Design and Synthesis of Esters as Protein Kinase C (PKC)-C1 Domain Regulators

A dissertation submitted to the

Indian Institute of Technology Guwahati as

Partial fulfillment for the Degree of

Doctor of Philosophy in Chemistry

Submitted by

Narsimha Mamidi

Department of Chemistry

Indian Institute of Technology Guwahati

Assam-781039, India

April-2014

INDIAN INSTITUTE OF TECHNOLOGY GUWAHATI

Department of Chemistry

STATEMENT

I do hereby declare that the matter embodied in this thesis is the result of investigations carried out by me in the Department of Chemistry, Indian Institute of Technology Guwahati, India under the supervision of assistant proferssor Dr. Debasis Manna.

In keeping with the general practice of reporting scientific observations, due acknowledgements have been made wherever the work described is based on the findings of other investigators.

21st April, 2014 **Narsimha Mamidi**
IIT Guwahati

INDIAN INSTITUTE OF TECHNOLOGY GUWAHATI

Department of Chemistry

CERTIFICATE

This is to certify that Narsimha Mamidi has been working under my supervision since July, 2009 as a regular registered Ph. D. student. I am forwarding his thesis entitled **"Design and Synthesis of Esters as Protein Kinase C (PKC)-C1 Domain Regulators"** being submitted for the Ph. D. (Science) Degree of this Institute. I certify that he has fulfilled all the requirements according to the rules of this institute regarding the investigations embodied in his thesis and this work has not been submitted elsewhere for a degree.

21st April, 2014
IIT Guwahati

Dr. Debasis Manna
Supervisor
Department of Chemistry
IIT Guwahati

Dedicated

To

My Parents, Brothers and Sister

Acknowledgements

It would have not been possible to write this doctoral thesis without the help and support of the kind people around me, to only some of whom it is possible to give particular mention here.

First and foremost, my heartful thanks to my thesis supervisor Dr. Debasis Manna for his precious suggestion, incisive guidance and decisive insights during the entire course of Ph.D. research. His true scientific spirit has helped me a lot during my research work. I am also thankful to him for giving me freedom to pursue my own ideas and I find myself privileged to have worked under his kind guidance. My everlasting gratitude goes towards him.

I would like to acknowledge my sincere gratitude to all my doctoral committee members, Prof. Gopal Das, Dr. Subhendu Sekhar Bag and Dr. Anil Mukund Limaye for their insightful advices and valuable suggestions. My honest regards to all the faculty of the Department of Chemistry for their motivation and encouragement.

I wish to acknowledge my sincere gratitude to the Council of Scientific and Industrial Research (CSIR), India for financial support and IIT Guwahati for all the facilities that were made available to me. I also thank Central Instrument Facility (CIF), IIT Guwahati for providing the instrument facility and DST for providing the X-ray facility.

My sincere thanks also go to the NMR and mass spectrometry employees Chandan and Singh da for their efforts with measuring my samples. For the X-ray structure analysis I would like to thank Mr. Babulal Das and Himanshu sekhar Jana for his help.

I would like to thank all my group members Sukhamoy Gorai, Rituparna Borah, Dipjyoti Talukdar and Sourav Paul, Subhankar, Narayana Sinha, Rakesh Mukhergy, Chandramohan Jana, Jashobanta Sahoo. I extend my sincere thanks to other friends in the department Dr. Chaitanya, Dr. Somasekhar Bondalapati, Dr. Murali Reddy, Dr. C. Mouli Reddy and Dr. Ramana for their valuable suggestions.

I also take this opportunity to thank all of my Ph.D. batchmates (July, 2009), the other research scholars in the Chemistry Department and all my IITG friends, who have shared their thoughts and views with me.

I am very much thankful to my best friends in IITG, especially Bigyan Ranjan Jaali, Kamali Gogoi, Kotipally, Himanshu, Renjith B, Sidick Basha R, Kishore, Kiran for their everyday help and support in all aspects.

My heartful thanks also go to my dearest friends from outside IITG, Sudhakar Madiri, Hemalatha Madiri, Nagaiah Dasari, Dhanjujaya Rao, Dasharatha, Salaiah, Naveen Kumar, Ramesh

Mukkamula, Naganna, Narender Reddy, Ramesh P and Venkanna D for their constant support and for being ever ready to lend a helping hand whenever I needed help at home.

Most importantly, my Ph. D. endeavours would not have been completed without the endless love, unending support, tolerance and blessings from my family. I wish to express my sincere gratitude to my parents, my brothers and sister. They are the main soul and inspiration for each and every step that I achieve in my life.

Narsimha Mamidi

List of Abbreviations

(1,4,5)IP_3	Phosphatidylinositol-1,4,5 trisphosphate
ADP	Adenosine-5´-diphosphate
Ag_2O	Silver(I) oxide
AGC	Adenine–Guanine–Cytosine
aPKCs	Atypical protein kinases
ATP	Adenosine-5´-triphosphate
Bn	Benzyl
BnBr	Benzyl bromide
cPKCs	Classical protein kinases
DAG	*sn*-1,2-diacyl glycerol
DAT	Diacyltetrol
DAT-PA	Diacyltetrol-phosphatidic acid
DAT-PG	Diacyltetrol-phosphatidylglycerol
DAT-PS	Diacyltetrol-phosphatidylserine
DCC	*N*,*N*-dicyclohexylcarbodiimide
DMAP	4-dimethylaminopyridine
DMSO	dimethylsulfoxide
DPP	12-deoxyphorbol-13-phenylacetate
DPPA (PA)	1,2-dipalmitoyl-sn-glycero-3-phosphate (sodium salt) (Phosphatidic acid)
DPPC (PC)	1,2-dipalmitoyl-sn-glycero-3-phosphocholine (Phosphatidylcholine)
DPPE (PE)	1,2-dipalmitoyl-sn-glycero-3-phosphoethanolamine (Phosphatidyl ethanolamine)
DPPG (PG)	1,2-dipalmitoyl-sn-glycero-3-phospho-(1'-rac-glycerol) (sodium salt) (Phosphatidylglycerol)
DPPS (PS)	1,2-dipalmitoyl-sn-glycero-3-phospho-L-serine (sodium salt); (Phosphatidylserine)
DTT	Dithiothreitol
ER	Endo reticulum
ESI	Electrospray ionization
FRET	Fluorescence resonance energy transfer
GROMACS	GROningen MAchine for Chemical Simulations
GST	Glutathione S-Transferase
HIV	Human immunodeficiency virus
HRMS	High resolution mass spectrometry
Hsp70	Heat-shock protein 70
IL-V	Indolactam V

IR	Infra-red
$LiAlH_4$ (LAH)	Lithium aluminium hydride
LNCaP	Lymph node carcinoma of the prostate
m.p.	Melting point
m/z	Mass to charge ratio
Mol. Dock.	Molecular Docking
MRCK	Myotonic dystrophy kinase-related Cdc42-binding kinases
NaH	Sodium hydride
NES	Nuclear Export Signals
NLS	Nuclear Localization Signals
NMR	Nuclear magnetic resonance
nPKCs	Novel protein kinases
Pd-C	Palladium on activated charcoal
PDK	Pyruvate dehydrogenase kinase or Pyruvate dehydrogenase complex kinase
PH	Pleckstrin homology
PKA	Protein Kinase A
PKC	Protein Kinase C
PKD	Protein Kinase D
PLC	Phospholipase C
PLD	Phospholipase D
PMSF	Phenylmethylsulfonyl fluoride
ppm	parts per million
Pst	Pseudosubstrate
$PtdIns(4,5)P_2$	Phosphatidylinositol-4,5 bisphosphate
p-TsOH	*p*-Toluenesulfonic acid
r.t.	room temperature
RasGRPs	Ras guanyl nucleotide-releasing protein
R_f	Retention factor
SDS-PAGE	Sodium dodecyl sulfate- Polyacrylamide gel electrophoresis
TBAF	*n*-Tetrabutylammonium fluoride
TBDPS	*tert*-Butyldiphenylsilyl
THF	Tetrahydrofuran
TLC	Thin Layer Chromatography
TPA	12-O-tetradecanoyl phorbol 13-acetate

Abbreviations for intensities of ^{1}H-NMR signals			
s	singlet	m	multiplet
d	doublet	brs	broad signal
dd	doublet of doublet	Hz	Hertz
t	triplet	MHz	Mega-Hertz
p	pentate		

Amino Acid	**3-Letter symbol**	**1-Letter symbol**	**Amino Acid**	**3-Letter symbol**	**1-Letter symbol**
Alanine	Ala	A	Methionine	Met	M
Arginine	Arg	R	Phenylalanine	Phe	F
Asparagine	Asn	N	Proline	Pro	P
Aspartic acid	Asp	D	Pyrrolysine	Pyl	O
Cysteine	Cys	C	Selenocystein	Sec	U
Glutamic acid	Glu	E	Serine	Ser	S
Glutamine	Gln	Q	Threonine	Thr	T
Glycine	Gly	G	Tryptophan	Trp	W
Histidine	His	H	Tyrosine	Tyr	Y
Isoleusine	Ile	I	Valine	Val	V
Leusine	Leu	L			

Compound and inhibitor constants and parameters

EC_{50}	The concentration of an compound which causes 50% of a maximal effect
IC_{50}	The concentration of an inhibitor which causes 50% inhibition
IG_{50}	The concentration of an inhibitor which causes 50% growth inhibition
K_I	Inhibitor dissociation constant
K_D	Dissociation constant

Contents

Abstract

The contents of my thesis have been divided into six chapters based on the results of experimental work performed during the complete course of research period. The introductory chapter (chapter 1) of the thesis presents the structure, activation and C1 domain of protein kinase C (PKC). In addition, C1 domain targeted ligands including natural products, synthetic compounds and the synthesis of biological active ester molecules using different approaches. Chapter 2 describes design, synthesis and protein binding properties of diacyltetrol (DATs) lipids. Chapter 3 illustrates development of diacyltetrol based anionic hybrid lipids as protein kinase C-C1 domain regulators. Chapter 4 presents (hydroxylmethyl)phenyl ester analogues as C1 domain regulators. In chapter 5, C1 domain targeted alkyl cinnamates synthesis is described. Chapter 6 describes $Zn(OTf)_2$ catalyzed chemoselective esterification of carboxylic acids.

Protein kinase C (PKC) family of serine/threonine kinases are the major cellular receptor for diacylglycerol (DAG)/phorbol esters. DAG depended PKC activation controls several cellular pathways by phosphorylating the target proteins. Dysregulation of these cellular pathways causes numerous diseases including cancer, diabetes, stroke, heart failure and Alzheimer's disease. Therefore, PKC isoenzymes particularly in the cancer field have been a subject of intensive research and drug development. PKC isoforms can be activated by natural products such as phorbol esters, prostratin, ingenol, indolactam V, iridal, bryostatin and their derivatives. However, except bryostatin most of them act as tumor promoters, due to their higher binding affinity. In addition, synthesis and structural modifications of these natural products are laborious for the specific and selectivity among the C1 domains of PKC isoforms. Therefore, there is a clear and unmet need to design simple surrogates, whose structure can be easily modified to achieve higher specificity and selectivity among the C1 domains of the PKC isoenzymes. Most of the reported PKC-C1 domain ligands have ester subunits, as an essential pharmacophore within their complex structure. However, only few methods can be used for synthesis of bioactive esters. In this regard, we developed esters as PKC-C1 domain regulators as well as $Zn(OTf)_2$ catalyzed selective esterification method in this thesis.

Initially, we designed diacyltetrols (DAT **1—4**) as PKC-C1 domain regulators and synthesis was accomplished within four to seven steps from (+)-diethyl L-tartrate as starting material (*Scheme 1*). In addition, we studied *in-vitro* protein binding properties with C1 domain of PKC isoforms using Trp-fluorescence quenching method. The calculated EC_{50} values for DATs compounds varied in the range of 0.35-3.08 μM. The binding pattern was assessed using molecular docking analysis. The stronger C1 domain binding capabilities of DATs with two hydroxyl/hydroxymethyl groups prompted us to design DAT based anionic hybrid phospholipids to obtain better C1 domain binding affinity and PKC isoform selectivity.

Therefore, to develop effective PKC regulators and understand the importance of anionic hybrid phospholipids in the protein activation, we developed flexible DAT-PA/PS/PG anionic hybrid phospholipids, where PA = phosphatidic acid, PS = Phosphatidylserine and PG = Phosphatidylglycerol). The synthesis was accomplished within seven to nine steps from (+)-diethyl L-tartrate as starting material (*Scheme 1*).

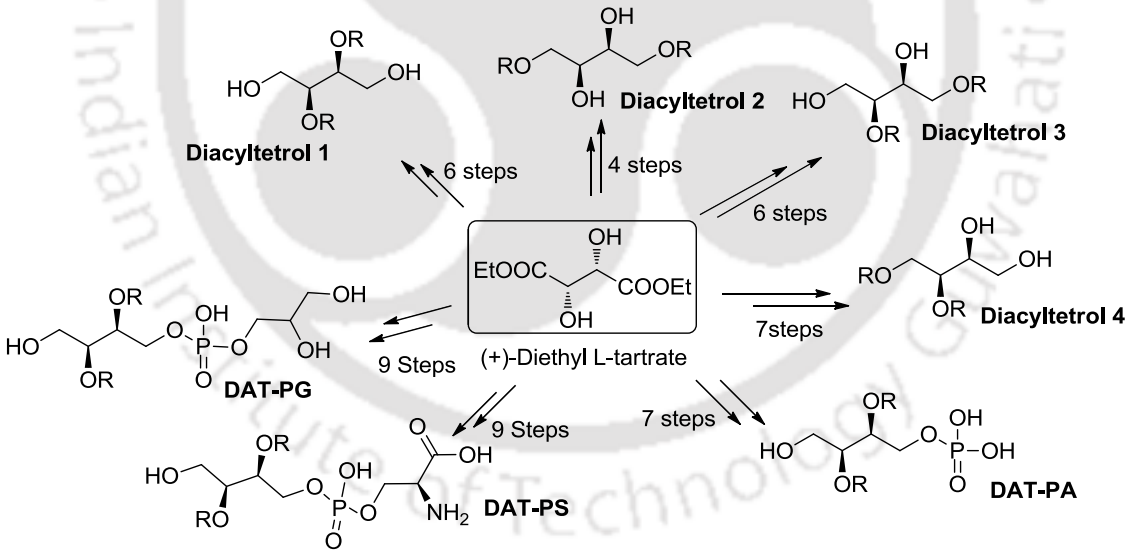

Scheme 1: *Synthetic Route to Diacyltetrols (DATs) and DAT-PA$_{8/16/18}$/PS$_{8/16/18}$/PG$_{8/16/18}$ Lipids.*

One pot multicomponent phosphorylation methodology was developed using OBn[(*i*-Pr)$_2$N]$_2$P for phosphorylation of alcohols in the part of DAT-PA/PS/PG synthesis. Further, we studied *in-vitro* protein binding properties with C1 domain of PKC isoforms using FRET. The binding results showed that DAT-PS anionic phospholipids specifically interact with PKCδ-C1b subdomains with stronger affinity (1.84-2.47 μM) than natural DAG. Further, DAT-PA and DAT-PG prefer to bind with PKCθ-C1b and PKCα-C1a respectively and anionic lipid headgroup play a significant role in binding. Molecular docking analysis was performed to understand the binding pattern of esters with C1 domain of PKC isoforms.

Due to structural flexible backbone, DATs and DAT-anionic lipids allows the ligands to increase the number of possible rotamers within the protein binding site. This makes the flexible ligands much less specific than expected. Therefore, we developed rigid phenyl backbone bearing (hydroxylmethyl)phenyl esters and alkyl cinnamates as PKC activators. The synthesis of (hydroxylmethyl)phenyl esters was accomplished within two to three steps using commercially available protocatechualdehyde, vanillin and isovanillin as the starting materials (*Scheme 2*). Whereas, the synthesis of alkyl cinnamates was accomplished within three steps starting from protocatechualdehyde using Knoevenagel condensation and Verley–Doebner modification of Knoevenagel condensation (*Scheme 2*). Then, we studied *in-vitro* binding properties using Trp-fluorescence techniques and the calculated EC_{50} values for (hydroxylmethyl)phenyl esters varied in the range of 0.91-1.02 μM whereas alkyl cinnamates showed in the range of 0.54-2.98 μM with PKCδ-C1b subdomain respectively.

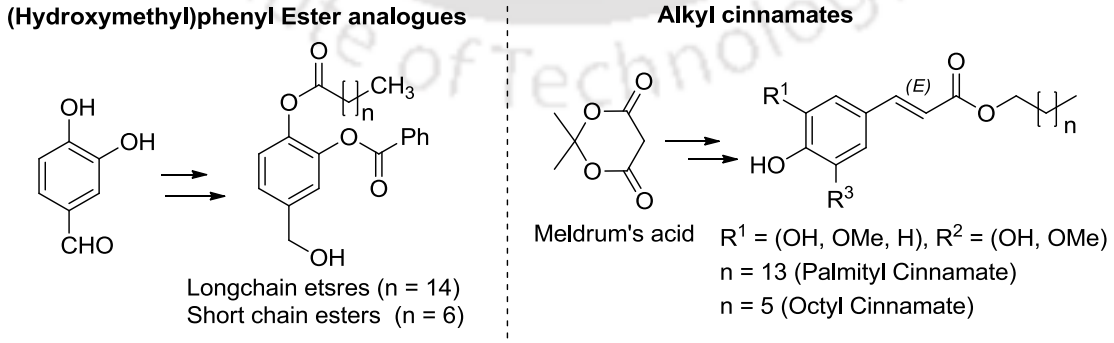

Scheme 2: *Synthetic Route to (hydroxylmethyl)phenyl Esters and Alkylcinnamates.*

Finally, docking analysis also suggested that the synthesized ester molecules interact with C1 domain of PKC isoforms and form hydrogen bonds with the backbone of the C1 domains in a similar binding fashion of DAG and phorbol esters.

Above developed DATs, DAT-anionic phospholipids, (hydroxylmethyl)phenyl esters and alkyl cinnamates are ester based C1 domain ligands. During the synthesis of these esters we faced some problems like chemo/regioselectivity, racemization, harsh reaction conditions, lower yield of desired products and longer reaction time. Therefore, to address these problems we developed a mild and efficient $Zn(OTf)_2$ promoted chemoselective esterification/amidation of the hydroxyl group bearing carboxylic acids in the presence of Ph_3P and I_2 *via* acyloxyphosponium ion intermediate (*Scheme 3*). This methodology was successfully utilized for the efficient synthesis of these PKC regulators in higher yields.

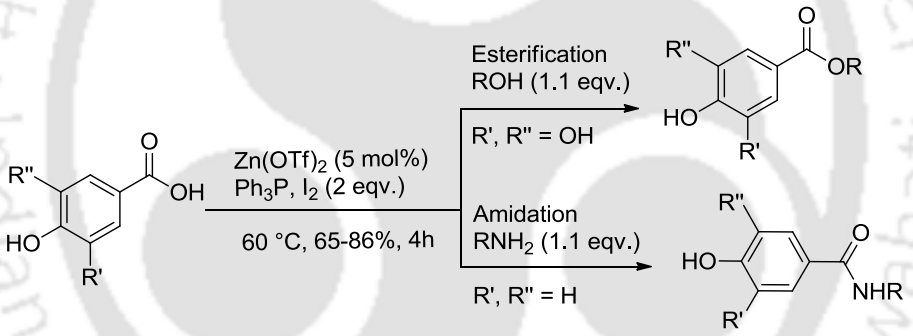

Scheme 3: *$Zn(OTf)_2$ Catalyzed Esterification/Amidation of Hydroxyl Group Bearing Acids.*

In conclusion we developed small molecules (esters) as PKC-C1 domain regulators. One-pot phosphorylation, time depended hydrogenation and $Zn(OTf)_2$ promoted esterification method has been developed. Detailed binding parameters of C1 domain of PKC isoforms were measured using fluorescence techniques and docking analysis was used to study binding pattern of esters with C1 domain. These esters can be used for the development of therapeutics against cancer and other diseases. Further, this concept can be extended to the drug design against Alzielmer's as well.

CHAPTER 1

Protein kinase C and its Ester Based Activators

1. Introduction

Protein kinases are one of the largest and most functionally diverse gene families. They control several key cellular functions, including cell growth, differentiation, proliferation and others, by phosphorylating the target proteins.[1-5] There are over 500 protein kinases present in the human genome that comprise about 2% of all human genes. Protein kinases are considered as potential therapeutic targets since their mutations and dysregulation influence the key cellular functions that create several human diseases, including immunological disorders, cancer and others.[1-6] However, the catalytic domain is subsequently homologous among the protein kinases. This sets the limit for the development of protein kinase inhibitors. Interestingly, some protein kinases have regulatory domain as part of their structure that assist them to activate the target proteins by controlling their localization and cellular function. Protein kinase C (PKC) family of proteins is an example of such class of protein kinases, which consists membrane binding C1 and C2 domain. The C1 domain is structurally conserved, contains only one ligand binding site and is found within a small number of kinases. These offers selectivity advantage for PKC proteins and make C1 domain an attractive drug target.[7] Consequently, the major portion of this thesis deals with the development of novel compounds targeted to bind the C1 domain of PKC.

For diseases like cancer and others, one of the most deliberated protein kinases is the PKC (EC 2.7.11.13) family of proteins. Initially the involvement of PKCs in signal transduction was not discovered. Later, the studies of calcium and anionic phospholipid-dependent diacylglycerol (DAG)-binding connected PKCs with signal transduction.[8] The isolation of other structurally related PKC isoenzymes and their detailed structural analysis and functional studies led to a sudden increase of research dedicated in elucidating their roles in signal-transduction pathways.

Currently, PKC is considered as a potent therapeutic target not only in cancer, but also in neurological, immunological, and cardiovascular diseases.[9-11] However, due to the presence of highly homologous catalytic domain among the protein kinases, the C1 domain present at the regulatory unit is considered as the major targets for drug designing in the

cancer field. In this regard, PKC enzyme activities are controlled by the C1 domain targeted natural compounds, its derivatives and also synthetic small molecules.

Esters are one of the major pharmacophores in various PKC-C1 domain active natural and synthetic ligands. However, there are only a few reported esterification methods in the literature that are suitable for the synthesis of such biological active esters in high yield. This compelled researchers to develop new methods suitable for esterification of the biologically complex acids or alcohols. In general, esterification is carried out either by acid or base catalysis. The familiar esterification methods are condensation of acids with alcohols using reactive acylating reagents like acyl chlorides and acid anhydrides.[12] However, most of these reagents limit the functional group tolerance. Mitsunobu esterification method is one of the convenient methods for the selective esterification of hydroxyl bearing carboxylic acids, but it results inversion in stereochemical configuration.[13] Therefore, these methods are not suitable for the synthesis of ester containing complex natural products and hydroxyl groups bearing bioactive molecules. Hence, the developments of new esterification methods are required to overcome these problems.

2. Review of the Literature

2.1. Protein kinases

Protein kinases modify the target proteins by phosphorylation. There are 518 protein kinase genes are present in the human genome, and they constitute only 2% of all human genes.[6] However, up to 30% of all human proteins are known to be directly or indirectly modified by protein kinase activity, and most of the signal transduction pathways in eukaryotic cells are also regulated by the kinase activity. Depending on the phosphorylation of the hydroxyl group of various amino acids present at the surface of the target proteins, the protein kinases are classified as serine/threonine kinases (EC 2.7.11.1), tyrosine kinases (EC 2.7.10.1 and 2.7.10.2), and dual specific kinases (EC 2.7.12.1).[14] It is also important to note that the specificity of the phosphorylation of above mentioned amino acids depends on the adjacent amino acids of the target proteins.[15] These protein phosphorylations play a significant role in a wide range of cellular processes including metabolism, transcription, cell cycle progression, cytoskeletal rearrangement, cell movement, apoptosis, differentiation and others.[9-11] Due to these insightful effects of protein kinases under cellular environment, their activity is highly regulated. The activity of kinases are turned on or off by phosphorylation (sometimes by autophosphorylation), by binding of activator / inhibitor proteins, or small molecules, or by

controlling their location in the cell relative to their substrates. Protein kinases are considered as potential therapeutic targets since mutations and dysregulation play crucial roles in multiple human diseases, affording the possibility of developing modulators (inhibitors) of these enzymes for the treatment of cancer and other disease.[16,17]

Figure 2.1.1 shows a cartoon diagram of the protein kinase-dependent phosphorylation process. In the phosphorylation reaction, adenosine-5´-triphosphate (ATP, **1**) first interacts with protein kinase and forms a kinase-ATP complex, then the target protein moves towards the protein kinase-ATP complex and form a ternary complex. The protein kinase then transfer the γ-phosphate group of ATP to the hydroxyl group of the target protein, and it releases the adenosine-5'-diphosphate (ADP, **2**). However, this sequence of phosphorylation and ADP release process may be also in reverse order depending on the protein kinases.

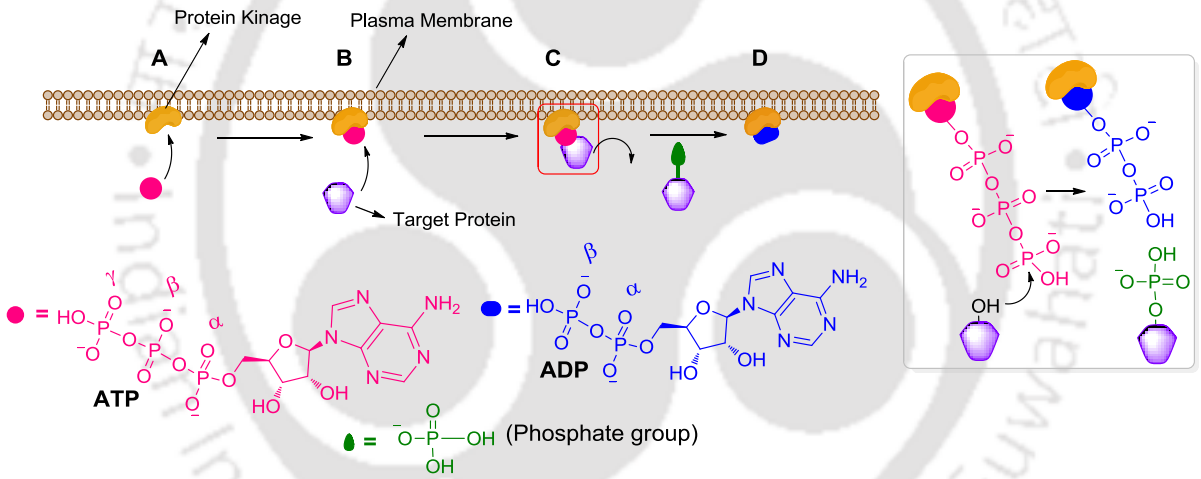

Figure 2.1.1: *Phosphorylation of target proteins by protein kinases;* ***A)*** *a protein kinase binds ATP,* ***B)*** *a target protein binds to the protein kinase-ATP complex,* ***C)*** *the protein kinase transfers a phosphate group from ATP to the target protein and the phosphorylated target protein leaves the complex,* ***D)*** *a protein kinase-ADP complex and a phosphorylated target protein as products. Adenosine-5´-triphosphate (ATP,* ***1****), adenosine-5´-diphosphate (ADP,* ***2****).*

The phosphorylated targeted protein then undergoes a conformational change, subsequently activating or deactivating the target enzyme. Thereby, this phosphorylated enzyme can participate in the subcellular relocation and association with other proteins.[6,18]

2.2. Protein kinase C

PKC isoenzymes belong to the larger subclass of protein kinases called adenine−guanine−cytosine (AGC) kinases and serine/threonine kinases. PKC is a crucial cellular receptor for DAG/tumor promoting phorbol esters.[19,20] In 1980s, PKC was first discovered as "the receptor" for the phorbol esters, later several studies revealed the key role of PKCs in cell signalling processes.[21,22] PKC isoenzymes play a pivotal role in the physiological and pathophysiological events including, malignant transformation, cell proliferation, differentiation, cell cycle progression and cancer,[7,23] diabetes,[24] stroke, heart failure and Alzheimer's disease.[25-27] Therefore, PKC isoforms in the cancer field have been a subject of demanding research and drug development. Detail biological studies and x-ray crystal structure of the phorbol ester bound PKCδ-C1b domain showed that phorbol ester and lipophilic second messenger *sn*-1,2-diacyl glycerol (DAG (**4**), *Figure 2.2.1*) molecules interact with the PKC isoenzyme through their C1 domain. This interaction stimulates these enzymes and endorses their association with the membrane lipids, by inducing the translocation of cytosolic PKCs to the inner leaflet of the cellular membrane.[16] The PKC enzyme family consists of at least 11 known isoforms, categorized as conventional or classical (α, γ, and βI, βII), novel (δ, ε, η and θ), and atypical (ζ, ι/λ) subgroups.[28] All PKCs are activated by anionic phospholipids, particularly phosphatidylserine (PS (**3**), *Figure 2.2.1*).[29]

In addition, conventional PKCs require both Ca^{2+} and DAG for an activation, whereas novel PKCs require only DAG. The third group, atypical PKCs, requires neither DAG nor Ca^{2+} for activation. All these isoenzymes have a regulatory moiety, and it contains two key functionalities: an autoinhibitory sequence (pseudosubstrate) and one or two membrane targeting modulates (C1 and C2 domains). Other families of signaling proteins such as Ras guanyl nucleotide-releasing protein (RasGRPs), myotonic dystrophy kinase-related Cdc42-binding kinases (MRCK), chimerins, Unc-13 scaffolding proteins, protein kinase D (PKD), and the DAG kinases β and γ also shares C1 domain with PKC isoforms.[11,30,31] Several structurally distinct forms of DAG are available in the mammalian cells that selectively interact with the C1 domain containing proteins.

Under equilibrium conditions, the cellular DAG concentrations are generally low in mammalian cells.[32,33] When cells are stimulated by G-protein-coupled receptors, receptor tyrosine kinases and others, hydrolysis of the phosphatidylinositol-4,5 bisphosphate ($PtdIns(4,5)P_2$) catalyzed by phosphatidylinositol-specific phospholipase C (PLC, EC

3.1.4.11) rapidly produces DAGs at the inner-plasma membrane (PM) that activate PKC and other proteins.[8,34,35] The other product of PtdIns(4,5)P_2 hydrolysis, inositol-1,4,5-triphosphate ((1,4,5)IP_3) induces the release of Ca^{2+} from ER which also activate various proteins, including Ca^{2+}-dependent PKC isoforms. DAGs can also be produced from phosphatidylcholine (PC) by concerted action of phospholipase D (PLD) and phosphatidic acid phosphohydrolase, presumably at internal membranes, such as ER and Golgi membranes.[33] Phorbol esters (**5**, *Figure 2.2.1*) are natural products, extracted from the seeds of Croton tiglium L.[36] The phorbol ester was identified to interact with the C1 domain through the same binding site as of DAG. However, many of the phorbol ester derivatives are tumor promoters.[37-39]

The inactive conformation of PKC effectively localize at the cellular cytoplasm.[18] After phosphorylation by phosphoinositide dependent kinase (PDK) and other enzymes, followed by Ca^{2+} binding to the C2 domain, PKC localize to different cellular membranes, including plasma membrane, perinuclear membrane and Golgi membrane. The isoform specific cellular functions of PKC are mainly due to their individual subcellular localization. At the cellular membranes, the C1 domain binds to DAG in the presence of anionic phospholipids. In addition, the interaction of membrane phospholipids with the C2 domain also anchor the enzymes to the membrane.

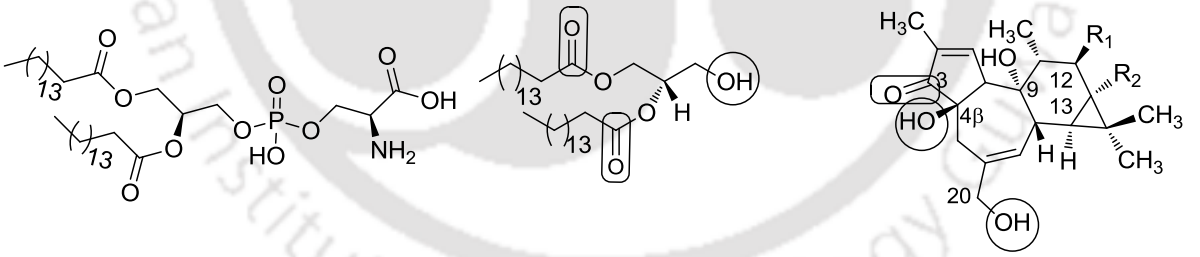

Figure 2.2.1: *The structures of phosphatidyl-L-serine (PS, **3**), 1,2-diacylglycerol (DAG, **4**) and phorbol esters (**5**). Functional groups that interact with the C1 domain are highlighted.*

It is also important to mention that DAG binding to the C1 domain pulls out the pseudosubstrate from the active site of the catalytic domain and the released pseudosubstrate interact with the negatively charged membrane surface. After this DAG dependent membrane organisation, the PKC isoenzymes becomes fully functional and ready to phosphorylate

serine and threonine residues in proper sequence context. However, when DAG is phosphorylated to phosphatidic acid or hydrolyzed to glycerol and constituent fatty acids the PKCs and DAG binding proteins get deactivated and relocalized to the cytoplasm of the cell.[30,39-42] When validating the therapeutic target enzyme, the selection of true isoform of PKC is extremely important since the different isoforms of PKCs show specific biological effects. Inhibition or activation of the target isoform should be considered as the different isoforms can produce divergent outcomes. In addition, several studies already described the independent biological functions of the regulatory domain of PKCs.[43] Therefore, C1 domains have become an attractive target in designing selective PKC ligands.

2.2.1. Structure, Activation and Regulation

Structure—The PKC family of proteins consist of a single polypeptide chain with a highly conserved C-terminal catalytic domain (approximately 44 kDa) and a less conserved N-terminal regulatory domain (approximately 18–40 kDa) connected by a proteolytically labile hinge region (*Figure 2.2.1.1*). When this hinge is cleaved a constitutively active kinase domain is formed, which is entirely free from the autoinhibition imposed by the regulatory domain. The catalytic region is highly preserved among the PKC isoenzymes, but the regulatory domain is less consistent.[44] However, the regulatory domain contains several shared subregions.

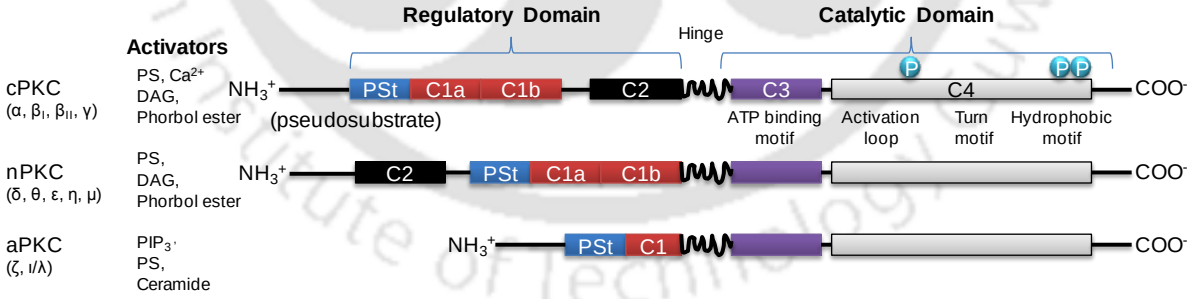

Figure 2.2.1.1: Structures *and domains of protein kinase C isoforms. Pst = pseudosubstrate, PB1 = Phox and Bem 1.*

The N-terminal regulatory domain of PKC proteins contains an autoinhibitory sequence and one or two membrane targeting domains (DAG / phorbol ester-binding C1 domain and Ca^{2+}-binding C2 domain).[11] The aPKCs have a Ca^{2+} independent C2 domain and an atypical C1 domain that binds PtdIns(3,4,5)P_3, PS and ceramide but not DAG. However, a

protein-protein interacting PB1 (Phox and Bem 1) domain that binds PB-containing scaffolds is present in the aPKCs. The aPKC isoform activation is due to the protein-protein interactions and phosphorylation of the activation loop by PDK-1 enzyme.[45,46]

Priming Phosphorylations of PKC—The PKCs isoenzymes in its immature conformations are localized at the cytoplasm.[18] PKCs become fully mature (priming phosphorylations) by a series of ordered phosphorylation reactions that are essential for the enzymes to gain catalytic competence and appropriate intracellular localization. The PKC requires two (aPKCs) or three (cPKCs and nPKCs) phosphorylations for its complete maturation.[41,47] The phosphorylation positions are conserved among PKC isoenzymes as well as among other AGC kinases. The first adaptation is an auto-phosphorylation or a PDK-1-catalyzed phosphorylation of a threonine residue at the activation loop of the catalytic domain of PKCs. This phosphorylation produces a negative charge in the peptide-binding domain and consequently, stabilizes the mature conformation. The second phosphorylation of threonine/serine residue at the conserved turn motif further stabilizes the PKCs and is essential for catalytic activity.[47] Once the PKC isoenzymes are phosphorylated at the C-terminal sites, the activation loop-phosphate is dispensable, immediately selective dephosphorylation occurs without the loss of any enzymatic activity. Therefore, phosphorylation at the turn motif of a mature PKC is essential for catalytic activity. The third modification (for cPKCs) is an autophosphorylation of the serine (S)/threonine (T) residue, 19 residues C-terminal to the turn motif. It is reported that, the third phosphorylation occurs at S/T residue within a conserved FXXFS/TF/Y hydrophobic motif. Where F stands for Phenylalanine, Y stands for Tyrosine while S and T represent the serine and threonine phosphoacceptor amino acid, respectively and X can be any amino acid. [48,49] For cPKC and nPKCs, this motif can also be transphosphorylated. The aPKCs do not have this S/T residue at the hydrophobic motif. It is reported that this essential phosphorylation in the hydrophobic moiety of aPKCs can be produced from glutamic acids residue instead of S/T residue. In addition to these phosphorylations, other S/T residues of the enzyme can also be phosphorylated under physiological conditions.[16]

Activation and Regulation of PKC—Activation of the PKC isoenzymes is the result of several actions that take place in the enzyme (*Figure 2.2.1.2*). The pseudosubstrate of the regulatory domain is an amino acid sequence with multiple basic residues, which is well

recognized by the substrate binding domain (Figure 4). When PKC is in the inactive conformation, the interaction of pseudosubstrate and substrate binding domain prevents PKCs to phosphorylates its substrates.

PKC activation initiate when the C2 domain binds to anionic lipids and Ca^{2+} (only cPKCs), providing the required energy to release the pseudosubstrate from the active site.[16,46] This allows the C2 domain to translocate to the cell membrane, consequently the C1 domain (of cPKCs and nPKCs) translocate to the cellular membrane and binds to DAG (**4**)/phorbol ester (**5**). This allows the PKC to undergo a conformational change, allowing the pseudosubstrate to move out from the ATP-binding site. Now the PKC is the fully active form and it can phosphorylates other amino acid residues. This conformational change of the PKCs reveals the hinge region between catalytic domain and the C2 domain. The hinge region becomes proteolytically labile, and if it is cleaved a constitutively active kinase domain is formed.[50]

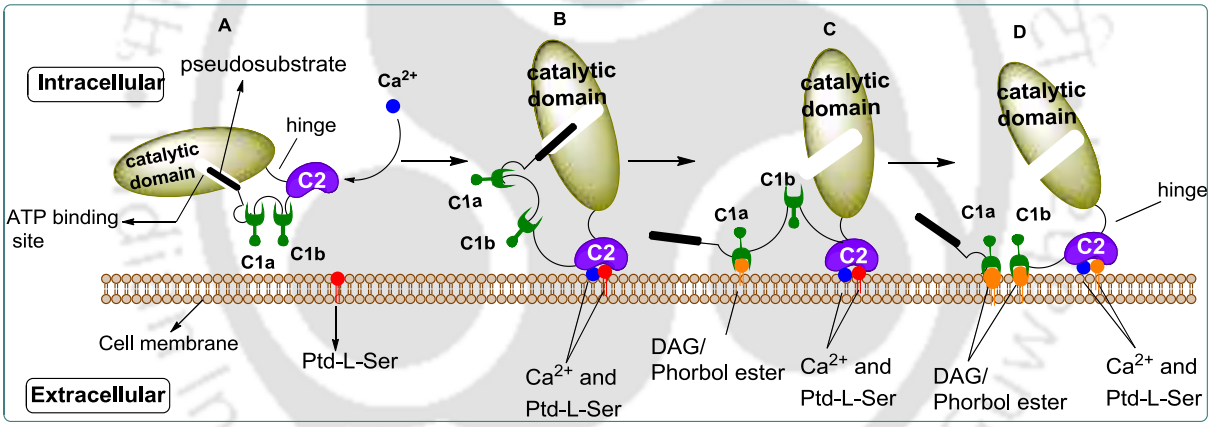

Figure 2.2.1.2: *Activation of cPKCs.* ***A)*** *In the inactive conformation, the pseudosubstrate is bound to the catalytic site of the kinase domain.* ***B)*** *The C2 domain binds* Ca^{2+} *and phosphatidyl-L-serine (PS,* ***3****) and the domain localizes to the cell membrane.* ***C)*** *The C1a domain binds diacylglycerol (DAG,* ***4****)/phorbol ester (****5****) at the cell membrane and a conformational change has moved the pseudosubstrate off the catalytic site. The C1b domain is still in front of the ATP-binding site, producing a low activity state of the catalytic site.* ***D)*** *The active conformation where the C1b domain is not anymore at the front of the catalytic domain but binds DAG (****4****)/phorbol ester (****5****) at the membrane.*

The activation or regulation of aPKCs is not affected by the DAG (**4**)/phorbol esters (**5**) or Ca^{2+} ion. The regulation of aPKCs is affected by their interaction with phospholipids,

PDK-1, the PB1 domain and other proteins. However, the activation of aPKC can be also regulated by the nuclear localization signals (NLS) and nuclear export signals (NES). It is also important to mention that phosphorylated and subsequently activated PKCs become highly sensitive to dephosphorylation. Membrane-bound PKCs is two orders of magnitude more sensitive to dephosphorylation or down-regulation than cytoplasmic PKCs.[51] The dephosphorylation of the PKCs also takes place if cells are activated by phorbol esters (**5**). Other reported PKC regulation pathways are caveolin-dependent targeting to endosomes, ubiquitin-mediated proteolysis, and binding of the heat-shock protein 70 (Hsp70).[52-56]

2.2.2. The C1 Domain of Protein Kinase C

The DAG-/phorbol esters-binding C1 domain is a cysteine-rich region of approximately 50 amino acid residues, present in all PKC isoenzymes. There are two functionally non-equivalent C1 domains (C1a and C1b) positioned in tandem within the regulatory domain of classical and novel PKC isozymes.[57] Whereas the C1 domain of aPKC has a single copy of the domain, it is called atypical because it does not bind DAG-/phorbol esters.[59] The C1a and C1b domains have different binding affinity for PKC isoenzymes. The PKCα-C1a and PKCθ-C1b subdomains shows higher DAG binding affinity than the C1b and C1a subdomain respectively, which have been explained by the presence of a single tyrosine residue only found in the C1b domain of the cPKCs. In all other C1 domains, this residue is tryptophan instead of tyrosine. For PKCδ-C1b/a subdomains, conflicting results have been reported regarding their DAG binding affinity. The C1b domain of PKCδ binds phorbol ester (**5**) with higher affinity than the C1a domain. PKCα C1a and C1b domains have equal binding affinity for phorbol ester (**5**). Available X-ray crystal structure and NMR solution structure showed that the C1 domains contain two zinc finger motifs, where His and Cys residues at opposite ends of the primary sequence coordinates with the Zn^{2+} ions to stabilize the domain, and two pulled apart β-sheets form the ligand binding pockets. The "top" part of the C1 domain structure is hydrophobic in nature and contains the DAG (**4**)/phorbol ester (**5**) binding site. The binding site is deep, narrow and contains polar group between two β-sheets (*Figure 2.2.2.1*).[60] The negatively charged amino acids are present at the "bottom" part of the C1 domain. The "central" part of the C1 domain is hydrophilic in nature.

In atypical C1 domains, the ligand binding pocket is compromised and module cannot bind with phorbol esters or diacylglycerol.[59] Elucidation of the structure of PKC*δ*-C1b subdomain reveal that the formation of C1 domain-DAG (**4**)/phorbol ester (**5**) complex

allows the C1 domain to be partly buried in the membrane bilayer, so that the positively charged residues at the central portion of the domain, could interact with anionic phospholipids. It is presumed that, to overcome the enthalpy penalty due to the interactions between the hydrophilic residues and the bilayer, the hydrophobic ligands acts like a lid on the top of the domain to produce a continuous hydrophobic surface and thus masking the hydrophilic residues for membrane interaction.[59,60] The ligand binding does not result in significant conformational change in the, tertiary structure of the domain. The X-ray crystal structure of the C1b domain complexed with phorbol 13-*O*-acetate (**7**) reveals that ligand interact with the C1 domain mainly through hydrogen bond interaction and hydrophobic interactions (*Figure 2.2.2.2*). The C20 hydroxyl group of **7** is hydrogen bonded with the carbonyls of Leu251 and Thr242 and, with the backbone amide hydrogen of Thr242. The C4 hydroxyl and C3 carbonyl group of **7** are hydrogen bonded with the carbonyl and the backbone amide proton of Gly253, respectively. It is also reported that C13 carbonyl group of **7** is also crucial for high-affinity binding with C1 domain of PKC. It is hypothesized that the C13 carbonyl group could be hydrogen bonded with the backbone amide proton of Gly253.The number of C1 domain-containing proteins is significantly smaller than the number of PKs.

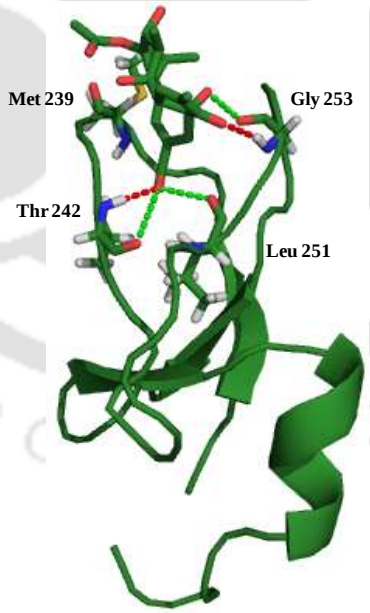

Figure 2.2.2.1: *Crystal structure of PKC δ-C1b domain (1PTR) complexed with phorbol ester (**5**).*

The catalytic domain, in particular, the ATP-binding site of PKC isoenzymes is substantially homologous among the PKs. Therefore, C1 domain provides an attractive target for designing selective PKC modulators.[30,31,61,62]

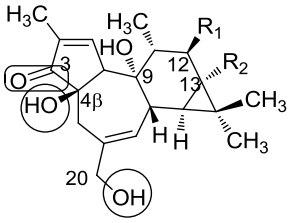

$R_1 = O_2C(CH_2)_{12}CH_3$, R_2 = OAc (PMA, **6**)
R_1 = OH, R_2 = OAc (**7**)
$R_1 = O_2C(CH_2)_8CH_3$, R_2 = OH (**8**)
R_1 = OH, $R_2 = O_2C(CH_2)_8CH_3$ (**9**)
R_1, R_2 = OH (Phorbol, **10**)

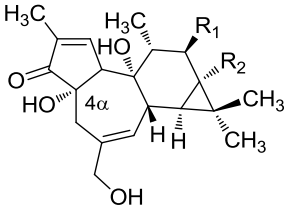

$R_1 = O_2C(CH_2)_{12}CH_3$,
R_2 = OAc (4α-Phorbol,**11**)

Figure 2.2.2.2: *Structures of phorbols* ***6-11****. Functional groups that interact with the C1 domain are highlighted.*

2.3. The C1-Domain as a Target for Natural and Synthetic Compounds

As mentioned earlier, the C1 domain is unique to PKC and few other proteins, which offers a selectivity advantage among the protein kinases and make the C1-domain an attractive drug target. Several natural compounds and synthetic compounds specifically target PKC-C1 domain. Among these ligands, most of them interact with the C1 domain through similar interaction mode as of DAG (**4**)/phorbol ester (**5**). These natural ligands are structurally complex and synthetically laborious. Therefore, the pharmacophores of the natural ligands have been used to design simplified compounds. Here, some of the C1 domain targeted natural compounds and simplified synthetic derivatives have been presented.

Prostratin and its Synthetic Analogues

Prostratin (**12**, 12-deoxyphorbol-13-acetate) and 12-deoxyphorbol-13-phenylacetate (DPP, **13**) are non-tumor promoting diterpenes (*Figure 2.3.1*) which were isolated from the extracts of *Homalanthus nutans* and used in traditional medicine to treat yellow fever and other conditions.[60] These diterpenes induce HIV expression in primary cells and latently infected cell lines.[60,63] Prostratin (**12**) and DPP (**13**) structurally resembles with the phorbol ester without the C12-hydroxy/acyl group found in phorbols (*Figure 2.3.1*). Both Prostratin (**12**) and DPP (**13**) contain ester groups at C13 position. However the reported results show that this small deference in the chemical structure makes these molecules non-tumor promoters.[59]

All these ligands strongly interact with the mixture of PKC isoforms, e.g. the prostratin analog **16** shown the K_i value 1.6 nM. Prostratin (**12**) and DPP (**13**) also interact with the C1 domains of PKC isoenzymes in the same manner as of phorbol esters (**5**). The mechanistic studies showed that these two ligands act as HIV inhibitor based on a PKC-dependent mechanism.[64] Prostratin (**12**) has been advanced into preclinical trial for cancer cell lines.[65] Even though, prostratin based ligands are non-tumor-promoters, but its development is inadequate because of its complex chemical structure and laborious synthetic procedures.

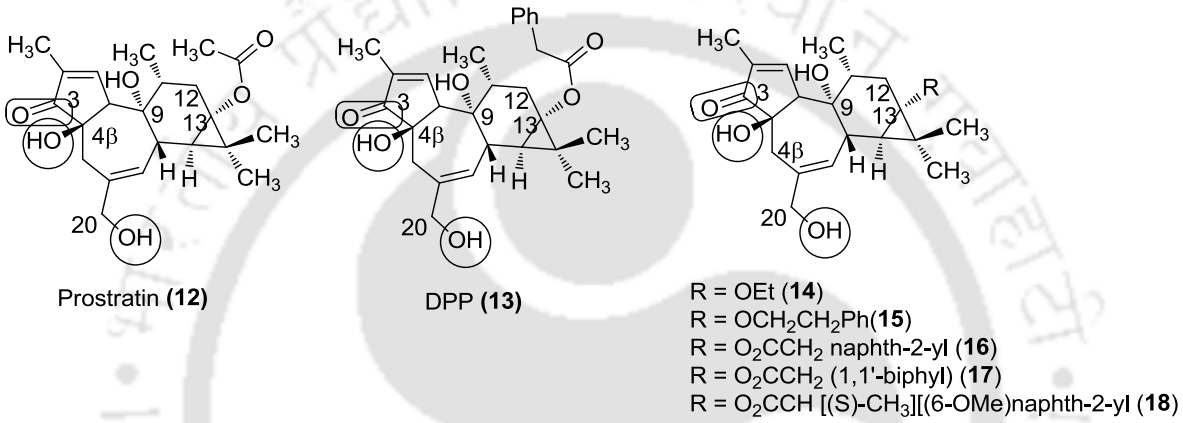

Figure 2.3.1: *Structures of the natural prostratin diterpenes (**12** and **13**) and synthetic analogues (**14-18**). Functional groups that are thought to interact with the C1 domain are highlighted.*

Ingenol and its Synthetic Analogues

Ingenol (**19**) is a member of the phorboid family and a highly polyoxygenated tetracyclic diterpenoid natural product, extracted from *Euphorbia ingens*.[66] Ingenol and its derivates show remarkable biological properties to mimic DAG (**4**) and it functions as endogenous activators of protein kinase (PKC). Further, they are found to demonstrate antitumor or tumor promoting, antileukemic, and anti-HIV properties and used in traditional medicine to treat skin diseases, asthma and migraine.[63,64] The ingenols (**19** and **20**, *Figure 2.3.2*) are structurally resembled with phorbol esters (**5**). The ingenols (**19** and **20**) have an additional hydroxyl group at C5 carbon on the seven-membered ring but which is not found in phorbol esters (**5**). Moreover, in ingenols (**19** and **20**) the C9 hydroxyl group of the phorbols is oxidized into a carbonyl and the six-membered ring of the phorbols is converted as a seven-

membered ring. Although, there is no ester group at C12 or C13 position like phorbol ester, but ingenol contain ester group at C3 position.

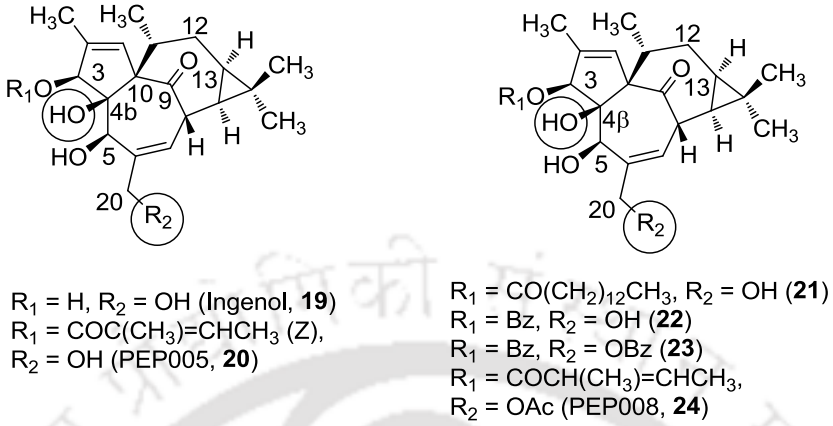

Figure 2.3.2: *Structures of the natural ingenols (**19** and **20**) synthetic ingenol analogues (**21-24**). Functional groups that are thought to interact with the C1 domain are highlighted.*

The C3 carbonyl in the five-membered ring of phorbols is replaced with an acyl or hydroxy group. These structural differences in the ingenols make them more hydrophilic than the phorbol esters.[67] The ingenols (**19** and **20**) binds with C1 domain of PKC in the same manner of phorbol esters (**5**). Then compounds **21** and **22** show strong binding interaction with PKCα (K_i value 7 nM and K_i 0.14 nM respectively).[65,68] However, **21** and **22** were found to be tumor-promoting. Interestingly, a dibenzoate derivative (**23**, K_i = 240 nM for PKCα) was found to be induce apoptosis in Jurkat cells through caspase-3 activation but not through PKC mediated activation.[65,68] Because compound **23** may not form the same interaction with groove in the biding site of PKC C1 domain the same as **21**. Ingenol angelate, or PEP008 (**24**) is a selective activator of the classical and novel PKC isoenzymes and show permanent growth arrest in solid tumors cell lines such as melanoma, breast and colon.[69]

Bryostatin and its Synthetic Analogues

Bryostatins (**25** and **26**, *Figure 2.3.3*) is a well-known macrolide lactone which was isolated from the marine organism *Bugula neritina* and *bacterial symbiont*.[70,71] These natural products are potent modulators (activators) of PKC. Bryostatins interact with the C1 domain of PKC isoenzymes in a similar fashion as of phorbol esters, (**5**) or DAG (**4**).[72] Bryostatin 1 (**25**) has shown activity against a variety of cancers.

It has shown potent activity related to a number of other diseases and conditions, including diabetes, stroke, and Alzheimer's disease. Bryostatin 1 (**25**) is under clinical trial for several diseases including, cancers, Alzheimer's disease and also acting as activators of effector cells of the immune system.[73,74] The involvement of bryostatin 1 becomes more realistic, when it is described that at least one mechanism for function of this compound involves activity on C1 domain containing PKC isozymes and other proteins. Bryostatin 1 (**25**) competes for binding with DAG (**4**) and phorbol esters (**5**) and the carbonyl group of C1 domain and the hydroxyl group of C19 and C26 of bryostatin 1 interacts with the PKC-C1 domains (*Figure 2.3.3*). Both bryostatin 1 (**25**) and bryostatin 2 (**26**) contain ester groups at C19 position. Furthermore, bryostatin 1 (**25**) induces the translocation of PKCδ protein almost exclusively to the nuclear membrane. Bryostatins strongly inhibit the binding of the tumor-promoting phorbol esters to PKCs and stimulate enzymatic activity both in-vitro and in-vivo.[75] However, the total syntheses of these highly complex macrocyclics are laborious and requires over 40 linear steps.[76,77] Hence, several research groups are interested in reducing the required steps to synthesize various bryostatin derivatives.

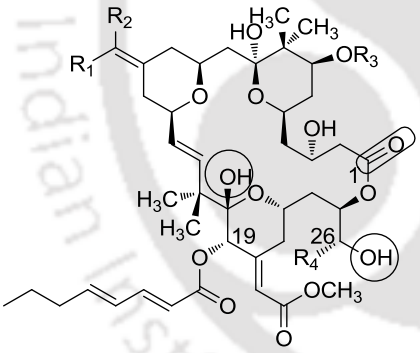

Compound	R_1	R_2	R_3	R_4
Bryostatin 1 (**25**)	COOMe	H	Ac	Me
Bryostatin 2 (**26**)	COOMe	H	H	Me

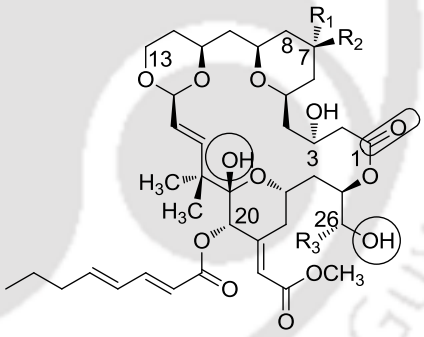

Compound	R1	R2	R3	K_i (nm)
27	H	H	Me	3.4
28	H	H	H	0.25[a]
29	H	OAc	H	13
30	H	OH	H	100
31	OH	H	H	1000

Figure 2.3.3: *Structures of the natural bryostatins (**25** and **26**) and synthetic bryostatin analogs (**27-31**). Functional groups that are thought to interact with the C1 domain are highlighted. The K_i values are also shown. [a]Wender and co-workers also reported a K_i value of 3.1 nM for the same derivative.*[79]

Recently, Wender and co-workers synthesized simplified derivatives (**27-31**, *Figure 2.3.3*) of bryostatin 1 (**25**) in a drastically reduced number of reaction steps.[76,78] When the methyl group was removed from C26 of compound **27** it produced compound **28**[77] (**K_i** value of 0.25 nM for rat brain PKC isoenzymes) was showed better binding affinities for rat brain PKC isoenzymes than **27** (K_i value of 3.4 nM for rat brain PKC isoenzymes).[59] However, the addition of acetoxy group to C7 of **27** the binding affinity of resulted compound **29** was decreased (K_i value to 13 nM for rat brain PKC isoenzymes). However, the addition of a hydroxyl group to C7 (compound **30** and **31**) reduced the binding affinity even further.[78] It has been hypothesized that these differences in binding affinities are because of the C8 gem-dimethyl groups found in the natural bryostatins, that shield a polar C7 group. Furthermore, the C3 hydroxyl group of bryostatins is essential for high binding affinity.[59]

Indolactam, Benzolactam and its Synthetic Analogues

Indolactam V (IL-V, **32**, *Figure 2.3.4),* is a 3,4-fused tricyclic indole containing natural product, isolated from *Streptoverticillium blastmyceticum* NA39-17.[80] Indolactam and its derivatives are potent activator of various PKC isoenzymes (K_i of 80 nM for PKCδ), but they are tumor promoters.[81] The structure of Indolactam-V (IL-V, **32**) is very similar to that of the teleocidins but, it lacks the hydrophobic group at 6,7-position of the indole ring of teleocidins (*Figure 2.3.4*).[80] The teleocidins (teleocidin B-4, **33**, *Figure 2.3.4*) are a family of 12-*O*-tetradecanoyl phorbol 13-acetate (TPA) type tumor promoters and aplysiatoxins. Teleocidins, indolactam and the benzolactam directly competes with phorbol esters for binding with PKCs. The primary hydroxyl groups of indolactams form hydrogen bonds to Thr113 and Leu119 in the groove of the PKCδ C1b domain.[80] In addition, the lactam N-hydrogen is hydrogen bonded to Leu119 and the C11 carbonyl group acts as a hydrogen bond acceptor for backbone proton of Gly124. Furthermore, the indole rings of indolactams are thought to have CH/π-interactions with Pro112 of PKCδ.[82] Even though, indolactam and its derivatives are potent activator of various protein kinase C (PKC) isozymes but tumor promoters. To improve the selective binding affinity of indolactam analogues with the C1 domain and to develop non-tumor-promoters, Endo and co-workers synthesized the benzolactam derivative based on the teleocidin **33** chemical structure.[83] In benzolactam derivatives the indole ring was replaced with a benzene ring and which have an 8-membered lactam moiety (**33**, *Figure 2.3.4*).

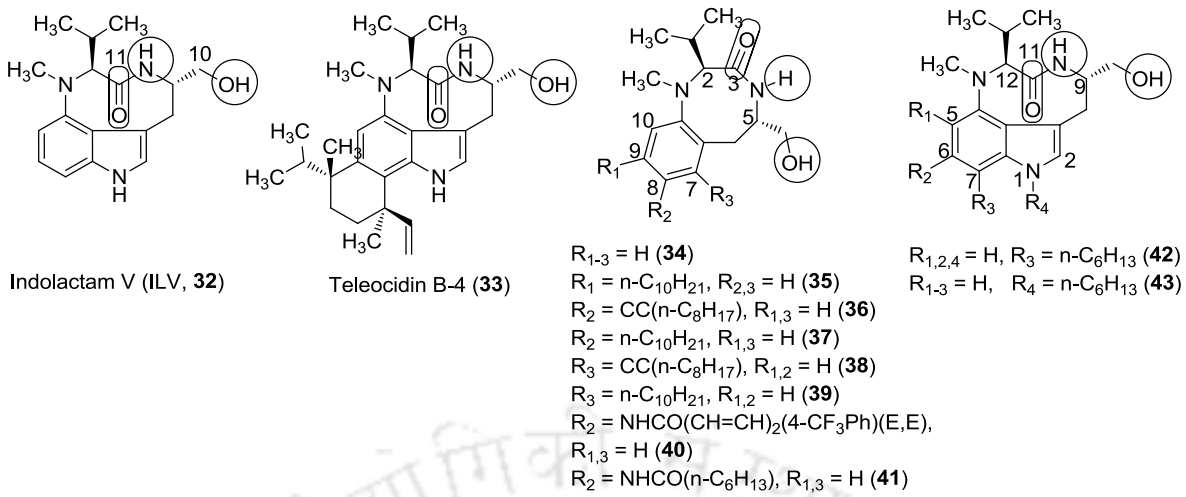

Figure 2.3.4: *Structures of indolactam (**32**), teleocidin B-4 (**33**) and synthetic benzolactams (**34**-**41**) and indolactams (**42** and **43**). Functional groups that interact with the C1 domain are highlighted.*

Benzolactam **34** was showed weak binding affinity with PKCδ (K_i = 1700 nM) whereas lipophilic side chain contained benzolactam analogue **35** was showed better binding affinity with PKCδ (K_i =1.8 nM). After that several benzolactams (**36**-**41**) and indolactams (**42** and **43**) derivative have been synthesized by various research groups (*Figure 2.3.4*).[84-90] Many of these synthetic compounds improved selective binding affinity with PKC than naturally occurring indolactam family of compounds. In addition, the benzolactams bind to the regulatory domain of PKC with the same interactions as the indolactams.

Iridals and its Synthetic Analogues

The iridals (**44** and **45**) are a family of exceptional monocyclic, bicyclic, or spirocyclic triterpenoids, extracted from sword lilies (*Figure 2.3.5*).[91,92] These complex natural products showed promising biological properties, including PKC activation, tumour promotion, skin irritancy, nerve growth factor elevation, and others. Recently, two of iridals (**44** and **45)** have been reported with selective binding affinity for PKCα-C1 domain (K_i values of 84 nM and 76 nM respectively).[93] Recent studies revealed that the iridals are less affected by multi-drug resistance expressing cell lines than doxorubicin and paclitaxel.[94] Arseniyadis and co-worker reported the first total synthesis of an iridal (**46**) in 20 steps (*Figure 2.3.5*).[95]

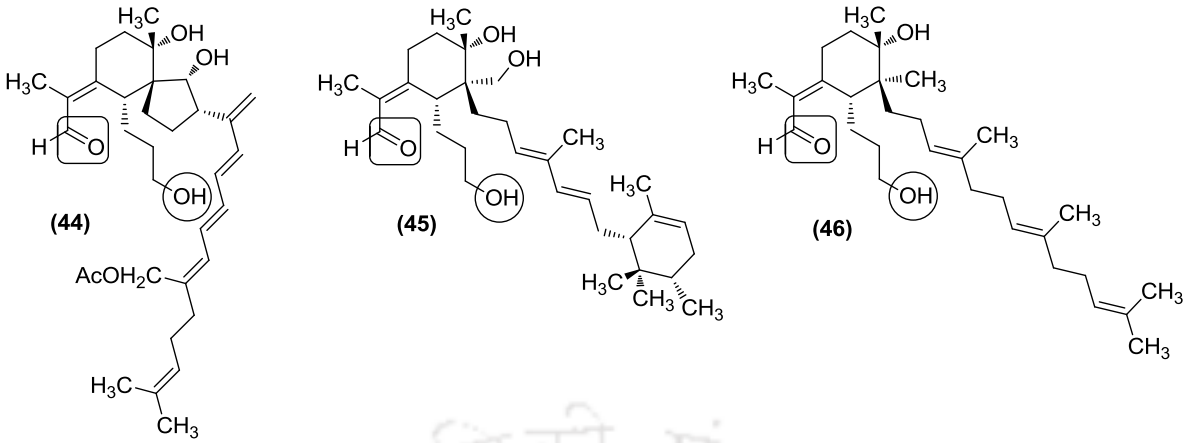

Figure 2.3.5: *Structures of iridals (**44-46**). Functional groups that interact with the C1 domain are highlighted.*

DAG-lactones

Recent studies on PKC-natural product interactions, clearly pointed out that PKC recognize ligands because of the presence of selective pharmacophores within the interatomic distance and hydrophobicity associated with the ligand surface. Blumberg and Marquez groups designed a series of conformationally constrained DAG-lactone derivatives as PKC activators, using simpler DAG (**4**) structure. These compounds are synthetically accessible containing all the required pharmacophores for their interaction with the C1 domain and the constrained structure reduce the entropic penalty caused by flexible DAG (**4**) upon binding to the C1 domain.[36,96,97] The DAG-lactones have stronger binding affinity than DAG, but weaker binding affinity than phorbol esters. To understand the role of hydrophobic group in PKC-C1 domain binding they prepared DAG-lactones with several lipophilic side chains such as the acyl- and alkylidene groups (**47**-**50**, *Figure 2.3.6*).[97] They also reported that (2R)-enantiomer of compound **47** specifically interacts with PKCα isoform (K_i value increased up to 1.45 nM).[98] The optically pure (2*R*)-DAG-lactones were prepared within 11 linear steps; whereas the synthesis of many natural products required more number of reaction steps. DAG γ-lactones have two binding mode such as "*sn-1*" and "*sn-2*" mode for the C1 domain (*Figure 2.3.6*).[98,99] The molecular docking analysis of DAG-lactones revealed that, in the "*sn-1*" mode the acyl group of lactones was forming hydrogen bond with Gly253 of PKC C1 domain whereas alkylidine functional group was pointing towards the lipid membranes.

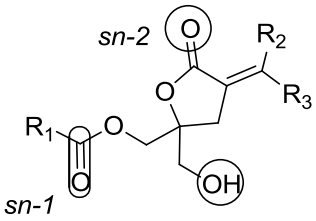

R_1 = *t*-Bu, R_2 = $CH_2CH(i\text{-Bu})_2$, R_3 = H (**47**)
R_1,R_2 = $CH_2CH(i\text{-Pr})_2$, R_3 = H (**48**)
R_1 = 4-(Me_2N)Ph, R_2 = 4-(NO_2)Ph, R_3 = H (**49**)
R_1 =$CH_2CH(i\text{-Pr})_2$, R_2 = $CH_2(i\text{-Pr})_2$, R_3 = H (**50**)

Figure 2.3.6: *Structures of synthetic DAG-lactones (**47-50**). Functional groups that are thought to interact with the C1 domain are highlighted.*

The hydroxyl group of DAG-lactones was hydrogen bonded with Thr242 and Leu251of C1 domain same as C20 hydroxyl group of phorbol ester (**5**). Additionally, in the "*sn-2*" mode the carbonyl functional group of lactones ring hydrogen bonded with Gly253 of C1 domain and the alkyl chain of the acyl group was pointed to the lipid membranes whereas the hydroxyl group is hydrogen-bonded to Thr242 and Leu251. However, many DAG-lactones have shown the selective binding with the mixture of PKC isoenzymes.[100,101] The compound **49** showed selective binding affinity with a mixture of C1 domain of PKC isoforms.[101] However, when the compound **49** interacted with PKCδ the K_i values of the isolated C1a and C1b domain were 2780 and 1.78 nM, respectively. Whereas, compound **49** interacted with the PKCα with K_i values of the C1a and C1b domain were 610 and > 10000 nM, respectively.[36]

It is also reported that, several DAG-lactones have shown antiproliferative and proapoptotic activity, especially **47** and its pure enantiomer of (2R)-**47** exhibited proapoptotic activities in lymph node carcinoma of the prostate (LNCaP) cells.[102,103] In addition, the DAG-lactones **47** and **50** have also shown to be active in HIV-1 eradication, in *ex vivo* culture experiments.[104] The structural analysis of these reported C1 domain ligands clearly showed that most of them contain at least one ester group, which is considered one of their major pharmacophores.

2.4. General Methods for the Synthesis of Hydroxyl Group Bearing Esters

Over the years several strategies have been developed for the chemoselective synthesis of esters, which include Lewis acid catalysts,[105-111] imidazole carbamates,[112] DCC/DMAP reaction,[113] triphenylphosphene, iodine conditions such as Mitsunobu reaction and Garegg-Samuelsson reaction.[112,114] However, only few methods can be used for the synthesis biological active esters. Some of them we showed below.

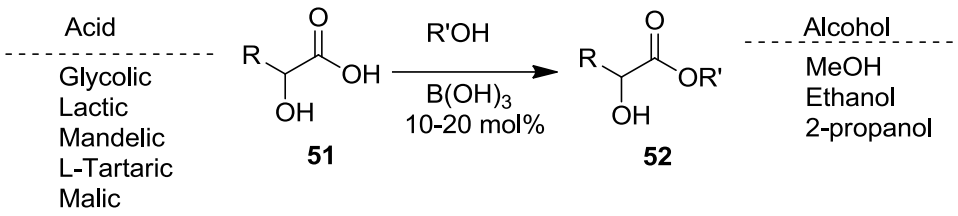

Scheme 2.4.1: *Boric Acid Catalyzed Chemoselective Esterification of α-Hydroxycarboxylic Acids*

Houston and co-worker reported the chemoselective esterification of α-hydroxyl carboxylic acids in the presence 10-20 mol% of boric acid at mild temperature (*scheme 2.4.1*). This method successfully converted several α-hydroxycarboxylic acids into their methyl esters in presence of excess of MeOH in good yield, whereas secondary alcohols yields were moderate.[105]

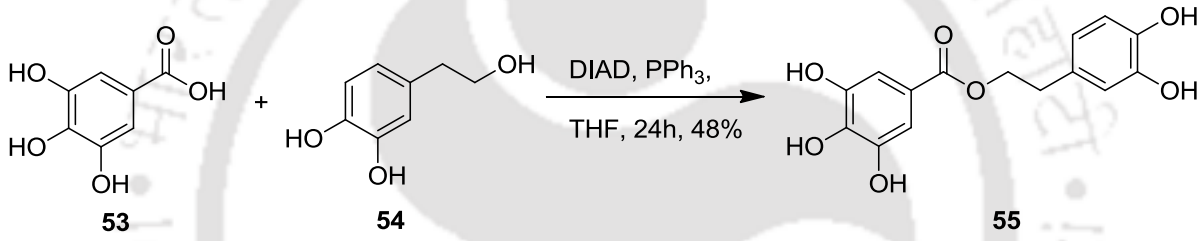

Scheme 2.4.2: *Chemoselective Esterification based on the Mitsunobu reaction*

Mitsunobu reaction is one the most effective method in the literature for the selective esterification of carboxylic acids. Appendino and co-workers demonstrated the selective esterification between Phenolic alcohol and phenolic acid under Mitsunobu reaction conditions in 48% of yield (*Scheme 2.4.2*). This method has shown broad application in the modern organic synthesis.[107]

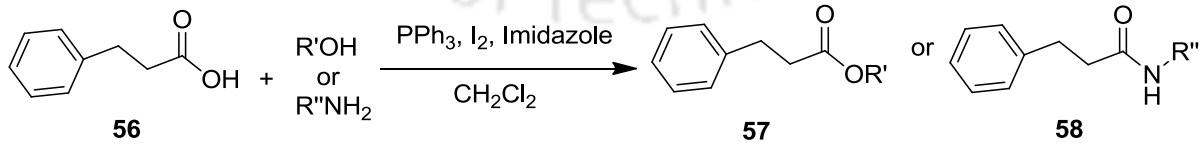

Scheme 2.4.3: *Chemoselective Esterification based on the Garegg-Samuelsson Reaction*

Recently, Rafael Robles and co-workers explored a mild and selective esterification of carboxylic acids based on the Garegg–Samuelsson reaction conditions in the presence of triphenylphosphine, iodine, and imidazole as shown in *Scheme 2.4.3.*[114]

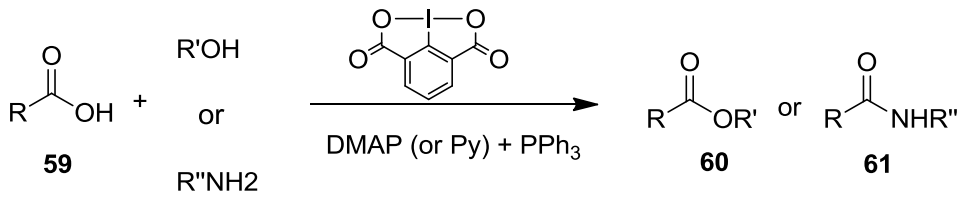

Scheme 2.4.4: *Hypervalent Iodine (III) Reagent Iodosodilactone Catalysed Esterification.*

In addition, Chi Zhang and co-workers demonstrated using hypervalent iodine reagent iodosodilactone as an efficient regenerated coupling reagent for direct esterification/amidation with triphenylphosphine and 4-dimethylaminopyridine (*scheme 2.4.4*). This process successfully achieved for the synthesis of macrocyclic lactones, amides, as well as peptides without racemization.[115]

In a similar approach Selva and co-workers reported chemoselective esterification of hydroxyl group bearing carboxylic acids (**62** and **64**) using dimethyl carbonate (DMC) and catalytic amount of NaY faujasite at 165°C in good yield (*scheme 2.4.5*). [116a]

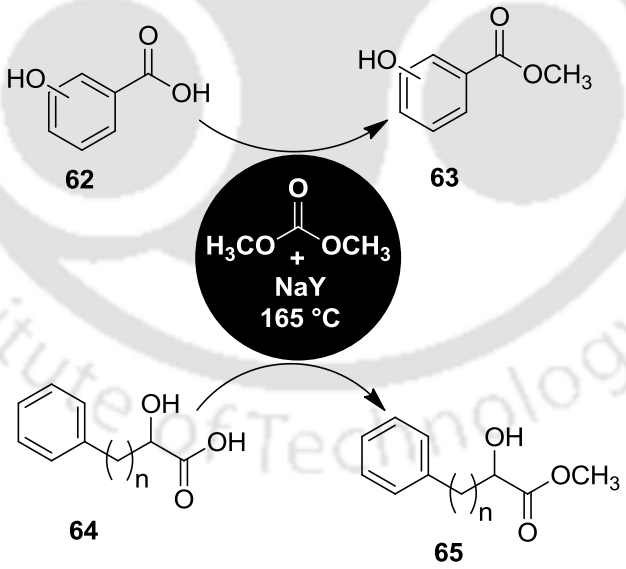

Scheme 2.4.5: *NaY Catalysed Esterification of Hydroxyl Group Bearing Carboxylic Acids.*

Muraleedharan and co-worker reported the chemoselective esterification of carboxylic acids as well as deprotection of Boc/THP/TBDMS groups in the presence of catalytic amount of $SmCl_3$ in a good yield (Scheme 2.4.6).[116b] Further, Appendino and co-workers described $CeCl_2$ catalyzed chemoselective esterification (Scheme 2.4.6).[116c] Yamamoto and co-workers established the N-polystyrene-bound 4-boronopyridinium chloride as reusable catalyst for the chemoselective esterification of carboxylic acids (Scheme 2.4.6).[116d]

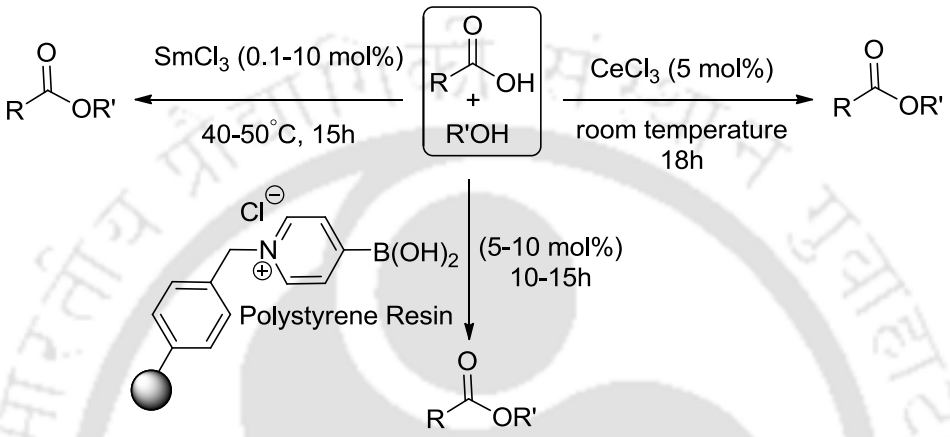

Scheme 2.4.6: *Lewis Acids Promoted Chemoselective Esterification Methods*

In addition, Mashima and co-workers demonstrated the enzyme like tetranuclear zinc cluster $[Zn_4(OCOCF_3)_6O]$ and alkoxy-bridged dinuclear Cobalt complex $[Co_8(OCO^tBu)_{12}O_2]$ promoted chemoselective transesterification methods in the presence of alkyl amines (Scheme 2.4.7).[116e,f]

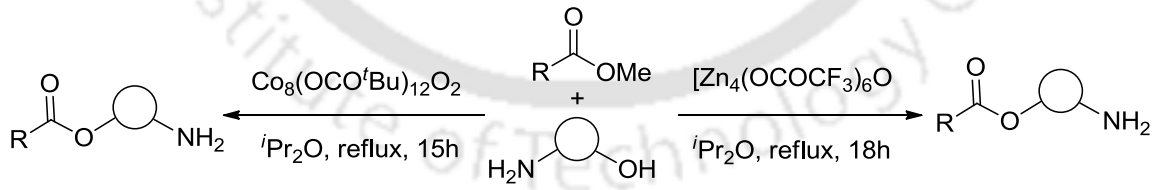

Scheme 2.4.7: *$Zn_4(OCOCF_3)_6O$ and $Co_8(OCO^tBu)_{12}O_2$ Promoted Chemoselective Esterification.*

Concluding Remarks

In general, PKC family of enzymes activate the target protein by phosphorylating the serine and/or threonine residues. Therefore, PKC enzymes plays an important role in several physiological and pathophysiological events including, malignant transformation, cell proliferation, differentiation, and cancer, diabetes, stroke, heart failure and Alzheimer's disease. Recent studies showed that the PKC dependent cellular functions can be controlled by activating its DAG-responsive C1 domains. There are many natural compounds (e.g. bryostatin 1 (**25**) and PEP005 (**20**)) that show potent binding to the C1 domain of PKC enzymes. The C1 domain binding ligands can be obtained from natural sources, but the isolated yields are usually very low with a need to be produced from sensitive ecosystems such as seas and oceans.

In addition, the compounds often have highly complex structures and therefore the total syntheses of the compounds are laborious. However, studies with these compounds have yielded valuable pharmacophores, which have been used to develop structurally simplified synthetic analogues of the complex natural compounds. For example, several research groups have achieved in simplifying the chemical structure of the natural bryostatins and those derivatives showed better potency than natural bryostatins. In addition, by using the pharmacophors of phorbol ester, newly designed compounds showed increased binding affinities for the PKC as well as decreased the reaction steps. However, the biological potential of synthetic ingenols has been shown disappointing; but the discovery of new naturally occurring ingenols is encouraging. Ingenol angelate (PEP005, **20**) has been shown to be a potential treatment of skin tumors and PEP008 (**24**), another naturally occurring ingenol derivative, has only recently been reported to arrest the growth of a variety of solid tumors *in vitro*. Moreover, synthesized indo- and benzolactam derivative have also shown a potent binding to the C1 domain of PKC as well as potent drug candidates against the cancer. In addition, conformationally constrained DAG-lactone derivatives are another family of potent C1 domain ligands that depict a good correlation between the synthetic small molecules and PKC activity. This suggests that synthesis of C1-domain targeted small molecules is very important in developing PKC regulators. Most of the reported PKC-C1 domain ligands have ester subunits, as an essential pharmacophore within their complex structure. However, due the structural complexity of these ligands, regular esterification does not work efficiently. In this regard mild and selective esterification methods are required for the synthesis of such biologically active molecules.

CHAPTER 2

Design, Synthesis and Protein Binding Properties of Diacyltetrol Lipids

This chapter describes rational design and synthesis of diacyltetrol lipids (DATs) from (+)-diethyl L-tartrate as starting material. It illustrates detailed *in-vitro* binding properties of DAT lipids with C1b subdomain of PKCδ and PKCθ by using the fluorescence techniques. The molecular docking analysis provides the binding orientation of diacyltetrol lipids within the C1 domain binding site.

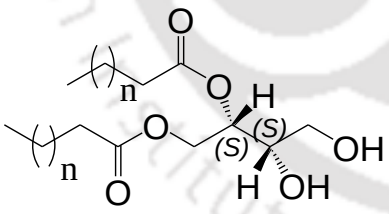

4b (n = 6)

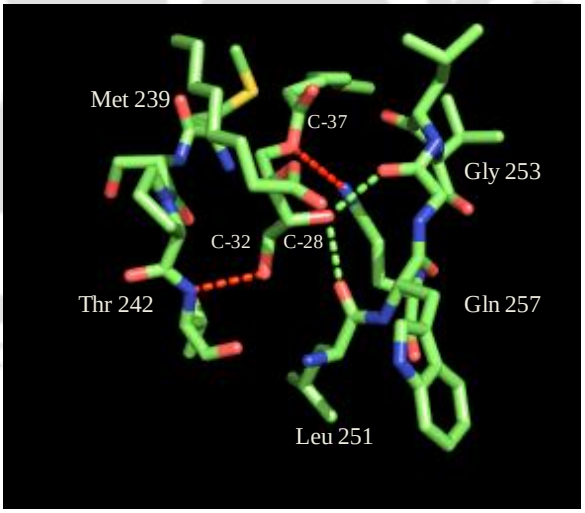

2.1. Background and Focus of the Present Work

PKC family of serine/threonine kinases is a major cellular receptor for DAG/phorbol esters. PKC isoenzymes play an important role in pathology of several diseases such as cancer, diabetes, stroke, heart failure and Alzheimer's disease.[11,23,117,118] Therefore, PKC isoforms particularly in the cancer field have been a subject of intensive research and drug development.[7] The PKC isoforms are activated by DAGs and transmit their signal by phosphorylating specific proteins. The DAG/phorbol esters selectively interact with the proteins containing a C1 domain. This interaction induces their translocation to the discrete subcellular compartments. For some of the C1 domain containing proteins, such translocation leads to activation.[11,119,120] Therefore, C1 domains have become an attractive target in designing selective PKC ligands.[58,119,121]

A number of structurally complex and rigid natural compounds such as phorbol esters,[122] bryostatins,[123] teleocidins,[87] aplysiatoxins,[124] ingenols,[67] and others is reported to interact with the DAG binding C1 domain containing proteins. Recently reported novel PKC isoforms specific indolactam[86] and benzolactam[85] derivatives are also structurally complex. Therefore, modification and large-scale production of these structurally complexes are quiet challenging. Some of these reported compounds have very strong affinity for C1 domains (~ 1000 fold stronger) in comparison with the flexible, natural DAG agonists. The family of conformationally constrained DAG-lactones overcomes the spread in potency between the natural product ligands and DAG.[96,97,125-127] Therefore, there is a clear and unmet need to design simple surrogates, whose structure could be easily modified to achieve higher specificity and selectivity among the C1 domains of the PKC isoforms. This chapter describes the synthesis and binding properties of a novel class of tetrol based lipids, diacyltetrols (DATs), to the C1b subdomains of PKCδ and PKCθ. The measured binding parameters showed that DATs interact with the C1b subdomains of PKC isoforms through the DAG or phorbol ester binding site and forms hydrogen bonds with the residues at the activator binding site. The results clearly suggest that the positions of two hydroxyl groups play an important role in recognizing C1 domains of PKC isoforms.

Design of Tetrol Based C1 Domain Ligands— The structures of C1 domain binding natural product ligands revealed the presence of more than one hydroxyl group. For example, the phorbol esters interact with the C1 domain through two hydroxyl groups including the other functionalities.[128,129] The X-ray structure of phorbol-13-O-acetate bound PKCδ C1b shows

that the hydroxyl groups attached to C-20 and C-4, including the carbonyl group on C-3, form hydrogen bonds with the protein residues.[129] This leads us to develop diacyltetrols (DATs) containing two of the phorbol ester pharmacophores, the hydroxyl and the carbonyl functionalities within the same molecule. The DATs have very high structural similarity to the natural diacylglycerols (DAGs). The lipids **1**, **3** and **4** contain at least one hydroxymethyl group just as DAGs, whereas compound **2** have only two hydroxyl groups (*Figure 2.1.1*).

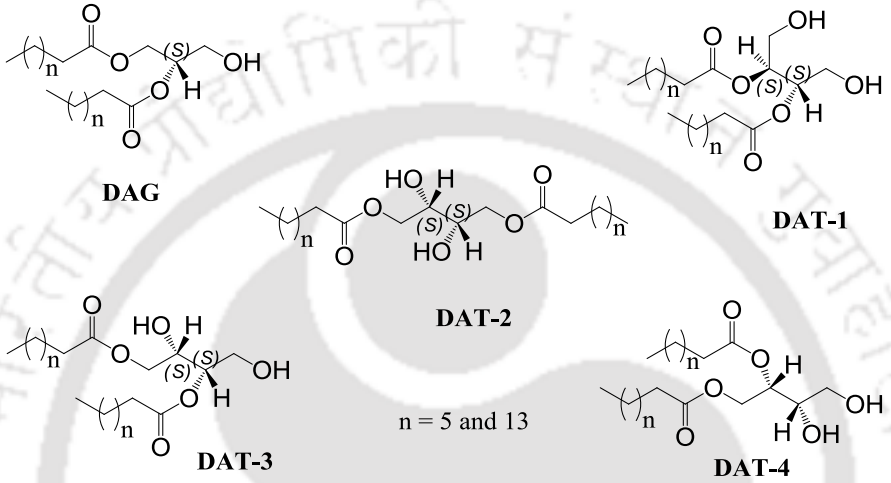

Figure 2.1.1: *Structure of DAG and synthesized tetrol based C1 domain ligands*

The positions of the hydroxyl groups were varied to get more insight on which two hydroxyl groups would be better anchored to the binding pocket of the C1 domain. The presence of an additional hydroxyl group also gives us the opportunities for further development of PKC isoforms specific and selective tetrol based ligands. The lipids were synthesized from commercially available (+)-diethyl L-tartrate. The C2 symmetric (+)-diethyl L-tartrate was used to avoid mixing of enantiomeric products during synthesis. The choice of stereochemistry of lipids is crucial, as the diversity of stereochemistry of these structures complicates the specificity. The (+)-diethyl-L-tartrate provides the stereochemistry as there in natural DAGs at the sn-2 position. The tetrol based lipids 1,4-dihydroxy-diacyltetrol (**1**), 2,3-dihydroxy-diacyltetrol (**2**), 1,3-dihydroxy-diacyltetrol (**3**) and 1,2-dihydroxy-diacyltetrol (**4**) were synthesized in four to seven steps from the starting material. DATs with long (palmitic acid) and short chain (octanoic acid) fatty acids were synthesized in order to study the impact of hydrophobicity on the binding affinity.

Synthesis of Diacyltetrols— The DAT analogues were synthesized via a modified reported reaction protocol using commercially available (+)-diethyl L-tartrate (*Scheme 2.1.1*) as the starting material. The DAT analogs **1a** and **1b** were first synthesized to explore the role of two hydroxymethyl groups of the same molecule in binding with the PKC-C1 domains. The cyclopentylidene acetal[130,131] was first introduced into diol of (+)-diethyl L-tartrate (**5**) and then reduction of ester of fully protected tartrate analogue **6** by 2.2 equiv of lithium aluminium hydride[132] resulted in bishydroxymethyl compound **7** in 78% yield (two steps).[131] Subsequently, dibenzylation[133] of compound **7** and cautious elimination of the cyclopentylidene acetal under mild acidic conditions yielded diol **9** in 68% yield (two steps).

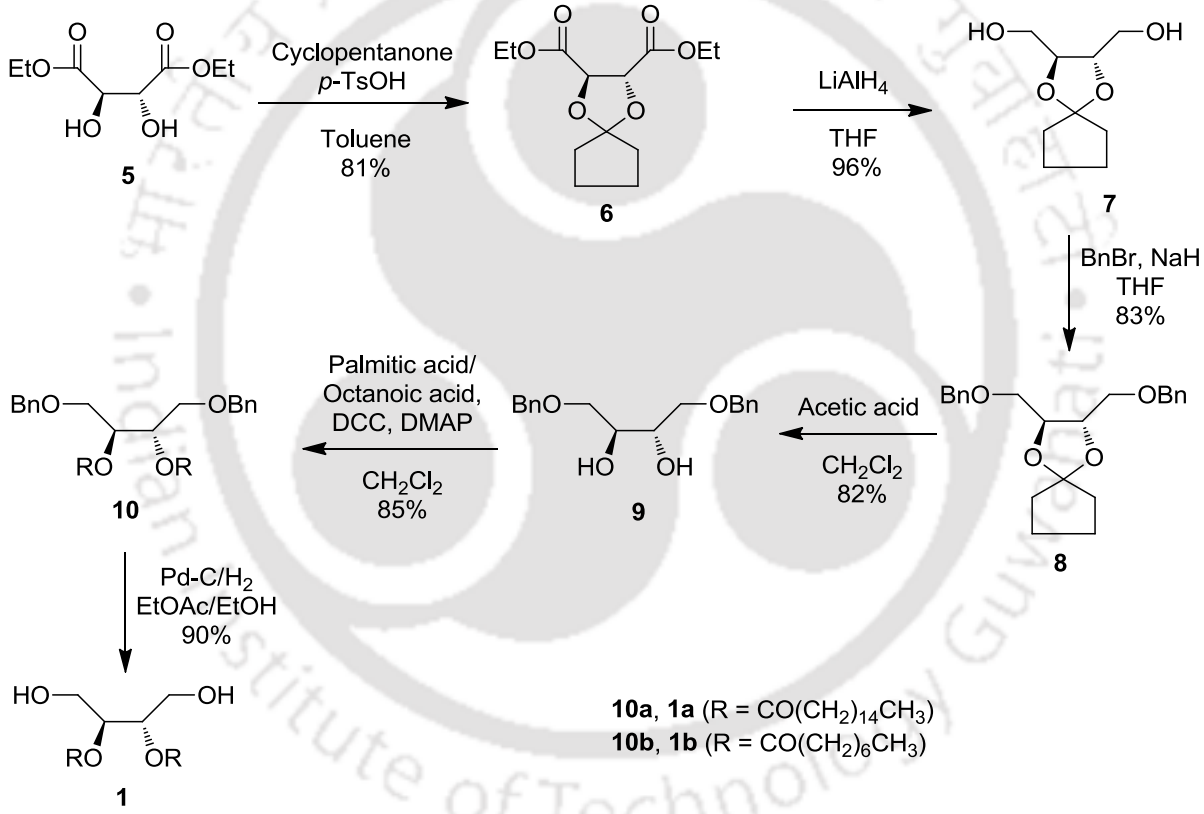

Scheme 2.1.1: *Synthesis route to 1,4-dihydroxy-diacyltetrol (**1**).*

After that acyl chains were introduced into **9** using a model DCC-mediated coupling method[134] with commercially available palmitic acid and octanoic acid to yield **10a** and **10b**, respectively, in 85–90% yield. In the end, the benzyl groups were separated using 0.1 equiv. of 10% Pd–C under hydrogenation environment[135] to produce compound **1a** and **1b** in 90% yield. To identify the role of two hydroxymethyl groups in binding with the PKC-C1 domain, compound **2a** and **2b** with two hydroxyl groups were synthesized. The DAT analogs **2a** and

2b were prepared from the bishydroxymethyl intermediate **7** (*Scheme 2.1.2*). DCC-mediated coupling reaction[134] of compound **7** with palmitic acid and octanoic acid yielded **11a** and **11b** respectively, in 80–85% yield. Deprotection of the cyclopentylidene acetal under mild acidic environment produced compounds **2a** and **2b** in 82% yield.

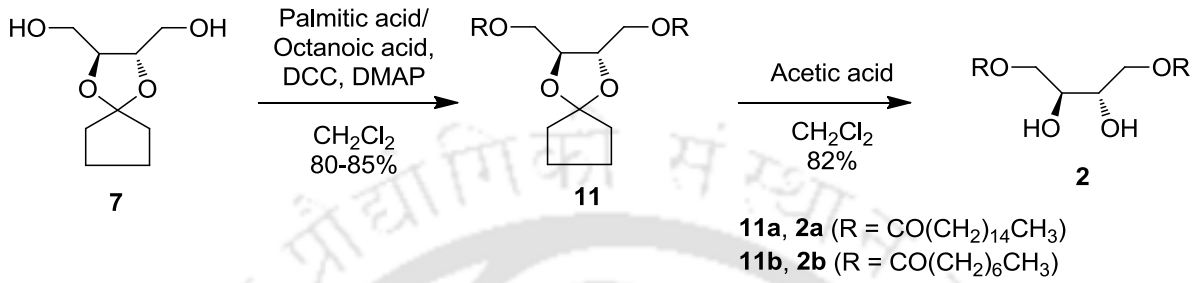

Scheme 2.1.2: *Synthesis route to 2,3-dihydroxy-diacyltetrol (**2**).*

For better understanding of the usefulness of both hydroxyl and hydroxymethyl functional groups in their binding with the PKC-C1 domains, compounds **3** and **4** including hydroxyl and hydroxymethyl functional groups at 1,3 and 1,2 positions, respectively were also synthesized (*Scheme 2.1.4*).

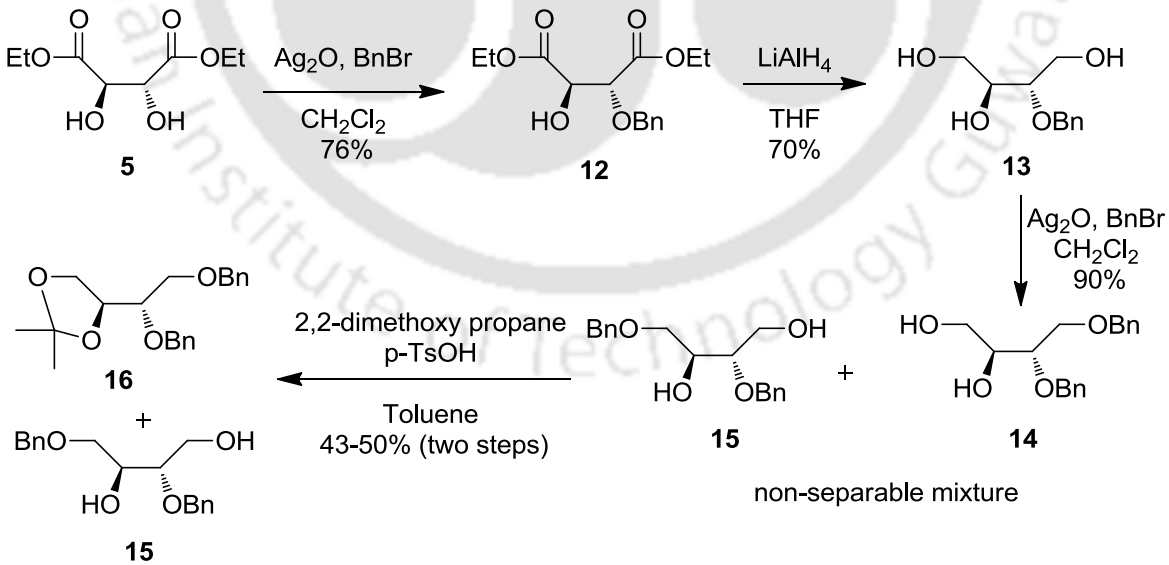

Scheme 2.1.3: *Synthesis route to (2S,3S)-2,4-bis (benzyloxy)butane-1,3-diol (**15**) and (S)-4-((S)-1,2-bis(benzyloxy)ethyl)-2,2-dimethyl-1,3-dioxolane (**16**).*

For the synthesis of compound **3** and **4**, (+)-diethyl L-tartrate (**5**) was first mono-protected with the benzyl group using 1.5 equiv. of Ag_2O in anhydrous dichloromethane[136] and additional ester reduction by 2.5 equiv. of lithium aluminium hydride resulted compound **13** (in 63%yield, two steps). Benzylation of compound **13** using 1.5 equiv. of Ag_2O in anhydrous dichloromethane[136] produced a mixture of 1,2-diol (**14**) and 1,3-diol (**15**) compounds as the main products (*scheme 2.1.3*). Regioselective reaction of the mixture of compound **14** and **15** via acetonide formation[130,132,137] produced compound **16** (44% yield, two steps) and compound **15** (43% yield, two steps). The acyl chains were then introduced into **15** using the model DCC-mediated coupling method[134] with palmitic acid to produce **17a** and octanoic acid to yield **17b**. Removal of benzyl groups from **17a** and **17b** using 0.1 equiv. of 10% Pd–C under hydrogenation environment yielded compound **3a** and **3b** in 77–91% yield.[135] Deprotection of benzyl groups from **16** and subsequent esterification yielded compound **19**[134] in 81-84% yield. Finally, cautious removal of the acetonide group from **19** using 80% acetic acid (aqueous solution) in dichloromethane resulted compound **4a** and **4b** in 75% yield.

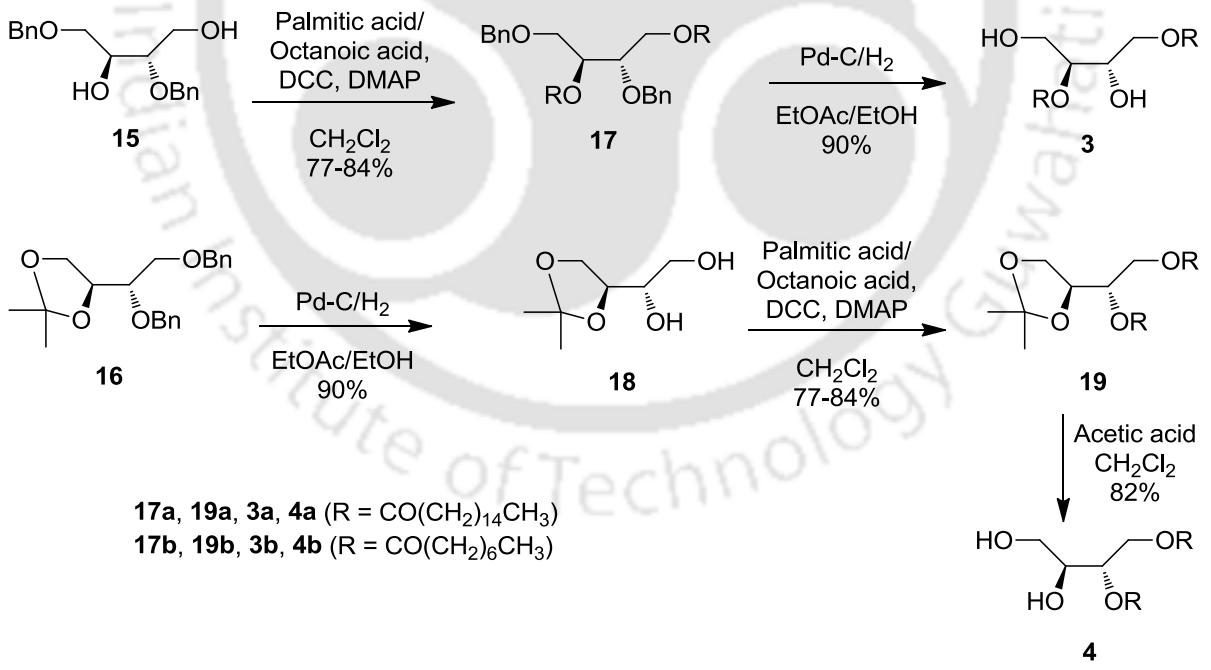

Scheme 2.1.4: *Synthesis route to 1,3-dihydroxy-diacyltetrol (**3**) and 1,2-dihydroxy-diacyltetrol (**4**).*

Measurement of Protein Binding Parameters ─ Intrinsic fluorescence is extensively used as a tool to observe changes in protein conformation and to depict conclusion regarding their local structure and dynamics. The inherent fluorescence of the PKC-C1b subdomains is because of the presence of a Trp (Trp-252 in delta, and Trp-253 in theta) and Tyr residues (Tyr-236 and Tyr-238 in PKCδ, Tyr-249 and Tyr-251 in PKC-θ). The alteration in conformation or microenvironment of the proteins caused by ligands can be measured by fluorescence spectroscopy. The binding affinity of diacyltetrols (DATs) and diacylglycerols (DAGs) for PKC-C1b subdomains was measured by Trp-fluorescence quenching method and the EC_{50} value was calculated using the Hill equation. The representative plot of ligand dependent PKCδ-C1b fluorescence quenching values were shown in Figure 2.1.2. The calculated EC_{50} values showed that compound **4** with different alkyl chain lengths interact with the PKCδ-C1b subdomains with stronger affinity (3.08-4.85 μM), whereas the other compounds had comparable affinity for both the proteins (*Table 2.1.1*).

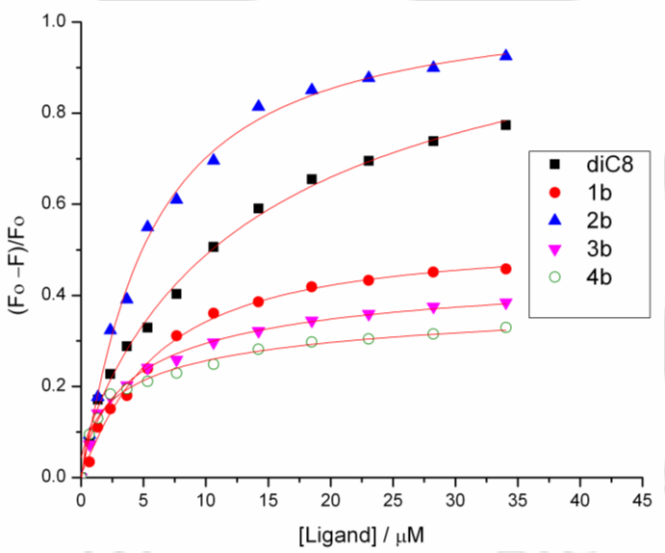

Figure 2.1.2: *Binding of ligands with PKCδ C1b. Representative plot of fluorescence intensity of PKCδ C1b (2 μM) in buffer (50 mM Tris, 150 mM NaCl, 50 μM $ZnSO_4$, pH 7.4) in the presence of varying concentration of* ***DAG$_8$*** *(■),* ***1b*** *(●),* ***2b*** *(▲), 3b (▼) and* ***4b*** *(○), where F and F_0 are fluorescence intensity in the presence and absence of the ligand, respectively. Solid lines indicate the fit using Hill equation.*

It is also essential to mention that the calculated EC_{50} values of DAG_{16} and DAG_8 are in agreement with the reported results.[138] The results also show that compound **4b** have 3.1-fold and 1.7-fold stronger binding affinity for PKCδ-C1b and PKCθ-C1b protein, respectively than the DAG_8.

Table 2.1.1: *EC_{50} values for the binding of DAGs and DATs with the PKCδ C1b and PKCθ C1b proteins[a] at room temperature.*

Compound	EC_{50} (μM)		xLogP3
	PKCδ C1b	PKCθ C1b	
DAG_{16}	6.68	7.59	14.04
1a	4.29	3.70	13.42
2a	4.92	4.63	13.42
3a	3.72	3.21	13.42
4a	3.34	3.08	13.42
DAG_8	15.39	6.12	5.11
1b	5.89	4.15	4.49
2b	5.29	4.98	4.49
3b	5.07	4.03	4.49
4b	4.85	3.59	4.49

[a]*Protein concentration is 2 μM in buffer (50 mM Tris, 150 mM NaCl, 50 μM $ZnSO_4$, pH 7.4)*

The binding parameters also point out that DATs have superior binding affinity for PKCθ-C1b than to the PKCδ-C1b, probably because of the additional hydrogen bond formation. Overall, the DATs have stronger binding affinity for the PKC-C1b subdomains than natural DAGs, possibly due to the existence of an additional hydroxyl group within the DAT compounds. A similar Trp-fluorescence quenching based binding analysis of the long chain DAT compounds were also performed to understand the essentiality of hydrophobicity for their PKC-C1 domain interactions. The calculated EC_{50} values showed that both the C1b subdomains showed a similar dependency on the hydrophobicity for all the compounds (*Table 2.1.1*). The compound **4a** with XLOGP3 value of 13.42 showed the highest affinity of 3.08 μM. It is important to mention here that for compound **2a** and **2b** although the binding affinity difference among them is negligible but they have a clear difference in the hydrophobicity values. This abnormality could be due to the ligand binding orientation within the pocket. The octanol-water partition coefficients for all compounds were calculated using the program XLOGP3.Steady-state fluorescence anisotropy measurements of the proteins in the presence or absence of ligands were performed to obtain more information about their DAT binding capability.

The anisotropy values of the PKCθ-C1b subdomain increased from 0.05529 in buffer to 0.10959, 0.11008, 0.11620 and 0.12634 in presence of excess (10-fold) compounds, **1b**, **2b**, **3b** and **4b** respectively (*Table 2.1.2).* A similar increase in anisotropy values were also observed for PKCδ-C1b subdomain in presence of excess (10-fold) compounds. The anisotropy values of the proteins also increased in presence of DAGs.[138] This measurement indicate that the DAT compounds increase the rigidity of the surrounding environment of the protein in a similar manner to that of DAGs.

Table 2.1.2: *Anisotropy[a] values of DATs and DAGs in the presence and absence of the PKCδ and PKCθ C1b proteins at room temperature.*

Compound	PKCδ C1b	PKCθ C1b
Buffer[b]	0.05793 (0.0056)	0.05529 (0.0032)
DAG_{16}[c]	0.10282 (0.0061)	0.07268 (0.0037)
1a[c]	0.10434 (0.0064)	0.08161 (0.0049)
2a[c]	0.10971 (0.0058)	0.07754 (0.0035)
3a[c]	0.11389 (0.0049)	0.08333 (0.0043)
4a[c]	0.12106 (0.0054)	0.09531 (0.0058)
DAG_8[c]	0.09777 (0.0063)	0.10693 (0.0051)
1b[c]	0.10339 (0.0053)	0.10959 (0.0072)
2b[c]	0.10014 (0.0055)	0.11008 (0.0089)
3b[c]	0.10027 (0.0052)	0.11620 (0.0078)
4b[c]	0.10459 (0.0049)	0.12634 (0.0089)

*[a)]Values in the parenthesis indicate standard deviations. [b)]Protein, 2 μM in buffer (20 mM Tris, 160 mM NaCl, 50 μM $ZnSO_4$, pH 7.4). [c)]**DAG, 1, 2, 3** and **4**, 20 μM; protein 2 μM in buffer (20 mM Tris, 160 mM NaCl, 50 μM $ZnSO_4$, pH 7.4).*

To investigate the protein binding properties of the compounds under liposomal environment, Trp-based fluorescence quenching assay was performed using long chain DAT compounds (*Figure 2.1.3*). The measured binding parameters indicate that compound **4a** shows strong binding affinity for the PKC-C1 domains (*Table 2.1.3*). The measured values showed that compound **4a** has 2.4 and 3.6 fold stronger binding affinity for PKCθ-C1b and PKCδ-C1b, respectively than DAG_{16} under the similar experimental conditions. These measurements suggest that the DATs bind to the PKC-C1b subdomains in a similar manner as of DAGs.

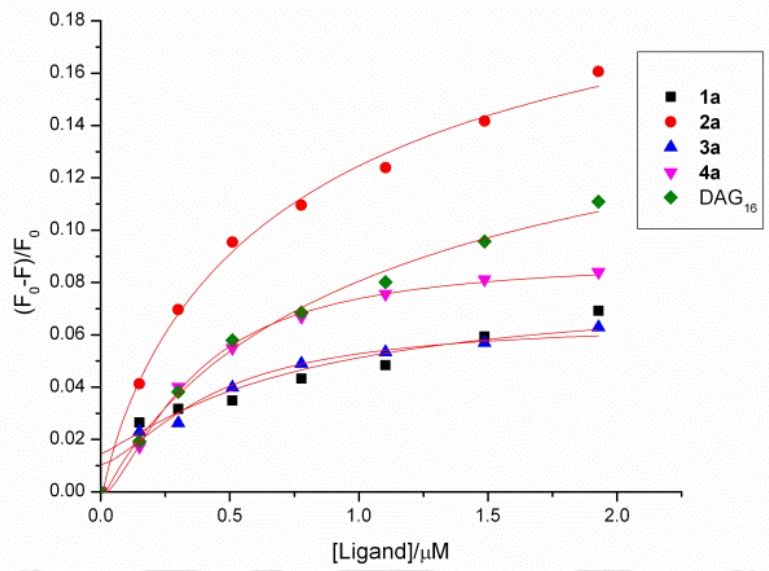

Figure 2.1.3: *Binding of liposome containing ligands with PKCδ-C1b. Representative plot of fluorescence intensity of PKCδ-C1b (500 nM) in buffer (50 mM Tris, 150 mM NaCl, 50 μM $ZnSO_4$, pH 7.4) in the presence of varying concentration of liposome containing* ***1a*** *(■),* ***2a*** *(●),* ***3b*** *(▲),* ***4a*** *(▼) and DAG16 (◆), where F and F_0 are fluorescence intensities in the presence and absence of ligand, respectively. Solid lines indicate the fit using Hill equation.*

Table 2.1.3: *EC_{50} values for the binding of DATs (**1a**–**4a**) and DAG_{16} containing liposomes[a] with the PKCδ-C1b and PKCθ-C1b proteins[b] at room temperature*

Compound	EC_{50}/nM	
	PKCδ C1b	PKCθ C1b
1a	0.76	0.81
2a	0.80	0.89
3a	0.44	0.58
4a	**0.35**	**0.48**
DAG_{16}	*1.25*	*1.16*

[a]Liposome composition, PC/PS/Ligand16 (80 -x : 20 : x, where x = 0-10). [b]Protein (0.5 μM) in buffer (50 mM Tris, 150 mM NaCl, 50 mM $ZnSO_4$, pH 7.4).

Competitive binding analysis was performed to prove that DATs interact with the PKC-C1b subdomains through the same DAG/phorbol ester binding site (*Figure 2.1.4*). Therefore, fluorescence-based binding assays confirm that PKC-C1b subdomains interact with the synthesized DATs in a lipid free system, as well as under liposomal environment.

The measured results also suggest that the long chain compounds can differentially influence PKC activation and their membrane localization properties. However, the differences in protein binding properties of the DATs are mostly due to the amino acid residues present within the binding pocket and the surface area of the binding pockets. The activating and/or protein binding properties of the synthesized DATs could be lower than the well known phorbol ester or other natural compounds under similar conditions. However, the binding parameters indicate that further modified DATs can interact differentially with the C1b subdomains and their interactions can modulate the PKC protein in an isoform specific manner.

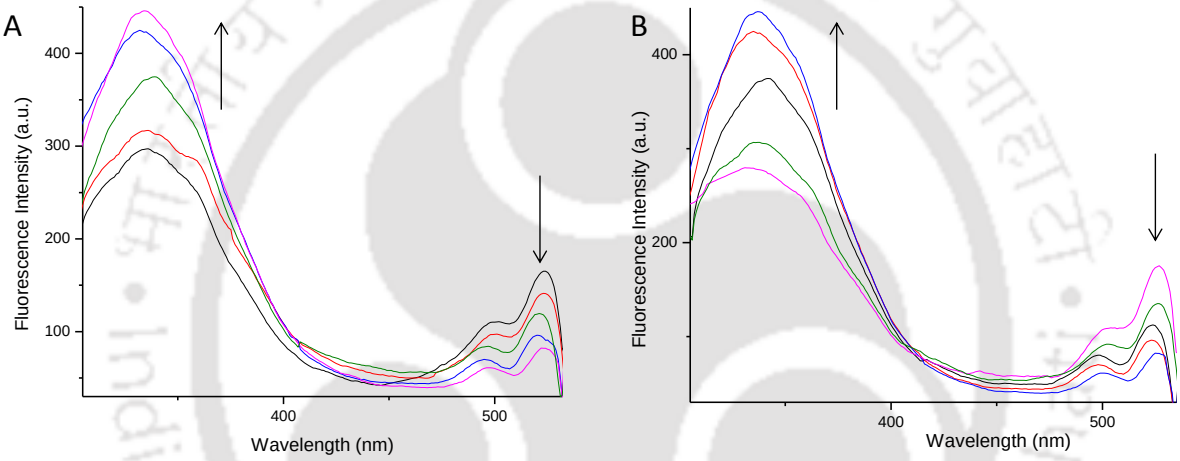

Figure 2.1.4: *Representative plot of competitive binding of DAT* ***4b*** *to PKCδ-C1b (A) and PKCθ-C1b (B) bound DAG containing liposomes. The curve represents the emission spectrum (λ_{ex} =280 nm) of a sample in which the protein (0.5 μM) was added to PC/PE/PS/DAG_{16}/NBD-PE (50:20:20:5:5) liposomes. The decrease in FRET efficiency between Trp residues (of PKCδ and PKCθ C1b subdomains) and NBD, caused by the displacement of protein from labelled liposomes, is demonstrated by the increase in Trp fluorescence (340 nm) and the concomitant decrease in NBD emission (524 nm).*

Molecular Docking Analysis ─The analyzed molecular models of ligand-bound protein revealed the binding orientation of the DATs within the DAG/phorbol ester binding site of the PKCδ-C1b subdomain. The molecular docking analysis were performed using the crystal coordinates of PKCδ-C1b subdomain complexed with phorbol-13-O-acetate (1PTR).[129] Thorough analysis of the model structures revealed that there were three and four probable

hydrogen bonds present among DAG-C1b subdomain and DATs-C1b subdomain docked structures, respectively (*Figure 2.1.5*). The analyzed model structures suggest that hydroxyl and carbonyl functions groups of the DAG_8 are primarily accountable for their interaction with the C1b subdomain.[139]

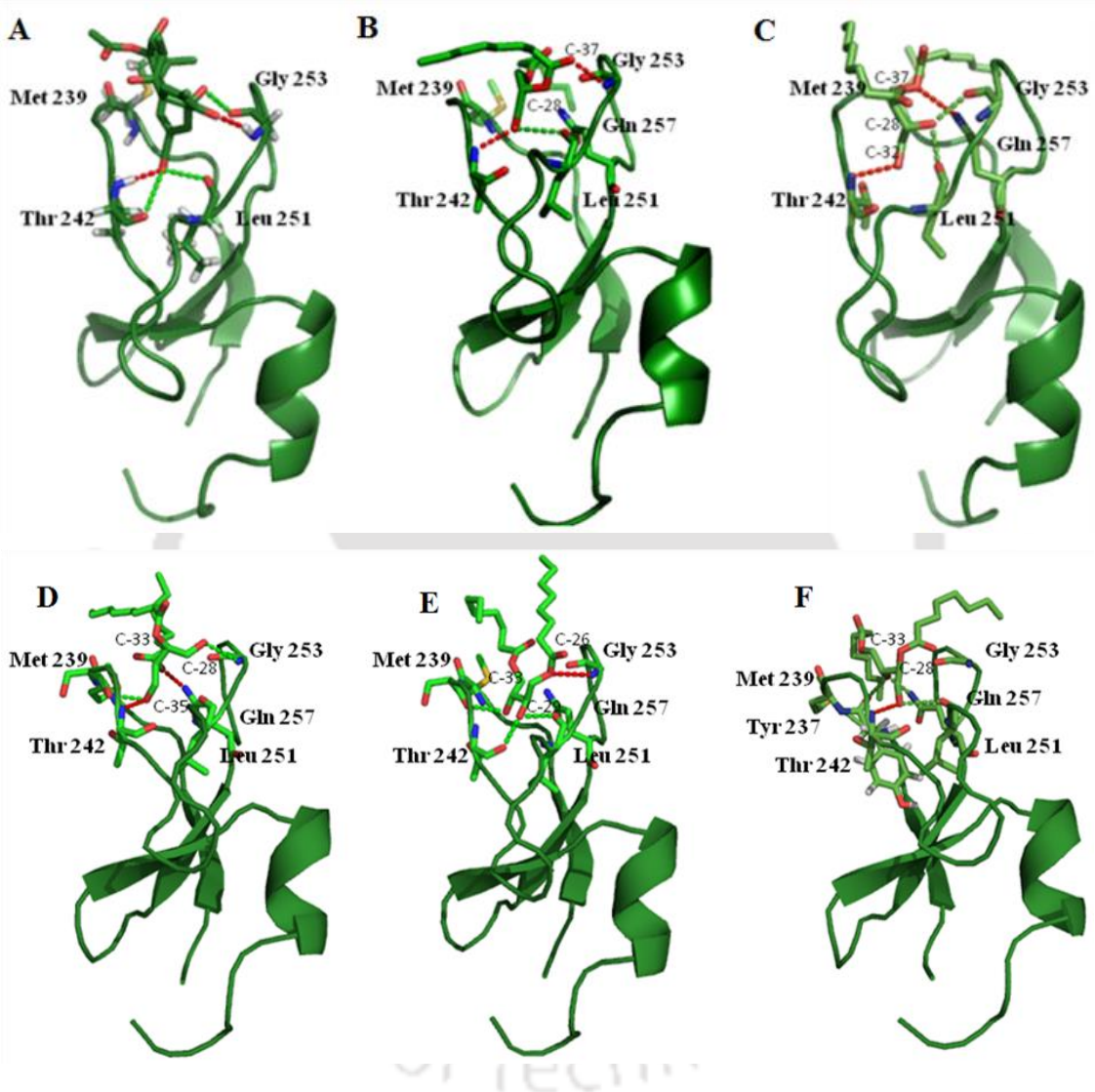

Figure 2.1.5: *Structures of ligand bound PKCδ-C1b subdomain. (A) Crystal structure of phorbol 13-O-acetate bound PKCδ-C1b; (B) modeled structure of DAG_8 docked into PKCδ C1b; (C) modeled structure of (**4b**); (D) modeled structure of (**1b**); (E) modeled structure of (**2b**); (F) modeled structure of (**3b**) docked into PKCδ-C1b. The modeled structures are generated using the Molegro Virtual Docker, version 4.3.0. The oxygen atoms and nitrogen atoms are shown in red and blue, respectively. The dotted line indicates possible hydrogen bonds.*

The hydroxyl group (C-28) of DAG_8 formed hydrogen bond with the carbonyl of Leu-251 and backbone amide proton of Thr-242 residues. In addition, the C-37 carbonyl group of DAG_8 formed hydrogen with the backbone amide proton of Gly-253 residue (*Figure 2.1.5 B*). The model structure also showed that the DATs were interacting with the PKCδ-C1b subdomain in a similar mode, as DAGs/phorbol esters (*Figure 2.1.5 A and B*). The backbone carbonyls and amide proton of the C1b subdomain also interact with the carbonyl and hydroxyl functional groups of DATs. Interestingly, the model structures also showed that DATs could form additional hydrogen bond with the polar amino acids. The backbone amide proton of Thr-242 and Gly-253 and, the carbonyl of Ser-240 form hydrogen bond with C-28 and C-35 hydroxyl groups of compound **1b**. The C-33 acyl pharmacophore of compound **1b** constructed a hydrogen bond with the Gln-257 side chain amine group (*Figure 2.1.5 D*). The compound **2b** also formed hydrogen bonds with the Ser-240, Thr-242 and Leu-251 thorough the C-29 and C-33 hydroxyl groups in a similar fashion. The other hydrogen bond was visualized between C-26 acyl group of **2b** and amide proton of Gly-253 (*Figure 2.1.5 E*). The C-28 hydroxyl functional group of **3b** formed hydrogen bond among the backbone carbonyl of Leu-251and amide proton of Thr-242. Whereas, the Tyr-238 and Gln-257 residues form hydrogen bond with the C-33 hydroxyl functional group of **3b** through the backbone carbonyl group and side chain amine proton, respectively (*Figure 2.1.5 F*). The C-28 hydroxyl functional group of compound **4b** formed hydrogen bond among the backbone carbonyls of Gly-253 and Leu-251. The C-37 ester group and C-32 hydroxyl group of compound **4b** formed hydrogen bond with the Gln-257-side chain amine proton and Thr-242-backbone amide proton, respectively (*Figure 2.1.5 C*).

The measured binding parameters and docking scores acquired from the model analysis do not always substantiate *(Table 2.1.4)*. This difference point out that proteins and compounds can experience conformational alterations under experimental circumstances. The analysis of the molecular models indicates that the strong binding affinity of the compounds **3** and **4** could be due to the structural difference, position of the hydroxymethyl and hydroxyl groups. This structural difference is helping them in anchoring to the binding site which is absent in compound **1** and **2**. Therefore the measured binding parameters of the compounds highlight both the importance of hydrophobicity and binding orientation of the ligands during their interaction with the C1b subdomains.[140] It is presumed that the hydrophobic residues (like Met-239, Phe-243, Leu-250, and Leu-254 for PKCδ C1b) surrounding the DAG/phorbol ester binding site of C1 domains interact with the hydrophobic part of the ligands.

The hydrophobic moiety of the DAT compounds may interact with the lipid bilayer during their interaction with the C1 domains, because the PKC isoenzymes are reported to interact with the lipid bilayer through its C1 domain for enzyme activity and regulation of several cellular pathways.

Table 2.1.4: *Docking score values obtained from the docking of DATs (with short chain length) and DAG_8 into the PKCδ C1b domains using Molegro Virtual Docker, version 4.3.0.*

Compound	Mol Dock score	Rerank score (kcal/mol)
DAG_8	-93.4027	-68.4225
1b	-103.005	-71.3153
2b	-107.654	-65.0598
3b	-100.492	-77.1676
4b	-113.135	-83.6599

Conclusion

In conclusion, this chapter demonstrated the detailed synthesis of diacyltetrols (DATs), and their binding properties with the C1b subdomains of PKCθ and PKCδ. Tetrol based lipids 1,4-dihydroxy-diacyltetrol (**1**), 2,3-dihydroxy-diacyltetrol (**2**), 1,3-dihydroxy-diacyltetrol (**3**) and 1,2-dihydroxy-diacyltetrol (**4**) with long (palmitic acid) and short chain (octanoic acid) fatty acids were synthesized from (+)-diethyl-L-tartrate. Synthesis of these tetrol lipids from the scratch provided the ability to generate pure samples of a single lipid structure and freedom to explore the role of hydroxyl and hydroxymethyl groups at different positions. The binding parameters and molecular docking analysis showed that DATs interact with the C1b subdomain of PKC isoforms through the diacylglycerol (DAG)/phorbol ester binding site and forms hydrogen bonds with the polar residues and backbone of the protein, at the same binding site, as that of DAG and phorbol esters. Compound **4b** with hydroxymethyl and hydroxyl groups at 1 and 2 positions, respectively, showed better binding affinity among the DATs. However, all the DATs with two hydroxyl/hydroxymethyl groups have stronger binding affinity for the C1 domains under the similar experimental conditions. Therefore, DAT molecules can be further used as research tools or lead compounds in PKC based drug development. Undoubtedly, further studies are needed to understand fully the importance of DATs in activation and regulation of PKC isoenzymes. Nevertheless, the present study demonstrates that a combination of experimental and computational approaches can provide valuable insight into the interaction of DATs with C1b subdomains of PKC isoforms.

The stronger C1 domain binding capabilities of DATs with two hydroxyl/hydroxymethyl groups prompted us to design DAT based anionic lipids to obtain better C1 domain binding affinity and PKC isoform selectivity.

2.2. Experimental Sections

2.2.1. Instrumentations and Characterization

All reagents were purchased from Sigma (St. Louis MO) and Merck (Mumbai, India) and used directly without further purification. Dry solvents were obtained according to the reported procedures. Column chromatography was performed using 60-120 mesh silica gel. Reactions were monitored by thin-layer chromatography (TLC) on silica gel 60 F254 (0.25 mm). ^{1}H NMR, ^{13}C NMR, and ^{31}P NMR spectra were recorded at 400, 100, and 162 MHz, respectively using a Varian AS400 spectrometer. Coupling constants (*J* values) are reported in hertz, and chemical shifts are reported in parts per million (ppm) downfield from tetramethylsilane using residual chloroform (δ = 7.24 for ^{1}H NMR, δ = 77.23 for ^{13}C NMR) as an internal standard. ^{31}P NMR spectra were recorded in $CDCl_3$ and calibrated to external standard 85% H_3PO_4. Multiplicities are reported as follows: s (singlet), d (doublet), t (triplet), m (multiplet), and br (broadened). Infrared (IR) spectra were recorded in KBr or neat using a Perkin-Elmer Spectrum One FT-IR spectrometer from 4000 to 450 cm^{-1}. Melting points were determined using a melting point apparatus and are uncorrected. Mass spectra were recorded using a Waters Q-TOF Premier mass spectrometry system, and data were analyzed using the built-in software. Melting points were determined using a Büchi B-545 melting point apparatus and are uncorrected. Optical rotation values were measured at room temperature on a Perkin-Elmer 343 polarimeter. 1,2-dipalmitoyl-sn-glycerol (DAG_{16}), 1,2-dioctanoyl-sn-glycerol (DAG_8), 1,2-dipalmitoyl-*sn*-glycero-3-phospho-L-serine (DPPS), 1,2-dipalmitoyl-*sn*-glycero-3-phosphate (DPPA), 1,2-dipalmitoyl-*sn*-glycero-3-phospho-(1'-*rac*-glycerol) (DPPG), 1,2-dioleoyl-*sn*-glycero-3-phosphoethanolamine-N-(5-dimethylamino-1-naphthalenesulfonyl) (NBD-PE), *N*-[5-(dimethylamino)naphthalene-1-sulfonyl]-1,2-dihexadecanoyl-*sn*-glycero-phosphoethanol -amine (Dansyl-PE) were purchased from Avanti Polar Lipids (Alabaster, AL). Ultrapure water (Milli-Q system, Millipore, Billerica, MA) was used for the preparation of buffers.

2.2.2. General procedure for the preparation of DAT esters (I)[134]: Palmitic acid/octanoic acid (2.2 equiv.), dicyclohexylcarbodiimide (2.2 equiv.) and *N*,*N*-dimethylaminopyridine (0.1 equiv.) were added to a solution of protected diol (1.0 equiv.) in anhydrous dichloromethane (8 mL) under a N_2 atmosphere. Stirring was continued for 12 h at room temperature. After completion of the reaction (monitored by TLC), the reaction mixture was filtered and washed (3x) with dichloromethane. The filtrate was concentrated under reduced pressure and the column chromatography was performed with silica gel and a gradient solvent system of 0-10% ethyl acetate to hexane to yield corresponding esters. The average yields were 77% to 85%.

2.2.3. General procedure for the deprotection of benzyl groups (II)[135]: To a solution of benzyl ether containing compounds (1 equiv.) in 10 mL of ethyl acetate/ethanol (3 : 1 ratio) was added 10% Pd–C (0.1 equiv.) and stirring was continued under a H_2 (80 psi) atmosphere, at room temperature for 8–9 h. After completion of the reaction (monitored by TLC), the catalyst (Pd–C) was filtered off through a pad of Celite and the solvent was removed under reduced pressure. The crude reaction mixture was purified by column chromatography with silica gel and a gradient solvent system of 5–25% of ethyl acetate to hexane to provide diol derivatives. The average yields were 77% to 98%.

2.2.4. General procedure for the deprotection of the cyclopentylidene and dimethyl acetal groups (III)[130,132]: To a stirring solution of protected tetrols (1 equiv.) in dichloromethane (10 mL), 3–5 mL of 80% acetic acid was added and stirring was continued at 40 $^{\circ}$C for 4–5 h. After completion of the reaction (monitored by TLC), the solvent was removed under reduced pressure to yield a residue. The residue was further dissolved in dichloromethane (10mL) and washed with saturated solution of sodium bicarbonate (3x). The organic layer was dried over anhydrous Na_2SO_4 and concentrated under reduced pressure. Purification by silica gel column chromatography and a gradient solvent system of 5–20% ethyl acetate to hexane yielded diol derivatives. The average yields were 75% to 82%.

2.2.5. General procedure for the preparation of cyclopentylidene ketal and acetonide of diols (IV)[130,131]: Method-A: To a stirring solution of diol (1 equiv.) in

toluene (50 mL) p-toluenesulfonic acid (0.1 equiv.) and cyclopentanone (2.5 equiv.) were added respectively. The solution was refluxed for 14 h and the azeotrope was collected in a Dean–Stark trap. The reaction mixture was then cooled to room temperature and reaction mixture was quenched by adding 20% solid $NaHCO_3$. After stirring for another 30 min at room temperature, the reaction mixture was filtered and concentrated under reduced pressure. The purification by silica gel column chromatography and a gradient solvent system of 0–20% ethyl acetate to hexanes yielded desired product.

Method-B: To a solution of diol (1 equiv.) in anhydrous THF (20 mL) were added *p*-toluene sulfonic acid (0.1 equiv.) and 2,2-dimethoxy propane (1.2 equiv.) under a N_2 atmosphere at room temperature. The reaction mixture was stirred at 65 $^{\circ}$C for 3 h. The reaction mixture was quenched by addition of anhydrous K_2CO_3 (1.4 equiv.). The solid residue was removed by filtration and washed with diethyl ether (3-5 mL). Solvent was removed under reduced pressure and purified by silica gel column chromatography (elution with ethyl acetate/hexane 5–15%) to furnish desired product.

2.2.6. General procedure for the reduction of esters with $LiAlH_4$ (V)[132]:

Protected ester (1 equiv.) in anhydrous THF (10 mL) was added dropwise to a suspension of lithium aluminium hydride (2.5 equiv.) in anhydrous THF (20 mL) at 0 $^{\circ}$C under a N_2 atmosphere. Stirring was continued at room temperature for 1 h and then the solution was refluxed for additional 6 h. After completion of the reaction (monitored by TLC), the temperature was lowered to 0 $^{\circ}$C and the reaction was cautiously quenched by addition of 1 mL of deionized water, followed by 1 mL of 10% NaOH and 2 mL of deionized water. The mixture was warmed to room temperature, and stirred until the gray color disappeared. The reaction mixture was filtered in a sintered glass crucible using Celite. Resulting solution was dried over anhydrous Na_2SO_4 and concentrated under reduced pressure. Column chromatography with silica gel and a gradient solvent system of 10–40% ethyl acetate to hexane yielded diol derivative (70-96%).

2.2.7. General procedure for the mono protection of diol and triol with Ag_2O (VI)[136]:

To a solution of alcohol (1 equiv.) in anhydrous dichloromethane (20 mL), silver oxide (Ag_2O, 1.5 equiv.) and benzyl bromide (1.1 equiv.) were added and stirred at

room temperature for 8 h under a N_2 atmosphere. After that the reaction mixture was filtered off through a pad of Celite. The solvent was removed under reduced pressure. The purification by silica gel column chromatography and a gradient solvent system of 10-20% ethyl acetate to hexane afforded protected alcohol. Average yields were 83-90%.

2.2.8. Purification of Proteins from Bacterial Cells: The PKCδ C1b and PKCθC1b subdomains fused with glutathione S-transferase (GST) were expressed in BL21 cells and purified as reported earlier.[141,142] The plasmids were a generous gift from Prof. Alexandra Newton (University of California, San Diego, USA). The protein expression was induced by the addition of 250 µM of isopropyl 1-thio-β-D-galactopyranoside and cells were harvested by centrifugation (5000xg for 10 min at 4 °C) after 14 h of incubation at 24 °C. The resulting pellet was resuspended in 20 mL of 20 µM Tris buffer, pH 8, containing 160 mM NaCl, 50 µM phenylmethylsulfonyl fluoride (PMSF), 2 mM dithiothreitol (DTT), and 0.1% Triton X-100. After sonication for 10 cycles the solution was centrifuged for 30 min (48 000xg at 4 °C). The supernatant was filtered and 500 µl of the glutathione S-transferase Tag resin was added. After incubating this mixture on ice for 1 h with mild shaking at 80 rpm, it was poured onto a column pre-rinsed with 20 mL of 20 mM Tris buffer, pH 8, containing 160 mM KCl. The non-specifically bound proteins were washed off with 100 mL of 20 mM Tris buffer, pH 8, containing 160 mM KCl, and 1 unit of thrombin in cleavage buffer was added to cleave the glutathione S-transferase tag and the column was stored at 4 °C for 12 h. The protein was then eluted in five fractions using 500 µl of 20 mM Tris buffer, pH 8, containing 160 mM KCl. Proteins were further purified by fast performance liquid chromatography (Akta Purifier) using a Superdext 75 column (GE Healthcare Biosciences), a mobile phase of 50 mm Tris, 100 mm NaCl, pH 7.4, and a flow rate of 0.5 mL min^{-1}.

2.2.9. Measurement of Binding Parameters using Fluorescence Spectroscopic Analysis: Fluorescence measurements were performed on a Fluoromax-4 spectrofluorometer using 10 mm path length quartz cuvettes with the slit width of 20 nm at room temperature. An excitation wavelength of 295 nm was applied to selectively excite the tryptophan residues in protein. Proper background corrections were made to avoid the contribution of buffer. For fluorescence titration, protein (2 µM) and varying concentration of ligands (0.67–40 µM for DATs of octanoic acid and 0.099–13 µM for DATs of palmitic acid)

were incubated in a buffer solution (50 mM Tris, 150 mM NaCl, 50 μM $ZnSO_4$, pH 7.4) at room temperature. Fluorescence intensity data, $(F_0\text{-}F)/F_0$, were plotted against the ligand concentration to generate the binding isotherms, where F and F_0 represent the fluorescence intensity at 350 nm in the presence and in the absence of ligand respectively. The EC_{50} values were calculated for all curves by fitting with the Hill equation using OriginLab software. Fluorescence anisotropy measurements were performed in the same fluorimeter using parallel and perpendicular polarizers. The tryptophan fluorescence of the proteins was recorded over 300–500 nm wavelengths by exciting at 295 nm using an excitation slit width of 2 nm. The anisotropy values were averaged over an integration time of 10 s, and a maximum number of five measurements were made for each sample. All anisotropy values of the proteins in the presence of compounds are the mean values of three individual determinations. The degree r of anisotropy in the tryptophan fluorescence of the proteins was calculated using the following equation at the peak of the protein fluorescence spectrum, where I_{VV} and I_{VH} are the fluorescence intensities of the emitted light polarized parallel and perpendicular to the excited light, respectively, and $G = I_{VH}/I_{HH}$ is the instrumental grating factor.

$r = (I_{VV}\text{-}GI_{VH})/ (I_{VV}+2GI_{VH})$

2.2.10. Liposome Binding Assay: The membrane binding of PKC C1b subdomains was analyzed by fluorescence quenching measurements. The protein (500 nM) was added to $PC/PS/Ligand_{16}$ (80-x: 20: x, where x = 0–10) liposomes prepared by an extrusion method,[142] and the emission spectra of protein were measured with the excitation wavelength of 295 nm. Fluorescence intensity data, $(F_0\text{-}F)/F_0$, were plotted against the liposome containing ligand concentrations to generate the binding isotherms, where F and F_0 represent the fluorescence intensity at 338 nm in the presence and in the absence of ligand containing liposomes, respectively. The EC_{50} values were calculated for all curves by fitting with the Hill equation using OriginLab software.

2.2.11. Molecular Docking Analysis: Molecular docking was performed using the crystal structure of PKCδ C1b subdomain complexed with phorbol-13-O-acetate (Protein Data Bank code: 1PTR).[129] The hydrogen as well as the side chains of Lys 234, Arg 273 and Glu 274 not visible in the X-ray structure was subsequently added to the protein. The energy minimized three-dimensional structure of ligands was prepared by using the GlycoBioChem PRODRG2 Server (http://davapc1.bioch.dundee.ac.uk/prodrg/). The GROningen MAchine

for Chemical Simulations (GROMACS) library of three-atom combination geometries employing a combination of short molecular dynamics simulations and energy minimizations was utilized for the conversion of 2D molecular structures to 3D structures. Ligand-protein docking was performed using the Molegro Virtual Docker software, version 4.3.0 (Molegro ApS, Aarhus, Denmark).[143] The binding site was automatically detected by the docking software and restricted within spheres with radius of 15 A˚. During virtual screening, the following parameters were fixed: number of runs 10, population size 50, crossover rate 0.9, scaling factor 0.5, maximum iteration 2000 and grid resolution 0.30. The docked results were evaluated on the basis of moledock and re-rank score. The poses were exported and examined with PyMOL software.

2.3. Spectroscopic Characterization of the Synthesized Compounds

2,3-Diethyl(2R,3R)-1,4-dioxaspiro[4.4]nonane-2,3-dicarboxylate (6)[130,131]: Using the general procedure IV (Method-A), starting from compound **5** (5.2 g, 25.22 mmol) compound **6** (5.6 g, 81%) was isolated as a yellow colorless oil. R_f 0.30 (EtoAc/Hexane, 1: 4); ^{1}H NMR (400 MHz, $CDCl_3$): δ_{ppm} 4.65 (s, 2H), 4.20 (q, J = 7.2 Hz, 4H), 1.93–1.88 (m, 2H), 1.82–1.75 (m, 2H), 1.67–1.62 (m, 4H), 1.24 (t, J=7.2Hz, 6H); ^{13}C NMR(100 MHz, $CDCl_3$): δ_{ppm} 169.1, 122.7, 76.6, 61.2, 36.2, 23.0, 13.6; FT-IR (KBr) *v* 2946, 2867, 1705, 1639, 1450, 1376, 1320, 1059 cm^{-1}.

[(2S,3S)-3-(hydroxymethyl)-1,4-dioxaspiro[4.4]nonan-2-yl]-methanol (7)[132]: Using the general procedure V starting from compound **6** (1.59 g, 5.8 mmol) compound **7** (1.05 g, 96%) was isolated as a colourless oil. R_f 0.32 (EtOAc/Hexane, 1 : 2); ^{1}H NMR (400 MHz, $CDCl_3$): δ_{ppm} 4.24–4.20 (m, 1H), 4.14–4.03 (m, 2H), 3.88–3.77 (m, 2H), 3.67–3.63 (m, 1H), 2.07 (s, 2H), 1.88–1.78 (m, 4H), 1.67–1.64 (m, 4H); ^{13}C NMR (100 MHz, $CDCl_3$): δ_{ppm} 119.1, 78.4, 62.4, 37.1, 23.3; FT-IR (KBr) *v* 3445, 2928, 1634, 1403, 1260, 1084 cm^{-1}; HR-MS m/z (%): calcd. for $C_9H_{16}O_4Na^+$ $[M+Na]^+$: 211.0946, found: 211.0951.

(2S,3S)-2,3-bis[(benzyloxy)methyl]-1,4-dioxaspiro[4.4]nonane (8): Sodium hydride (60% in mineral oil, 282.24 mg, 11.76 mmol) was first taken in a flame-dried round-bottom flask under a N_2 atmosphere and washed thrice with anhydrous hexane to remove mineral oil. Diol 7 (1 g, 4.89 mmol) in anhydrous THF (5 mL) was added dropwise to a stirred suspension of

NaH in anhydrous THF (15 mL) at 0 °C and stirred for 1 h. Then benzyl bromide (1.4 mL, 11.76 mmol) was added dropwise to the reaction mixture and stirred overnight at room temperature.[132] The reaction was quenched by a saturated solution of ammonium chloride and the residue was extracted with diethyl ether (3x20 mL). The organic layer was dried over anhydrous Na_2SO_4 and concentrated under reduced pressure. Column chromatography with silica gel and a gradient solvent system of 0-10% ethyl acetate to hexane yielded 8 (1.5 g, 83%) as a colorless oil. R_f 0.42 (EtOAc/Hexane, 1:6); ^{1}H NMR (400 MHz, $CDCl_3$): δ_{ppm} 7.25–7.15 (m, 10H), 4.46 (s, 4H), 3.90–3.89 (m, 2H), 3.52–3.46 (m, 4H), 1.75–1.72 (m, 4H), 1.57–1.56 (m, 4H); ^{13}C NMR (100 MHz, $CDCl_3$): δ_{ppm} 137.9, 128.2, 127.5, 119.4, 77.2, 73.3, 70.6, 37.2, 23.4; FT-IR (KBr) *ν* 3031, 2930, 2870, 1637, 1453, 1334, 1259, 1205, 1102, 907, 799, 736, 698, 604 cm^{-1}; HR-MS m/z (%): calcd. for $C_{23}H_{28}O_4Na^+$ $[M + Na]^+$: 391.1880, found: 391.1881.

(2S,3S)-1,4-bis(benzyloxy)butane-2,3-diol (9): Using the general procedure (III), starting from compound 8 (600 mg, 1.63 mmol) compound 9 (406.6 mg, 82%) was isolated as colorless oil. R_f 0.37 (EtoAc/Hexane, 1: 2); ^{1}H NMR (400 MHz, $CDCl_3$): δ_{ppm} 7.29–7.22 (m, 10H), 4.47 (s, 4H), 3.81–3.79 (m, 2H), 3.55–3.50 (m, 4H), 2.09 (s, 2H); ^{13}C NMR (100 MHz, $CDCl_3$): δ_{ppm} 137.7, 128.2, 127.6, 127.5, 73.1, 71.5, 70.4; FT-IR (KBr) *ν* 3304, 3029, 2919, 2862, 1638, 1454, 1386, 1362, 1261, 1090, 949, 907, 804, 750, 734, 696, 610 cm^{-1}; HR-MS m/z (%): calcd. For $C_{18}H_{22}O_4Na^+$ $[M + Na]^+$: 325.1410, found: 325.1420.

(2S,3S)-1,4-bis(benzyloxy)-3-(hexadecanoyloxy)butan-2-yl hexadecanoate (10a): Using the general procedure (I), starting from compound 9 (200 mg, 0.662 mmol) and palmitic acid (373.4 mg, 1.46 mmol) compound 10a (437.5 mg, 85%) was isolated as a white solid. Mp: 95–97 °C; R_f 0.45 (EtOAc/Hexane, 1: 9); $[\alpha]^{20}D$ = -9.2 (c 0.1, CH_2Cl_2); ^{1}H NMR (400 MHz, $CDCl_3$): δ_{ppm} 7.27–7.19 (m, 10H), 5.30 (m, 2H), 4.38 (dd, J = 12 Hz, J = 12 Hz, 4H), 3.47 (m, 4H), 2.23–2.20 (m, 4H), 1.52–1.50 (m, 4H), 1.18 (m, 48H), 0.81 (t, J = 5.8 Hz, 6H); ^{13}C NMR (100 MHz, $CDCl_3$): δ_{ppm} 173.2, 137.8, 128.5, 127.9, 73.3, 70.7, 62.4, 35.9, 34.2, 33.5, 32.7, 32.1, 31.0, 29.8, 29.6, 29.5, 29.4, 29.2, 26.4, 25.7, 25.6, 25.5, 24.9, 24.9, 22.8, 14.2; FT-IR (KBr) n 2926, 2854, 1711, 1639, 1458, 1263, 1160, 1108, 1026, 790, 713, 697 cm^{-1}; HR-MS m/z (%): calcd. for $C_{50}H_{82}O_6Na^+$ $[M + Na]^+$: 801.6004, found: 801.6005.

(2S,3S)-3-(hexadecanoyloxy)-1,4-dihydroxybutan-2-yl hexadecanoate (1a): Using the general procedure (II) starting from compound 10a (250 mg, 0.321 mmol) and 10% Pd–C (3.81 mg, 0.0321 mmol), compound **1a** (171 mg, 90%) was isolated as a white solid. Mp: 97–98 °C; R_f 0.36 (EtOAc/Hexane, 1:7); $[\alpha]^{20}D$ = -8.0 (c 0.1, CH_2Cl_2); ^1H NMR (400 MHz, $CDCl_3$): δ_{ppm} 5.29 (m, 2H), 3.77–3.70 (m, 4H), 2.12–2.11 (m, 2H), 1.92–1.86 (m, 2H), 1.71–1.61 (m, 4H), 1.25 (br s, 48H), 0.88 (m, 6H); ^{13}C NMR (100 MHz, $CDCl_3$): δ_{ppm} 173.4, 73.3, 62.4, 35.9, 34.2, 33.5, 32.7, 32.0, 30.9, 29.8, 29.6, 29.5, 29.4, 29.2, 26.4, 25.7, 25.6, 25.5, 24.9, 24.8, 22.8, 14.2; FT-IR (KBr) *v* 3448, 3301, 2919, 2850, 1733, 1638, 1549, 1463, 1384, 1248, 1121 cm^{-1}; HR-MS m/z (%): calcd. for $C_{36}H_{70}O_6Na^+$ $[M + Na]^+$: 621.5065, found: 621.5064.

(2S,3S)-1,4-bis(benzyloxy)-3-(octanoloxy)butan-2-yl octanoate (10b): Using the general procedure (I), starting from compound **9** (200 mg, 0.662 mmol) and octanoic acid (211 mg, 1.46 mmol) compound **10b** (313 mg, 85%) was isolated as colorless syrup. R_f 0.37 (EtOAc/Hexane, 1 : 9); $[\alpha]^{20}D$ = -6.7 (c 0.1, CH_2Cl_2); ^1H NMR (400 MHz, $CDCl_3$): δ_{ppm} 7.25–7.18 (m, 10H), 5.29 (m, 2H), 4.38 (dd, J = 12, J = 12 Hz, 4H), 3.47 (m, 4H), 2.28–2.19 (m, 4H), 1.57–1.49 (m, 4H), 1.20 (m, 16H), 0.80 (m, 6H); ^{13}C NMR (100 MHz, $CDCl_3$): δ_{ppm} 173.2, 137.8, 128.5, 127.9, 73.3, 70.7, 68.3, 34.4, 34.2, 31.8, 29.2, 29.15, 29.1, 29.0, 25.1, 24.8, 22.7, 14.2; FT-IR (KBr) *v* 2926, 2855, 1717, 1457, 1263, 1160, 1107, 1026, 804, 746, 713 cm^{-1}; HR-MS m/z (%): calcd. for $C_{34}H_{50}O_6Na^+$ $[M+Na]^+$: 577.3505, found: 577.3501.

(2S,3S)-1,4-dihydroxy-3-(octanoloxy)butan-2-yl octanoate (1b): Using the general procedure (II), starting from compound **10b** (250 mg, 0.451 mmol) and 10% Pd–C (5.34 mg, 0.0451 mmol), compound **1b** (152 mg, 90%) was isolated as a colourless oil. R_f 0.30 (EtOAc/Hexane, 1 : 4); $[\alpha]^{20}D$ = -11.0 (c 0.1, CH_2Cl_2); ^1H NMR (400 MHz, $CDCl_3$): δ_{ppm} 5.36–5.32 (m, 1H), 5.20–5.16 (m, 1H), 3.70–3.56 (m, 2H), 3.51–3.42 (m, 2H), 2.40–2.31 (m, 4H), 1.65–1.61 (m, 4H), 1.28–1.23 (m, 16H), 0.85 (m, 6H); ^{13}C NMR (100 MHz, $CDCl_3$): δ_{ppm} 173.2, 73.3, 62.4, 34.4, 34.2, 31.8, 29.2, 29.15, 29.1, 29.0, 25.1, 24.8, 22.7, 14.2; FT-IR (KBr) *v* 3434, 2961, 2926, 2854, 1733, 1638, 1461, 1261, 1095, 1024 cm^{-1}; HR-MS m/z (%): calcd. For $C_{20}H_{38}O_6Na^+$ $[M + Na]^+$: 397.2561, found: 397.2562.

[(2S,3S)-3-[(hexadecanoyloxy)methyl]-1,4-dioxapiro[4.4]nonan-2-yl]methyl hexadecanoate (11a): Using the general procedure (I), starting from compound **7** (300 mg,

1.6 mmol) and palmitic acid (900 mg, 3.51 mmol) compound **11a** (857 mg, 80%) was isolated as a white solid. Mp: 98–99 °C; R_f 0.35 (EtOAc/Hexane, 1 : 6); $[\alpha]^{20}D$ = -17.3 (c 0.1, CH_2Cl_2); ^1H NMR (400 MHz, $CDCl_3$): δ_{ppm} 4.20–4.08 (m, 2H), 3.93–3.78 (m, 2H), 3.62–3.59 (m, 2H), 2.35–2.26 (m, 4H), 1.89–1.83 (m, 4H), 1.76–1.56 (m, 8H), 1.18 (br s, 48H), 0.82–0.78 (m, 6H); ^{13}C NMR (100 MHz, $CDCl_3$): δ_{ppm} 173.2, 120.4, 76.0, 63.9, 49.8, 37.4, 36.1, 34.2, 32.9, 32.1, 31.0, 29.84, 29.8, 29.6, 29.56, 29.5, 29.4, 29.3, 26.5, 25.7, 25.5, 25.0, 24.9, 23.7, 22.8, 21.0, 14.3; FT-IR (KBr) *v* 2918, 2849, 1702, 1627, 1463, 1310, 1295, 1088, 940 cm^{-1}; HR-MS m/z (%): calcd. for $C_{41}H_{76}O_6Na^+$ $[M + Na]^+$: 687.5534, found: 687.5535.

(2S,3S)-4-hexadecanoloxy-2,3-dihydroxybutyl hexadecanoate (2a): Using the general procedure (III), starting from compound **11a** (500 mg, 0.7523 mmol) compound **2a** (370 mg, 82%) was isolated as a white solid. Mp: 95–96 °C; R_f 0.36 (EtOAc/Hexane, 1 : 7); $[\alpha]^{20}D$ = -10.0 (c 0.1, CH_2Cl_2); ^1H NMR (400 MHz, $CDCl_3$): δ_{ppm} 4.24–4.13 (m, 4H), 3.80 (m, 2H), 2.68 (br s, 2H), 2.36–2.30 (m, 4H), 1.60–1.58 (m, 4H), 1.23 (br s, 48H), 0.87–0.84 (m, 6H); ^{13}C NMR (100 MHz, $CDCl_3$): δ_{ppm} 174.4, 69.8, 65.5, 34.5, 34.4, 32.1, 29.9, 29.9, 29.7, 29.6, 29.5, 29.3, 25.1, 22.9, 14.3; FT-IR (KBr) *v* 3435, 2955, 2917, 2849, 1736, 1638, 1463, 1383, 1178, 1094 cm^{-1}; HR-MS m/z (%): calcd. for $C_{36}H_{70}O_6Na^+$ $[M + Na]^+$: 621.5065, found: 621.5065.

[(2S,3S)-3-[(octanoyloxy)methyl]-1,4-dioxapiro[4.4]nonan-2-yl]-methyl octanoate (11b): Using the general procedure (I), starting from compound **7** (300 mg, 1.6 mmol) and octanoic acid (506.18 mg, 3.51 mmol) compound **11b** (600 mg, 85%) was isolated as colourless oil. R_f 0.32 (EtOAc/Hexane, 1 : 7); $[\alpha]^{20}D$ = -7.3 (c 0.1, CH_2Cl_2); ^1H NMR (400 MHz, $CDCl_3$): δ_{ppm} 4.20–4.11 (m, 4H), 3.94–3.93 (m, 2H), 2.30–2.25 (m, 4H), 1.77–1.76 (m, 4H), 1.61–1.55 (m, 8H), 1.22 (br s, 16H), 0.82–0.79 (m, 6H); ^{13}C NMR (100 MHz, CDCl3): δ_{ppm} 174.1, 120.4, 75.9, 63.9, 49.9, 37.4, 35.9, 34.2, 32.7, 31.8, 31.0, 29.8, 29.2, 29.0, 26.4, 25.6, 25.4, 24.9, 32.6, 22.7, 20.9, 14.1; FT-IR (KBr) *v* 2918, 2849, 1703, 1627, 1463, 1310, 1295, 1088, 941 cm^{-1}; HR-MS m/z (%): calcd. for $C_{25}H_{44}O_6Na^+$ $[M + Na]^+$: 463.3030, found: 463.3031.

(2S,3S)-2,3-dihydroxy-4-(octanoloxy)butyloctanoate (2b): Using the general procedure (III), starting from compound **11b** (500 mg, 1.135 mmol) compound **2a** (349 mg, 82%) was isolated as a colourless oil. R_f 0.35 (EtOAc/Hexane, 1 : 4); $[\alpha]^{20}D$ = -9.2 (c 0.1, CH_2Cl_2); ^1H NMR (400 MHz, $CDCl_3$): δ_{ppm} 4.21–4.11 (m, 4H), 3.85–3.78 (m, 2H), 2.93 (br s, 2H), 2.36–

2.24 (m, 4H), 1.60–1.57 (m, 4H), 1.25 (br s, 16H), 0.86–0.82 (m, 6H); ^{13}C NMR (100 MHz, $CDCl_3$): δ_{ppm} 174.2, 69.7, 65.4, 34.4, 34.3, 31.8, 29.2, 29.1, 25.0, 22.8, 14.2; FT-IR (KBr) *v* 3449, 3300, 2928, 2854, 1746, 1637, 1547, 1446, 1375, 1229, 1117, 1050 cm^{-1}; HR-MS m/z (%): calcd. for $C_{20}H_{38}O_6Na^+$ $[M + Na]^+$: 397.2561, found: 397.2561.

(2R,3R)-diethyl 2-(benzyloxy)-3-hydroxysuccinate (12)[136]**:** Using the general procedure (VI), starting from compound **5** (1.0 g, 4.85 mmol) compound **12** (1.3g, 90%) was isolated as a slight yellow colored oil. R_f 0.35 (EtOAc/Hexane, 1 : 4); ^{1}H NMR (400 MHz, $CDCl_3$): δ_{ppm} 7.33–7.22 (m, 5H), 4.86 (d, J = 12 Hz, 2H), 4.59 (s, 1H), 4.21 (d, J = 12Hz, 1H), 4.34–4.28 (m, 2H), 4.13–4.02 (m, 2H), 3.39 (bs, 1H), 1.32 (t, J = 7 Hz, 3H), 1.16 (t, J = 7 Hz, 3H); ^{13}C NMR (100 MHz, CDCl3): δ_{ppm} 173.1, 169.3, 137.8, 128.6, 128.4, 128.2, 128.1, 78.3, 72.9, 72.3, 62.0, 61.5, 14.2, 14.0; FT-IR (KBr) *v* 3450, 2930, 1732, 1634, 1455, 1384, 1265, 1015, 861, 740, 700 cm^{-1}; HR-MS m/z (%): calcd. for $C_{15}H_{20}O_6Na^+$ $[M + Na]^+$: 319.1152, found: 319.1100.

(2S,3S)-3-(benzyloxy)-1,2,4-triol (13)[132]**:** Using the general procedure (V), starting from compound **12** (1.3 g, 4.39 mmol) compound **13** (656 mg, 70%) was isolated as a white solid. Mp: 77–78 °C [ref. 75.3–76.6 °C]; R_f 0.20 (EtOAC); $[\alpha]^{20}D$ = -27.3 (c 0.1, CH_2Cl_2); ^{1}H NMR (400 MHz, $CDCl_3$): δ_{ppm} 7.31–7.22 (m, 5H), 5.17 (br s, 3H), 4.51 (dd, J = 11.6, J = 11.6 Hz, 2H), 3.85–3.38 (m, 6H); ^{13}C NMR (100 MHz, $CDCl_3$): δ_{ppm} 137.9, 128.7, 128.2, 79.3, 72.7, 72.1, 63.4, 60.7; FT-IR (KBr) *v* 3403, 2938, 1638, 1454, 1213, 1050, 911, 742, 700 cm^{-1}; HR-MS m/z (%): calcd. For $C_{11}H_{16}O_4Na^+$ $[M + Na]^+$: 235.0941, found: 235.0942.

(2S,3S)-2,4-bis(benzyloxy)butane-1,3-diol (15) and (S)-4-((S)-1,2-bis(benzyloxy)ethyl)-2,2-dimethyl-1,3-dioxolane (16)[130,132,136,137]**:** Using the general procedure (VI), starting from compound **13** (650 mg, 3.065 mmol) mixture of compound **14** and **15** (700 mg, 76%) was isolated as colourless oil. R_f 0.30 (EtOAc/Hexane, 2 : 1); ^{1}H NMR (400 MHz, $CDCl_3$): δ_{ppm} 7.29–7.18 (m, 20H), 4.45 (s, 4H), 5.54 (dd, J = 11.6, J = 11.6 Hz, 4H), 3.91–3.89 (m, 1H), 3.77–3.72 (m, 3H), 3.64–3.57 (m, 4H), 3.55–3.47 (m, 4H), 2.51 (br s, 2H), 1.91 (br s, 2H); ^{13}C NMR (100 MHz, $CDCl_3$): δ_{ppm} 138.0, 137.9, 137.74, 137.7, 128.2, 127.9, 127.8, 127.74, 127.67, 127.62, 127.56, 127.53, 127.5, 78.6, 78.1, 73.2, 73.1, 72.6, 72.5, 72.4, 72.0, 70.8, 70.3, 69.5, 63.3, 61.0; FT-IR (KBr) *v* 3437, 2926, 2855, 1637, 1455, 1261, 1188, 1119, 802,

741, 698 cm^{-1}; HR-MS-m/z (%): calcd. for $C_{18}H_{22}O_4Na^+$ $[M + Na]^+$: 325.1410, found: 325.1397.

Using the general procedure IV (Method-B), starting from mixture of compound **14** and **15** (700 mg, 2.32 mmol) compound **16**(400 mg, 50%) was isolated as colourless oil and recover **15** (300 mg, 43%) as colourless oil. (2S,3S)-2,4-Bis(benzyloxy)butane-1,3-diol (**15**): R_f 0.30 (EtOAc/Hexane, 2 : 1); $[\alpha]^{20}D$ = -4.1 (c 0.1, CH_2Cl_2); ^1H NMR (400 MHz, $CDCl_3$): δ_{ppm} 7.35–7.28 (m, 10H), 5.20 (s, 2H), 4.80 (d, J = 11.2 Hz, 2H), 4.48 (d, J = 11.6 Hz, 2H), 4.12–4.10 (m, 2H), 3.91–3.81 (m, 4H); ^{13}C NMR (100 MHz, $CDCl_3$): δ_{ppm} 137.2, 135.6, 128.8, 128.7, 128.6, 128.4, 128.3, 78.8, 76.9, 73.0, 67.1, 63.5; FT-IR (KBr) *ν* 3430, 2925, 2855, 1628, 1455, 1383, 1261, 1188, 1120, 803, 746, 698 cm^{-1}; HR-MS m/z (%): calcd. for $C_{18}H_{22}O_4Na^+$ $[M + Na]^+$: 325.1410, found: 325.1397. (S)-4-((S)-1,2-Bis(benzyloxy)ethyl)-2,2-dimethyl-1,3-dioxolane (**16**): R_f 0.34 (EtOAc/Hexane , 1 : 1); $[\alpha]^{20}D$ = -19.5 (c 0.1, CH_2Cl_2); ^1H NMR (400 MHz, $CDCl_3$): δ_{ppm} 7.29–7.19 (m, 10H), 5.23(s, 2H), 4.64 (dd, J = 12 Hz, J = 12 Hz, 2H), 4.23–4.18 (m, 1H), 3.93–3.90 (m, 1H), 3.72–3.68 (m, 1H), 3.64–3.61 (m, 1H), 3.51–3.44 (m, 2H), 1.35 (s, 3H), 1.29 (s, 3H); ^{13}C NMR (100 MHz, $CDCl_3$): δ_{ppm} 138.2, 128.3, 127.8, 127.7, 109.2, 79.5, 76.5, 75.6, 72.7, 68.3, 63.3, 26.3, 25.3; FT-IR (KBr) *ν* 2925, 2852, 1637, 1462, 1381, 1262, 1100, 1020, 801, 669 cm^{-1}; HR-MS m/z (%): calcd. for $C_{21}H_{26}O_4Na^+$ $[M + Na]^+$: 365.1723, found: 365.1722.

(2S,3S)-1,3-bis(benzyloxy)-4-(hexadecanoyloxy)butan-2-yl hexadecanoate (17a): Using the general procedure (I), starting from compound **15** (200 mg, 0.662 mmol) and palmitic acid (373 mg, 1.456 mmol) compound **17a** (400 mg, 77%) was isolated as a white solid. Mp: 88–90 °C; R_f 0.36 (EtOAc/Hexane, 1 : 9); $[\alpha]^{20}D$ = -13.1 (c 0.1, CH_2Cl_2); ^1H NMR (400 MHz, $CDCl_3$): δ_{ppm} 7.26–7.16 (m, 10H), 5.28–5.24 (m, 1H), 5.19–5.15 (m, 1H), 4.56 (dd, J = 12, J = 11.6 Hz, 2H), 4.43 (s, 2H), 4.27–4.15 (m, 1H), 4.10–4.01 (m, 1H), 3.85–3.67 (m, 1H), 3.59–3.51 (m, 1H), 2.26–2.13 (m, 4H), 1.51 (m, 4H), 1.18 (br s, 48H), 0.78 (m, 6H); ^{13}C NMR (100 MHz, $CDCl_3$): δ_{ppm} 173.5, 173.4, 138.1, 128.6, 128.1, 128.03, 128.01, 127.9, 75.5, 73.4, 73.2, 69.4, 62.4, 34.4, 34.2, 34.1, 32.1, 29.9, 29.6, 29.5, 29.4, 29.3, 29.2, 26.3, 25.4, 25.1, 24.9, 24.9, 22.8, 14.2; FT-IR (KBr) *ν* 2921, 2846, 1732, 1638, 1455, 1109, 905, 801, 733, 696 cm^{-1}; HR-MS m/z (%): calcd. for $C_{50}H_{82}O_6Na^+$ $[M + Na]^+$: 801.6004, found: 801.6004.

(2S,3S)-4-(hexadecanoyloxy)-1,3-dihydroxybutan-2-yl hexadecanoate (3a): Using the general procedure (II), starting from compound **17a** (300 mg, 0.385 mmol) and 10% Pd–C (4.6 mg, 0.0385 mmol), compound **3a** (210 mg, 91%) was isolated as a white solid. R_f 0.40 (EtOAc/Hexane, 1 : 7); mp: 96–97 °C; $[\alpha]^{20}D$ = -5.7 (c 0.98, CH_2Cl_2); ^1H NMR (400 MHz, $CDCl_3$): δ_{ppm} 5.36–5.24 (m, 2H), 4.32–4.22 (m, 1H), 4.18–4.08 (m, 1H), 3.92–3.79 (m, 1H), 3.67–3.59 (m, 1H), 2.35–2.24 (m, 4H), 1.59–1.56 (m, 4H), 1.26 (br s, 48H), 0.87 (m, 6H); ^{13}C NMR (100 MHz, $CDCl_3$): δ_{ppm} 173.5, 173.3, 76.4, 72.7, 65.5, 61.6, 34.5, 34.4, 34.34, 34.3, 32.1, 29.9, 29.8, 29.6, 29.54, 29.5, 29.3, 25.1, 25.0, 22.9, 14.3; FT-IR (KBr) *ν* 3451, 2922, 2849, 1656, 1519, 1461, 1383, 1261, 1224, 1083 cm^{-1}; HR-MS m/z (%): calcd. for $C_{36}H_{70}O_6Na^+$ $[M + Na]^+$: 621.5065, found: 621.5066.

(2S,3S)-1,3-bis(benzyloxy)-4-(octanoyloxy)butan-2-yl octanoate (17b): Using the general procedure (I), starting from compound **15** (200 mg, 0.6619 mmol) and octanoic acid (210 mg, 1.456 mmol) compound **17b** (300 mg, 82%) was isolated as a colourless oil. R_f 0.40 (EtOAc/Hexane, 1 : 7); $[\alpha]^{20}D$ = -26.1 (c 0.1, CH_2Cl_2); ^1H NMR (400 MHz, $CDCl_3$): δ_{ppm} 7.25–7.18 (m, 10H), 5.27–5.25(m, 1H), 5.17–5.16 (m, 1H), 4.57 (dd, J = 12 Hz, J = 11.6 Hz, 2H), 4.44 (s, 2H), 4.24–4.16 (m, 1H), 4.10–4.02 (m, 1H), 3.84–3.72 (m, 1H), 3.58–3.52 (m, 1H), 2.27–2.13 (m, 4H), 1.53–1.49 (m, 4H), 1.19 (br s, 16H), 0.80 (m, 6H); ^{13}C NMR (100 MHz, $CDCl_3$): δ_{ppm} 173.5, 173.4, 138.1, 128.6, 128.2, 128.1, 128.0, 127.8, 76.5, 75.6, 73.4, 69.6, 62.4, 34.5, 34.43, 34.4, 34.29, 33.2, 31.8, 29.9, 29.2, 29.1, 25.1, 25.0, 22.8, 14.2; FT-IR (KBr) *ν* 2922, 2854, 1732, 1637, 1455, 1383, 1113, 733, 698, 630 cm^{-1}; HR-MS m/z (%): calcd. For $C_{34}H_{50}O_6Na^+$ $[M + Na]^+$: 577.3500, found: 577.3501.

(2S,3S)-1,3-dihydroxy-4-(octanoyloxy)butane-2-yl octanoate (3b): Using the general procedure (II), starting from compound **17b** (250 mg, 0.451 mmol) and 10% Pd–C (5.3 mg, 0.0451 mmol), compound **3b** (160 mg, 77%) was isolated as colourless oil. R_f 0.34 (EtOAc/Hexane, 1 : 7); $[\alpha]^{20}D$ = -15.1 (c 0.1, CH_2Cl_2); ^1H NMR (400 MHz, $CDCl_3$): δ_{ppm} 5.26–5.16 (m, 2H), 4.27–4.17 (m, 1H), 4.11–4.03 (m, 1H), 3.87–3.72 (m, 1H), 3.61–3.53 (m, 1H), 2.28–2.13 (m, 4H), 1.53–1.49 (m, 4H), 1.19 (br s, 16H), 0.80 (m, 6H); 13C NMR (100 MHz, CDCl3): δ_{ppm} 173.2, 173.1, 74.4, 70.5, 65.4, 62.7, 34.2, 34.0, 31.6, 29.0, 28.4, 28.3, 26.1, 25.2, 24.9, 24.7, 22.6, 14.4; FT-IR (KBr) *ν* 3449, 2955, 2926, 2851, 1733, 1705, 1640, 1463, 1382, 1235, 1197, 1109, 1096 cm^{-1}; HR-MSm/z (%): calcd. for $C_{20}H_{38}O_6Na^+$ $[M + Na]^+$: 397.2561, found: 397.2560.

(S)-1-((S)-2,2-dimethyl-1,3-dioxolan-4yl)ethane-1,2-diol (18): Using the general procedure (II), starting from compound **16** (300 mg, 0.876 mmol) and 10%Pd–C (10.37 mg, 0.0876 mmol), compound **18** (139 mg, 98%) was isolated as a colourless oil. R_f 0.35 (3: 1); $[\alpha]^{20}D$ = -27.3 (c 0.1, CH_2Cl_2); ^1H NMR(400 MHz, $CDCl_3$): δ_{ppm} 4.18–4.11 (m, 1H), 4.06–4.02 (m, 1H), 3.84–3.80 (m, 1H), 3.65–3.58 (m, 3H), 1.42 (s, 3H), 1.38 (s, 3H); ^{13}C NMR (100 MHz, $CDCl_3$): δ_{ppm} 109.2, 76.3, 72.2, 65.5, 63.4, 26.2, 25.1; FT-IR (KBr) *v* 3446, 2950, 2087, 1637, 1409, 1084, 1042 cm^{-1}; HR-MS m/z (%): calcd. for $C_7H_{14}O_4Na^+$ $[M + Na]^+$: 185.0784, found: 185.0786.

(1S)-1-[(4S)-2,2-dimethyl-1,3-dioxan-4-yl]-2-(hexadecanoyloxy)-ethyl hexadecanoate (19a): Using the general procedure (I), starting from compound **18** (70 mg, 0.4318 mmol) and palmitic acid (243.6 mg, 0.95 mmol) compound **19a** (224 mg, 81%) was isolated as a white solid. R_f 0.37 (EtOAc/Hexane, 1 : 7); mp: 86–88 °C; $[\alpha]^{20}D$ = -7.0 (c 0.1, CH_2Cl_2); ^1H NMR (400 MHz, $CDCl_3$): δ_{ppm} 5.13–5.09 (m, 1H), 4.26–4.17 (m, 2H), 4.11–4.06 (m, 1H), 3.98–3.94 (m, 1H), 3.73–3.69 (m, 1H), 2.30–2.20 (m, 4H), 1.57–1.51 (m, 4H), 1.36 (s, 3H), 1.28 (s, 3H), 1.19 (m, 48H), 0.81 (m, 6H); ^{13}C NMR (100 MHz, $CDCl_3$): δ_{ppm} 173.5, 173.4, 110.0, 74.5, 70.7, 65.6, 62.9, 34.4, 34.2, 34.1, 32.1, 29.9, 29.7, 29.54, 29.5, 29.3, 29.2, 26.3, 25.4, 25.1, 25.0, 24.9, 22.7, 14.3; FT-IR (KBr) *v* 2918, 2850, 1737, 1637, 1463, 1384, 1169, 1099, 1073 cm^{-1}; HR-MS m/z (%): calcd. for $C_{39}H_{74}O_6Na^+$ $[M + Na]^+$: 661.5378, found: 661.5377.

(2S,3S)-1-(hexadecanoyloxy)-3,4-dihydroxybutan-2-yl-hexadecanoate (4a): Using the general procedure (III), starting from compound **19a** (150 mg, 0.235 mmol) compound **4a** (105 mg, 75%) was isolated as a white solid. R_f 0.36 (EtOAc/Hexane, 1 : 9); mp: 97–98 °C; $[\alpha]^{20}D$ = -12.7 (c 0.1, CH_2Cl_2); ^1H NMR (400 MHz, $CDCl_3$): δ_{ppm} 5.23–5.19 (m, 1H), 4.36–4.27 (m, 2H), 4.21–4.16 (m, 1H), 4.08–4.04 (m, 1H), 3.83–3.79 (m, 1H), 2.40–2.30 (m, 4H), 1.67–1.61 (m, 4H), 1.29 (br s, 48H), 0.91 (m, 6H); ^{13}C NMR (100 MHz, $CDCl_3$): δ_{ppm} 173.5, 173.4, 74.5, 70.7, 65.6, 62.9, 34.4, 34.2, 34.1, 32.1, 29.9, 29.6, 29.54, 29.5, 29.3, 29.2, 26.3, 25.4, 25.1, 25.0, 24.9, 22.8, 14.3; FT-IR (KBr) *v* 3430, 2918, 2850, 1638, 1550, 1380, 1245, 1116 cm^{-1}; HR-MS m/z (%): calcd. for $C_{36}H_{70}O_6Na^+$ $[M + Na]^+$: 621.5065, found: 621.5064.

(1S)-1-[(4S)-2,2-dimethyl-1,3-dioxolan-4-yl]-2-(octanoyloxy)-ethyl octanoate (19b): Using the general procedure (I), starting from compound **18** (70 mg, 0.4318 mmol) and

octanoic acid (137 mg, 0.95 mmol) compound **19b** (150 mg, 84%) was isolated as a colourless oil. R_f 0.36 (EtOAc/Hexane, 1 : 7); $[\alpha]^{20}D$ = -8.3 (c 0.1, CH_2Cl_2); ^1H NMR (400 MHz, $CDCl_3$): δ_{ppm} 5.20–5.16 (m, 1H), 4.33–4.24 (m, 2H), 4.18–4.13 (m, 1H), 4.05–4.02 (m, 1H), 3.80–3.76 (m, 1H), 2.38–2.28 (m, 4H), 1.66–1.58 (m, 4H), 1.43 (s, 3H), 1.35 (s, 3H), 1.29 (m, 16 H), 0.88 (m, 6H); ^{13}C NMR (100 MHz, $CDCl_3$): δ_{ppm} 173.2, 173.1, 109.7, 74.4, 70.5, 65.4, 62.7, 34.2, 34.0, 31.6, 29.03, 29.0, 28.9, 26.1, 25.2, 24.9, 24.8, 22.6, 14.0; FT-IR (KBr) *v* 2922, 2856, 1738, 1642, 1455, 1382, 1222, 1161, 1108, 1071, 964 cm^{-1}; HR-MS m/z (%): calcd. for $C_{23}H_{42}O_6Na^+$ $[M + Na]^+$: 437.2874, found: 437.2885.

(2S,3S)-3,4-dihydroxy-1-(octanoyloxy)butane-2-yl octanoate (4b): Using the general procedure (III), starting from compound **19a** (150 mg, 0.235 mmol) compound **4a** (105 mg, 75%) was isolated as a colourless oil. R_f 0.35 (EtOAc/Hexane, 1 : 4); $[\alpha]^{20}D$ = -22.0 (c 0.1, CH_2Cl_2); ^1H NMR (400 MHz, $CDCl_3$): δ_{ppm} 5.23–5.19 (m, 1H), 4.36–4.28 (m, 2H), 4.20–4.16 (m, 1H), 4.08–4.04 (m, 1H), 3.83–3.80 (m, 1H), 2.40–2.30 (m, 4H), 1.67–1.64 (m, 4H), 1.31 (br s, 16H), 0.90 (m, 6H); ^{13}C NMR (100 MHz, $CDCl_3$): δ_{ppm} 179.1, 173.1, 74.4, 70.6, 65.4, 62.8, 34.1, 33.9, 31.6, 29.7, 29.01, 29.0, 28.9, 26.0, 25.1, 24.9, 24.8, 24.7, 22.5, 13.9; FT-IR (KBr) *v* 3451, 2926, 2855, 1745, 1633, 1456, 1372, 1229, 1165, 1047 cm^{-1}; HR-MS m/z (%): calcd. for $C_{20}H_{38}O_6Na^+$ $[M + Na]^+$: 397.2561, found: 397.2560.

2.4. NMR Spectra of the Synthesized Compounds

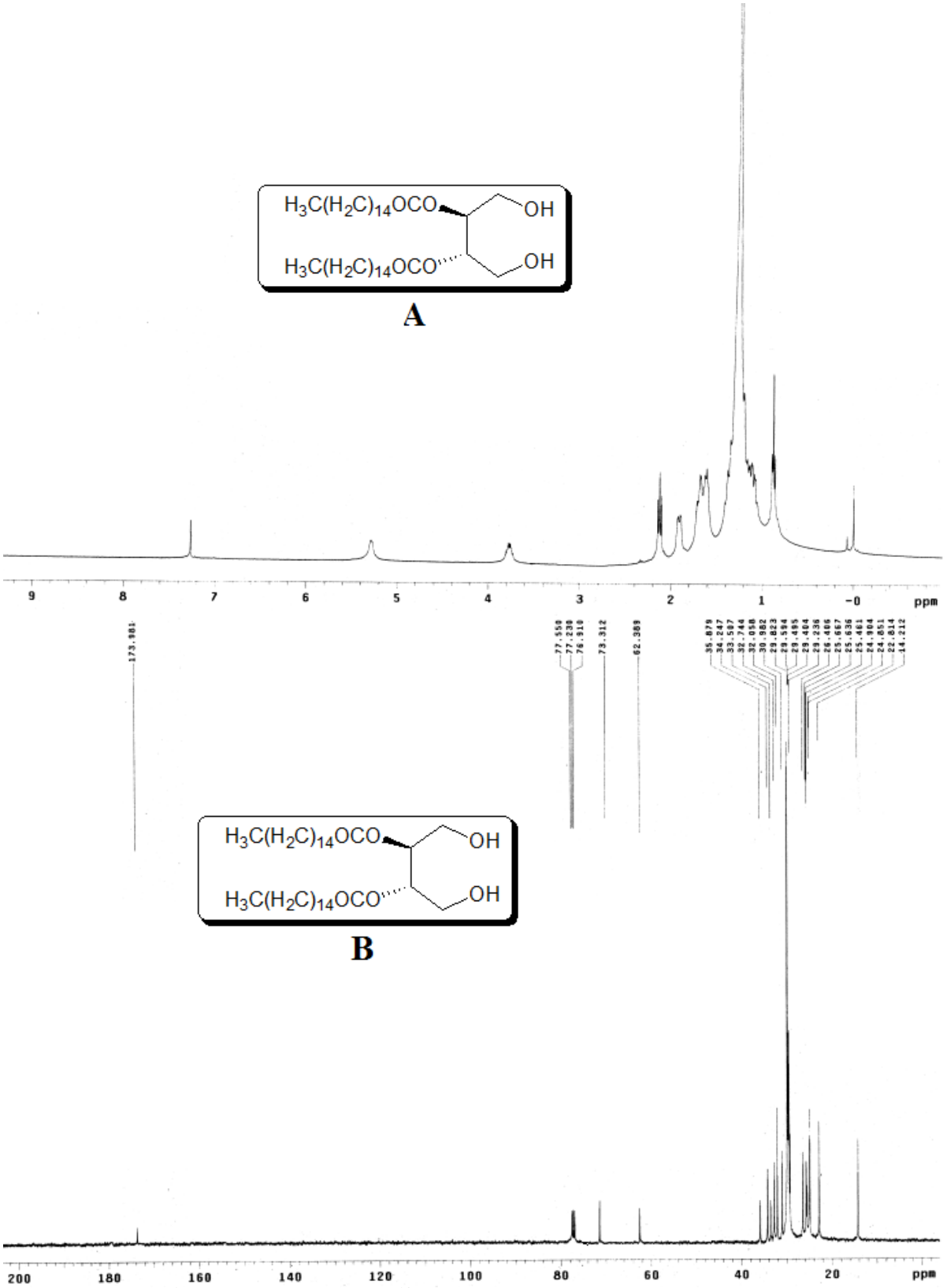

Figure 2.4.1: *^{1}H NMR (**A**) and ^{13}C NMR (**B**) of (2S,3S)-3-(hexadecanoyloxy)-1,4-dihydroxybutan-2-yl hexadecanoate (**1a**)*

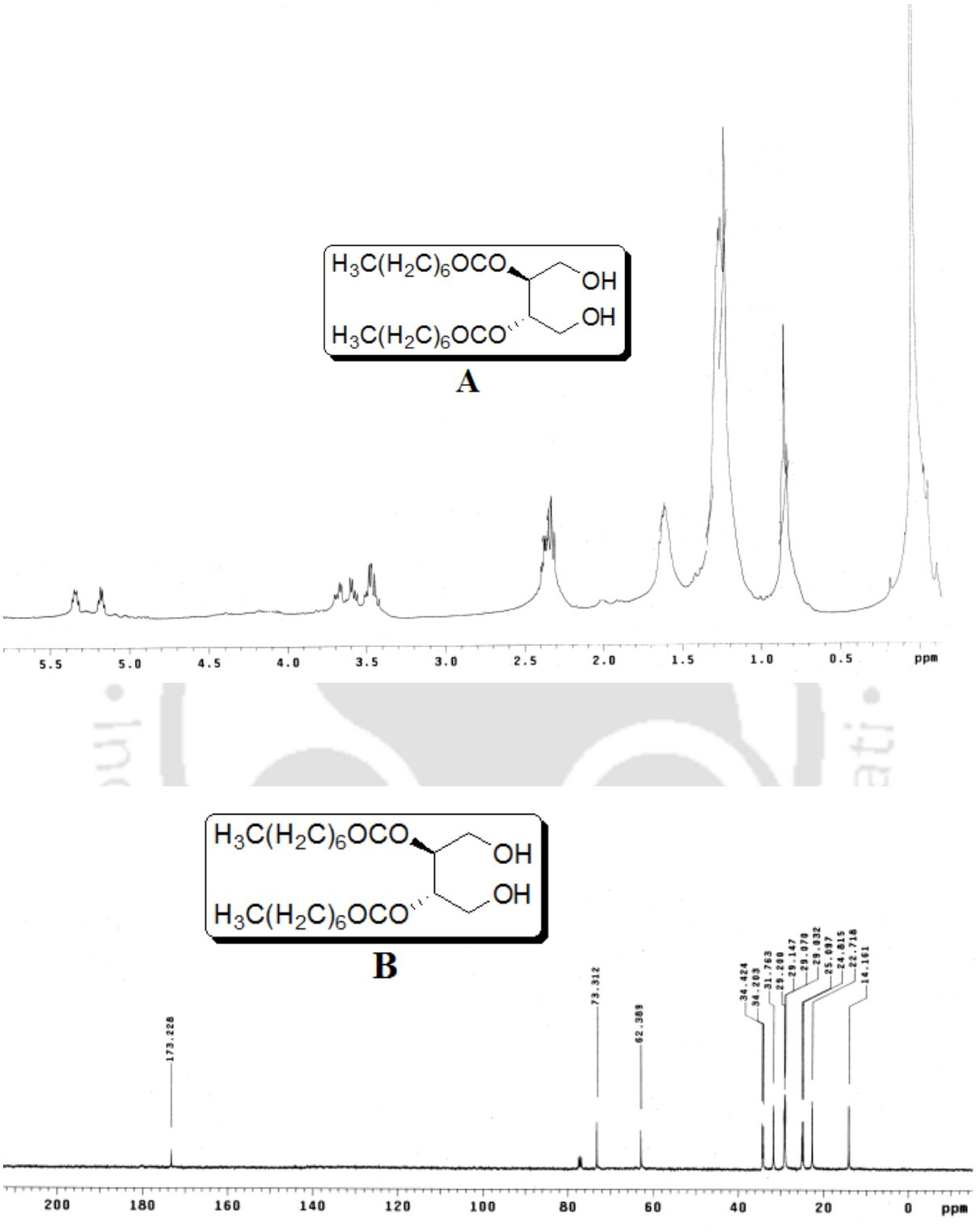

Figure 2.4.2: *^{1}H NMR (**A**) and ^{13}C NMR (**B**) of (2S,3S)-1,4-dihydroxy-3-(octanoloxy)butan-2-yl octanoate (**1b**)*

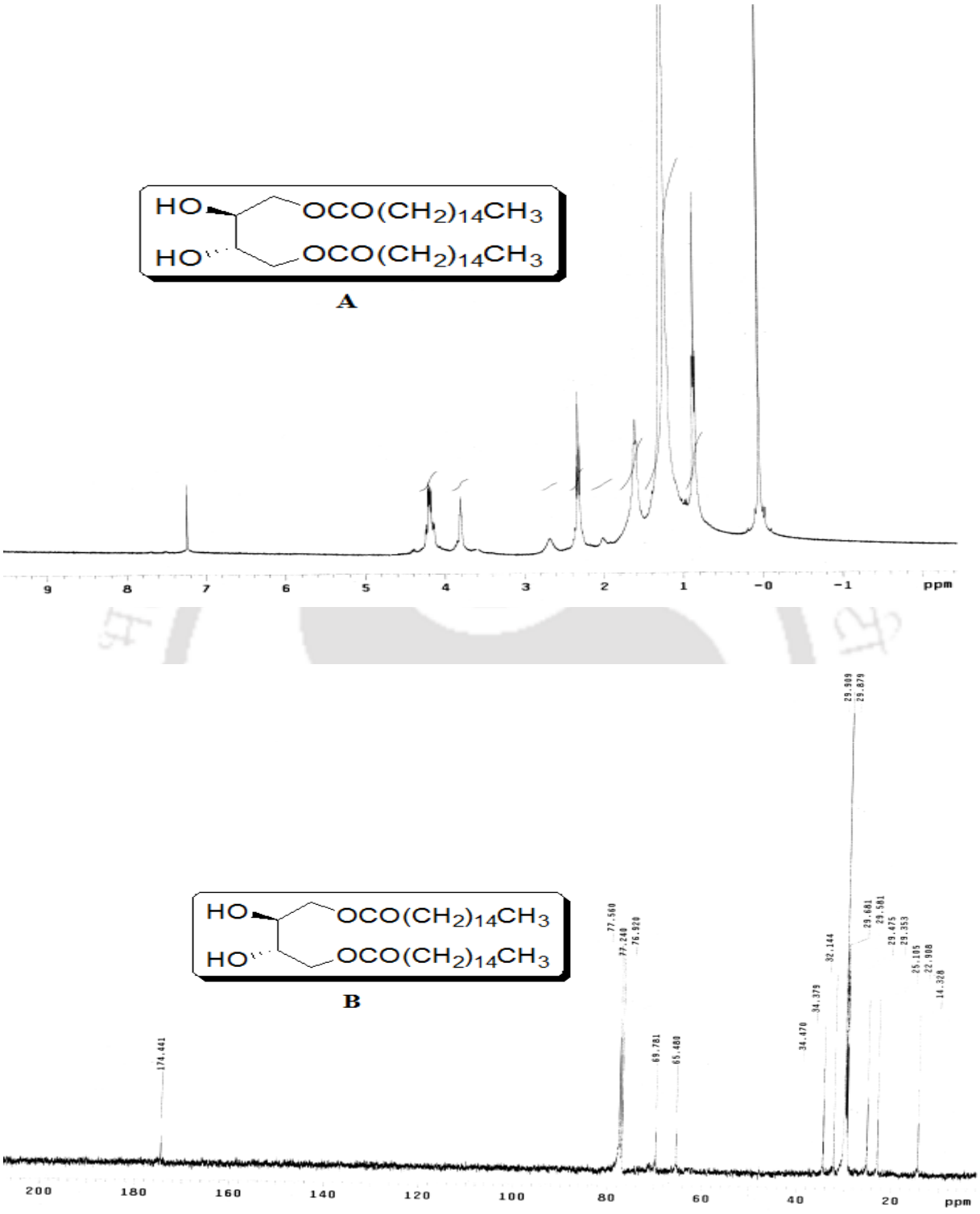

Figure 2.4.3: *^{1}H NMR (**A**) and ^{13}C NMR (**B**) of (2S,3S)-4-hexadecanoloxy-2,3-dihydroxybutyl hexadecanoate (**2a**)*

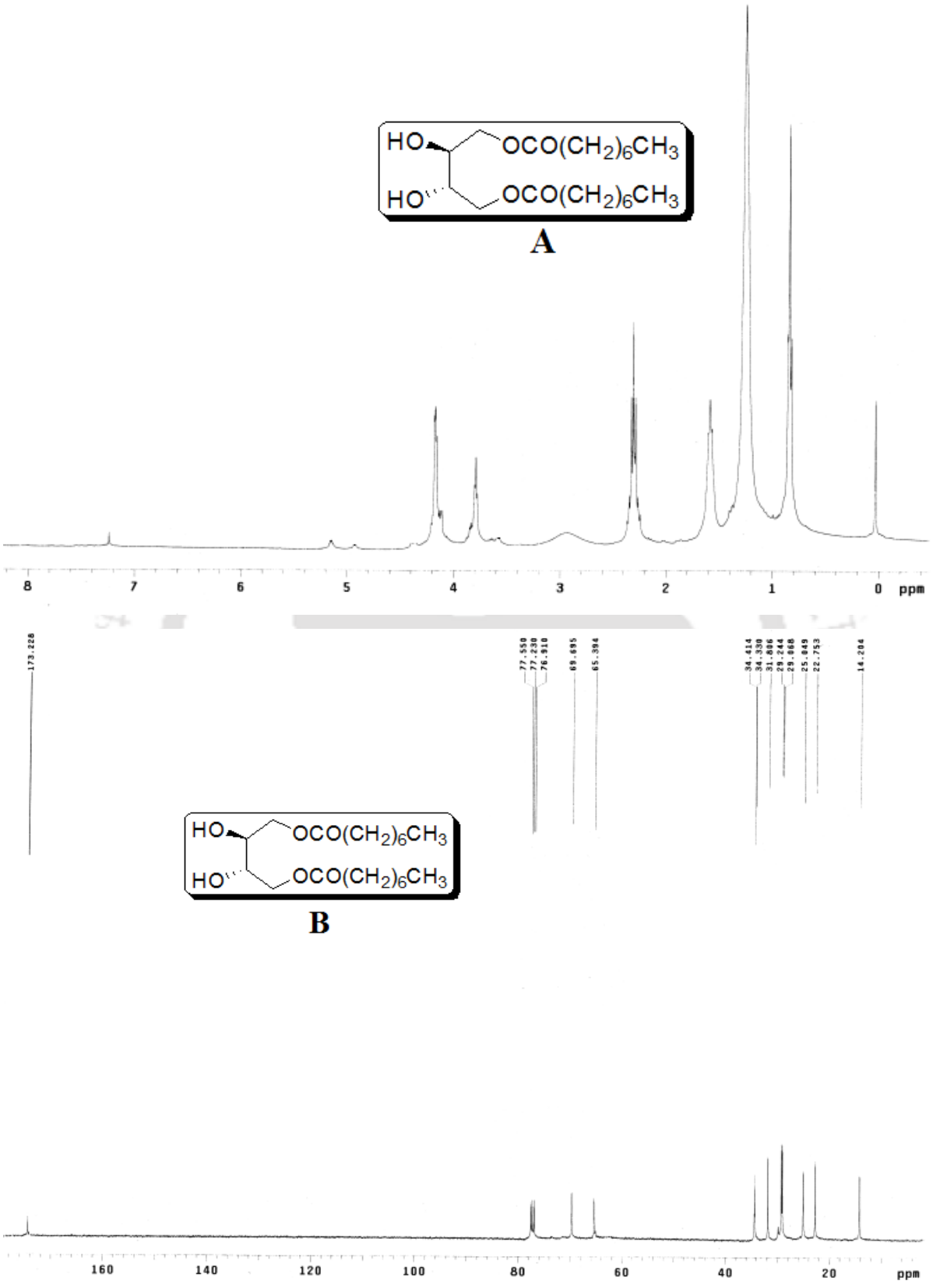

Figure 2.4.4: *^{1}H NMR (**A**) and ^{13}C NMR (**B**) of (2S,3S)-2,3-dihydroxy-4-(octanoloxy)butyloctanoate (**2b**)*

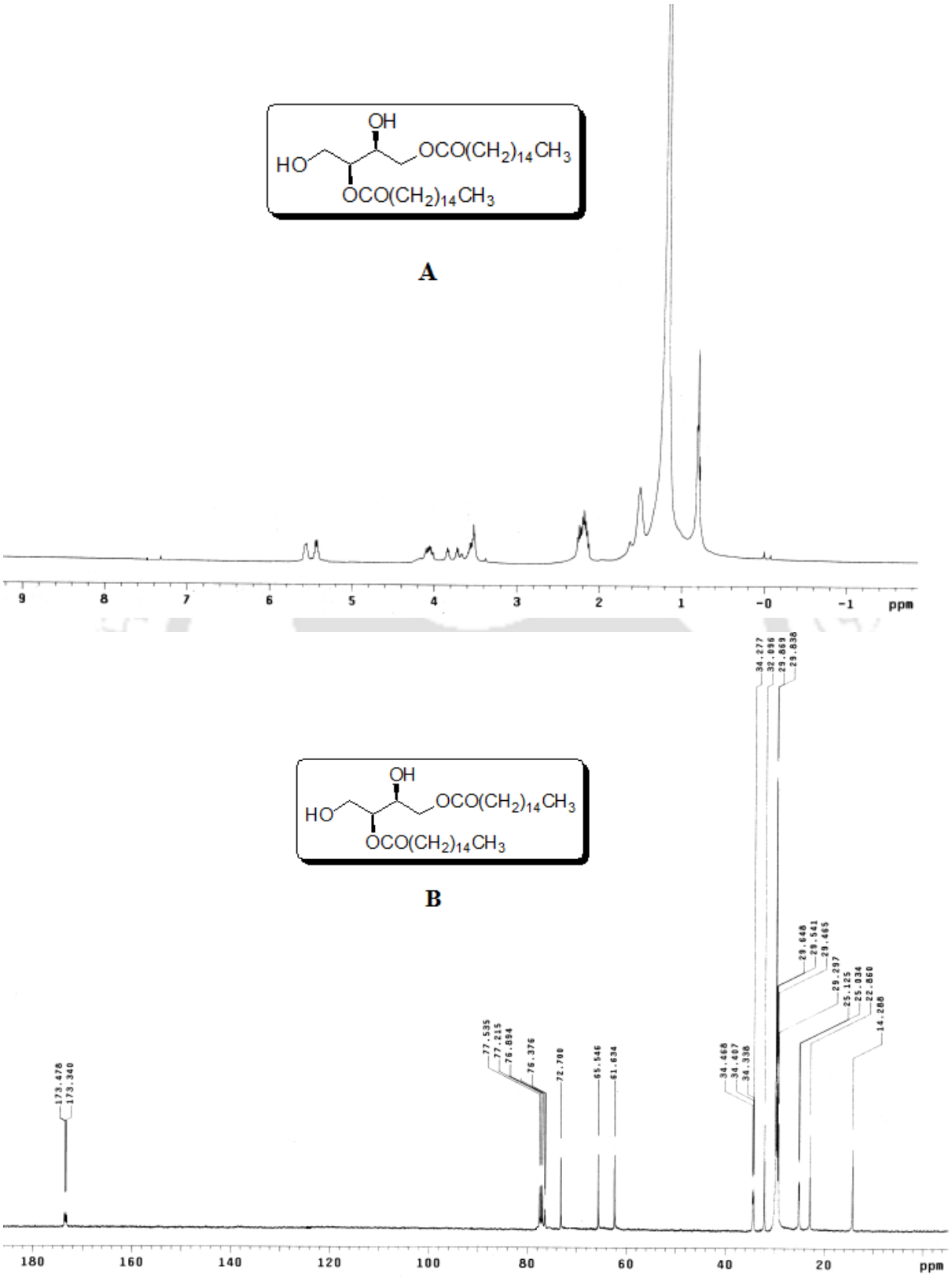

Figure 2.4.5: *^{1}H NMR (**A**) and ^{13}C NMR (**B**) of (2S,3S)-4-(hexadecanoyloxy)-1,3-dihydroxybutan-2-yl hexadecanoate (**3a**)*

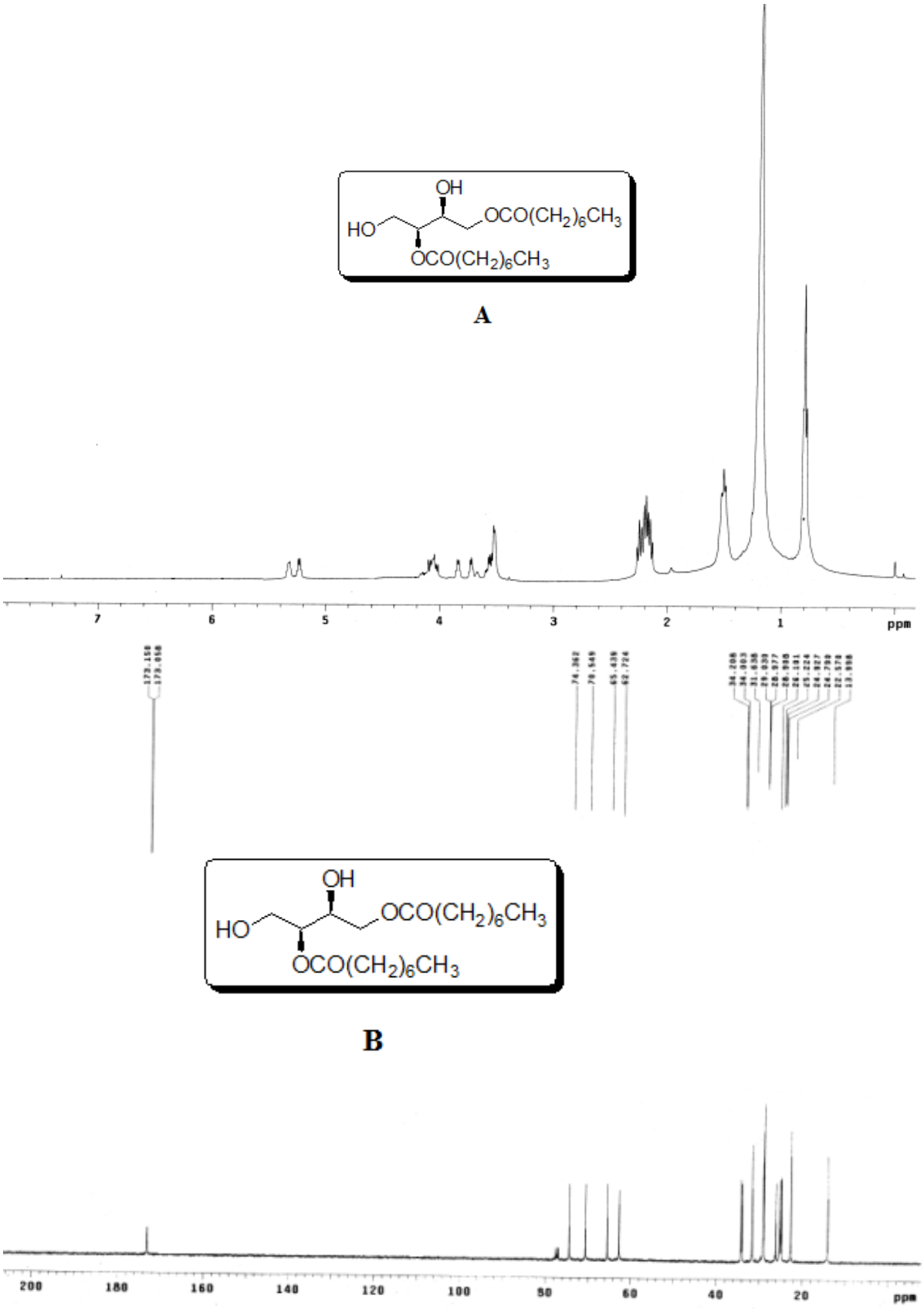

Figure 2.4.6: *^{1}H NMR (**A**) and ^{13}C NMR (**B**) of (2S,3S)-1,3-dihydroxy-4-(octanoyloxy)butane-2-yl octanoate (**3b**)*

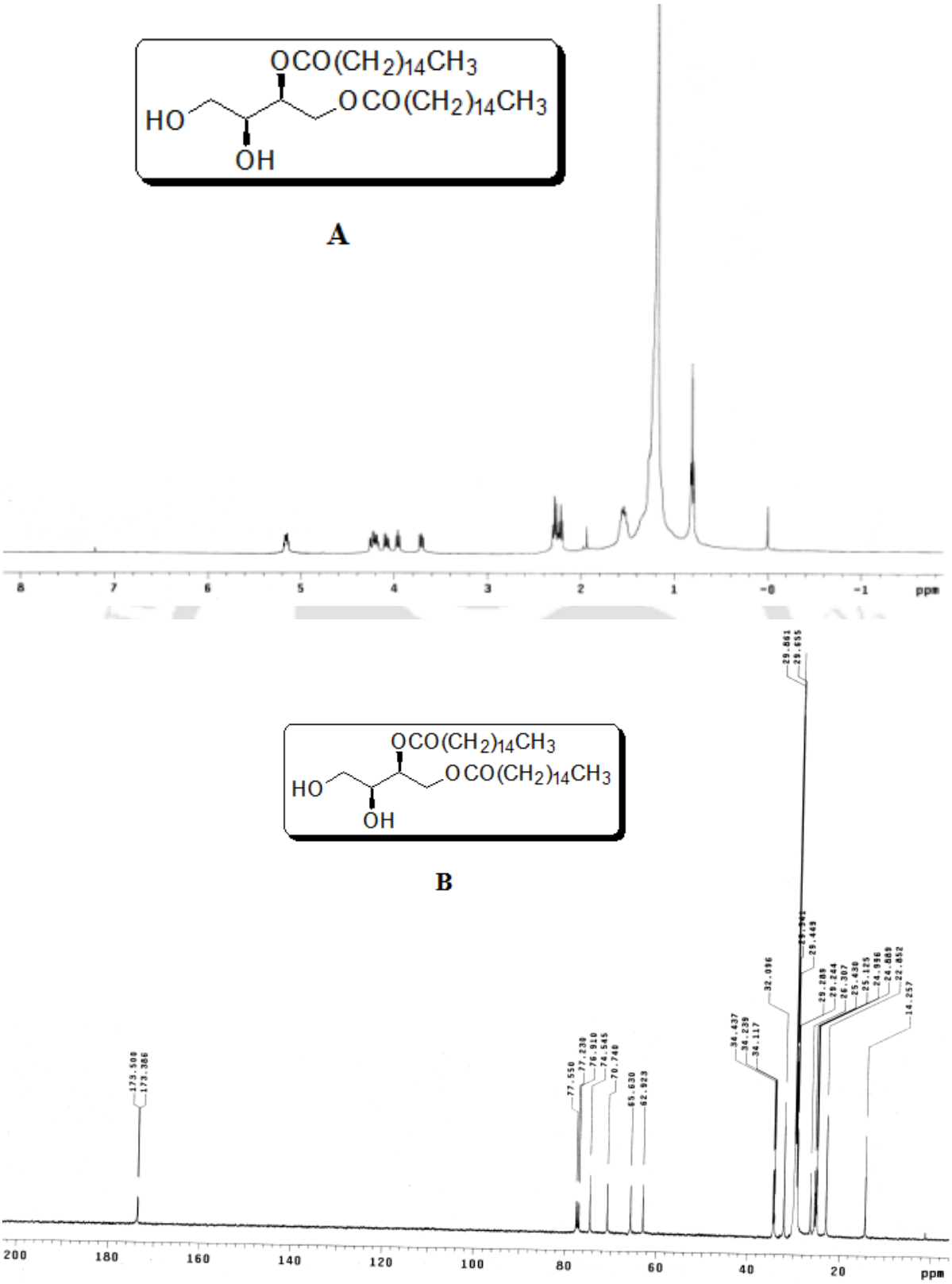

Figure 2.4.7: *^{1}H NMR (**A**) and ^{13}C NMR (**B**) of (2S,3S)-1-(hexadecanoyloxy)-3,4-dihydroxybutan-2-yl-hexadecanoate (**4a**)*

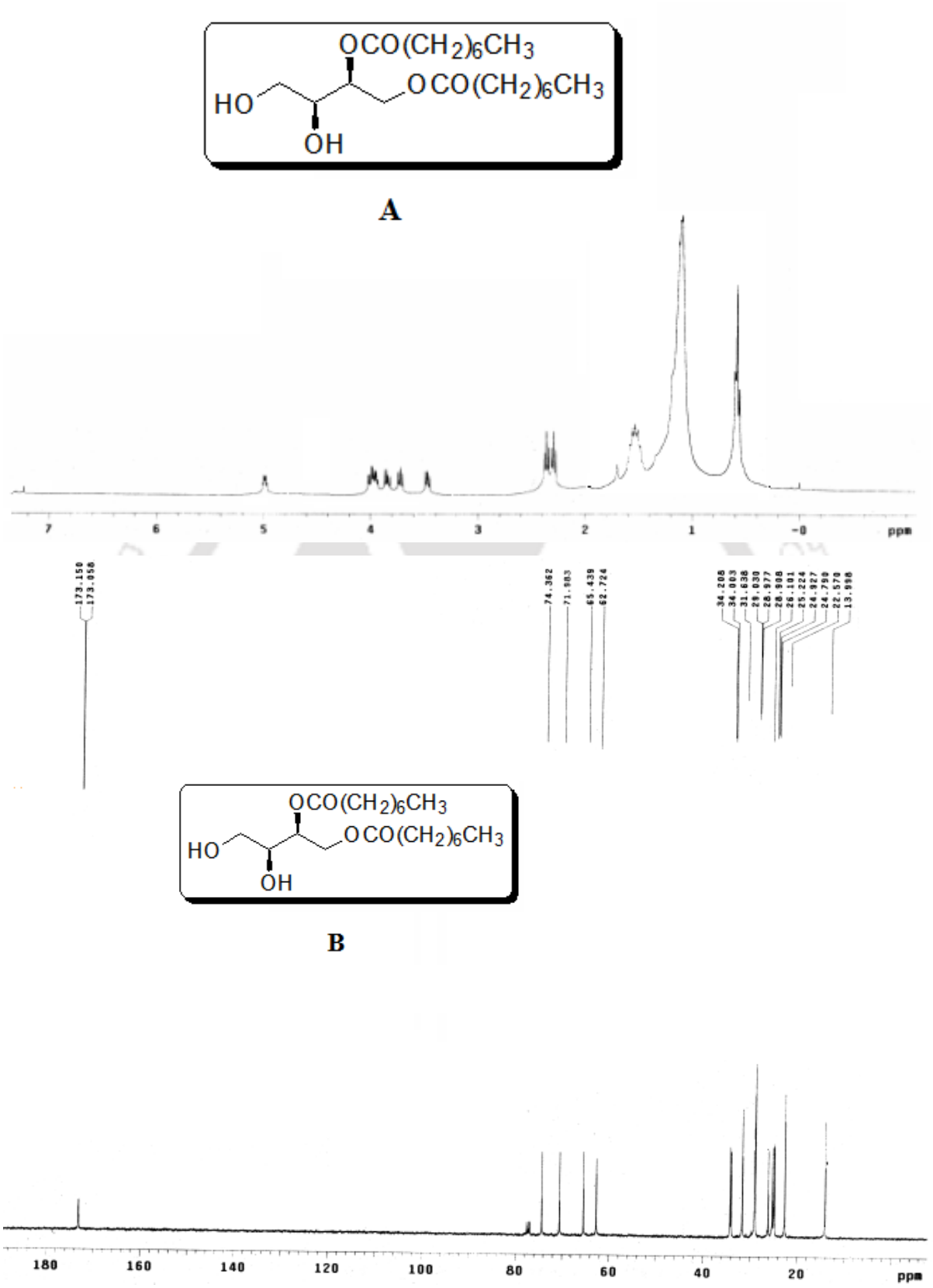

Figure 2.4.8: *^{1}H NMR (**A**) and ^{13}C NMR (**B**) of (2S,3S)-3,4-dihydroxy-1-(ocatnoyloxy)butane-2-yl octanoate (**4b**)*

CHAPTER 3

Development of Diacyltetrol Based Anionic Hybrid Lipids as Protein Kinase C (PKC)-C1 Domain Regulators

The present chapter demonstrates the design and synthesis of diacyltetrol based anionic hybrid lipids having both DAG and anionic phospholipid headgroups within the same molecule, such as diacyltetrol-phosphatidic acid (DAT-PA), diacyltetrol-phosphatidylserine (DAT-PS) and diacyltetrol-phosphatidylglycerol (DAT-PG)). It also describes the PKC-C1 domain binding properties of DAT-anionic hybrid lipids using Trp-fluorescence quenching assay both in monomeric form and under liposomal environment. Molecular docking analyses elucidate the binding orientation of the hybrid lipids within C1 domain binding sites of PKC isoforms.

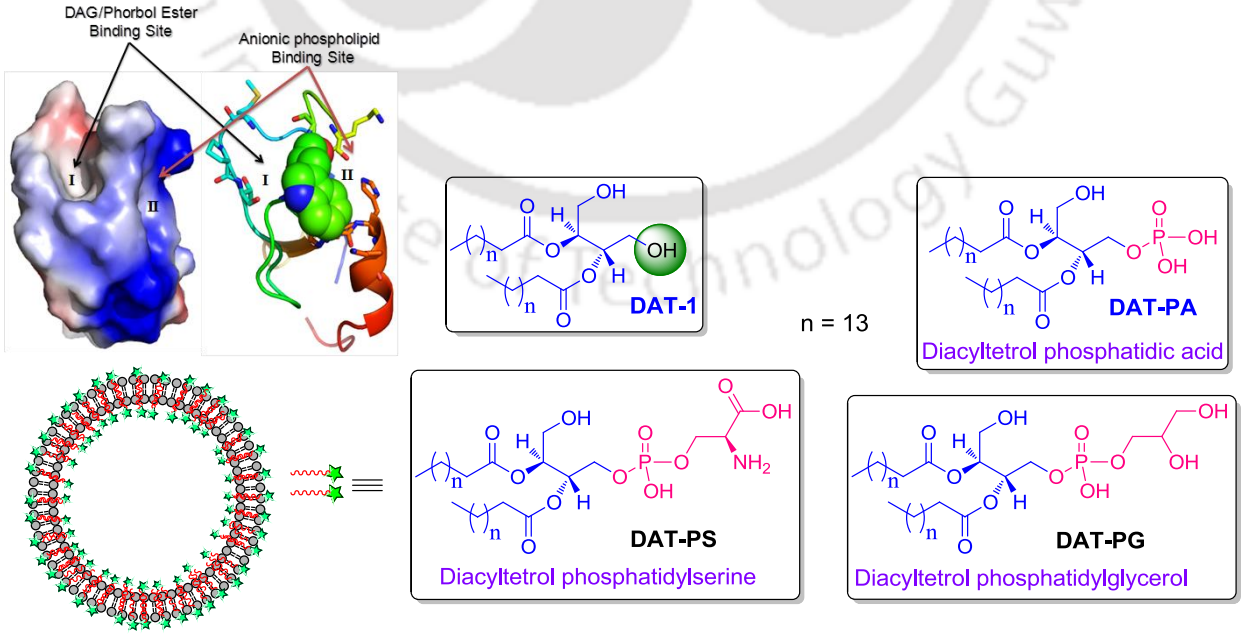

3.1. Background and Focus of the Present Work

The PKC isoforms are activated by DAGs and transmit their signal by phosphorylating specific proteins. The DAGs selectively interact with the C1 domain of PKC isoenzymes. This interaction induces their translocation to the discrete subcellular compartments. For some of the C1 domain containing proteins, such translocation leads to activation.[119,144] Detail mechanistic studies of PKC activation process shows that the cellular translocation of classical PKC isoenzymes to the plasma membrane is initially mediated by Ca^{2+} binding through C2 domain, followed by C1 domain-DAG interactions in the presence of anionic phospholipids. In contrast, only DAG binding to the C1 domain in the presence of anionic phospholipids activates novel PKC isozymes.[120,145] The C1 and C2 domains of PKC isoenzymes have strong binding affinities for anionic phospholipids, so it is difficult to use the whole-enzyme activity to characterize the role of anionic phospholipids in DAG binding affinity of PKCs. Previous studies also reported that the PKC-C1 domains have the determinants for the stereospecific interaction of the anionic phospholipids.[119,144,146,147] Accumulating evidences suggest that anionic phospholipids like PS, phosphatidic acid (PA) and phosphatidylglycerol (PG) enhance the DAG dependent membrane binding affinity and PKC activity; although the anionic phospholipid dependence varies considerably among the PKC isoenzymes. For the classical PKCs, PKCα and PKCβ_{II} prefer PS to PG, whereas PKCγ shows comparable affinity for PS and PG. Among the novel PKCs, PKCδ and PKCθ show a certain degree of PS selectivity, whereas PKCε shows preference for PA. In case of isolated C1b subdomains, similar selectivity have been observed for PKCδ, PKCθ and PKCε. Whereas the PKCβII-C1b subdomain shows little preference between PS and PG.[148-150] However, the reported experimental measurements used either only DAG or a combination of separate DAG and anionic lipid molecules in solution or under liposomal environment to determine the DAG dependent membrane binding capabilities of the effector proteins. Therefore, it is difficult to understand the role of both the lipid headgroups simultaneously in their effector protein binding capabilities. In addition, the modification of natural DAG structure, to attain higher membrane localization and activation of the targeted proteins in the presence of anionic lipids have been reported on several occasions, surprisingly, the design and synthesis of lipids having both DAG and anionic lipid headgroups within the same moiety (*Figure 3.1.1*) have never been attempted.

In the previous chapter, we described the synthesis of diacyltetrol (DAT) based lipids and detailed binding interaction study with C1 domains of PKC isoforms. The binding results revealed that compound **4** has shown 3 to 4 fold stronger binding affinity than DAGs for PKCδ-C1b and PKCθ-C1b, respectively.[151] To extend the utility of DAT based lipids as PKC modulators; we developed DAT-based hybrid anionic phospholipids. Hence, the present chapter describes the design, synthesis of diacyltetrol (DAT) based hybrid lipids having both DAG and anionic phospholipid headgroups within the same molecule and determining the anionic phospholipid dependent DAG binding affinity for the isolated C1 domains of PKCs. Herein, we report the synthesis of nine hybrid lipids with short and long chain lengths (DAT-PX_8, DAT-PX_{16} and DAT-PX_{18}; where PX = PA, PS, PG) for further biophysical analysis. We characterized the binding affinities of these hybrid lipids with the isolated C1 domains of PKCδ, PKCθ and PKCα. The measure binding parameters showed that PKCδ-C1b and PKCθ-C1a prefer DAT-PS and DAT-PA, respectively. Whereas, comparable binding affinity for all these hybrid lipids was observed for PKCα-C1b subdomain

Design and Synthesis of DAT-Anionic Hybrid Lipids─In the previous chapter we have reported a series of DAT based lipids as PKC-C1 domain regulators.[151] In our continued effort to develop improved PKC activators and understand the importance of anionic phospholipids in DAG/ligand binding, we selected DAT-**1** lipid with the 1,4-diol moiety. The structural analysis clearly showed that one of the hydroxymethyl groups of DAT-**1** lipid could be easily modified for further development of PKC regulators. The C1 domains of PKCs are reported to have anionic phospholipids dependent DAG binding affinity. So far, the anionic phospholipid dependencies in the DAG binding of the PKC-C1 domains were measured using separate molecules of DAG with PS/PA/PG phospholipids under liposomal environment.[148] To understand how C1 domain of PKCs will interact with the hybrid lipids having both DAG and anionic lipid headgroup, we synthesized a family of DAT based hybrid lipids, where one molecule of hybrid lipid contains either PS- or PA- or PG- headgroup along with the DAG headgroup (*Figure 3.1.1*). Therefore, these hybrid lipids are structural mimic of the DAG and PS/PA/PG lipids. The hydrophobic interactions are difficult to model. Hence, we also used hybrid lipids with longer chain length to study the impact of different functionality and 'lipid tail' on the binding affinity.

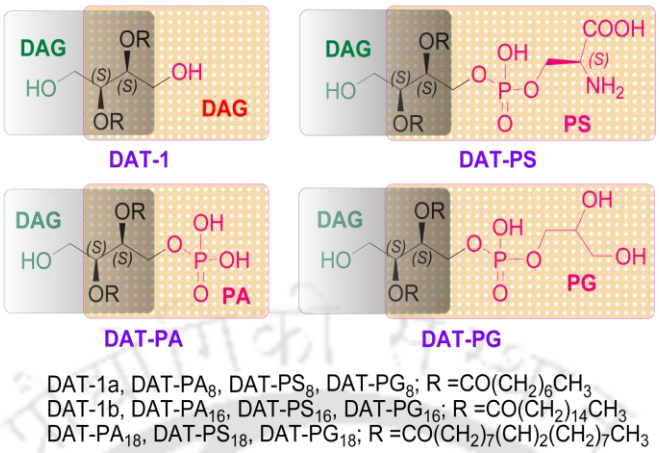

Figure 3.1.1: *Structure of the hybrid lipids used for the present study*.

It has also been reported that, lipids with unsaturated acyl groups are abundant in cellular membranes and more potent in PKC activation than the saturated ones.[58,145,152,153] Consequently, we used hybrid lipids with unsaturated fatty acid (oleic acid). The hybrid lipids were synthesized from commercially available (+)-diethyl L-tartrate. The C_2 symmetric diethyl L-tartrate was used to avoid mixing of enantiomeric products during synthesis. The choice of stereochemistry of lipids is crucial as the diversity of stereochemistry of these structures complicates the specificity. The (+)-diethyl- L-tartrate provides the stereochemistry as there in natural DAGs and anionic lipids at the sn-2 position.[151] The hybrid lipids DAT-PX (where PX = PA, PS, PG) were synthesized in seven to nine steps. DAT-PA_8 lipid was initially synthesized to investigate the role of additional PA headgroup within the same molecule in binding with the PKC-C1 domains. We first prepared protected alcohol **4** from (+)-diethyl L-tartrate in three steps according to the reported procedures (*Scheme 3.1.1*).[136,151] The phosphate headgroup, protected as a phosphotriester, was then installed using dibenzyl diisopropylphosphoramidite to afford compound **5** in high yield (92%).[136] Careful removal of the isopropylidene group under mild acidic conditions furnished diol **6** in 82% yield. The acyl chains were then introduced into the diol **6** using a standard *N,N'*-Dicyclohexylcarbodiimide (DCC) mediated coupling reaction with readily available caprylic acid, palmitic acid and oleic acid to produce compound **7a, 7b** and **7c** respectively in 86% yield. Finally, the benzyl groups were removed using catalytic amount of 10% Pd–C under hydrogenation conditions to access DAT-PA_8, DAT-PA_{16} and DAT-PA_{18} in

90% yield. We used DAT-PA_{16} with palmitic acid to study the impact of alkyl chain length on the binding affinity.

***Scheme 3.1.1*:** *Synthetic route to DAT-PA lipids*

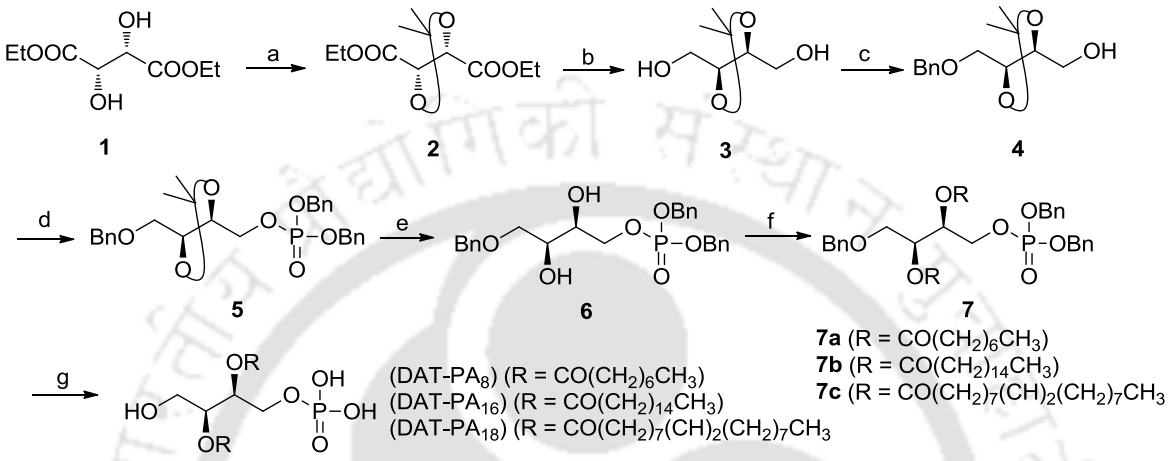

Reagents and conditions: (a) 2,2-dimethoxypropane, p-TsOH, toluene, Dean stark apparatus, 8 h, 84%; (b) $LiAlH_4$, THF, 0-65°C, 7 h, 98%; (c) BnBr, Ag_2O, CH_2Cl_2, rt, 8h, 84%; (d) dibenzyl diisopropylphosphoramidite, 1H-tetrazole, CH_2Cl_2, rt, 4h, then meta-chloroperbenzoic acid, -20 °C to rt, 1 h, 92%; (e) p-TsOH, methanol, rt, 4 h, 82%; (f) octanoic acid/palmitic acid/oleic acid, N,N-dicyclohexylcarbodiimide, 4-dimethylaminopyridine, CH_2Cl_2, rt, 12 h, 86%; (g) 10% Pd-C, H_2 (80 psi), rt, 30 min, 90%.

To understand the role of unsaturated lipids in PKC-C1 domain binding, we also used DAT-PA_{18} with oleic acid. However, during the synthesis of DAT-PA_{18} from **7c**, the deprotection of benzyl group in the presence of olefin double bond proved to be particularly challenging.[154] To avoid the problems associated with the uncontrolled hydrogenation, we optimized the time dependent regioselective catalytic hydrogenation reaction conditions. After several attempts, we found that 0.1 equivalent of 10% Pd-C in EtOH/EtOAc (1:3) solvent system under 80-psi pressure of hydrogen gas yielded desired product in sufficient amount within 30 minutes of the reaction time results were outlined in the Table 3.1.1.

Table 3.1.1: Optimization of the catalytic hydrogenation reaction conditions for the deportation of benzyl ether of intermediate ***7c***

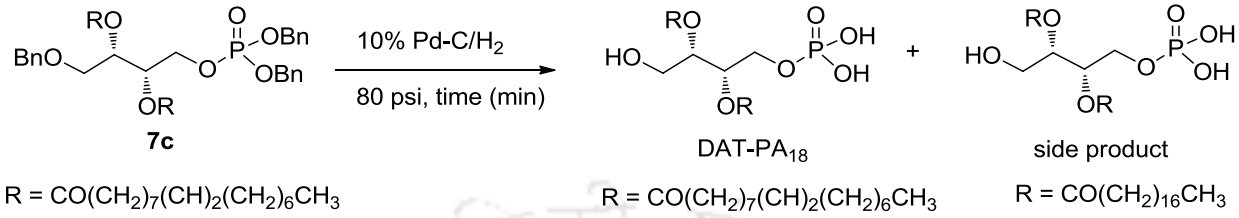

R = $CO(CH_2)_7(CH)_2(CH_2)_6CH_3$ R = $CO(CH_2)_7(CH)_2(CH_2)_6CH_3$ R = $CO(CH_2)_{16}CH_3$

Entry	Catalyst	Solvent system	Time(min)	% Yield ($DAT\text{-}PA_{18}$:side product)
1	Pd-C/H_2 (10%)	EtOH/EtoAc (1:3)	180 min	10:90
2	Pd-C/H_2 (10%)	EtOH/EtoAc (1:3)	120 min	20:80
3	Pd-C/H_2 (10%)	EtOH/EtoAc (1:3)	60 min	35:65
4	**Pd-C/H_2 (10%)**	**EtOH/EtoAc (1:3)**	**30 min**	**90:10**
5[a]	Pd-C/H_2 (10%)	EtOH/EtoAc (1:3)	15 min	60:05

[a] *starting material has been recovered.*

The PS dependency in the DAG binding of the PKC-C1 domains has been extensively studied by several research groups. To understand the importance of PS headgroup in the DAG binding of PKC-C1 domains, we synthesized $DAT\text{-}PS_8$ hybrid lipids from protected alcohol **4** (*Scheme 3.1.3*). Initially, we attempted to synthesize **16** by directly installing protected PS head headgroup onto protected alcohol **4**. However, removal of isopropylidene group under mild acidic environment led to a significant amount of hydrolysis of phosphotriester group. Thus, this approach was not feasible (*Scheme 3.1.2*). Therefore, we prepared **11** from protected alcohol **4** to optimize one-pot multicomponent reaction for the synthesis of DAT-PS compounds. To avoid the problems associated with the hydrolysis of phosphotriester group, we focused on the development of a route in which isopropylidene group would be removed, prior to the installation of protected PS head headgroup. For the efficient synthesis of DAT-PS compounds, the diol **9** was prepared from protected alcohol **4** using TBDPS protection under basic condition,[155] followed by careful removal of isopropylidene group under mild anionic condition (S*cheme 3.1.3*).[151] The silylated diol **9** was subjected to a DCC-mediated coupling reaction with caprylic acid, palmitic acid and octanoic acid resulted **10a, 10b** and **10c** respectively in 80-86% yield.

Scheme 3.1.2: *General approach for the synthesis of DAT-PS/PG lipids*

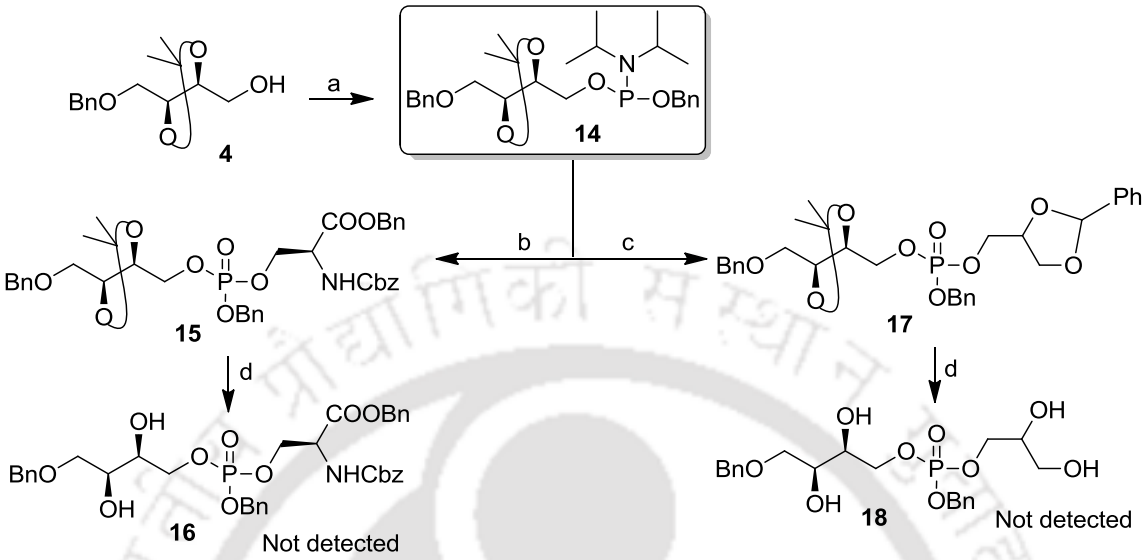

Reagents and conditions: (a) O-benzyl N,N,N',N'-tetraisopropyl phosphoramidite, 1H-tetrazole,CH_2Cl_2, rt, 4h, 72%. (b) benzyl (S)-1-((benzyloxy)carbonyl)-2-hydroxyethyl carbamate/(2-phenyl-1,3-dioxan-4-yl)methanol, 1H-tetrazole, CH_2Cl_2, rt, 5 h then meta-chloroperbenzoic acid, -20 °C to rt, 1 h, 75%; (c) (2-phenyl-1,3-dioxan-4-yl)methanol, 1H-tetrazole, CH_2Cl_2, rt, 5 h then meta-chloroperbezoic acid, -20 °C to rt, 1 h, 73%; (d) p-TsOH, methanol, rt, 4 h.

The TBAF-assisted removal of TBDPS group furnished the key intermediates **11a-c** in 98% yields.[155] One-pot multicomponent phosphorylation reaction of protected alcohols **11a-c**, protected serine[156] and O-benzyl *N,N,N',N'*-tetraisopropyl phosphorodiamidite in the presence of 1*H*-tetrazole, followed by oxidation using *meta*-chloroperbenzoic acid yielded phosphorylated compounds **12a-c**. Finally, the benzyl groups were removed using optimized catalytic hydrogenation reaction conditions, to access DAT-PS_8, DAT-PS_{16} and DAT-PS_{18} respectively in 90% yield. Similarly, to understand the importance of PG head group in DAG binding of PKC-C1 domains, we prepared DAT-PG series of hybrid lipid. The protected alcohol **11a-c** was coupled with the 1,2-O-benzylidene glycerol, using one-pot phosphorylation reaction conditions to furnish intermediate **13a-c** as shown in the Scheme 3.1.3.

The targeted 1,2-*O*-benzylidene glycerol was prepared from glycerol according to the reported procedures.[157,158] Finally, the deprotection of benzyl groups under optimized catalytic hydrogenation reaction conditions provided DAT-PG_8, DAT-PG_{16} and DAT-PG_{18} respectively in 90% yield (*Scheme 3.1.3*).

Scheme 3.1.3: *Optimized Synthetic route to DAT- PS/PG lipids*

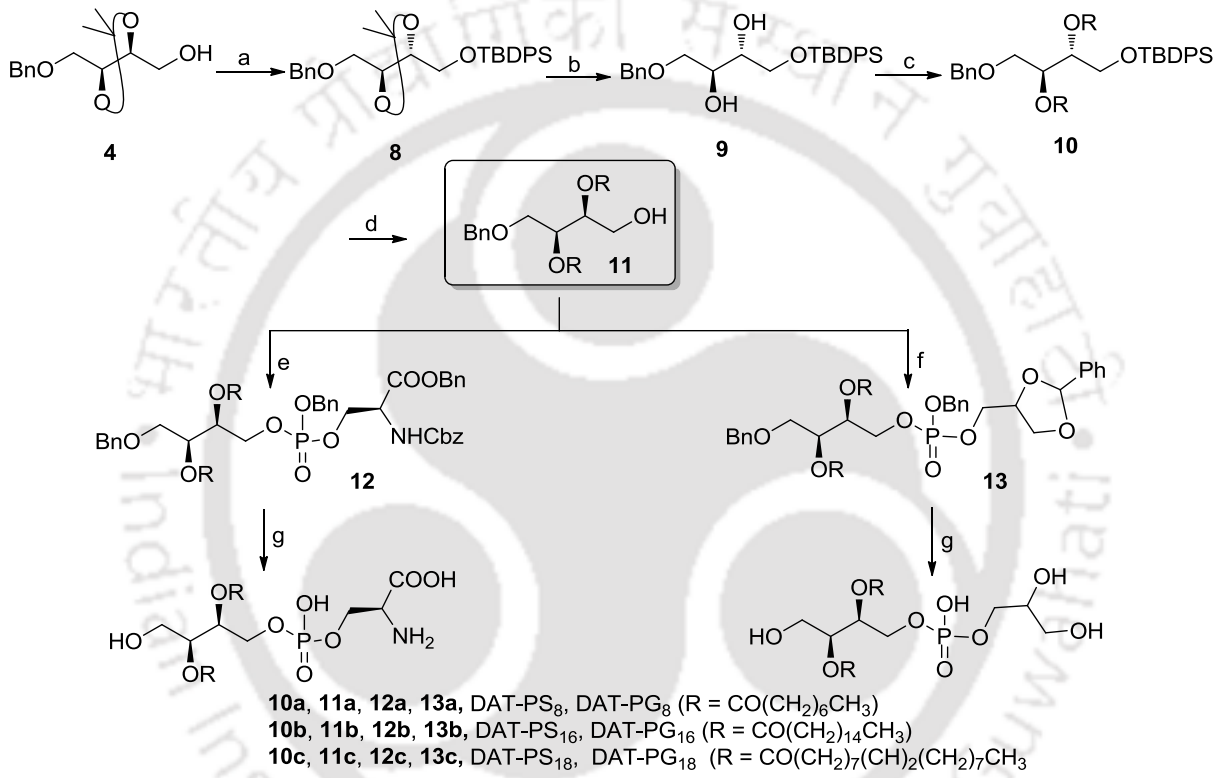

Reagents and conditions: (a) TBDPSCl, imidazole, 4-dimethylaminopyridine, CH_2Cl_2, rt, 12 h, 98%; (b) p-TsOH, methanol, rt, 4 h, 85%; (c) octanoic acid/palmitic acid/oleic acid, N,N-dicyclohexylcarbodiimide, 4-dimethylaminopyridine, CH_2Cl_2, rt, 12 h, 86%; (d) TBAF (solution 1.0 M in THF), 1 h, 98%; (e) O-benzyl N,N,N',N'-tetraisopropyl phosphoramidite, 1H-tetrazole, benzyl (S)-1-((benzyloxy)carbonyl)-2-hydroxyethyl carbamate/(2-phenyl-1,3-dioxan-4-yl)methanol, CH_2Cl_2, 5 h, rt, then meta-chloroperbenzoic acid, -20 °C to rt, 1 h, 83%; (f) O-benzyl N,N,N',N'-tetraisopropyl phosphorodiamidite, 1H-tetrazole, (2-phenyl-1,3-dioxan-4-yl)methanol, CH_2Cl_2, 5 h, rt, then meta-chloroperbenzoic acid, -20 °C to rt, 1 h, 83%; (g) 10% Pd-C, H_2 (80 psi), rt, 30 min, 90%.

Measurement of Protein Binding Parameters─ Structural and functional studies of the PKC-C1 domains have revealed that Thr-12, Leu-21, and Gly-23 residues play a crucial role in DAG binding. The hydrophobic residues present along the circumference of the binding pocket facilitate the insertion of the C1 domain into the membrane after DAG binding, thereby stabilizing the formation of the ternary (ligand-receptor-membrane) binding complex. Their membrane interaction is also facilitated by a ring of positively charged residues located around the middle of the domain that potentially interact with the anionic phospholipids like PS, PA, or PG (*Figure 3.1.2*).[11,150,151,160] In this study PKCα-C1a, PKCδ-C1b and PKCθ-C1b subdomains were used to measure the binding properties of the synthesized hybrid lipids in monomeric form by using intrinsic fluorescence quenching method and steady-state fluorescence anisotropy measurements. Förster resonance energy transfer (FRET)-based competitive binding assay under liposomal environment was also used to measure their ligand binding affinities and specificities.

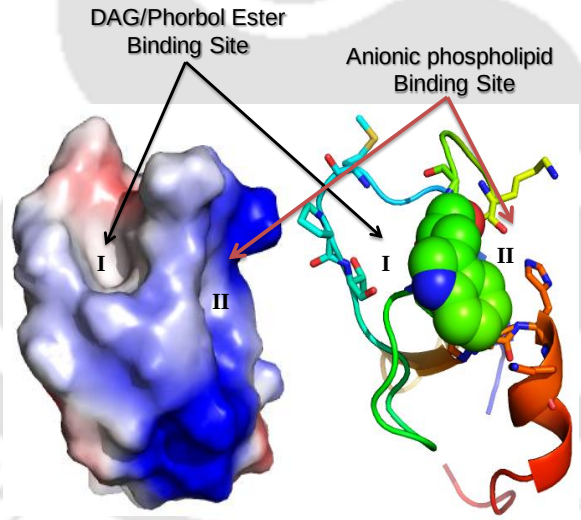

Figure 3.1.2: *Structure of PKCδ-C1b subdomain (1PTR). The arrows indicate the DAG/phorbol ester and anionic phospholipid binding sites. I and II indicate the ligand binding sites within the PKCδ-C1b subdomain.*

Interaction with Soluble Ligands— Fluorescence spectroscopy is a useful technique to detect ligand-induced change in protein conformation or microenvironment. The intrinsic fluorescence of the PKC-C1b/a subdomains is due to the presence of a single tryptophan (Trp-22), phenylalanine and tyrosine residues. The Trp-22 residue is also present close to the DAG binding pocket of the C1b/a subdomains of PKCδ, PKCθ and PKCα.[138,151,159] The ability of the proteins to bind ligands in monomeric form was calculated from the ligand-induced Trp-fluorescence quenching data (*Figure 3.1.3*). The calculated values showed that the hybrid lipids with different chain length interact with the C1b/a subdomain with highest binding affinity (1.49—2.07 μM) and other lipids with comparable binding affinities for all three proteins. We have recently reported that, the DAT-**1** with two hydroxymethyl groups compared to one in DAG showed ~2-fold stronger binding affinity for PKCδ-C1b subdomain.[151] An intriguing finding was the pivotal role played by the hybrid lipids in the binding of the C1b/a subdomains. The results showed that PKCδ-C1b subdomain has 5-fold stronger binding affinity for DAT-PS_8 than DAG_8.

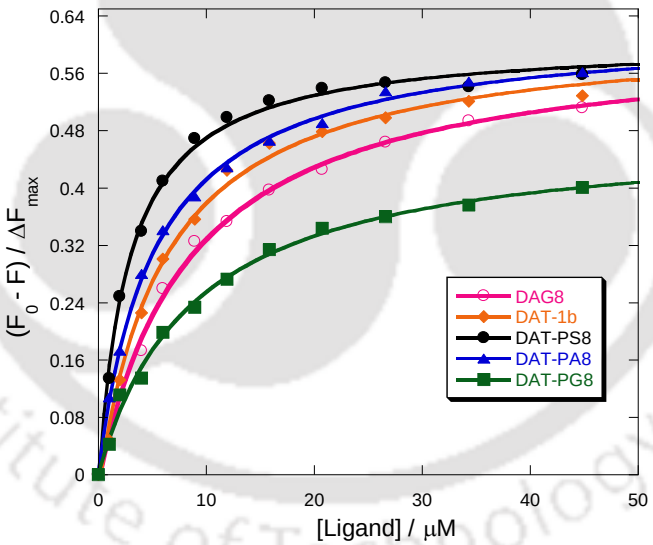

Figure 3.1.3: *Binding isotherms of ligands with PKCδ-C1b. Representative plot of fluorescence intensity of PKCδ-C1b (1 μM) in buffer (20 mM Tris, 160 mM NaCl, 50 μM $ZnSO_4$, pH 7.4) in the presence of varying concentration of DAG_8, DAT-**1b**, DAT-PS_8, DAT-PA_8 and DAT-PG_8, where F and F_0 are fluorescence intensity in the presence and absence of the ligands, respectively. The solid lines are nonlinear least squares best fit curves.*

The other anionic hybrid lipid, DAT-PA_8 showed ~2-fold stronger binding affinity, whereas, DAT-PG_8 did not show any substantial preference for PKCδ-C1b subdomain than DAG_8. In the case of PKCθ-C1b subdomain, although DAT-PA_8 showed 2.5-fold stronger binding affinity than DAG_8, but there was no significant differences in binding potencies for all the three hybrid lipids. However, no significant preference for the hybrid lipids was observed for PKCα-C1a subdomain.

To understand the importance of hydrophobicity of the ligands in C1-domain binding, a similar analysis was performed with the long chain hybrid lipids. All three proteins showed similar patterns of dependence on the hydrophobicity of the compounds (*Table 3.1.2*). For DAT-PX_8 and DAT-$PX_{16/18}$ (PX stands for PA, PS or PG) ligands, although there is a distinct difference in hydrophobicity, but the differences in binding affinities are small for all three proteins. This could be due to the binding orientations of proteins with the ligands.

Table 3.1.2: K_D (ML) values for the binding of ligands with the PKCδ-C1b, PKCθ-C1b, and PKCα-C1a proteins[a] at room temperature.

Compound	K_D (ML) (μM)		
	PKCδ-C1b	PKCθ-C1b	PKCα-C1a
DAG_8	12.41 ± 0.59	6.74 ± 0.54	14.58 ± 0.44
DAT-**1b**	5.85 ± 0.48	4.83 ± 0.36	8.78 ± 0.41
DAT-PA_8	5.35 ± 0.23	2.53 ± 0.26	5.98 ± 0.34
DAT-PS_8	2.47 ± 0.21	2.70 ± 0.17	8.85 ± 0.45
DAT-PG_8	8.89 ± 0.43	3.27 ± 0.22	5.58 ± 0.28
DAG_{16}	7.04 ± 0.43	6.35 ± 0.37	8.31 ± 0.23
PA_{16}	9.43 ± 0.45	—	—
PS_{16}	7.72 ± 0.57	—	—
PG_{16}	8.54 ± 0.62	—	—
DAG_{16} + PA_{16} (1:1)	6.43 ± 0.45	—	—
DAG_{16} + PS_{16} (1:1)	3.01 ± 0.35	—	—
DAG_{16} + PG_{16} (1:1)	6.44 ± 0.48	—	—
DAT-**1a**	4.31 ± 0.25	3.89 ± 0.30	6.85 ± 0.11
DAT-PA_{16}	4.26 ± 0.21	2.07 ± 0.10	5.46 ± 0.34
DAT-PS_{16}	1.84 ± 0.17	2.27 ± 0.19	5.66 ± 0.23
DAT-PG_{16}	5.34 ± 0.22	2.63 ± 0.31	4.83 ± 0.38
DAT-PA_{18}	3.23 ± 0.19	1.49 ± 0.11	4.66 ± 0.51
DAT-PS_{18}	1.60 ± 0.11	1.70 ± 0.18	5.54 ± 0.43
DAT-PG_{18}	4.26 ± 0.31	2.24 ± 0.12	4.52 ± 0.34

[a] *Protein, 1 μM in buffer (20 mM Tris, 160 mM NaCl, 50 μM $ZnSO_4$, pH 7.4) Values represent the mean ± S.D. from triplicate measurements.*

The overall higher binding affinities of the hybrid lipids with long chains were presumably due the interaction of long chains with the hydrophobic amino acids, surrounding the binding pocket of the C1 domains. Therefore, binding affinities of the hybrid lipids highlight the importance of ligand hydrophobicity and binding orientation. The hybrid lipids, DAT-PX_{16} showed stronger binding affinities for the PKCδ-C1b subdomain compared to only DAG_{16}, PS_{16}, PA_{16}, or PG_{16} lipids. This indicates that isolated PKC-C1 domains may first interact with the anionic lipids due to electrostatic interaction and then strongly interacts with the DAG. Another intriguing result was that there were substantial differences in the binding affinity between hybrid lipids and 1:1 lipid mixture of DAG with anionic phospholipids.

Steady-state fluorescence anisotropy measurements of the proteins suggest that the presence of the ligands in monomeric form increases the rigidity of the surrounding environment of the protein in a manner similar to that of DAGs (*Table 3.1.3).* Therefore, the increases in anisotropy values of the proteins in the presence of the ligands also support their ligand binding.

Table 3.1.3: Anisotropy[a] values of the ligands in the presence and absence of the PKCδ, PKCθ and PKCα C1b/a Proteins at room temperature.

Compound	PKCδ C1b	PKCθ C1b	PKCα C1a
buffer[b]	0.0746 (0.0007)	0.0682 (0.0222)	0.0522 (0.0071)
DAG_8[c]	0.2493 (0.0616)	0.3372 (0.0774)	0.1669 (0.0222)
DAT-**1b**[c]	0.3606 (0.0322)	0.3611 (0.0997)	0.4517 (0.0734)
DAT-PS_8[c]	0.4435 (0.0634)	0.4356 (0.0736)	0.3065 (0.0109)
DAT-PA_8[c]	0.2862 (0.0613)	0.4888 (0.0871)	0.3321 (0.0904)
DAT-PG_8[c]	0.3670 (0.0476)	0.3381 (0.1314)	0.2608 (0.0421)
DAG_{16}[c]	0.2737 (0.0630)	0.3993 (0.0814)	0.1958 (0.0188)
DAT-**1a**[c]	0.2953 (0.0786)	0.4413 (0.0758)	0.3802 (0.0165)
DAT-PS_{16}[c]	0.3509 (0.0761)	0.4525 (0.0914)	0.3417 (0.0075)
DAT-PA_{16}[c]	0.2828 (0.0694)	0.4713 (0.0631)	0.2843 (0.0887)
DAT-PG_{16}[c]	0.2773 (0.0304)	0.3282 (0.0620)	0.3542 (0.0571)
DAT-PS_{18}[c]	0.4341 (0.0126)	0.5147 (0.0357)	0.5730 (0.0166)
DAT-PA_{18}[c]	0.5664 (0.0368)	0.5038 (0.0648)	0.6770 (0.0469)
DAT-PG_{18}[c]	0.3856 (0.0475)	0.3827 (0.0821)	0.3841 (0.0407)

*[a]Values in parenthesis indicate standard deviations. [b]Protein, 1 μM in buffer (20 mM Tris, 160 mM NaCl, 50 μM $ZnSO_4$, pH 7.4). [c]**Ligands**, 10 μM; protein, 1 μM in buffer (20 mM Tris, 160 mM NaCl, 50 μM $ZnSO_4$, pH 7.4)*

Interaction with Ligand-Associated Liposomes—PKC proteins are reported to interact with the membrane through their lipid-binding C1 and C2 domains. The PKC-C1 domains have both a membranes binding surface and a lipid-binding groove. The binding properties of the isolated C1 domains with the ligands under liposomal environment were quantitatively measured by protein-to-membrane FRET-based binding assay. The Trp residue of the PKC-C1b/a subdomains serve as the FRET donor, and a low density of membrane-embedded, dansyl-PE (dPE) lipids serve as the acceptors.[159,161,162]

DAG_8 was titrated into the solution containing C1b/a-subdomain-bound liposomes. The decrease in the protein-to-membrane FRET signal (*Figure 3.1.4*) was monitored to measure the displacement of protein from the liposomes surface to the bulk solution, and apparent inhibitory constant [$K_I(DAG_8)_{app}$] calculation. Figure 3.1.5 represents DAG_8 promoted displacement of PKCδ-C1b subdomain from ligand associated liposomes (PC/PE/dPE/DAT-PX_{16}). The values of $K_I(DAG_8)_{app}$ depend on ligand concentration and the background lipid composition in the liposomes as well as the affinities of the C1b/a subdomains for ligands/DAG_8.

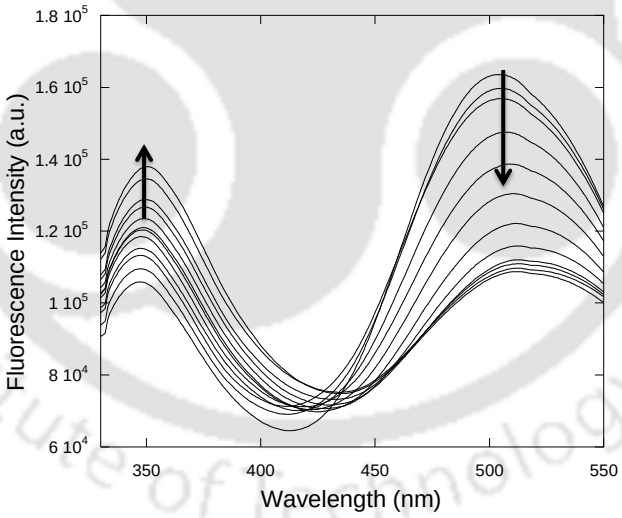

Figure 3.1.4*: Representative protein-to-membrane FRET experiment under liposomal environment. Addition of increased concentration of compound DAG_8 (0-80 μM) to PKCδ C1b subdomain (1 μM) bound to the active liposome (PC/PE/dPE/DAT-PS_{16} (75/15/5/5)) decreases the FRET signal at 505 nm. All the measurements were performed in 20 mM Tris, pH 7.4 containing 160 mM NaCl and 50 μM $ZnSO_4$.*

This assay showed that the synthesized hybrid lipids interact with the C1 domains under liposomal environment. The results also showed that higher concentration of DAG_8 was required for the displacement of PKCδ-C1b protein from the DAT-$PS_{16/18}$ associated liposomes. The PKCθ-C1b subdomain showed highest binding affinity for DAT-$PA_{16/18}$ associated liposomes. Whereas, PKCα-C1a subdomain showed slight preference for DAT-$PG_{16/18}$ lipids. Finally, the equilibrium dissociation constant ($K_D(L_{16/18})$) for the C1b/a subdomains binding to the liposome-associated targeted ligand was calculated using equation 4 (see experimental section 3.2.10).

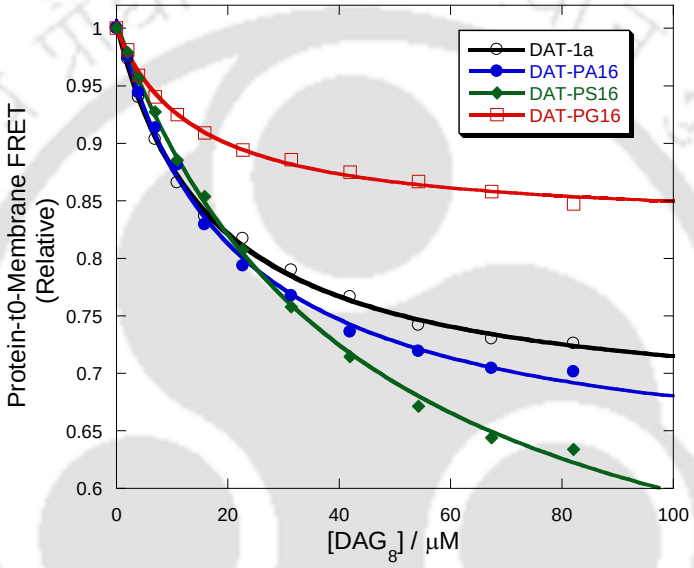

Figure 3.1.5: *Competitive displacement assay for the PKCδ-C1b subdomain (1 μM) bound to liposome containing ligands DAT-1a (○), DAT-PA_{16} (●), DAT-PS_{16} (♦), DAT-PG_{16} (□). The bound complex was titrated with the DAG_8.*

Comparison of the equilibrium dissociation constant also revealed that PKCδ-C1b and PKCθ-C1b subdomains have higher binding affinity for the DAT-$PS_{16/18}$ and DAT-$PA_{16/18}$ associated liposomes, respectively (*Table 3.1.4*). From the binding affinity results, it can be concluded that PKCδ-C1b, PKCθ-C1b and PKCα-C1a showed different binding affinities depending on the anionic phospholipids headgroup present in the hybrid lipids.

Table 3.1.4: Equilibrium parameters for PKCδ-C1b and PKCθ-C1b protein[a] binding to the ligand associated liposomes[b/c] at room temperature.

Compound	$K_I(DAG_8)_{app}$ (μM)			$K_D(L_{16/18})$ (nM)		
	PKCδ-C1b	PKCθ-C1b	PKCα-C1a	PKCδ-C1b	PKCθ-C1b	PKCα-C1a
DAT-1a	17.14 ± 1.21	**23.08 ± 2.48**	9.68 ± 1.32	883.50 ± 11.23	**533.13 ± 12.26**	6365.90 ± 33.23
DAT-PA_{16}	20.59 ± 1.90	**41.81 ± 3.23**	15.38 ± 1.38	686.08 ± 11.87	**136.99 ± 8.94**	1447.56 ± 39.32
DAT-PA_{18}	29.88 ± 3.23	**46.95 ± 5.89**	15.46 ± 1.80	318.75 ± 8.72	**86.20 ± 4.34**	1134.79 ± 23.27
DAT-PS_{16}	**43.65 ± 2.65**	32.88 ± 2.95	10.34 ± 1.83	**115.74 ± 7.86**	195.04 ± 8.91	3186.72 ± 29.21
DAT-PS_{18}	**46.26 ± 4.24**	34.72 ± 3.05	11.36 ± 2.55	**94.22 ± 6.89**	135.40 ± 10.09	2503.47 ± 28.12
DAT-PG_{16}	14.33 ± 7.67	**22.73 ± 1.91**	19.52 ± 1.57	1562.20 ± 14.17	**344.12 ± 15.29**	864.73 ± 19.23
DAT-PG_{18}	14.74 ± 1.99	**23.17 ± 1.86**	22.18 ± 2.21	1062.98 ± 25.89	**281.47 ± 9.81**	673.14 ± 4.29

*[a)]Protein (1 μM) in buffer (20 mM Tris, 150 mM NaCl, 50 μM $ZnSO_4$, pH 7.4). [b)]Active liposome composition, PC/PE/PS/dPE/DAT-**1a** (55/15/20/5/5). [c)]Active liposome composition, PC/PE/dPE/$Ligand_{16/18}$ (75/15/5/5).*

These results validate that not only DAG but also anionic phospholipids are crucial for binding of the C1 domains to the membrane. There are reports on plausible Trp fluorescence quenching by the anionic phospholipids, due to their ability to donate a proton from the phosphate ion to the indole chromophore.[163] Detailed structural analysis showed that the Trp residue present close to both the DAG/phorbol ester and anionic phospholipids binding sites (I and II, *Figure 3.1.2*). However, comparative protein binding measurements between 1:1 lipid mixture of DAG with anionic phospholipids and hybrid lipids clearly indicate that, the hybrid lipids have a certain degree of preference for the C1 domain, under the measure experimental conditions. All these measured binding parameters indicate that the hybrid lipids bind either to the DAG/phorbol ester-binding site or with the positively charged residues located around the C1 domain. However, these binding parameters do not point out the genuine binding site of the C1 domain for the hybrid lipids. To determine the actual binding site of the hybrid lipid within the C1 domain, we performed molecular docking analysis to both the possible binding sites (I and II, *Figure 3.1.2*). Theoretical binding energy for each conformation and distribution of ligands between the two sites showed that these hybrid lipids bind to both the site with little preference for anionic lipid binding site *(Figure 3.1.6)*.

Therefore, all these measurements indicate that the binding of these hybrid lipids binding to PKC C1 domain follows a critical mechanism. These lipids (i) either can binding to the DAG/phorbol ester binding site (I) and shows Trp fluorescence quenching due to its displacement from hydrophobic environment to aqueous environment, or (ii) bind to the anionic lipid binding site (II) and quench Trp fluorescence due to transfer of proton from phosphate to indole chromophore and subsequent DAG_8 binding to the site (I) can cause a conformational change leading to the displacement of protein from membrane surface.

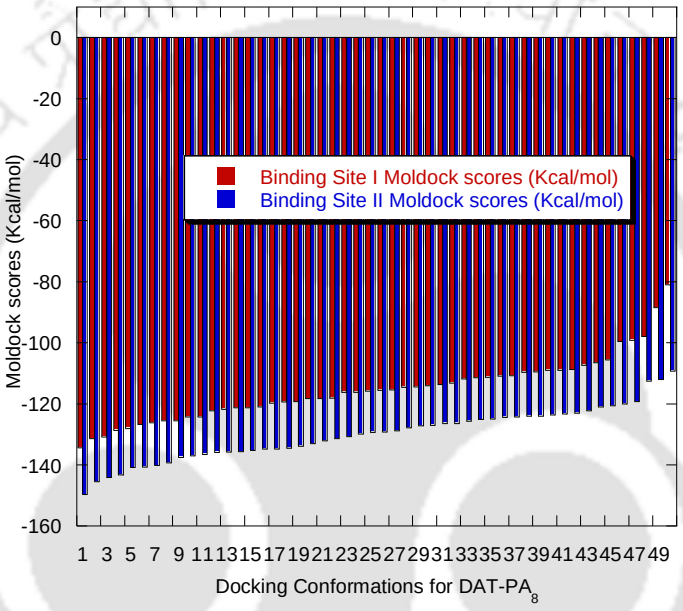

Figure 3.1.6: *Theoretical binding energy calculation and distribution of DAT-PA_8 between the DAG/phorbol ester binding site (I) and anionic lipid binding site (II) of the PKCδ-C1b subdomain (1PTR).*

Extent of Membrane Localization— We performed fluorescence quenching experiments using ligand-containing liposomes (PC/cholesterol/$ligand_{16}$/NBD-PE) to understand the relationship between the protein binding properties of the ligands and the extent of their localization at the bilayer/water interface. The NBD dye in NBD-PE lipid is embedded close to the bilayer/water interface, providing a useful marker for surface interactions of bilayer-active ligands.[151,159]

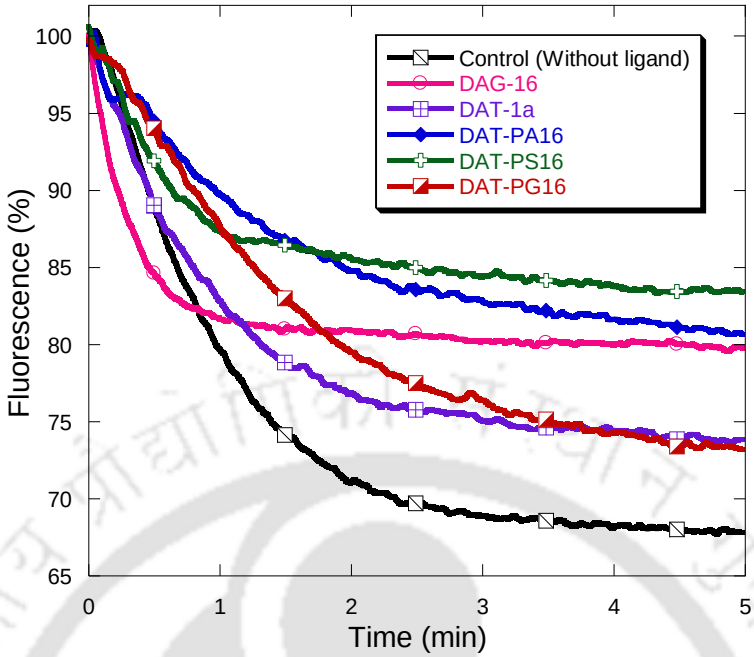

Figure 3.1.7: *Fluorescence quenching of NBD-PE embedded in PC/cholesterol/ligand$_{16}$/NBD-PE (44.5:44.5:10:1) liposomes. Sodium dithionite, 0.6 µM; control, without ligand.*

It is necessary to emphasize that, the rate of sodium dithionite-induced NBD fluorescence quenching showed significant differences among the ligand-associated liposomes (*Figure 3.1.7*). The measured quenching rates suggest that, the NBD dye became more "shielded" from the soluble dithionite quencher, because of the presence of ligands in the liposomes. The results also imply that these ligands are more localized at the bilayer/water interface and more accessible for protein binding than DAG and DAT-**1a**. Therefore, NBD-quenching result is in complete correlation with their protein binding properties in the liposome environment. Hence, measured binding parameters showed that the DAT based hybrid lipids interact differentially with C1b/a subdomain of PKCδ, PKCθ and PKCα, both in the monomeric form and under liposomal environment. Modifications of the acyl chain length showed a modest effect on the binding affinity. However, modification of headgroup of DAT based lipids showed a strong effect on the binding. Overall, these results validate that not only DAG but also anionic phospholipids are crucial for binding of the C1 domains to the membranes and long chain hybrid lipids can differentially influence the in vitro membrane interaction properties of the PKCδ, PKCθ, and PKCα.

Therefore, the hydrid lipid-C1 domain binding is driven by both electrostatic and hydrophobic interactions. However, it is important to emphasize that the hybrid lipid specificity of the C1 domains is not in accordance with the reported anionic lipid specificity, measured using isolated DAG and anionic phospholipids. The specificity and binding affinity difference among the three proteins could be due to the difference in the interacting residues and areas of the activator-binding sites. The binding results also show that these compounds have higher binding affinity for PKCθ-C1b than for PKCδ-C1b and PKCα-C1a, possibly because of the additional hydrogen bonds. The molecular docking analysis indicate that the hybrid lipids can interact with the C1 domain through both DAG/phorbol ester binding site and anionic phospholipid binding site with slight preference for the second one. However, the relative binding parameters clearly showed that these hybrid lipids bind to the C1 domains and presence of additional anionic lipid headgroup within the same molecule enhanced the C1 domain binding affinity and specificity of the hybrid lipids.

Conclusion

In conclusion, this chapter demonstrated the detailed synthesis of diacyltetrols (DATs) based anionic hybrid lipids, and their protein binding properties. Tetrol based hybrid lipids DAT-$PX_{8/16/18}$ with long (palmitic acid and oleic acid) and short chain (octanoic acid) fatty acids were synthesized from (+)-diethyl-L-tartrate. Synthesis of these hybrid lipids from the scratch provided the ability to generate pure samples of a single lipid structure and freedom to explore the role of hydroxymethyl group and anionic lipid headgroups in protein binding. These tetrol-based hybrid lipids are structural mimic of DAG and anionic phospholipids having both DAG and anionic phospholipid headgroups within the same molecule. The fluorescence based protein binding parameters were measured in monomeric form and under the liposomal environment. The measured results show that these lipids interact with the PKC-C1 domain in an isoform-specific manner and the presence of anionic lipid headgroup plays a significant role in their binding properties. PKCδ-C1b specifically interacts with DAT-PS lipid, whereas, PKCθ-C1b and PKCα-C1a prefers DAT-PA and DAT-PG to the other lipids. This also makes these hybrid lipids as potential regulator of PKC isoforms and can be further developed as research tools or lead compound in drug development. This study should help account for different cellular function

and regulation capabilities of the proteins in which both DAG and anionic phospholipid binding sites resides.

The abilities of these flexible tetrol based lipid and/or anionic hybrid lipids encouraged us to design (hydroxymethyl)phenyl ester analogues as PKC-C1 domain activators. The (hydroxymethyl)phenyl ester analogues contain the required hydroxymethyl group and ester groups, but with phenyl backbone instead of glycerol or tetrol backbones in DAG or DATs, respectively.

3.2. Experimental Section

3.2.1. Instrumentations and Characterization

As described in chapter 2 section 2.2.1.

3.2.2. General Procedure for the Deprotection of Isopropylidene Group (I)[151]:

To a stirring solution of isopropylidene protected compounds (1.0 equiv) in methanol (5 mL), *p*-TsOH (0.1 equiv) was added and stirring was continued at room temperature for 4 h. After completion of the reaction (monitored by TLC), the solvent was removed under reduced pressure to yield a residue. The residue was further dissolved in dichloromethane (10mL) and washed with a saturated solution of sodium bicarbonate (3×). The organic layer was dried over anhydrous Na_2SO_4 and concentrated under reduced pressure. Purification by silica gel column chromatography and a gradient solvent system of 20–30% ethyl acetate to hexane yielded diol derivatives.

3.2.3. General Procedure for the Preparation of Esters (II)[151]: Caprylic acid/palmitic acid/oleic acid (2.2 equiv), dicyclohexylcarbodiimide (2.2 equiv) and *N*,*N*-dimethylaminopyridine (0.1 equiv) was added to a solution of protected alcohol (1.0 equiv.) in anhydrous dichloromethane (5 mL), under a N_2 atmosphere. Stirring was continued for 12 h at room temperature. After completion of the reaction, the reaction mixture was filtered and washed (3×) with dichloromethane. The filtrate was concentrated under reduced pressure, and the

column chromatography was performed with silica gel, and a gradient solvent system of 2–5% ethyl acetate to hexane to yielded corresponding esters.

3.2.4. General Procedure for the Deprotection of Benzyl Groups (III): The removal of benzyl ether group using 0.1 equivalents of 10% Pd-C, under 80 psi of H_2 gas for 3 h produced the desired compounds (yield ~ 90%) with saturated tail groups. Unfortunately, in case of oleoyl compounds reduction of oleic double was detected. Removal of benzyl protecting groups in the presence of olefin double bond proved to be particularly challenging. To overcome this problem, the time dependent regioselective catalytic hydrogenation reaction conditions were optimized. Several trials were attempted with Pd-C catalyst concentrations, solvent systems and the reaction time. However, the reaction with 0.1 equivalents of 10% Pd-C under 80 psi of H_2 gas in EtOH/EtoAc (1:3) solvent system produced the targeted compound within 30 min. After completion of the reaction, the catalyst (Pd–C) was filtered off through a pad of Celite and washed with 30 ml of MeOH. Removal of solvent under reduced pressure yielded the targeted compounds.

3.2.5. General Procedure for the Deprotection of TBDPS Group (IV)[156]: To a stirring solution of TBDPS protected compound (1.0 equiv) in THF (5.0 mL) was added commercially available TBAF (2.0 equiv, 1.0 M solution in THF) at room temperature and stirring was continued for 1 h. After completion of the reaction, the solvent was removed under reduced pressure to yield a residue. The residue was dissolved in EtOAc (20 mL) and washed with a saturated solution of sodium bicarbonate (3×). The organic layer was dried over anhydrous Na_2SO_4 and concentrated under reduced pressure. Column chromatography with silica gel and a gradient solvent system of 7–10% ethyl acetate to hexane yielded alcohol derivatives.

3.2.6. General Procedure for the One-pot Phosphorylation of Protected Alcohols to Prepare DAT-PS and DAT-PG Derivatives (V): To an ice-cooled stirring suspension of O-benzyl *N*,*N*,*N*′,*N*′-tetraisopropyl phosphoramidite (1.1 equiv) and 1*H*-tetrazole (6.0 equiv), protected alcohol (1.0 equiv) in anhydrous dichloromethane (2 mL) was

added under N_2 atmosphere. After continuous stirring for 30 min benzyl, (S)-1-((benzyloxy)carbonyl)-2-hydroxyethylcarbamate or (the 2-phenyl-1,3-dioxan-4-yl)methanol (1.0 equiv) in anhydrous dichloromethane (2 mL) was added. The reaction mixture was stirred for another 5 h at room temperature and cooled to -20 °C, and a solution of *meta*-chloroperbenzoic acid (1.5 equiv) in dichloromethane (2 mL) was added. Finally, the reaction mixture was stirred for 1 h at room temperature, diluted with dichloromethane (30 mL), washed (3×) with 10% aqueous $NaHCO_3$ (10 mL) and brine (10 mL). The organic layer was dried over anhydrous Na_2SO_4 and concentrated under reduced pressure. Column chromatography with silica gel and a gradient solvent system of 27–30% ethyl acetate to hexane yielded corresponding phosphates compound.

3.2.7. Synthesis of Dibenzyl ((4S,5S)-5-((benzyloxy)methyl)-2,2-dimethyl-1,3-dioxolan-4-yl)methyl phosphate (5)[154]: To a stirring solution of protected alcohol **4** (252 mg, 1.0 mmol) in anhydrous dichloromethane, (2.5 mL) suspension of dibenzyldiisopropylphosphoramidite (518 mg, 1.5 mmol) and *1H*-tetrazol (420 mg, 6.0 mmol) in anhydrous dichloromethane (2.5 mL) were added at room temperature under a N_2 atmosphere. Stirring was continued for another 4 h and cooled to -20 °C, and a solution of *meta*-chloroperbenzoic acid (259 mg, 1.5 mmol) was added. The reaction mixture was stirred for 1 h at room temperature, diluted with 30 mL of dichloromethane, washed (10% aqueous $NaHCO_3$, brine). Resulting solution was dried over anhydrous Na_2SO_4 and concentrated under reduced pressure. Column chromatography with silica gel and a gradient solvent system of 25–30% ethyl acetate to hexane yielded phosphoester **5** (470 mg, 92%).

3.2.8. Synthesis of (((4S,5S)-5-((benzyloxy)methyl)-2,2-dimethyl-1,3dioxolan-4-yl)methoxy)(*tert* butyl)diphenylsilane (8)[156]: To an ice-cooled stirring solution of *tert*-butylchlorodiphenylsilane (TBDPS-Cl) (340 µL, 1.31 mmol) in anhydrous dichloromethane (5 mL) were added triethylamine (182 µL, 1.31), catalytic amount of DMAP (15 mg, 0.12 mmol), and a solution of protected alcohol **4** (300 mg, 1.19 mmol) in dry dichloromethane (5 mL). The resulting mixture was allowed to warm up to room temperature and stirring was continued for 12 h at room temperature. After completion of the reaction, the solvent was removed under reduced

pressure to yield a residue. The residue was dissolved in dichloromethane (20 mL) and washed with saturated solution of $NaHCO_3$. The organic layer was dried over anhydrous Na_2SO_4 and concentrated under reduced pressure. Purification by silica gel column chromatography and a gradient solvent system of 3–5% ethyl acetate to hexane yielded **8** (572 mg, 98%).

3.2.9. Protein Purification: The PKCδ and PKCθ-C1b subdomains were expressed in *E. Coli* as a GST-tagged protein, purified by glutathione sepharose column and the GST tag were removed by the thrombin treatment using methods similar to those reported earlier.[138,151,159,164]

3.2.10. Fluorescence Measurements: To calculate the binding parameters under membrane free system, ligand-induced Trp fluorescence quenching measurements were performed on a Fluoromax-4 spectrofluorometer at room temperature. The stock solutions of compounds were freshly prepared by first dissolving complexes in spectroscopic-grade dimethylsulfoxide (DMSO) and then diluted with buffer. The amount of DMSO was kept less than 3% (by volume) for each set of experiment and had no effect on any experimental results. For fluorescence titration, protein (1 μM) and varying concentration of ligands were incubated in a buffer solution (20 mM Tris, 150 mM NaCl, 50 μM $ZnSO_4$, pH 7.4) at room temperature. Protein was excited at 280 nm, and emission spectra were recorded from 300 to 550 nm.[159] Proper background corrections were made to avoid the contribution of buffer and dilution effect.

The resulting plot of Trp fluorescence as a function of ligand concentration was subject to nonlinear least-squares best-fit analysis to calculate the apparent dissociation constant for ligands (K_D(ML)), using eq 1, which describes binding to a single independent site.

$$(F_0 - F) = \Delta F_{max}\left(\frac{[x]}{[x]+K_D(ML)}\right) + C \qquad (1)$$

Where, F and F_0 represented the fluorescence intensity at 339 nm in the presence and the absence of ligand respectively. The ΔF_{max} represents the calculated maximal fluorescence change; [x] represents the total monomeric ligand concentration.

Fluorescence anisotropy measurements were also performed on the same fluorimeter using similar methods described earlier.[159] All anisotropy values of the proteins in the absence or presence of compounds are the mean values of three individual determinations. The degree (r) of anisotropy in the tryptophan fluorescence of the proteins was calculated using eq 2, at the

peak of the protein fluorescence spectrum, where I_{VV} and I_{VH} are the fluorescence intensities of the emitted light polarized parallel and perpendicular to the excited light, respectively, and $G = I_{VH}/I_{HH}$ is the instrumental grating factor.

$$r = \frac{(I_{VV} - GI_{VH})}{(I_{VV} + 2GI_{VH})} \qquad (2)$$

Analysis of protein-to-membrane FRET based binding assay was used to measure the binding affinity and specificity of the selected ligands under a liposomal environment. In this assay, membrane-bound C1 domain was displaced from liposomes (PC/PE/dPE/Ligand$_{16/18}$ (75/15/5/5)) by the addition of the DAG_8. The vesicles composed of PC/PE/PS/dPE (60/15/20/5) and PC/PE/PS/dPE/DAT-**1a** (55/15/20/5/5) were used as control and for DAT-**1a** lipid, respectively. The stock solution of DAG_8 was titrated into the sample containing C1 domain (1 μM) and excess liposome (100 μM total lipid) in a buffer solution (20 mM Tris, 150 mM NaCl, 50 μM $ZnSO_4$, pH 7.4) at room temperature. The competitive displacement of protein from the membrane was quantitated using protein-to-membrane FRET signal (λ_{ex} = 280 nm and λ_{em} = 505 nm). Control experiments were performed to measure the dilution effect under similar experimental condition and the increasing background emission arising from direct dPE excitation. Protein-to-membrane FRET signal values as a function of DAG_8 concentration were subjected to nonlinear least-squares-fit analysis using eq 3 to calculate apparent equilibrium inhibition constants ($K_I(DAG_8)_{app}$) for DAG_8. Where, [x] represents the total DAG_8 concentration and ΔF_{max} represents the calculated maximal fluorescence change.

$$F = \Delta F_{max}\left(1 - \frac{[x]}{[x] + K_I(DAG_8)_{app}}\right) + C \qquad (3)$$

The equilibrium dissociation constant ($K_D(L_{16})$) for the binding of the C1 domains to the ligand-associated liposomes was calculated from eq 4, using $K_D(ML)$ and $K_I(DAG_8)_{app}$ values. Where, $[L_{16}]_{free}$ is the free ligand concentration (2.63 ± 0.04 μM). During calculation, the ligand concentration in the liposome interior was ignored, because of their inaccessibility for the protein. Thus, the protein accesses about half of lipids in the liposomes. The ligand concentration was used excess relative to the protein. The free ligand concentration was calculated by assuming that most of the protein would bind to the liposome and equimolar amount of ligand can be subtracted from the accessible ligand.

$$K_I(DAG_8)_{app} = K_D(ML)\left(1 + \frac{[L_{16}]_{free}}{K_D(L_{16})}\right) \qquad (4)$$

3.2.11. Extent of Membrane Localization: The extent of localization of the ligands at the liposome interface was studied by NBD fluorescence quenching method, using PC/Cholesterol/Ligand$_{16}$/NBD-PE liposomes (44.5/44.5/10/1) in 50 mM Tris buffer, pH 8.2, containing 150 mM NaCl, according to the reported procedure.[151,159]

3.3. Characterization of the Synthesized Compounds

Dibenzyl ((4S,5S)-5-((benzyloxy)methyl)-2,2-dimethyl-1,3-dioxolan-4-yl)methyl phosphate (5): Colorless oil. $[\alpha]^{20}_{D}$ = -10.1 (c 0.1, CH_2Cl_2); ^{1}H NMR (400 MHz, $CDCl_3$): δ_{ppm} 7.36-7.30 (m, 15H), 5.11-5.00 (m, 4H), 4.54 (s, 2H), 4.16-4.11 (m, 2H), 4.08-3.97 (m, 2H), 3.59-3.50 (m, 2H), 1.39 (s, 3H), 1.37 (s, 3H); ^{13}C NMR (100 MHz, $CDCl_3$): δ_{ppm} 137.9, 135.8, 135.6, 128.8, 128.6, 128.5, 128.1, 128.0, 127.8, 127.7, 110.1, 76.4, 73.6, 70.3, 69.5, 67.4, 67.3, 27.1, 26.9; ^{31}P NMR (161.9 MHz, $CDCl_3$): δ_{ppm} 0.59; HRMS (ESI) Calcd for $C_{28}H_{33}O_7PNa^+$ $[M+Na]^+$: 535.1862, Found: 535.1863.

Dibenzyl (2S,3S)-4-(benzyloxy)-2,3-dihydroxubutyl phosphate (6): Using the general procedure (I), starting from compound **5** (350 mg, 0.684 mmol) compound **6** (265 mg, 82%) was isolated as colorless oil. $[\alpha]^{20}_{D}$ = -22.4 (c 0.2, CH_2Cl_2); ^{1}H NMR (400 MHz, $CDCl_3$): δ_{ppm} 7.23-7.16 (m, 15H), 4.91 (d, 4H, J = 8.4 Hz), 4.39 (s, 2H), 4.00-3.95 (m, 2H), 3.74-3.68 (m, 2H), 3.45-3.43 (m, 2H); ^{13}C NMR (100 MHz, $CDCl_3$): δ_{ppm} 137.9, 135.7, 135.6, 128.6, 128.5, 128.0, 127.8, 73.5, 71.6, 70.5, 69.6, 69.4, 68.8; ^{31}P NMR (161.9 MHz, $CDCl_3$): δ_{ppm} 0.59; HRMS (ESI) Calcd for $C_{25}H_{29}O_7PNa^+$ $[M+Na]^+$: 495.1549, Found: 495.1546.

(2S,3S)-4-(benzyloxy)-1-{[bis(benzyloxy)phosphoryl]oxy}-3-(octanoyloxy)butan-2-yl octanoate (7a): Using the general procedure (II), starting from compound **6** (100 mg, 0.212 mmol) compound **7a** (132 mg, 86%) was isolated as colorless oil. $[\alpha]^{20}_{D}$ = -20.3 (c 0.2, CH_2Cl_2); ^{1}H NMR (400 MHz, $CDCl_3$): δ_{ppm} 7.35-7.25 (m, 15H), 5.37-5.34 (m, 1H), 5.29-5.25 (m, 1H), 5.04-4.98 (m, 4H), 4.45 (d, 2H, J = 6.4 Hz), 4.20-4.15 (m, 1H), 4.11-4.04 (m, 1H), 3.57-3.49 (m, 2H), 2.29 (t, 2H, J = 7.6 Hz), 2.22 (t, 2H, J = 7.8 Hz), 1.64-1.53 (m, 4H), 1.16 (br s, 16H), 0.87 (t, 6H, J = 6.2 Hz); ^{13}C NMR (100 MHz, $CDCl_3$): δ_{ppm} 172.8, 172.7, 137.6, 135.7, 128.6, 128.5, 128.0, 127.9, 127.8, 127.7, 73.3, 70.1, 69.9, 69.5, 67.9, 65.7, 34.2, 34.1, 31.7, 29.1, 29.0, 24.9,

24.8, 22.6, 14.1; ^{31}P NMR (161.9 MHz, $CDCl_3$): δ_{ppm} 0.09; HRMS (ESI) Calcd for $C_{41}H_{57}O_9PNa^+$ $[M+Na]^+$: 747.3638, Found:.747.3637.

(2S,3S)-4-(benzyloxy)-1-{[bis(benzyloxy)phosphoryl]oxy}-3-(hexadecanoyloxy)butan -2-yl hexadecanoate (7b): Using the general procedure (II), starting from compound **6** (100 mg, 0.21 mmol) compound **7b** (173 mg, 86%) was isolated as colorless oil. $[\alpha]^{20}_D$ = -15.4 (c 0.2, CH_2Cl_2); ^{1}H NMR (400 MHz, $CDCl_3$): δ_{ppm} 7.33-7.26 (m, 15H), 5.36-5.33 (m, 1H), 5.27-5.24 (m, 1H), 5.00 (t, 4H, J = 7.6 Hz), 4.45 (d, 2H, J = 7.2 Hz), 4.20-4.14 (m, 1H), 4.10-4.00 (m, 1H), 3.57-3.49 (m, 2H), 2.30 (t, 2H, J = 7.4 Hz), 2.22 (t, 2H, J = 7.8 Hz), 1.68-1.52 (m, 4H), 1.26 (br s, 48H), 0.88 (t, 6H, J = 6.8 Hz); ^{13}C NMR (100 MHz, $CDCl_3$): δ_{ppm} 172.9, 172.8, 137.6, 135.8, 128.6, 128.5, 128.1, 128.0, 127.9, 127.8, 73.4, 70.1, 70.0, 69.6, 68.0, 65.8, 34.3, 34.2, 32.0, 29.8, 29.6, 29.5, 29.4, 29.2, 25.0, 24.9, 22.8, 14.2; ^{31}P NMR (161.9 MHz, $CDCl_3$): δ_{ppm} 0.08; HRMS (ESI) Calcd for $C_{57}H_{89}O_9PNa^+$ $[M+Na]^+$: 971.6142, Found: 971.6142.

(2S,3S)-4-(benzyloxy)-1-{[bis(benzyloxy)phosphoryl]oxy}-3-[(9Z)-octadec-9-enoyloxy]butan-2-yl (9Z)-octadec-9-enoate (7c): Using the general procedure (II), starting from compound **6** (100 mg, 0.212 mmol) compound **7c** (170 mg, 80%) was isolated as yellow oil. $[\alpha]^{20}_D$ = -11.6 (c 0.1, CH_2Cl_2); ^{1}H NMR (400 MHz, $CDCl_3$): δ_{ppm} 7.43-7.19 (m, 15H), 5.39-5.30 (m, 4H), 5.25-5.22 (m, 1H), 5.17-5.98 (m, 4H), 4.52 (s, 2H), 4.40-4.36 (m, 1H), 4.20-4.10 (m, 1H), 3.97-3.95 (m, 1H), 3.73-3.63 (m, 1H), 3.55-3.44 (m, 1H), 2.37-2.26 (m, 4H), 2.00 (m, 8H), 1.62-1.60 (m, 4H), 1.30 (br s, 40H), 0.88 (t, 6H, J = 6.8 Hz); ^{13}C NMR (100 MHz, $CDCl_3$): δ_{ppm} 173.4, 173.2, 137.6, 135.5, 135.4, 134.9, 130.0, 129.7, 129.3, 128.7, 128.4, 128.3, 128.2, 128.0, 127.8, 127.7, 127.6, 127.5, 127.3, 126.9, 73.5, 71.4, 70.9, 69.2, 68.8, 67.3, 64.7, 34.2, 34.1, 31.9, 29.8, 29.7, 29.5, 29.3, 29.2, 29.1, 27.2, 26.6, 24.9, 24.8, 22.7, 14.2; ^{31}P NMR (161.9 MHz, $CDCl_3$): δ_{ppm} 1.73; HRMS (ESI) Calcd for $C_{61}H_{93}O_9P$ $[M+K]^+$: 1039.6194, Found: 1040.4760.

[(2S,3S)-4-hydroxy-2,3-bis(octanoyloxy)butoxy]phosphonic acid (DAT-PA$_8$): Using the general procedure (III), starting from compound **7a** (130 mg, 0.179 mmol) compound DAT-PA$_8$ (73 mg, 90%) was isolated as colorless oil. $[\alpha]^{20}_D$ = -12.6 (c 0.1, EtOH); ^{1}H NMR (400 MHz, $CDCl_3$): δ_{ppm} 5.26-5.19 (br s, 2H), 4.36-4.15 (br s, 4H), 2.29 (m, 4H), 1.55 (m, 4H), 1.23 (br s,

16H), 0.83 (m, 6H); ^{13}C NMR (100 MHz, $CDCl_3$): δ_{ppm} 176.7, 174.2, 71.2, 69.4, 67.4, 63.3, 34.2, 31.9, 29.8, 29.3, 29.1, 25.1, 24.9, 22.8, 14.2; ^{31}P NMR (161.9 MHz, $CDCl_3$): δ_{ppm} 1.09; HRMS (ESI) Calcd for $C_{20}H_{39}O_9PNa^+$ $[M+Na]^+$: 477.2229, Found: 477.2230.

[(2S,3S)-2,3-bis(hexadecanoyloxy)-4-hydroxybutoxy]phosphonic acid (DAT-PA$_{16}$): Using the general procedure (III), starting from compound **7b** (160 mg, 0.169 mmol) compound DAT-PA_{16} (104 mg, 90%) was isolated as white solid. m.p: 45-46 $^{\circ}$C; $[\alpha]^{20}_D$ = -9.8 (c 0.1, EtOH); ^{1}H NMR (400 MHz, $CDCl_3$): δ_{ppm} 5.23-5.06 (m, 2H), 4.79 (br s, 2H), 4.31-3.59 (m, 2H), 2.28-2.19 (m, 4H), 1.53-1.51 (m, 4H), 1.18 (br s, 48H), 0.8 (t, 6H, J = 6.6 Hz); ^{13}C NMR (100 MHz, $CDCl_3$): δ_{ppm} 176.9, 173.9, 71.0, 69.0, 66.2, 63.3, 34.1, 31.9, 29.6, 29.3, 29.1, 24.9, 24.8, 22.6, 13.9; ^{31}P NMR (161.9 MHz, $CDCl_3$): δ_{ppm} 1.44; HRMS (ESI) Calcd for $C_{36}H_{71}O_9P\ Na^+$ $[M+Na]^+$: 701.4733, Found: 701.4733.

[(2S,3S)-4-hydroxy-2,3-bis[(9Z)-octadec-9-enoyloxy]butoxy]phosphonic acid (DAT-PA$_{18}$): Using the general procedure (III), starting from compound **7c** (150 mg, 0.15 mmol) compound DAT-PA_{18} (99 mg, 90%) was isolated as a yellow oil. $[\alpha]^{20}_D$ = -18.2 (c 0.1, EtOH); ^{1}H NMR (400 MHz, $CDCl_3$): δ_{ppm}. 5.26 (m, 4H), 4.22-4.19 (m, 1H), 4.10-4.40 (m, 2H), 3.86-3.84 (m, 1H), 3.72-3.67 (m, 1H), 3.62-3.58 (m, 1H), 3.10 (br s, 1H), 2.78-2.24 (m, 4H), 1.94-1.93 (m, 8H), 1.55 (m, 4H), 1.23 (br s, 40H), 0.81 (t, 6H, J = 6.7 Hz); ^{13}C NMR (100 MHz, $CDCl_3$): 173.4, 129.8, 129.6, 78.0, 75.0, 64.0, 62.1, 36.6, 36.4, 34.0, 31.8, 29.7, 29.6, 29.5, 29.3, 29.1, 29.0, 27.1, 25.0, 24.8, 23.7, 23.6, 22.6, 14.0; ^{31}P NMR (161.9 MHz, $CDCl_3$): δ_{ppm} -1.59; HRMS (ESI) Calcd for $C_{40}H_{76}O_9P$ $[M+H]^+$: 731.5227, Found: 731.5228.

(((4S,5S)-5-((benzyloxy)methyl)-2,2-dimethyl-1,3dioxolan-4-yl)methoxy)(*tert*-butyl) diphenylsilane (8): Colourless oil. $[\alpha]^{20}_D$ = -14.3 (c 0.1, CH_2Cl_2); ^{1}H NMR (400 MHz, $CDCl_3$): δ_{ppm} 7.68-7.63 (m, 5H), 7.44-7.28 (m, 10H), 4.59 (dd, 2H, J = 12.0 Hz, J = 12.0 Hz), 4.26-4.21 (m, 1H), 3.92-3.88 (m, 1H), 3.81-3.73 (m, 2H), 3.67-3.63 (m, 1H), 3.60-3.56 (m, 1H), 1.43 (s, 3H), 1.41 (s, 3H), 1.03 (s, 9H); ^{13}C NMR (100 MHz, $CDCl_3$): δ_{ppm} 138.2, 135.7, 133.2, 129.9, 128.5, 127.8, 127.7, 109.5, 78.4, 76.9, 73.6, 71.1, 64.3, 27.3, 27.1, 26.9, 19.3; HRMS (ESI) Calcd for $C_{30}H_{38}O_4SiNa^+$ $[M+Na]^+$: 513.2437, Found: 513.2439.

[(2S,3S)-4-(benzyloxy)-2,3-dihydroxybutoxy](tert-butyl)diphenylsilane (9): Using the general procedure (I), starting from compound **8** (550 mg, 1.12 mmol) compound **9** (429 mg, 85%) was isolated as colorless oil. $[\alpha]^{20}_{D}$ = -26.7 (c 0.2, CH_2Cl_2); ^{1}H NMR (400 MHz, $CDCl_3$): δ_{ppm} 7.60-7.55 (m, 5H), 7.35-7.14 (m, 10H), 4.41 (dd, 2H, J = 11.6 Hz, J = 11.2 Hz), 3.77-3.72 (m, 3H), 3.66-3.56 (m, 2H), 3.45-3.42 (m, 1H), 2.62 (br s, 2H), 0.97 (s, 9H); ^{13}C NMR (100 MHz, $CDCl_3$): δ_{ppm} 138.1, 135.8, 135.7, 135.0, 133.2, 130.1, 129.9, 128.6, 128.5, 128.1, 128.0, 127.8, 79.7, 72.8, 72.7, 71.9, 63.9, 26.9, 19.4, 19.3; HRMS (ESI) Calcd for $C_{27}H_{35}O_4Si$ $[M+H]^+$: 451.2305, Found: 451.2302.

(2S,3S)-4-(benzyloxy)-1-[(tert-butyldiphenylsilyl)oxy]-3-(octanoyloxy)butan-2-yl octanoate (10a): Using the general procedure (II), starting from compound **9** (200 mg, 0.44 mmol) compound **10a** (266 mg, 86%) was isolated as colorless oil; $[\alpha]^{20}_{D}$ = -11.3 (c 0.2, CH_2Cl_2); ^{1}H NMR (400 MHz, $CDCl_3$): δ_{ppm} 7.67-7.63 (m, 5H), 7.43-7.27 (m, 10H), 5.40-5.37 (m, 1H), 5.21-5.17 (m, 1H), 4.58 (dd, 2H, J = 12.0 Hz, J = 12.0 Hz), 4.35-4.26 (m, 1H), 4.19-4.12 (m, 1H), 3.83-3.66 (m, 2H), 2.29-2.20 (m, 4H), 1.58-1.55 (m, 4H), 1.26 (br s, 16H), 1.05 (s, 9H), 0.87 (t, 6H, J = 6.2 Hz); ^{13}C NMR (100 MHz, $CDCl_3$): δ_{ppm} 173.4, 173.0, 138.1, 135.8, 135.7, 135.6, 133.3, 133.2, 133.1, 129.9, 128.5, 128.0, 127.9, 78.0, 75.5, 73.2, 70.5, 62.7, 34.3, 34.2, 31.8, 29.2, 29.1, 26.9, 25.1, 25.0, 24.9, 22.7, 19.3, 19.2, 14.2; HRMS (ESI) Calcd for $C_{43}H_{63}O_6Si$ $[M+H]^+$: 703.4394, Found: 703.4398.

(2S,3S)-4-(benzyloxy)-1-[(tert-butyldiphenylsilyl)oxy]-3-(hexadecanoyloxy)butan-2-yl hexadecanoate (10b): Using the general procedure (II), starting from compound **9** (200 mg, 0.44 mmol) compound **10b** (354mg, 86%) was isolated as colorless oil. $[\alpha]^{20}_{D}$ = -13.8 (c 0.1, CH_2Cl_2); ^{1}H NMR (400 MHz, $CDCl_3$): δ_{ppm} 7.67-7.63 (m, 5H), 7.43-7.25 (m, 10H), 5.40-5.36 (m, 1H), 5.21-5.17 (m, 1H), 4.58 (dd, 2H, J = 12.0 Hz, J = 12.0 Hz), 4.35-4.26 (m, 1H), 4.20-4.11 (m, 1H), 3.82-3.66 (m, 2H), 2.28-2.19 (m, 4H), 1.57-1.55 (m, 4H), 1.25 (br s, 48H), 1.05 (s, 9H), 0.88 (t, 6H, J = 6.8 Hz); ^{13}C NMR (100 MHz, $CDCl_3$): δ_{ppm} 173.3, 173.1, 138.1, 135.8, 135.7, 135.6, 133.3, 133.1, 129.9, 128.4, 128.0, 127.9, 127.8, 78.0, 75.5, 73.2, 70.5, 62.7, 34.3, 34.2, 32.1, 29.8, 29.6, 29.5, 29.4, 29.3, 26.9, 25.1, 24.9, 22.8, 19.3, 19.2, 14.2; HRMS (ESI) Calcd for $C_{59}H_{94}O_6Si$ Na^+ $[M+Na]^+$: 949.6717, Found: 949.6719.

(2S,3S)-4-(benzyloxy)-1-[(tert-butyldiphenylsilyl)oxy]-3-[(9Z)-octadec-9-enoyloxy]butan-2-yl (9Z)-octadec-9-enoate (10c): Using the general procedure (II), starting from compound **9** (200 mg, 0.44 mmol) compound **10c** (373 mg, 80%) was isolated as colorless oil. $[\alpha]^{20}_{D}$ = -10.8 (c 0.1, CH_2Cl_2); ^{1}H NMR (400 MHz, $CDCl_3$): δ_{ppm} 7.63-7.60 (m, 3H), 7.43-7.25 (m, 12H), 5.44-5.41 (m, 1H), 5.37-5.33 (m, 4H), 5.31-5.27 (m, 1H), 4.46 (dd, 2H, J = 17.8 Hz), 3.73 (d, 2H, J = 4.8 Hz), 3.58 (d, 2H, J = 4.8 Hz), 2.29-2.21 (m, 4H), 2.01-1.99 (m, 8H), 1.62-1.56 (m, 4H), 1.27 (br s, 40H), 1.02 (s, 9H), 0.88 (t, 6H, J = 6.8 Hz); ^{13}C NMR (100 MHz, $CDCl_3$): δ_{ppm} 173.1, 173.0, 137.9, 135.8, 135.7, 133.2, 133.1, 130.2, 130.0, 129.9, 128.5, 127.9, 73.4, 72.3, 70.5, 68.5, 62.4, 34.5, 32.1, 30.0, 29.9, 29.7, 29.5, 29.4, 29.3, 27.4, 27.3, 26.9, 25.1, 25.0, 22.9, 19.3, 14.3; HRMS (ESI) Calcd for $C_{63}H_{98}O_6Si$ $[M+H]^+$: 979.7211, Found: 979.7212.

(2S,3S)-4-(benzyloxy)-1-hydroxy-3-(octanoyloxy)butan-2-yl octanoate (11a): Using the general procedure (IV), starting from compound **10a** (200 mg, 0.29 mmol) compound **11a** (132 mg, 98%) was isolated as a colourless oil; $[\alpha]^{20}_{D}$ = -16.8 (c 0.1, CH_2Cl_2);^{1}H NMR (400 MHz, $CDCl_3$): δ_{ppm} 7.37-7.27 (m, 5H), 4.63 (dd, 2H, J = 11.2 Hz, J = 11.6 Hz), 4.37-4.33 (m, 1H), 4.29-4.23 (m, 1H), 4.19-4.10 (m, 2H), 3.89 (m, 1H), 3.68-3.61 (m, 1H), 2.68 (br s, 1H), 2.36-2.24 (m, 4H), 1.63-1.28 (m, 4H), 1.28 (br s, 16H), 0.88 (t, 6H, J = 6.6 Hz), ^{13}C NMR (100 MHz, $CDCl_3$): δ_{ppm} 173.9, 173.7, 137.6, 128.6, 128.2, 76.4, 73.1, 69.6, 65.0, 62.7, 34.3, 34.2, 31.8, 29.2, 29.0, 25.0, 22.7, 14.2; HRMS (ESI) Calcd for $C_{27}H_{44}O_6Na^+$ $[M+Na]^+$: 487.3036, Found: 487.3036.

(2S,3S)-4-(benzyloxy)-3-(hexadecanoyloxy)-1-hydroxybutan-2-yl hexadecanoate (11b): Using the general procedure (IV), starting from compound **10b** (300 mg, 0.32 mmol) compound **11b** (216 mg, 98%) was isolated as a white solid. m.p: 50-51 $^{\circ}$C; $[\alpha]^{20}_{D}$ = -18.0 (c 0.2, CH_2Cl_2); ^{1}H NMR (400 MHz, $CDCl_3$): δ_{ppm} 7.26-7.19 (m, 5H), 4.57 (dd, 2H, J = 11.6 Hz, J = 11.6 Hz), 4.29-4.25 (m, 1H), 4.19-4.15 (m, 1H), 4.11-4.04 (m, 2H), 3.82-3.80 (m, 1H), 3.60-3.56 (m, 1H), 2.64 (br s, 1H), 1.24-2.16 (m, 4H), 1.53-1.50 (m, 4H), 1.18 (br s, 48H), 0.80 (t, 6H, J = 6.6 Hz); ^{13}C NMR (100 MHz, $CDCl_3$): δ_{ppm} 173.8, 173.6, 137.6, 128.6, 128.2, 76.4, 73.1, 69.6, 64.9, 62.7, 34.3, 34.2, 32.1, 29.8, 29.6, 29.5, 29.4, 29.3, 25.0, 22.8, 14.2; HRMS (ESI) Calcd for $C_{43}H_{77}O_6$ $[M+H]^+$: 689.5720, Found: 689.5717.

(2S,3S)-4-(benzyloxy)-1-hydroxy-3-[(9Z)-octadec-9-enoyloxy]butan-2-yl (9Z)-octadec-9-enoate (11c): Using the general procedure (IV), starting from compound **10c** (300 mg, 0.31 mmol) compound **11c** (225 mg, 98%) was isolated as a yellow oil. $[\alpha]^{20}_{D}$ = -16.0 (c 0.2, CH_2Cl_2); ^{1}H NMR (400 MHz, $CDCl_3$): δ_{ppm} 7.41-7.26 (m, 5H), 5.39-5.30 (m, 4H), 5.24-5.20 (m, 1H), 5.10-5.08 (m, 1H), 4.52 (s, 2H), 4.40-4.36 (m, 1H), 4.19-4.10 (m, 1H), 3.98-3.94 (m, 1H), 3.74-3.66 (m, 1H), 3.56-3.47 (m, 1H), 2.37-2.26 (m, 4H), 2.00 (m, 8H), 1.62-1.60 (m, 4H), 1.30 (br s, 40H), 0.88 (t, 6H, J = 6.8 Hz); ^{13}C NMR (100 MHz, $CDCl_3$): δ_{ppm} 173.5, 173.3, 137.6, 134.9, 130.0, 129.7, 129.5, 128.5, 127.9, 127.7, 127.6, 73.6, 71.4, 70.9, 69.4, 64.8, 34.3, 34.1, 32.0, 29.8, 29.7, 29.6, 29.4, 29.3, 29.2, 27.3, 27.2, 26.6, 25.0, 24.9, 22.8, 14.2; HRMS (ESI) Calcd for $C_{47}H_{81}O_6$ $[M+H]^+$: 741.6033, Found: 741.6032.

(2S,3S)-1-({[(2S)-2-amino-3-(benzyloxy)-3-oxopropoxy](benzyloxy)phosphoryl} oxy)-4-(benzyloxy)-3-(octanoyloxy)butan-2-yl octanoate (12a): Using the general procedure (V), starting from O-benzyl *N*,*N*,*N'*,*N'*-tetraisopropyl phosphorodiamidite (109 mg 0.33 mmol), benzyl (S)-1-((benzyloxy)carbonyl)-2-hydroxyethylcarbamate (100 mg, 0.30 mmol) and compound **11a** (139 mg, 0.30 mmol) compound **12a** (235 mg, 83%) isolated as colourless oil ;; $[\alpha]^{20}_{D}$ = -15.1 (c 0.1, EtOH); ^{1}H NMR (400 MHz, $CDCl_3$): δ_{ppm} 7.33-7.25 (m, 20H), 6.00 (d, 1H, J = 7.2 Hz), 5.36-5.32 (m, 1H), 5.27-5.23 (m, 1H), 5.19 (s, 2H), 5.09 (s, 2H), 5.02-4.94 (m, 2H), 4.49-4.41 (m, 3H), 4.18-4.14 (m, 1H), 4.09-4.04 (m, 1H), 3.95 (dd, 2H, J = 11.2 Hz, J = 11.2 Hz), 3.55-3.48 (m, 2H), 2.33-2.20 (m, 4H), 1.63-1.52 (m, 4H), 1.26 (br s, 16 H), 0.87 (m, 6H); ^{13}C NMR (100 MHz, $CDCl_3$): δ_{ppm} 173.2, 173.0, 170.8, 156.7, 137.8, 136.5, 135.8, 135.6, 128.8, 128.7, 128.6, 128.3, 128.2, 128.0, 127.9, 127.7, 73.5, 70.3, 70.1, 69.8, 68.1, 67.5, 67.3, 66.2, 63.2, 56.6, 34.4, 34.3, 31.9, 29.9, 29.3, 29.2, 25.1, 22.8, 22.7, 14.3; ^{31}P NMR (161.9 MHz, $CDCl_3$): δ_{ppm} 0.17; HRMS (ESI) Calcd for $C_{52}H_{68}NO_{13}PNa^+$ $[M+Na]^+$: 968.4326, Found: 968.4326.

2S,3S)-1-({[(2S)-2-amino-3-(benzyloxy)-3-oxopropoxy](benzyloxy)phosphoryl}oxy)-4-(benzyloxy)-3-(hexadecanoyloxy)butan-2-yl hexadecanoate (12b): Using the general procedure (V), starting from O-benzyl *N*,*N*,*N'*,*N'*-tetraisopropyl phosphorodiamidite (109 mg 0.33 mmol), benzyl (S)-1-((benzyloxy)carbonyl)-2-hydroxyethylcarbamate (100 mg, 0.30 mmol) and compound **11b** (210 mg, 0.30 mmol) compound **12b** (291 mg, 83%) isolated as a

white solid. m.p: 70-71 °C; $[\alpha]^{20}_{D}$ = -17.6 (c 0.1, EtOH); ^{1}H NMR (400 MHz, $CDCl_3$): δ_{ppm} 7.32-7.25 (m, 20H), 5.90 (d, 1H, J = 7.6 Hz), 5.35-5.32 (m, 1H), 5.26-5.23 (m, 1H), 5.18 (s, 2H), 5.09 (s, 2H), 5.00-4.97 (m, 2H), 4.48-4.44 (m, 3H), 4.18-4.14 (m, 1H), 4.08-4.04 (m, 1H), 3.93 (dd, 2H, J = 11.2 Hz, J = 10.8 Hz), 3.55-3.48 (m, 2H), 2.32-2.19 (m, 4H), 1.60-1.51 (m, 4H), 1.25 (br s, 48 H), 0.88 (t, 6H, J = 6.8 Hz); ^{13}C NMR (100 MHz, $CDCl_3$): δ_{ppm} 172.9, 172.8, 170.6, 156.5, 137.5, 136.2, 135.5, 135.4, 135.3, 128.6, 128.5, 128.4, 128.3, 128.2, 128.1, 128.0, 127.8, 127.7, 73.3, 69.9, 69.7, 69.6, 67.9, 67.2, 67.0, 65.7, 62.8, 56.4, 34.2, 34.0, 31.9, 29.7, 29.5, 29.4, 29.3, 29.1, 24.9, 24.8, 22.7, 14.1; ^{31}P NMR (161.9 MHz, $CDCl_3$): δ_{ppm} 0.14; HRMS (ESI) Calcd for $C_{68}H_{101}NO_{13}P$ $[M+H]^+$: 1170.7011, Found: 1170.7010.

(2S,3S)-1-(benzyloxy)-4-{[(benzyloxy)[(2S)-3-(benzyloxy)-2-{[(benzyloxy)carbonyl] amino}-3-oxopropoxy]phosphoryl]oxy}-3-[(9Z)-octadec-9-enoyloxy]butan-2-yl (9Z)-octadec-9-enoate (12c): Using the general procedure (V), starting from compound **11c** (150 mg, 0.2 mmol) compound **12c** (202 mg, 83%) was isolated as a yellow oil. $[\alpha]^{20}_{D}$ = -19.2 (c 0.1,EtOH); ^{1}H NMR (400 MHz, $CDCl_3$): δ_{ppm} 7.41-7.25 (m, 20H), 5.76 (d, 1H, J = 8.0 Hz), 5.42-5.30 (m, 4H), 5.21 (s, 2H), 5.12 (s, 4H), 4.58-4.50 (m, 2H), 4.40-4.35 (m, 1H), 4.19-4.12 (m, 2H), 4.02-3.92 (m, 3H), 3.74-3.67 (m, 1H), 3.56-3.48 (m, 2H), 2.37-2.26 (m, 4H), 2.06-2.00 (m, 8H), 1.65-1.60 (m, 4H), 1.27 (br s, 40H), 0.88 (t, 6H, J = 6.8 Hz); ^{13}C NMR (100 MHz, $CDCl_3$): δ_{ppm} 173.5, 173.4, 170.6, 156.4, 137.6, 136.2, 135.5, 135.3, 135.0, 130.2, 130.0, 129.8, 128.8, 128.7, 128.6, 128.4, 128.3, 128.1, 128.0, 127.9, 73.7, 71.5, 71.3, 69.6, 69.1, 67.6, 67.4, 65.0, 63.4, 56.4, 34.4, 34.3, 32.1, 30.0, 29.9, 29.7, 29.5, 29.4, 29.3, 27.4, 27.3, 26.7, 25.1, 25.0, 22.9, 14.3; ^{31}P NMR (161.9 MHz, $CDCl_3$): δ_{ppm} 2.23; HRMS (ESI) Calcd for $C_{72}H_{105}NO_{13}P$ $[M+H]^+$: 1222.7318, Found: 1222.7319.

(2S)-2-amino-3-({hydroxy[(2S,3S)-4-hydroxy-2,3-bis(octanoyloxy)butoxy] phosphoryl}oxy) propanoic acid (DAT-PS$_8$): Using the general procedure (III), starting from compound **12a** (136 mg, 0.14 mmol) compound DAT-PS_8 (70 mg, 90%) was isolated as a yellow oil; $[\alpha]^{20}_{D}$ = -25.7 (c 0.1, EtOH); ^{1}H NMR (400 MHz, $CDCl_3$ + DMSO-d_6): δ_{ppm} 5.66 (d, 1H, J = 8.4 Hz), 4.86-4.82 (m, 1H), 4.00-3.90 (m, 2H), 3.84-3.80 (m, 1H), 3.74-3.70 (m, 1H), 3.62 (dd, 2H, J = 3.6 Hz, J = 3.6 Hz), 3.50-3.44 (m, 1H), 2.10 (t, 2H, J = 7.4 Hz), 1.97 (t, 2H, J = 7.6 Hz), 1.33-1.26 (m, 4H), 0.96 (br s, 16H), 0.56 (t, 6H, J = 6.8 Hz); ^{13}C NMR (100 MHz, $CDCl_3$ + DMSO-

d_6): δ_{ppm} 173.0, 172.7, 79.2, 74.1, 70.3, 65.2, 62.7, 62.5, 55.6, 34.1, 33.9, 31.4, 30.6, 29.5, 28.8, 28.7, 28.2, 26.0, 25.1, 24.8, 24.6, 22.4, 14.0; ^{31}P NMR (161.9 MHz, $CDCl_3$): δ_{ppm} 0.04; HRMS (ESI) Calcd for $C_{23}H_{45}NO_{11}P$ $[M+H]^+$: 542.2730, Found: 542.2731.

(2S)-2-amino-3-({[(2S,3S)-2,3-bis(hexadecanoyloxy)-4-hydroxybutoxy](hydroxy) phosphoryl}oxy)propanoic acid (DAT-PS$_{16}$): Using the general procedure (III), starting from compound **12b** (200 mg, 0.17 mmol) compound DAT-PS_{16} **(**117 mg, 90%) was isolated as a white solid. m.p: 140-141 $^{\circ}$C; $[\alpha]$ $^{20}_D$ = -23.2 (c 0.2, EtOH); ^{1}H NMR (400 MHz, $CDCl_3$ + DMSO-d_6): δ_{ppm} 5.67 (d, 1H, J = 8.0 Hz), 4.88-4.84 (m, 1H), 4.02-3.92 (m, 2H), 3.86-3.81 (m, 1H), 3.77-3.72 (m, 1H), 3.66 (dd, 2H, J = 10.0 Hz, J = 10.0 Hz), 3.52-3.46 (m, 1H), 2.05 (t, 2H, J = 7.4 Hz), 1.99 (t, 2H, J = 7.4 Hz), 1.35-1.27 (m, 4H), 0.96 (br s, 48H), 0.58 (t, 6H, J = 6.8 Hz); ^{13}C NMR (100 MHz, $CDCl_3$ + DMSO-d_6): δ_{ppm} 173.2, 173.0, 79.3, 74.1, 70.3, 65.3, 62.7, 62.5, 55.8, 34.1, 33.9, 31.7, 29.5, 29.3, 29.2, 29.1, 28.9, 28.8, 28.2, 26.0, 25.1, 24.8, 24.6, 22.5, 14.0; ^{31}P NMR (161.9 MHz, $CDCl_3$): δ_{ppm} 0.60; HRMS (ESI) Calcd for $C_{39}H_{77}NO_{11}P$ $[M+H]^+$: 766.5234, Found: 766.5234.

(2S)-2-amino-3-({hydroxy[(2S,3S)-4-hydroxy-2,3-bis[(9Z)-octadec-9-enoyloxy] butoxy]phosphoryl}oxy)propanoic acid (DAT-PS$_{18}$): Using the general procedure (III), starting from compound **12c** (150 mg, 0.12 mmol) compound DAT-PS_{18} (88 mg, 90%) was isolated as a yellow oil. $[\alpha]$ $^{20}_D$ = -17.8 (c 0.1,EtOH); ^{1}H NMR (400 MHz, $CDCl_3$): δ_{ppm} 5.66 (d, 1H, J = 8.0 Hz), 4.95-4.87 (m, 4H), 3.79-3.73 (m, 2H), 3.62-3.58 (m, 2H), 3.51-3.48 (m, 1H), 3.38-3.31 (m, 2H), 3.19-3.12 (m, 2H), 1.85-1.81 (m, 4H), 1.61-1.59 (m, 8H), 1.73-1.14 (m, 4H), 1.02 (m, 40H), 0.47 (t, 6H, J = 6.6 Hz); ^{13}C NMR (100 MHz, $CDCl_3$ + DMSO-d_6): δ_{ppm} 175.1, 172.1, 129.1, 128.9, 78.5, 75.7, 65.6, 62.1, 61.8, 55.2, 33.4, 31.1, 28.9, 28.7, 28.5, 28.4, 28.3, 27.6, 26.3, 26.0, 24.6, 24.1, 21.9, 13.4; ^{31}P NMR (161.9 MHz, $CDCl_3$): δ_{ppm} 0.69; HRMS (ESI) Calcd for $C_{43}H_{80}NO_{11}P$ $[M+Na]^+$: 840.5367, Found: 841.0718.

(2S,3S)-4-(benzyloxy)-1-{[(benzyloxy)[(2-phenyl-1,3-dioxolan-4-yl)methoxy] phosphoryl]oxy }-3-(octanoyloxy)butan-2-yl octanoate (13a): Using the general procedure (V), starting from compound **11a** (150 mg, 0.32 mmol) compound **13a** (212 mg, 83%) was isolated as a yellow oil; $[\alpha]$ $^{20}_D$ = -23.1 (c 0.1, CH_2Cl_2); ^{1}H NMR (400 MHz, $CDCl_3$): δ_{ppm} 7.64-

7.51 (m, 5H), 7.46-7.26 (m, 10H), 6.15 (s, 1H), 5.00-4.95 (m, 2H), 4.88-4.83 (m, 2H), 4.69 (s, 2H), 4.66-4.55 (m, 1H), 4.35-4.25 (m, 5H), 4.17-4.14 (m, 1H), 3.91-3.88 (m, 1H), 3.69-3.66 (m, 1H), 2.33-2.27 (m, 4H), 1.63-1.60 (m, 4H), 1.28 (br s, 16H), 0.88 (t, 6H, J = 6.4 Hz); ^{13}C NMR (100 MHz, $CDCl_3$): δ_{ppm} 174.1, 171.9, 135.6, 135.3, 134.7, 130.3, 130.1, 129.2, 128.7, 128.6, 128.5, 128.3, 127.8, 127.4, 127.2, 106.9, 76.3, 73.2, 72.2, 69.7, 65.4, 65.0, 62.7, 62.4, 62.3, 34.3, 34.2, 31.8, 31.1, 29.8, 29.2, 29.1, 25.0, 24.1, 22.7, 14.3, 14.2; ^{31}P NMR (161.9 MHz, $CDCl_3$): δ_{ppm} 1.52, 1.06; HRMS (ESI) Calcd for $C_{44}H_{61}O_{11}P$ $[M+H]^+$: 797.4030, Found: 797.4031.

(2S,3S)-4-(benzyloxy)-1-{[(benzyloxy)({[(4S)-2-phenyl-1,3-dioxolan-4-yl]methoxy}) phosphoryl]oxy}-3-(hexadecanoyloxy)butan-2-yl hexadecanoate (13b): Using the general procedure (V), starting from compound **11b** (150 mg, 0.22 mmol) compound **13b** (186 mg, 83%) was isolated as a white solid. m.p: 126-127 $^{\circ}$C; $[\alpha]^{20}_D$ = -25.7 (c 0.1, CH_2Cl_2); ^{1}H NMR (400 MHz, $CDCl_3$): δ_{ppm} 7.59-7.57 (m, 5H), 7.44-7.27 (m, 10H), 6.15 (s, 1H), 5.00-4.95 (m, 2H), 4.89-4.83 (m, 2H), 4.66 (s, 2H), 4.60-4.55 (m, 1H), 4.35-4.23 (m, 5H), 4.18-4.15 (m, 1H), 3.93-3.89 (m, 1H), 3.69-3.65 (m, 1H), 2.33 (t, 4H, J = 7.4 Hz), 1.64-1.59 (m, 4H), 1.26 (br s, 48H), 0.88 (t, 6H, J = 6.6 Hz); ^{13}C NMR (100 MHz, $CDCl_3$): δ_{ppm} 173.8, 173.6, 140.9, 137.5, 135.5, 129.8, 128.4, 128.3, 128.2, 128.1, 127.9, 127.3, 127.2, 126.9, 107.5, 76.2, 72.9, 72.3, 70.5, 69.3, 67.5, 67.3, 64.7, 62.1, 34.1, 31.8, 29.6, 29.4, 29.3, 29.2, 29.1, 26.3, 24.8, 23.8, 23.7, 22.6, 14.0, 13.9; ^{31}P NMR (161.9 MHz, $CDCl_3$): δ_{ppm} 1.75, 1.28; HRMS (ESI) Calcd for $C_{60}H_{94}O_{11}P$ $[M+H]^+$: 1021.6534, Found: 1021.6536.

(2S,3S)-4-(benzyloxy)-1-{[(benzyloxy)({[(4S)-2-phenyl-1,3-dioxolan-4-yl]methoxy}) phosphoryl]oxy}-3-[(9Z)-octadec-9-enoyloxy]butan-2-yl (9Z)-octadec-9-enoate (13c): Using the general procedure (V), starting from compound **11c** (150 mg, 0.20 mmol) compound **13c** (178 mg, 83%) was isolated as a yellow oil. $[\alpha]^{20}_D$ = -13.2 (c 0.1,CH_2Cl_2); ^{1}H NMR (400 MHz, $CDCl_3$): δ_{ppm} 7.40-7.26 (m, 15H), 6.16 (s, 1H), 5.40-5.30 (m, 4H), 5.24-5.20 (m, 1H), 5.10-5.08 (m, 1H), 4.98-4.83 (m, 1H), 4.52 (s, 2H), 4.40-4.25 (m, 3H), 4.20-4.12 (m, 3H), 3.98-3.95 (m, 1H), 3.74-3.66 (m, 1H), 3.56-3.46 (m, 2H), 2.37-2.26 (m, 4H), 2.00 (m, 8H), 1.61-1.59 (m, 4H), 1.27 (br s, 40H), 0.88 (t, 6H, J = 6.8 Hz); ^{13}C NMR (100 MHz, $CDCl_3$): δ_{ppm} 173.8, 173.5, 137.5, 135.6, 135.3, 130.1, 129.9, 129.8, 129.7, 129.1, 128.6, 128.5, 128.4, 128.0, 127.8, 127.7, 127.3, 106.8, 77.7, 77.6, 73.6, 71.4, 71.3, 70.8, 69.4, 64.8, 62.2, 34.3, 34.2, 32.0, 29.8, 29.6, 29.4, 29.3,

29.2, 27.3, 27.2, 26.6, 25.0, 24.9, 22.8, 14.2; ^{31}P NMR (161.9 MHz, $CDCl_3$): δ_{ppm} 2.14, 1.68; HRMS (ESI) Calcd for $C_{64}H_{98}O_{11}P$ $[M+H]^+$: 1073.6847, Found: 1073.6850.

(2,3-dihydroxypropoxy)[(2S,3S)-4-hydroxy-2,3-bis(octanoyloxy)butoxy] phosphinic acid (DAT-PG$_8$): Using the general procedure (III), starting from compound **13a** (136 mg, 0.17 mmol) compound DAT-PG$_8$ (81 mg, 90%) was isolated as a yellow oil. $[\alpha]^{20}_D$ = -25.7 (c 0.1 EtOH); ^{1}H NMR (400 MHz, $CDCl_3$): δ_{ppm} 7.14 (br s, 1H), 5.20-5.16 (m, 2H), 4.33-4.25 (m, 2H), 4.18-4.13 (m, 1H), 4.06-4.02 (m, 1H), 3.94-3.88 (m, 2H), 3.80-3.76 (m, 1H), 3.70-3.65 (m, 2H), 3.48 (br s, 1H), 2.42-2.28 (m, 4H), 1.97-1.71 (m, 4H), 1.26 (br s, 16H), 0.88 (t, 6H, J = 6.6 Hz), ^{13}C NMR (100 MHz, $CDCl_3$): δ_{ppm} 173.5, 173.4, 74.5, 70.7, 65.6, 62.9, 55.8, 49.9, 35.9, 34.2, 32.8, 32.1, 31.8, 31.0, 29.8, 29.6, 29.6, 29.5, 29.4, 29.2, 29.1, 29.0, 26.4, 26.2, 25.6, 25.4, 25.0, 24.9, 22.8, 22.7, 14.2, 14.1; ^{31}P NMR (161.9 MHz, $CDCl_3$): δ_{ppm} 6.06, 0.15; HRMS (ESI) Calcd for $C_{23}H_{45}O_{11}P$ $[M+Na]^+$: 551.2597, Found: 551.2598.

[(2S,3S)-2,3-bis(hexadecanoyloxy)-4-hydroxybutoxy][(2S)-2,3-dihydroxypropoxy] phosphinic acid (DAT-PG$_{16}$): Using the general procedure (III), starting from compound **13b** (150 mg, 0.15 mmol) compound DAT-PG$_{16}$ (102 mg, 90%) was isolated as a white solid. m.p: 80-81 $^{\circ}$C; $[\alpha]^{20}_D$ = -25.7 (c 0.1, EtOH); ^{1}H NMR (400 MHz, $CDCl_3$): δ_{ppm} 7.16 (br s, 1H), 5.19-5.18 (m, 1H), 4.44-4.40 (m, 1H), 4.33-4.24 (m, 2H), 4.20-4.12 (m, 2H), 4.05-4.01 (m, 1H), 3.92-3.86 (m, 1H), 3.80-3.78 (m, 1H), 3.72-3.65 (m, 1H), 3.48-3.46 (m, 1H), 2.42-2.27 (m, 4H), 1.97-1.92 (m, 2H), 1.73-1.60 (m, 2H), 1.25 (br s, 48H), 0.88 (t, 6H, J = 6.6 Hz); ^{13}C NMR (100 MHz, $CDCl_3$): δ_{ppm} 173.7, 173.6, 74.5, 70.9, 70.7, 68.9, 65.6, 64.8, 62.9, 34.4, 34.3, 32.9, 31.0, 29.9, 29.6, 29.5, 29.4, 29.3, 26.5, 26.3, 25.8, 25.7, 25.5, 25.1, 25.0, 24.9, 22.9, 14.3; ^{31}P NMR (161.9 MHz, $CDCl_3$): δ_{ppm} 5.69, -0.22; HRMS (ESI) Calcd for $C_{39}H_{78}O_{11}P$ $[M+H]^+$: 753.5280, Found: 753.5281.

[(2S)-2,3-dihydroxypropoxy][(2S,3S)-4-hydroxy-2,3-bis[(9Z)-octadec-9-enoyloxy] butoxy]phosphinic acid (DAT-PG$_{18}$): Using the general procedure (III), starting from compound **13c** (140 mg, 0.13 mmol) compound DAT-PG$_{18}$ (94 mg, 90%) was isolated as a yellow oil. $[\alpha]^{20}_D$ = -19.2 (c 0.1,EtOH); ^{1}H NMR (400 MHz, $CDCl_3$): δ_{ppm} 7.27 (br s, 1H), 5.31-5.29 (m, 4H), 4.55-4.51 (m, 1H), 4.45-4.36 (m, 2H), 4.31-4.24 (m, 2H), 4.21-4.13 (m, 1H), 4.04-

3.98 (m, 1H), 3.91-3.89 (m, 1H), 3.84-3.76 (m, 1H), 3.60-3.57 (m, 2H), 2.54-2.39 (m, 4H), 2.09-2.04 (m, 8H), 1.95-1.72 (m, 4H), 1.37 (br s, 40H), 0.99 (t, 6H, J = 6.8 Hz); ^{13}C NMR (100 MHz, $CDCl_3$): δ_{ppm} 173.7, 173.6, 128.5, 126.8, 74.5, 70.7, 68.9, 65.6, 64.8, 62.9, 62.4, 34.2, 34.0, 32.9, 32.1, 31.0, 29.9, 29.6, 29.5, 29.4, 29.3, 26.5, 25.8, 25.7, 25.5, 25.4, 25.1, 25.0, 24.9, 22.9, 14.3; ^{31}P NMR (161.9 MHz, $CDCl_3$): δ_{ppm} 0.81, -1.28; HRMS (ESI) Calcd for $C_{43}H_{82}O_{11}P$ $[M+H]^+$: 805.5595, Found: 805.5594.

3.4. Selected Spectra of DAT-Anionic Lipids

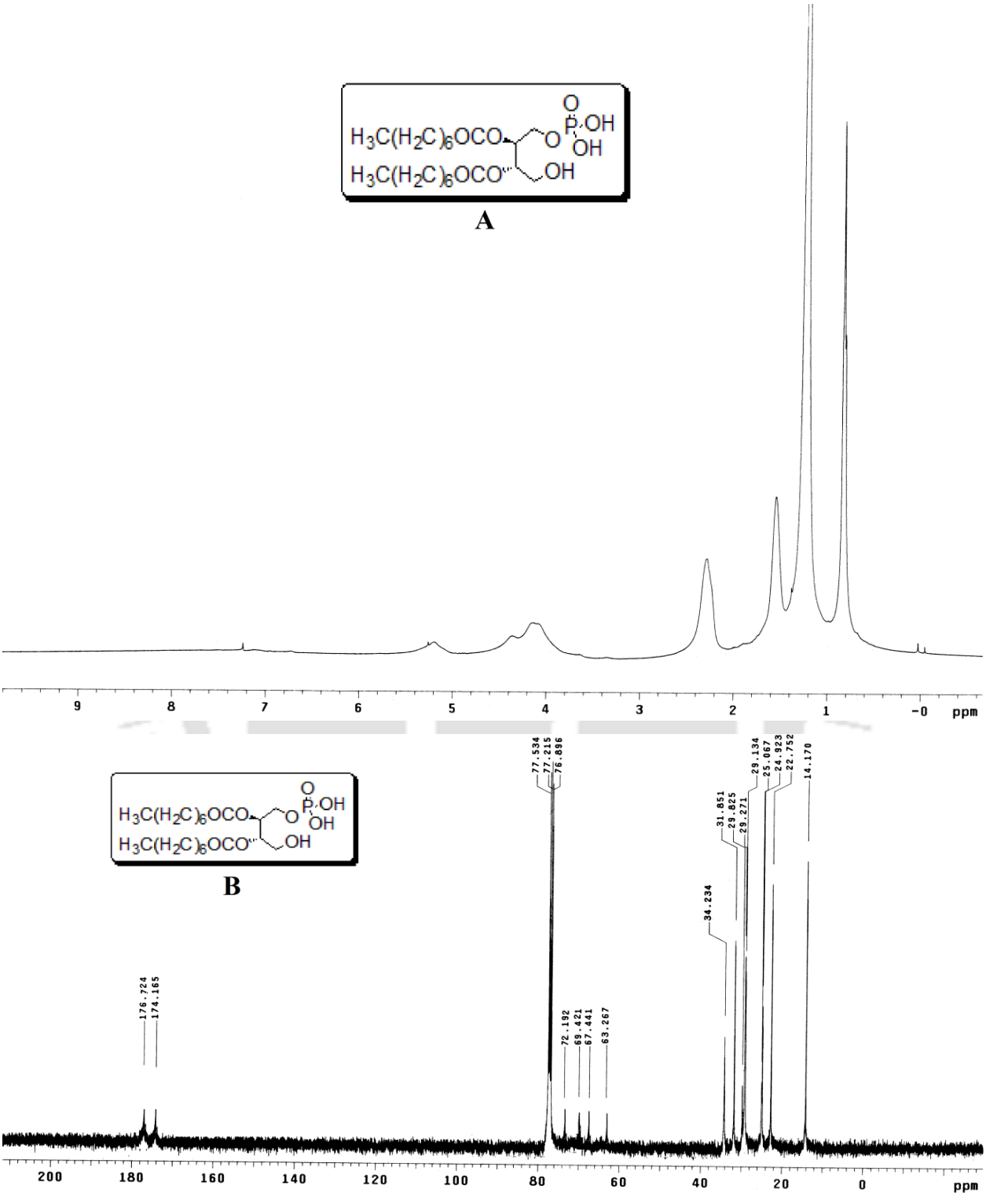

Figure 3.4.1: *^{1}H NMR (A) and ^{13}C NMR (B) spectra of DAT-PA_8*

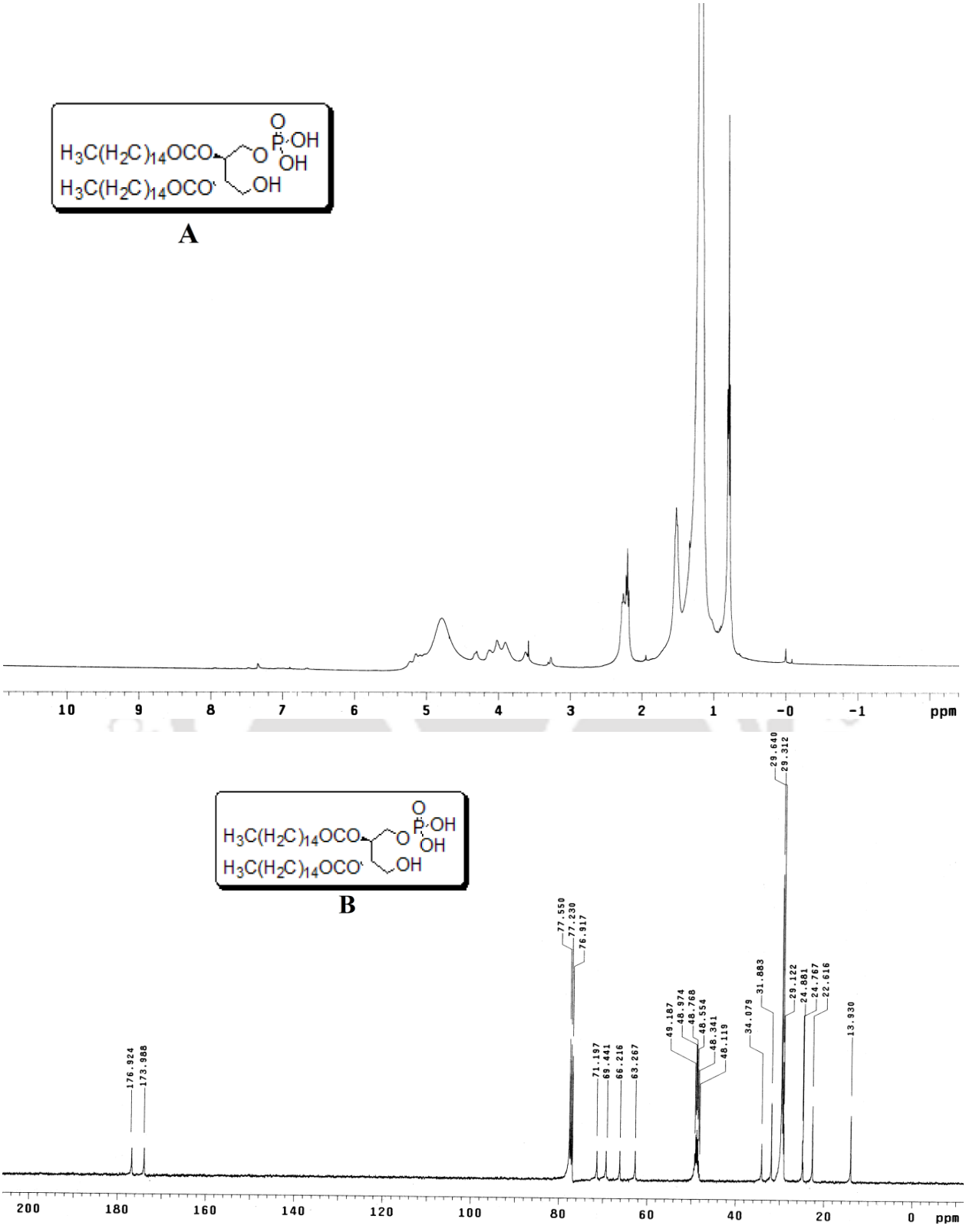

Figure 3.4.2: *^{1}H NMR (A) and ^{13}C NMR (B) spectra of DAT-PA_{16}*

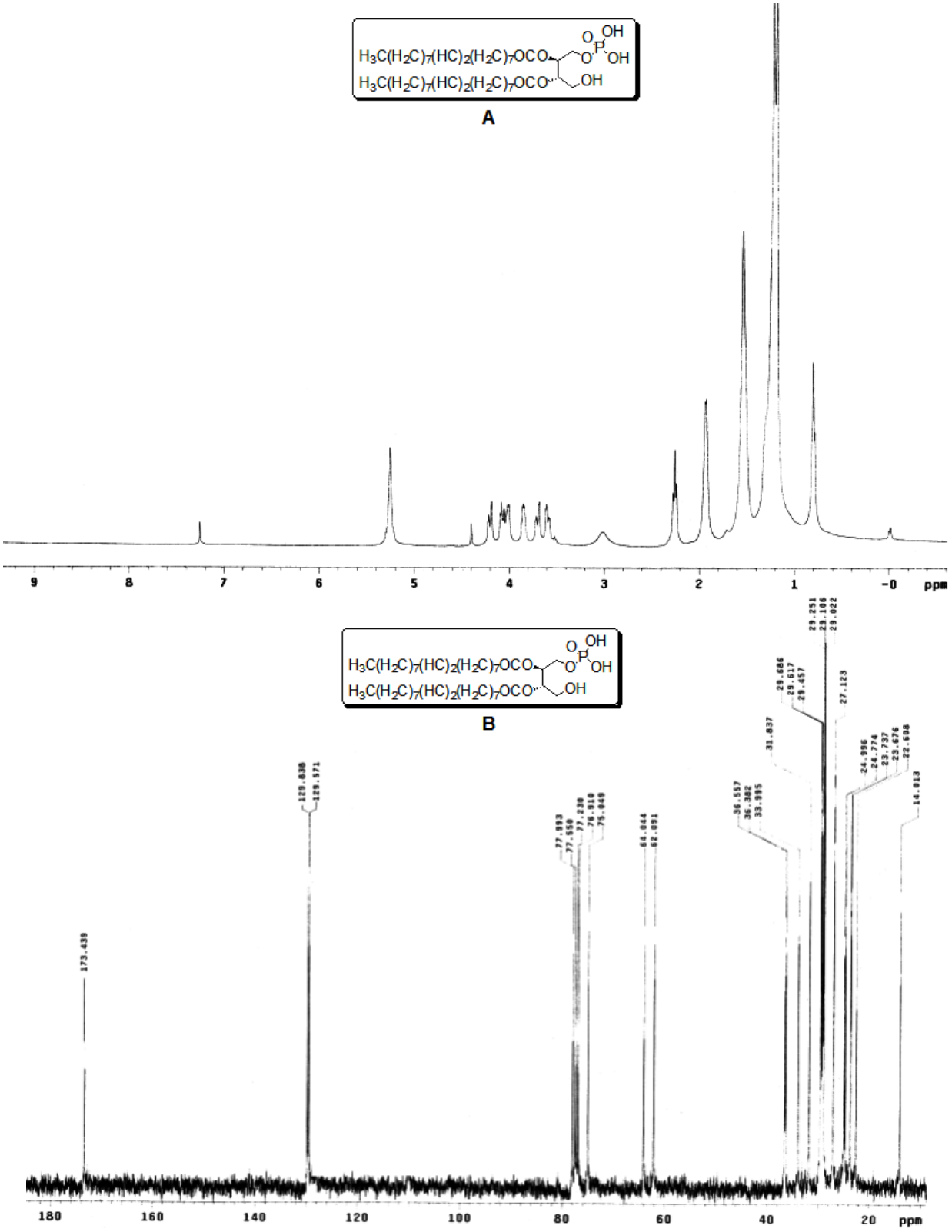

Figure 3.4.3: *^{1}H NMR (A) and ^{13}C NMR (B) spectra of DAT-PA_{18}*

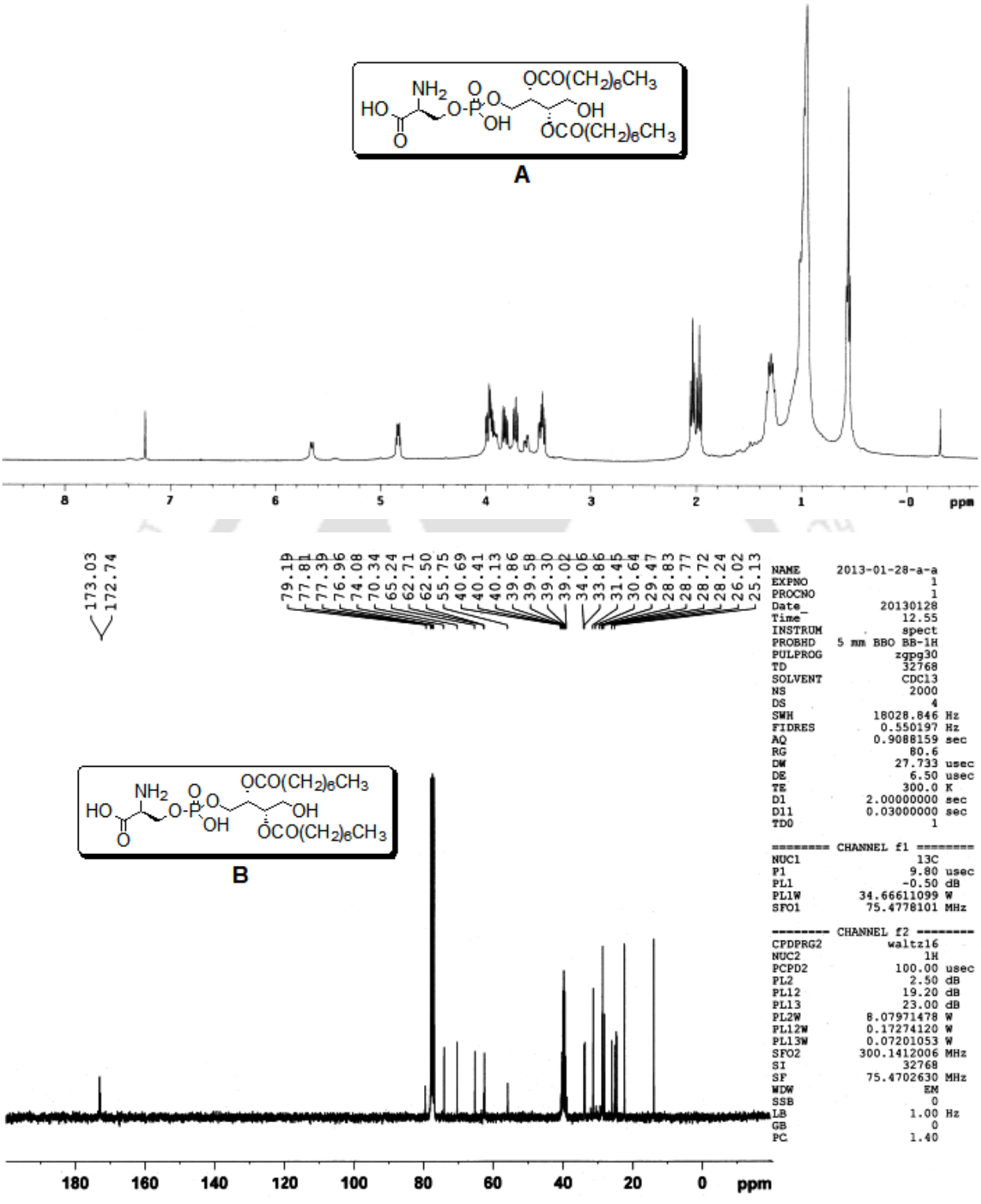

Figure 3.4.4: *^{1}H NMR (A) and ^{13}C NMR (B) spectra of DAT-PS_8*

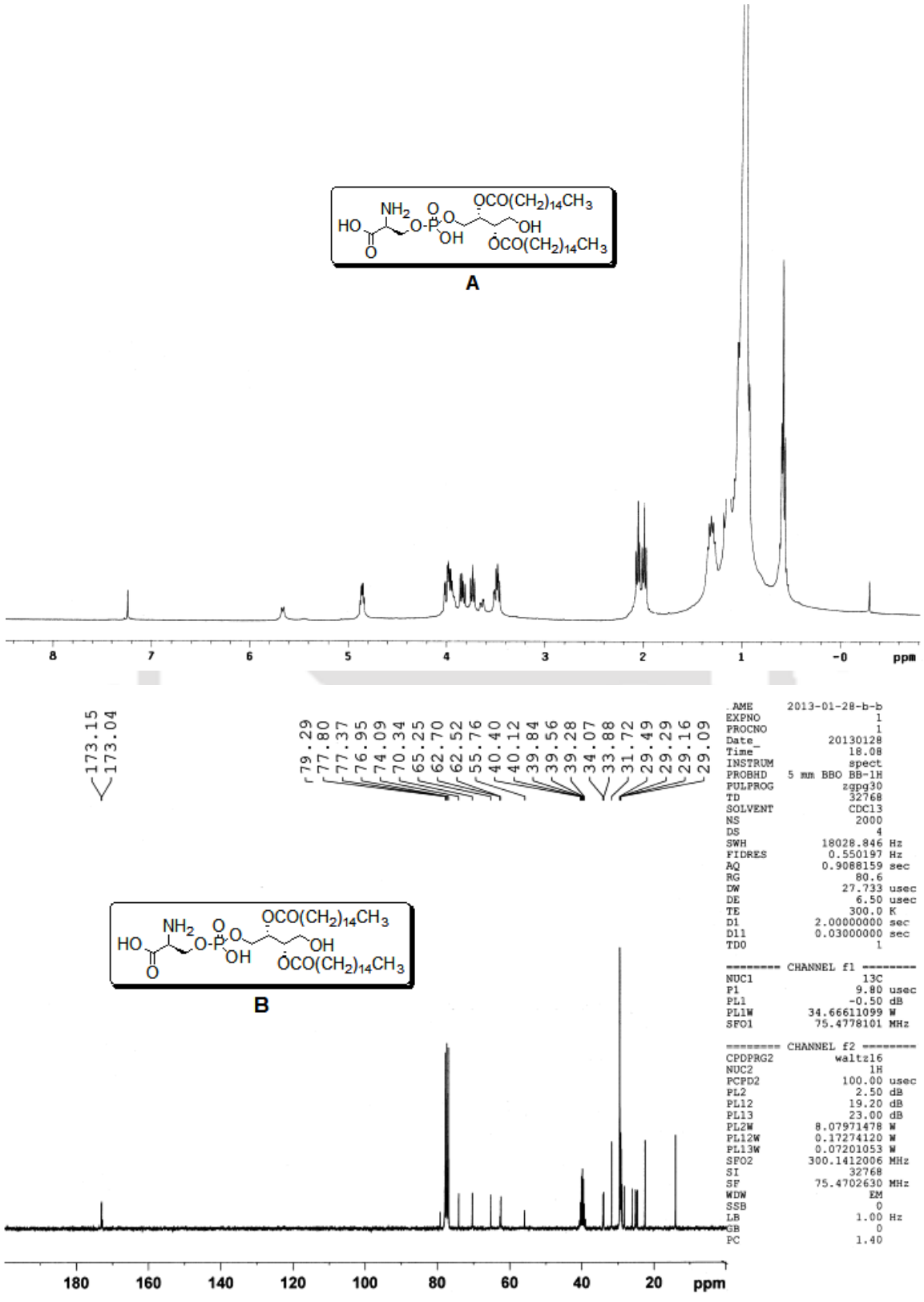

Figure 3.4.5: *^{1}H NMR (A) and ^{13}C NMR (B) spectra of DAT-PS_{16}*

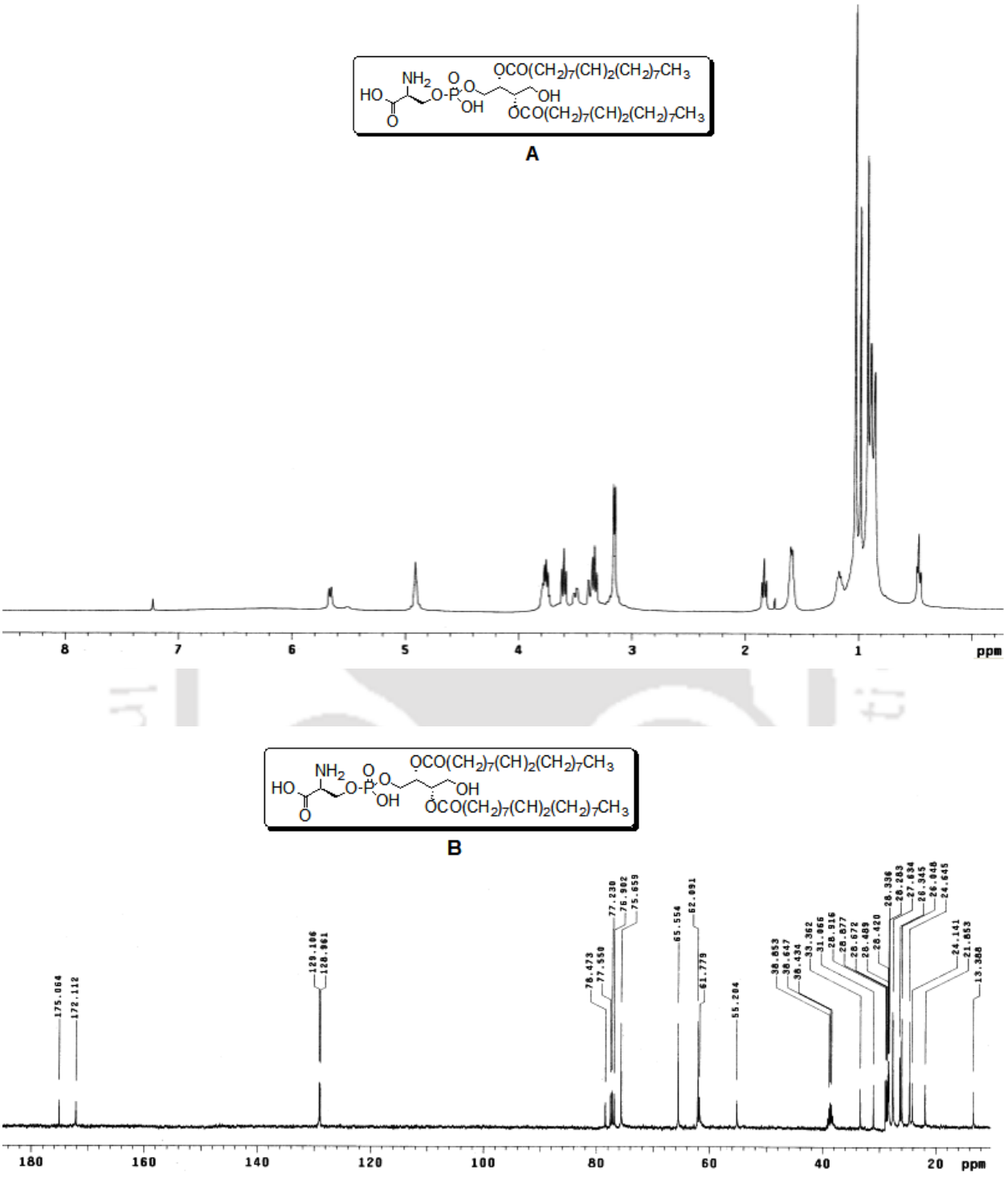

Figure 3.4.6: *^{1}H NMR (A) and ^{13}C NMR (B) spectra of DAT-PS$_{18}$*

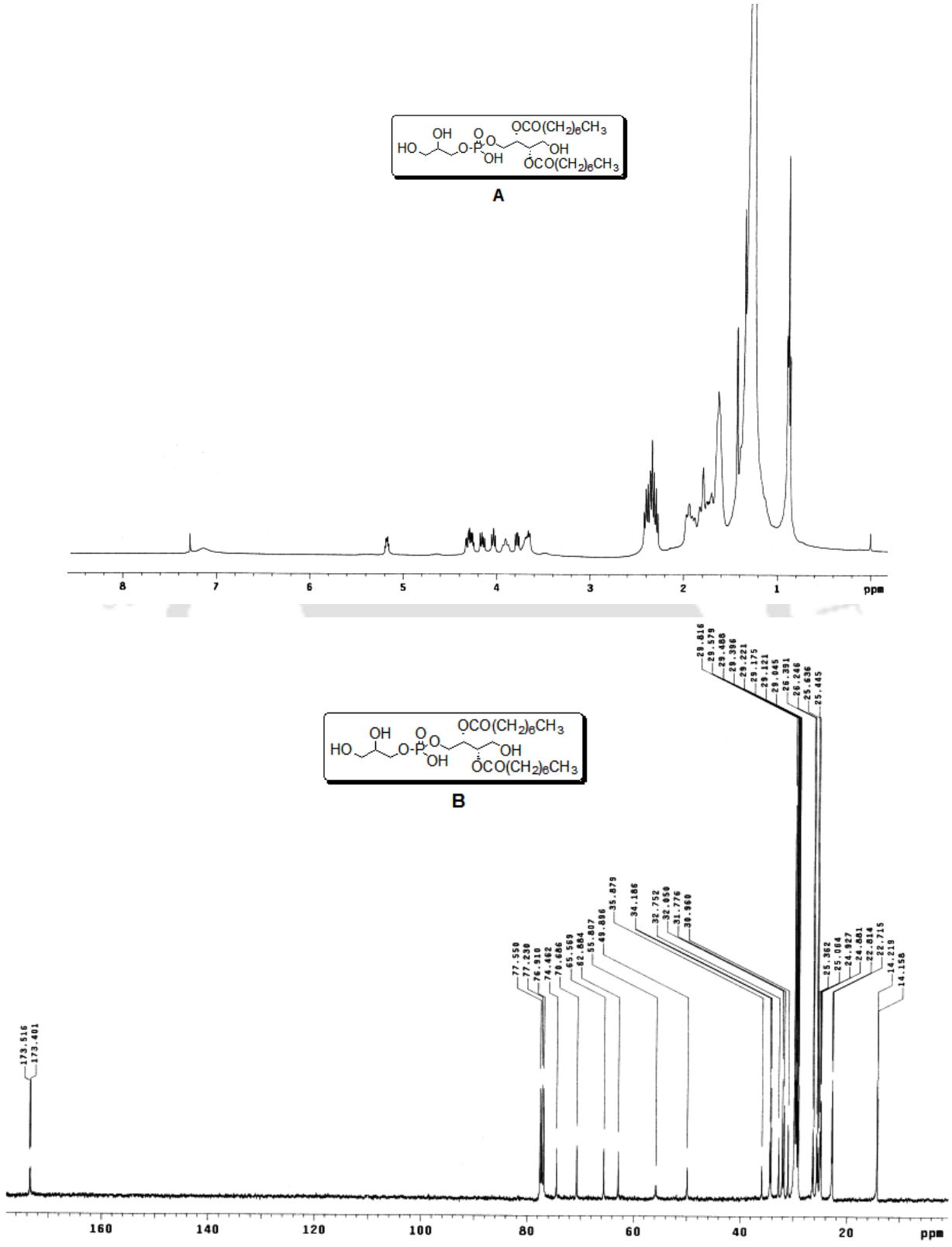

Figure 3.4.7: *^{1}H NMR (A) and ^{13}C NMR (B) spectra of DAT-PG$_8$*

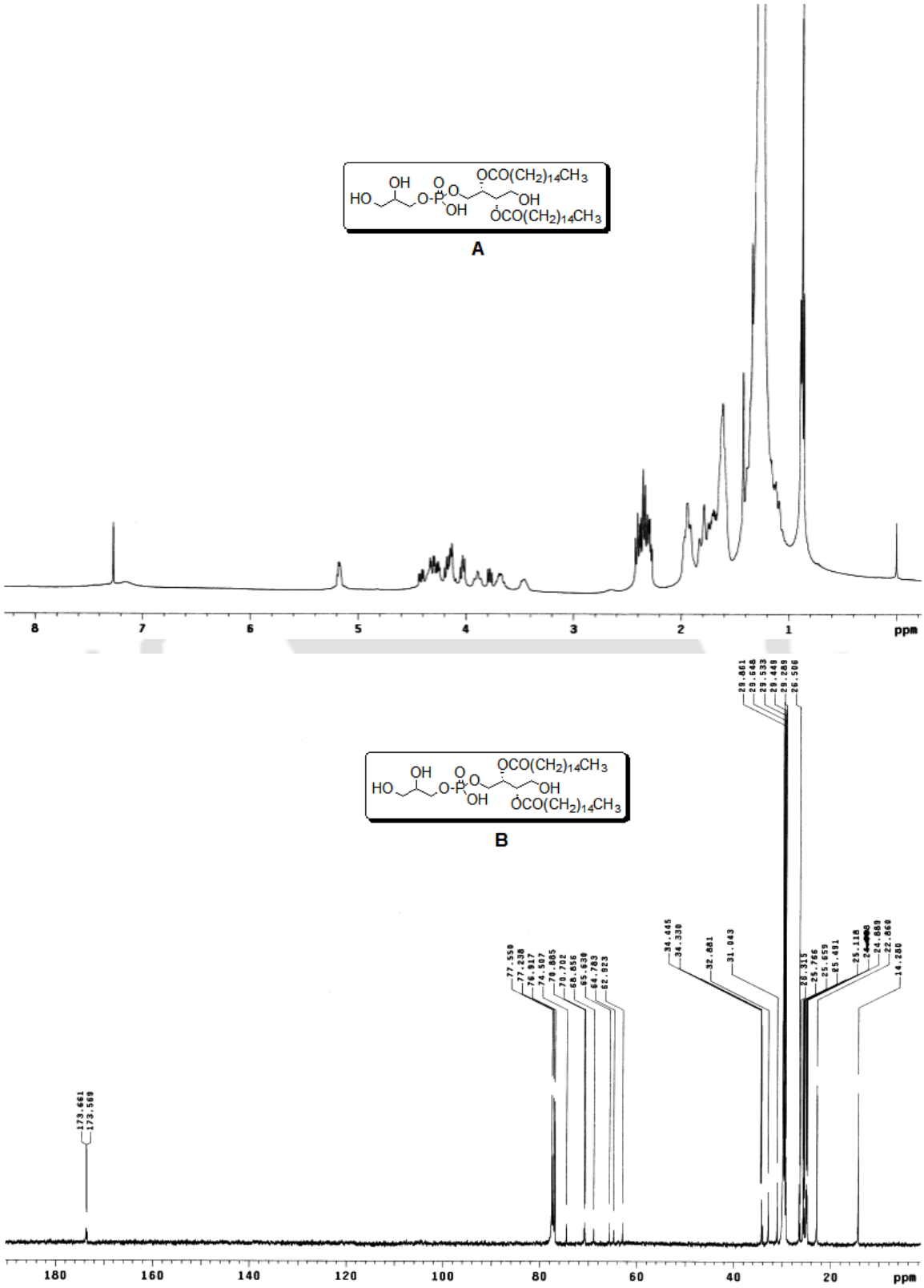

Figure 3.4.8: *^{1}H NMR (A) and ^{13}C NMR (B) spectra of DAT-PG$_{16}$*

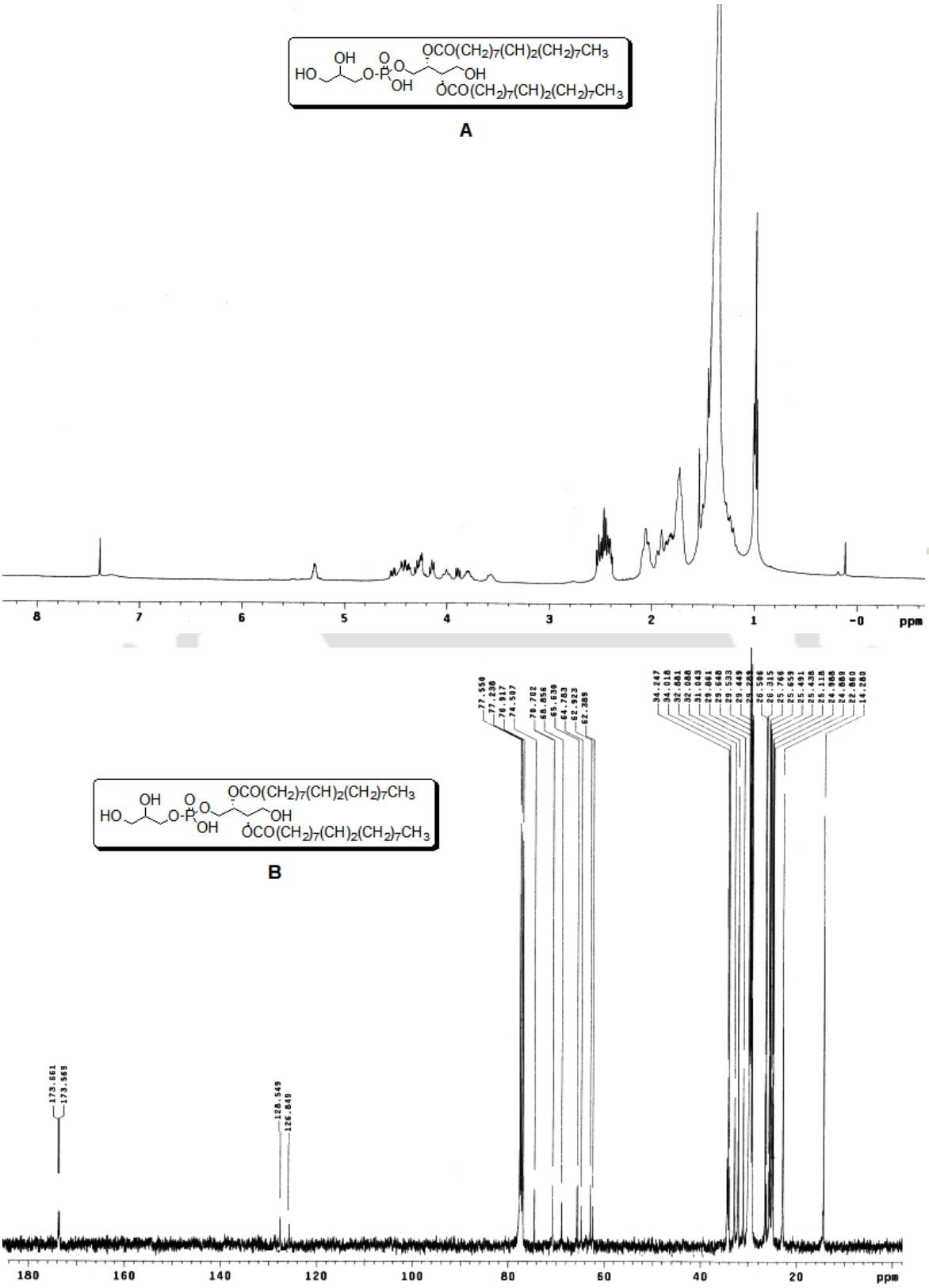

Figure 3.4.9: *^{1}H NMR (A) and ^{13}C NMR (B) spectra of DAT-PG$_{18}$*

3.5. ^{31}P NMR Spectra of DAT-Anionic Lipids

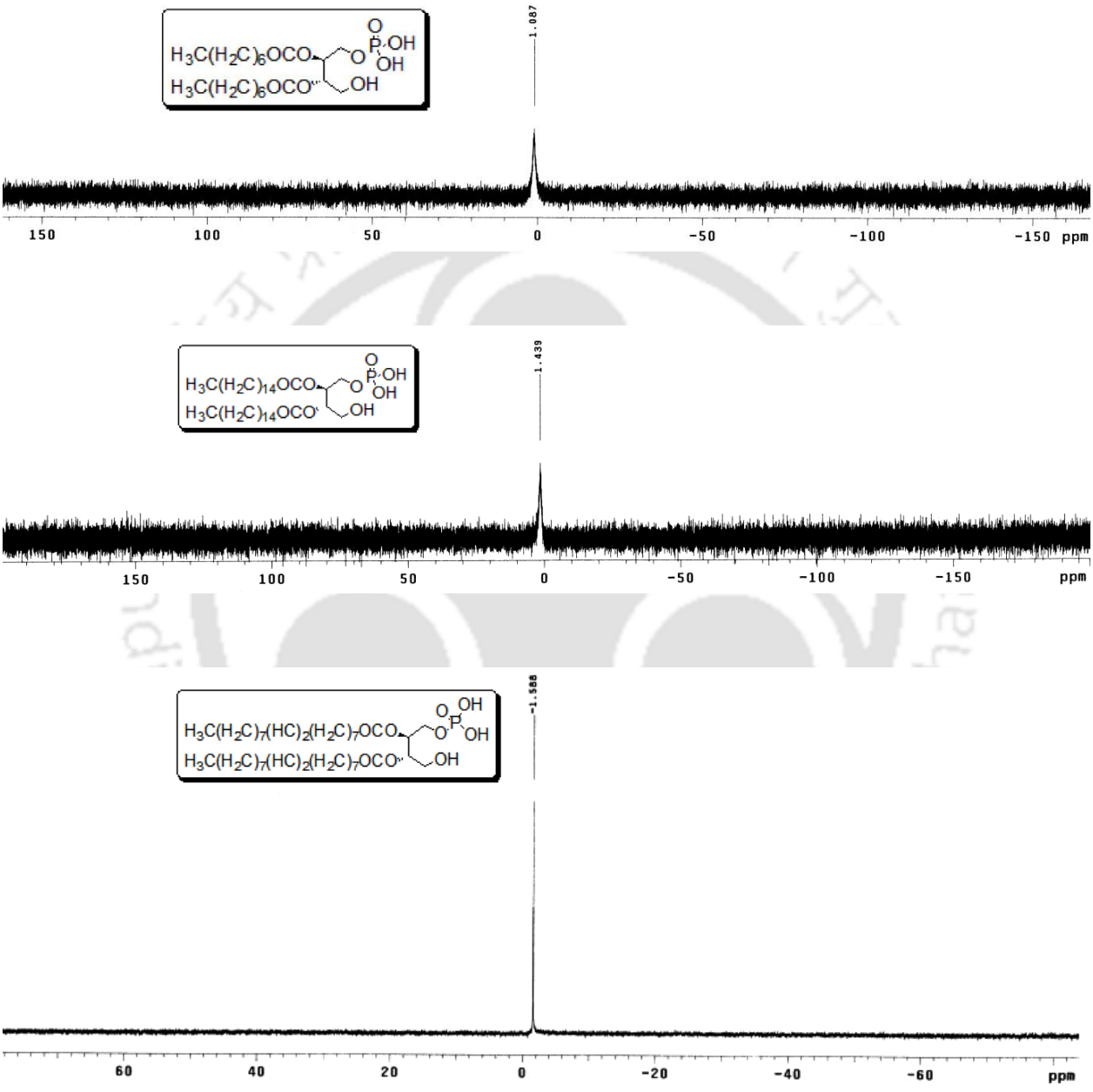

Figure 3.5.1: *^{31}P NMR spectra of compound DAT-PA$_8$, DAT-PA$_{16}$, and DAT-PA$_{18}$*

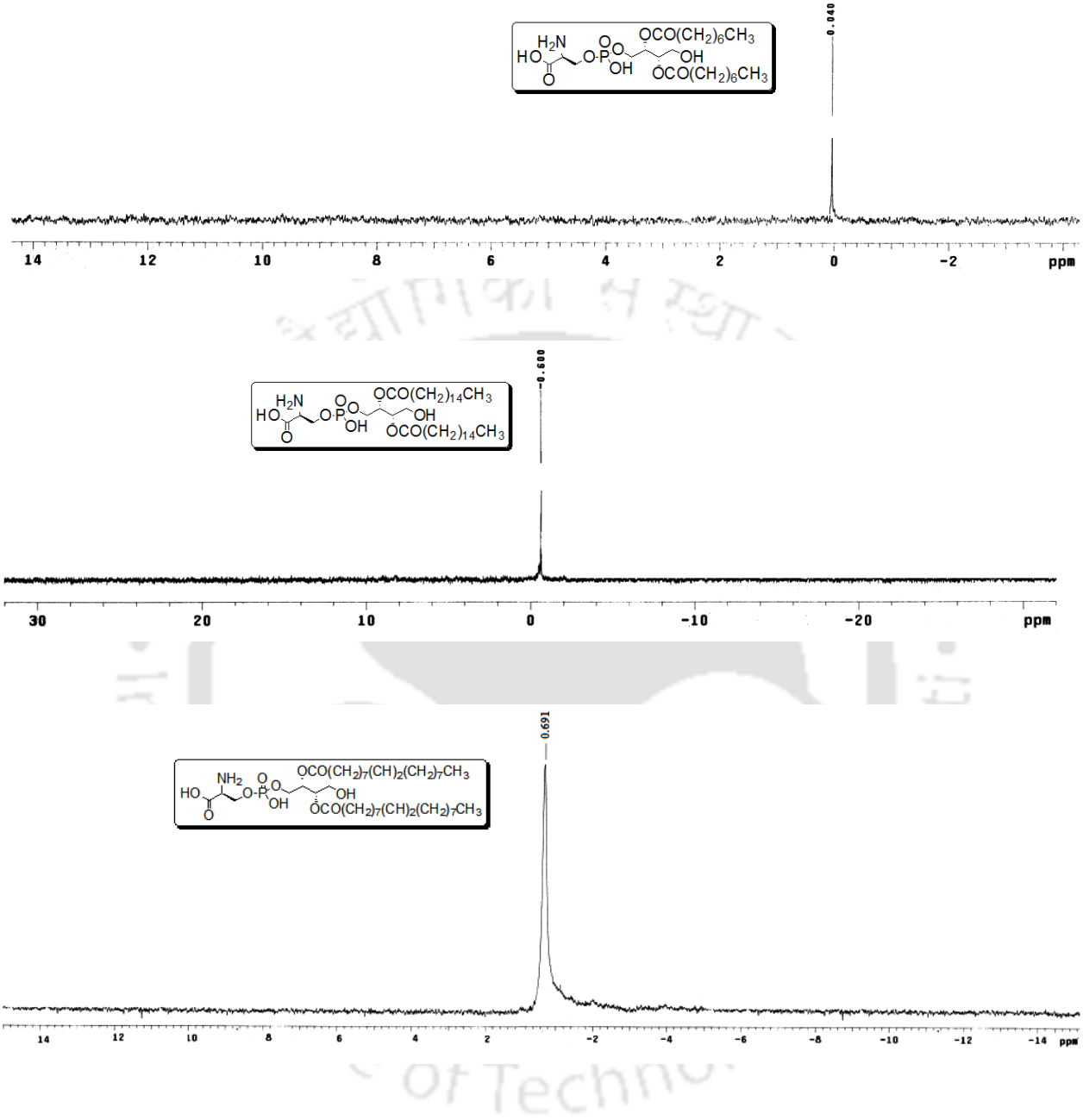

Figure 3.5.2: *^{31}P NMR spectra of compound DAT-PS_8, DAT-PS_{16}, and DAT-PS_{18}*

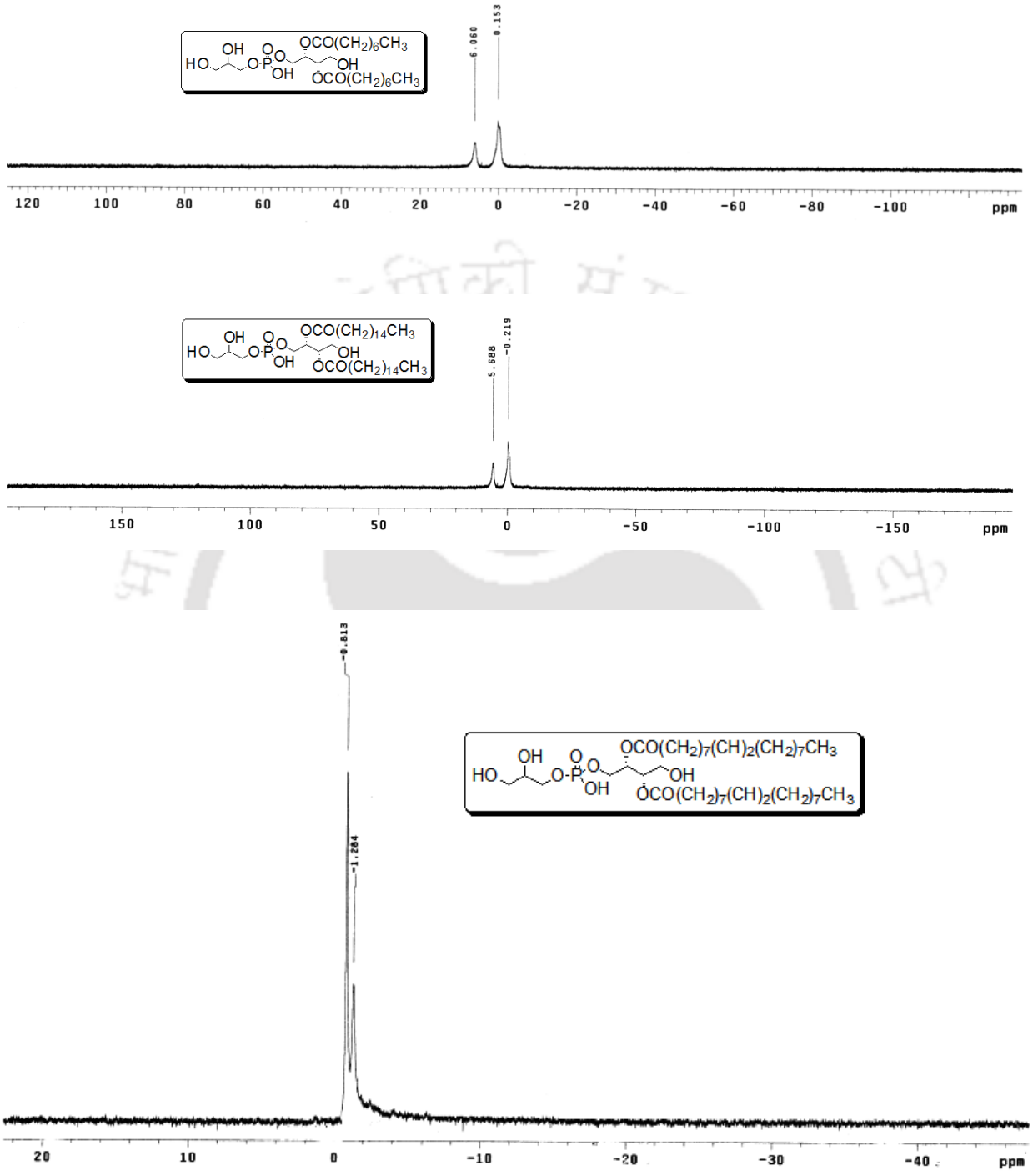

Figure 3.5.3: *^{31}P NMR spectra of compound DAT-PG$_8$, DAT-PG$_{16}$, and DAT-PG$_{18}$*

CHAPTER 4

(Hydroxylmethyl)phenyl Ester Analogues as Protein Kinase C-C1 Domain Regulators

This chapter presents rational design and synthesis of (hydroxymethyl)phenyl ester analogues as PKC-C1 domain regulators. These esters analogous were synthesized using biologically active protocatechualdehyde. It describes the importance of the hydroxymethyl group, hydrophobic side chains, and an ester group at the ortho position. It also describes a detailed *in-vitro* binding properties of (hydroxymethyl)phenyl ester analogues with the C1b subdomains of PKCδ and PKCθ isoenzymes.

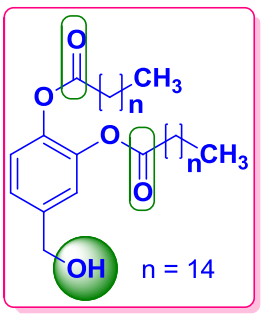

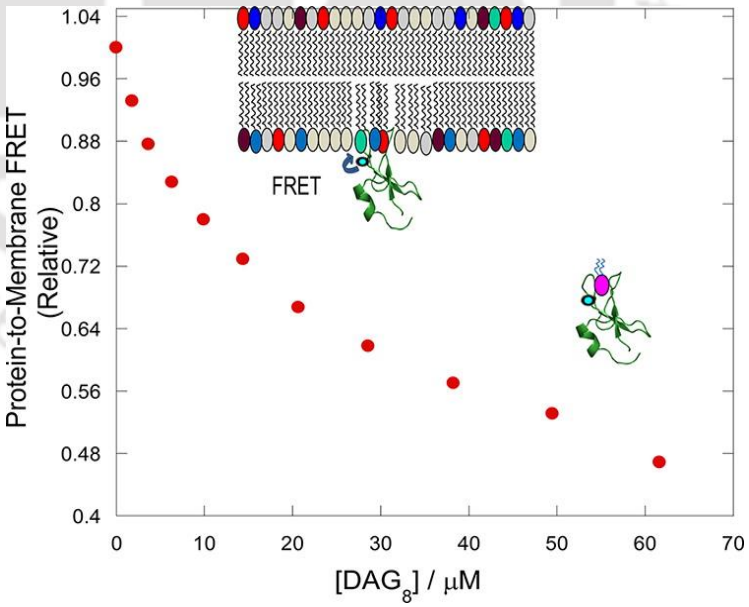

4.1. Background and Focus of the Present Work

The activation of C1 domain containing proteins, especially the PKCs are considered as an important drug target for the treatment of several diseases including cancer and others.[38,165] However, most of the high-affinity C1-domain ligands are a structurally complex natural product.[123] Therefore, structural modification and large-scale production of these compounds are quite difficult. In chapter 2 and 3, we described the design and synthesis of flexible diacyltetrols (DATs) and DAT-anionic phospholipids and its detailed *in-vitro* binding affinity with PKC C1 domain.[151,167] Both DATs and DAT-anionic lipids contain flexible tetrol backbone. It is presumed that structural flexibility allows the ligands to increase the number of possible rotameric forms within the binding site, and one of the rotameric form of the ligand is physiologically active. This makes the flexible ligands much less specific than expected. However, stronger C1 domain binding is also governed by the presence of requisite pharmacophores, proper orientation of the ligands inside the binding pocket and also their localization at the cellular membrane bilayer. From our previous studies, we recognize that the presences of hydroxymethyl and ester groups are very important for the C1 domain ligands. [151,167] Keeping these information in mind, we designed (hydroxymethyl)phenyl ester analogues. These compounds contain the required pharmacophores as of DAGs or DATs and the phenyl group that provides substantial rigidity than that of tetrol or glycerol backbones. In this context, the present chapter describes the synthesis and *in-vitro* binding properties of (hydroxymethyl)phenyl ester analogues to the C1b subdomains of PKCδ and PKCθ. The active (hydroxymethyl)phenyl ester analogues can compete with DAG binding to C1 domains of PKC. The hydroxylmethyl group and a suitable hydrophobic ester group of the compounds play an important role in recognizing the C1 domains of PKC isoenzymes.

Design and Synthesis─ The X-ray crystal structure of the PKCδ-C1b complexed with phorbol-13-*O*-acetate demonstrates that hydroxymethyl and carbonyl groups of the phorbol ester are mainly accountable for its interaction with the C1 domain.[127] The carbonyl group on C3 and the hydroxymethyl groups attached to C20, C4 of the phorbol ester forms hydrogen bonds with the backbone carbonyls or amide protons. The structure–activity studies also reported that the C9 hydroxyl group and C13 carbonyl group are also significant for binding of phorbol ester to the C1 domain. The biological activities and structure–activity relationship (SAR) studies reported that the phenyl backbone containing hydrophobic derivatives of isophthalic acid act as potential C1-domain ligands.

The molecular docking analysis of the isophthalic acid derivatives shows a similar interaction pattern with the PKCδ C1b subdomain as of phorbol esters and DAGs. The hydroxymethyl group and one of the carbonyl groups of dipentyl 5-(hydroxylmethyl)isophthalate form hydrogen bonds with the backbone carbonyls or amide protons of PKCδ C1 domain.[58,119,] On the contrary, the second carbonyl group of this isophthalate derivative shows no direct interactions with the C1 domain. However, it is anticipated that the protein-ligand complex might be stabilized either by a bridging water molecule or by an interaction with anionic phospholipids.[119] The hydrophobic side chains of the C1-domain ligands, including phorbol esters, DAGs, and isophthalic acid derivatives, are reported to interact either with the hydrophobic amino acids (Met-239, Phe-243, Leu-250, Trp 252, and Leu-254) surrounding the ligand binding cleft or with the hydrophobic moiety in the lipid bilayer.[97,127]

We selected (hydroxymethyl)phenyl ester analogues for the development of C1-domain-based PKC modulators. These compounds can be synthesized from the corresponding protocatechualdehyde, vanillin, and isovanillin and are easily derivatizable. These aldehydes are secondary plant metabolites and have many pharmacological effects, including antioxidant and antitumor activities.[166] The two hydroxyl groups of protocatechualdehyde provide access to incorporate different functionalities.

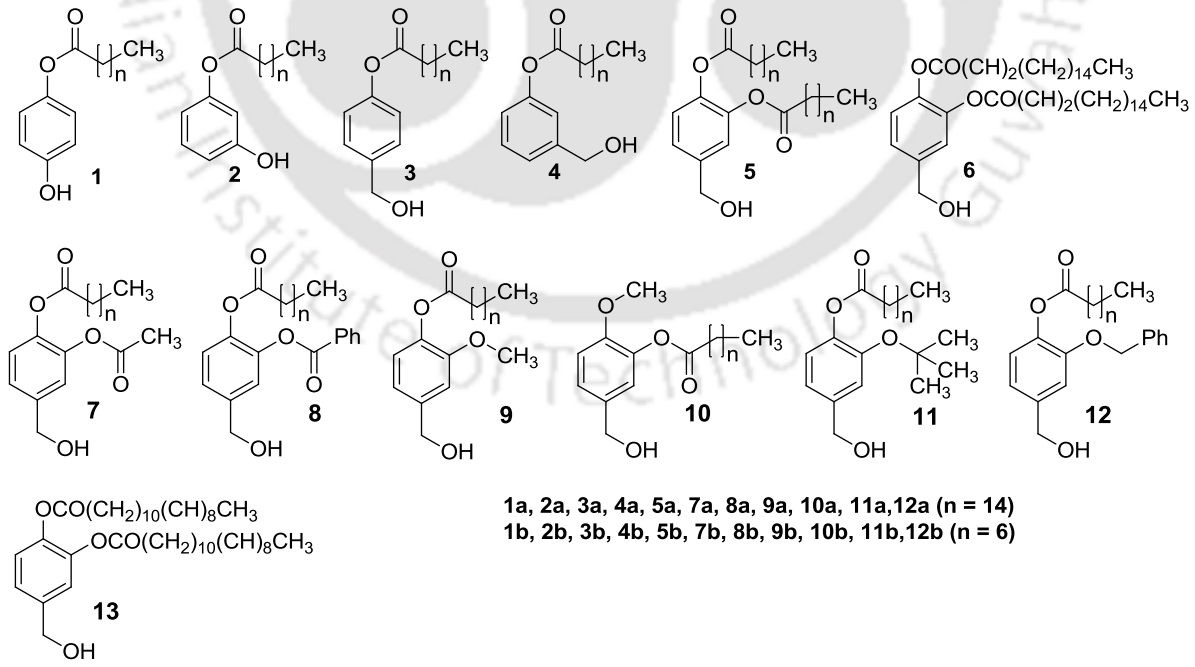

Figure 4.1.1: *Structures of the Synthesized Compounds Used for the Present Study*

They also allow the incorporation of two of the phorbol ester pharmacophores (the hydroxyl and carbonyl functionalities) within the same interatomic distance as in phorbol ester. The long alkyl chain attached to the hydroxyl group at the first position is useful for anchoring the ligands in the lipid bilayer/membranes and for interaction with anionic phospholipids. The second hydroxyl group is available to introduce different functionalities for optimization of the protein binding. The hydrophobic interactions are difficult to model. Thus, we synthesized a series of (hydroxymethyl)phenyl ester analogues with different side chains to study the impact of different functionalities and side chains on the binding affinity (*Figure 4.1.1*). We initially synthesized 4-(hydroxymethyl)phenyl diester analogue (**5**) in two steps using commercially available protocatechualdehyde as the starting material (*Scheme 4.1.1*). The compound **5**, with long (palmitic acid) and short (caprylic acid) chain fatty acids were synthesized to study the impact of alkyl chain length on the binding affinity.

To investigate the importance of the two ester groups with alkyl chains and interatomic distance between the phorbol ester pharmacophores in C1b subdomain binding, we prepared 3-(hydroxymethyl)phenyl ester (**3**) and 4-(hydroxymethyl)phenyl ester (**4**), with a monoester group at the meta and para positions, respectively. To investigate the importance of the hydroxymethyl group of compounds **3**–**5**, we prepared hydroxyphenyl ester analogues **1** and **2**, with required phorbol ester pharmacophores. It has also been reported that DAGs with unsaturated ester groups generated by PI-PLC are more potent in PKC activation than saturated forms produced by other pathways.[31,121,145,153] Therefore, we prepared 4-(hydroxymethyl)phenyl diester analogues **6** and **13** with unsaturated fatty acid (oleic acid and arachidonic acid, respectively). To understand the role of the long alkyl chain in the ortho position, we also prepared compounds **7** and **8** with acetic acid and benzoic acid, respectively. An ether group was also introduced to understand the importance of the ester group at the ortho position in C1-domain binding.

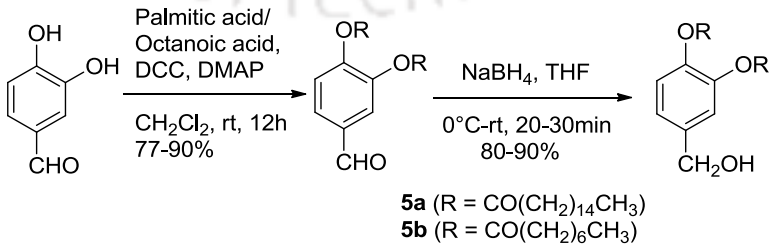

Scheme 4.1.1: *Synthesis Route to (Hydroxymethyl)phenyl Ester (**5**)*

The positions of the ester and ether groups of **9** and **10** were selected for further SAR studies. To increase the hydrophobicity of the ether-linked side chain, we prepared compounds **11** and **12** with *tert*-butyl and benzyl ether groups, respectively. Hydroxyphenyl ester analogues **1** and **2** were directly synthesized from the corresponding dihydroxybenzene, using the standard *N*,*N*′-Dicyclohexylcarbodiimide (DCC)-mediated coupling reaction with octanoic acid and palmitic acid.[134] The (hydroxymethyl)phenyl ester analogues (**3**–**6**, **13**) were conveniently synthesized in two steps using the commercially available corresponding hydroxybenzaldehydes as the starting material. The phenolic hydroxyl groups of the hydroxybenzaldehydes were esterified with octanoic acid, palmitic acid, oleic acid, and arachidonic acid using the DCC-mediated coupling reaction to produce the formylphenyl ester analogues. Subsequent reduction of the formyl group with $NaBH_4$ provided the target (hydroxymethyl)phenyl ester analogues **3**–**6** and **13**. For the preparation of compounds **7**, **8**, **11**, and **12**, we first synthesized 4-formyl-2-hydroxyphenyl octanoate/hexadecanoate from protocatechualdehyde using the DCC-mediated coupling reaction with octanoic acid and palmitic acid. The selective formations of these monoesters were characterized by NMR and mass spectral analyses. Further DCC-mediated coupling reaction with acetic acid/benzoic acid and subsequent reduction of the formyl group with $NaBH_4$ resulted in compounds **7** and **8**. Treatment of 4-formyl-2-hydroxyphenyl octanoate/hexadecanoate with *tert*-butyl iodide/benzyl bromide using Ag_2O and reduction of the formyl group with $NaBH_4$ yielded compounds **11** and **12**. Compounds **9** and **10** were prepared from vanillin and isovanillin respectively, through DCC-mediated esterification followed by reduction of the formyl group with $NaBH_4$.

Protein Binding– In the classical and novel PKC isoenzymes, the DAG-sensitive C1 domain is duplicated into a tandem C1 domain consisting of C1a and C1b subdomains. The C1b subdomains of PKCδ and PKCθ are reported to have sufficiently strong DAG binding affinities and to be easy to obtain in soluble form in sufficient amounts from bacterial cells. In the present study, these C1b subdomains were used to measure the in vitro binding potencies of the synthesized compounds in monomeric form by using intrinsic fluorescence quenching method. We also used Förster resonance energy transfer (FRET) based liposome binding assay and a competitive displacement assay to measure the ligand binding affinity and specificity under liposomal environment.[161,162]

Interaction with Soluble Ligands─ The intrinsic fluorescence of the PKC C1b subdomains is due to the presence of a single tryptophan (Trp-252 in delta, Trp-253 in theta) and tyrosine residues (Tyr-236 and Tyr-238 in delta, Tyr-249 and Tyr-251 in theta), and the change in the conformation or microenvironment caused by ligands can be detected by fluorescence spectroscopy. The single Trp residue is also present close to the DAG binding pocket of the C1b subdomains of PKCδ and PKCθ.[138,167] Figure 4.1.2 shows a representative plot of the fluorescence quenching data for PKCδ C1b in the presence of ligands.

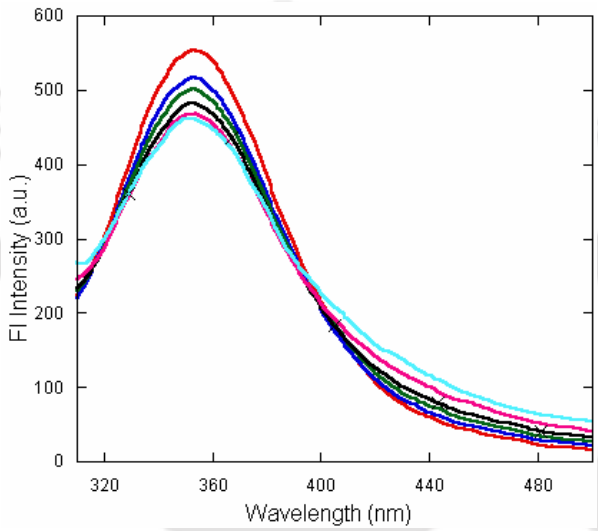

Figure 4.1.2: *Representative fluorescence quenching plot of PKCδ C1b protein by compound (**5a**). Addition of increased concentration of **5a** (0-10 μM**)** to PKCδ C1b (2 μM) quenched the intrinsic fluorescence intensity at 340 nm (λ_{ex} = 280 nm).*

The measured binding affinities revealed that compounds **5**, **6**, **8**, and **13** (*Figure 4.1.3*) with different chain lengths interact with the C1b subdomains with the highest affinity (0.54-1.15 μM) and that other compounds have comparable binding affinities for both proteins (*Table 4.1.1*). Monomeric ligands **5b** and **8b** show more than 5-fold stronger binding affinity than DAG_8 for PKCδ protein. The binding results also show that (hydroxymethyl)phenyl esters have higher binding affinity for PKCθ C1b than for PKCδ C1b, possibly because of the additional hydrogen bonds. The molecular models of ligand-bound protein showed that there were three possible hydrogen bonds between DAG and PKCδ C1b, whereas compounds **5b** and **8b** showed four hydrogen bonds with PKCδ C1b. The experimental binding results and docking score values obtained from the models do not always agree (*Table 4.2.1*).

This difference indicates that both proteins and compounds can undergo conformational changes under experimental conditions.

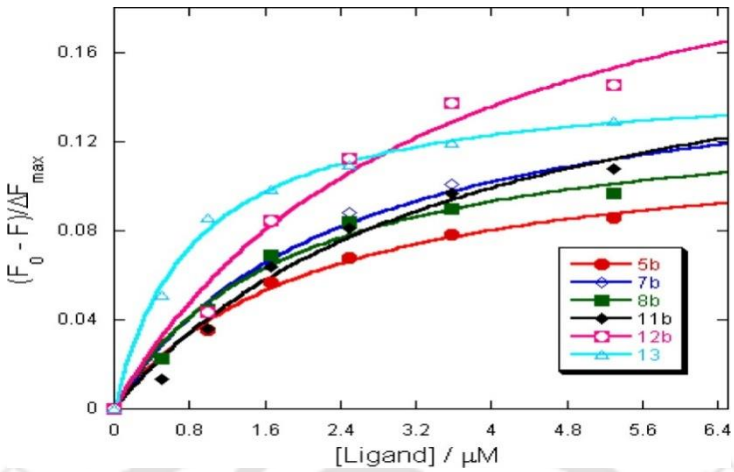

Figure 4.1.3: *Binding of ligands with PKCδ C1b. Representative plot of fluorescence intensity of PKCδ C1b (2 μM) in buffer (20 mM Tris, 160 mM NaCl, 50 μM $ZnSO_4$, pH 7.4) in the presence of varying concentrations of* ***5b*** *(●),* ***7b*** *(◊),* ***8b*** *(■),* ***11b*** *(♦),* ***12b*** *(□), and* ***13*** *(△), where F and F_0 are the fluorescence intensities in the presence and absence of the ligands, respectively. The solid lines are nonlinear least-squares best-fit curves.*

To understand the importance of hydrophobicity of the compounds in C1-domain binding, a similar analysis was performed with the long-chain (hydroxymethyl)phenyl esters. The two proteins showed similar patterns of dependence on the hydrophobicity of the compounds (*Table 4.1.1*). For compounds **8a** (XLOGP3 = 9.46) and **8b** (XLOGP3 = 5.13), although there is a distinct difference in hydrophobicity, the difference in binding affinity is very small for the two proteins. This could be due to the binding orientations with the C1b subdomains through the hydroxymethyl group. The molecular docking analysis also indicates that the overall high binding affinities of compounds **5** and **8** are probably associated with the presence of hydroxymethyl and carbonyl functionalities within the same interatomic distance as in phorbol ester. The hydrophobic amino acids surrounding the binding site of the C1 domain also interact with the hydrophobic side chains of the ligands. Thus, the binding affinity values of (hydroxymethyl)phenyl esters highlight the importance of ligand hydrophobicity and binding orientation, in a manner similar to those reported for C1-domain ligands.

***Table 4.1.1*:** *K_D (ML) Values for the Binding of Ligands with the PKCδ C1b and PKCθ C1b Proteins[a] at Room Temperature*

compound	K_D(ML) (μM)				K_D(ML) (μM)		
	PKCδ C1b	PKCθ C1b	XLOGP3	compound	PKCδ C1b	PKCθ C1b	XLOGP3
DAG_{16}	7.02 ± 0.33	7.47 ± 0.48	14.04	DAG_8	10.17 ± 0.68	6.29 ± 0.44	5.11
1a	6.17 ± 0.26	–	8.64	**1b**	7.25 ± 0.49	–	4.31
2a	5.83 ± 0.28	–	8.56	**2b**	6.94 ± 0.37	–	4.22
3a	5.13 ± 0.31	–	8.11	**3b**	5.26 ± 0.28	–	3.78
4a	4.78 ± 0.31	–	8.11	**5b**	1.23 ± 0.17	1.17 ± 0.11	6.53
5a	1.10 ± 0.09	1.07 ± 0.05	15.19	**7b**	1.33 ± 0.13	1.27 ± 0.13	3.53
6	1.03 ± 0.07	–	14.95	**8b**	1.02 ± 0.16	0.99 ± 0.13	5.13
7a	1.27 ± 0.08	1.26 ± 0.11	7.87	**9b**	2.32 ± 0.19	1.98 ± 0.17	3.75
8a	0.91 ± 0.15	0.81 ± 0.08	9.46	**10b**	3.87 ± 0.16	–	3.75
9a	1.98 ± 0.19	1.59 ± 0.09	8.09	**11b**	1.87 ± 0.13	1.74 ± 0.22	4.74
10a	3.45 ± 0.18	–	8.09	**12b**	1.96 ± 0.18	1.84 ± 0.11	5.02
11a	1.84 ± 0.11	1.62 ± 0.03	9.07	**13**	**0.83 ± 0.09**	**0.54 ± 0.12**	13.54
12a	1.67 ± 0.15	1.71 ± 0.05	9.35				

[a]*Protein (1 μM) in buffer (20 mM Tris, 160 mM NaCl, 50 μM $ZnSO_4$, pH 7.4).*

Table 4.1.2: *Anisotropy[a] Values of the Ligands in the Presence and Absence of the PKCδ and PKCθ C1b Proteins at Room Temperature*

compound	**PKCδ C1b**	**PKCθ C1b**	**compound**	**PKCδ C1b**	**PKCθ C1b**
buffer[b]	0.0439 (0.0045)	0.0667 (0.0073)	DAG_8[c]	0.0978 (0.0063)	0.1069 (0.0051)
DAG_{16}[c]	0.1028 (0.0061)	0.0727 (0.0037)	**1b**[c]	0.0596 (0.0077)	–
1a[c]	0.1424 (0.0026)	–	**2b**[c]	0.0856 (0.0013)	–
2a[c]	0.0994 (0.0063)	–	**3b**[c]	0.0562 (0.0032)	–
3a[c]	0.0892 (0.0045)	–	**4b**[c]	0.0660 (0.0026)	–
4a[c]	0.0768 (0.0032)	–	**5b**[c]	0.0874 (0.0161)	0.1111 (0.0046)
5a[c]	0.0685 (0.0065)	0.0984 (0.0156)	**7b**[c]	0.0565 (0.0042)	0.0884 (0.0005)
6[c]	0.0915 (0.0008)	–	**8b**[c]	0.0850 (0.0119)	0.0896 (0.0022)
7a[c]	0.0862 (0.0051)	0.0973 (0.0025)	**9b**[c]	0.0834 (0.0047)	0.0933 (0.0008)
8a[c]	0.0838 (0.0077)	0.0903 (0.0028)	**10b**[c]	0.0673 (0.0038)	–
9a[c]	0.0889 (0.0075)	0.0946 (0.0006)	**11b**[c]	0.0766 (0.0029)	0.0945 (0.0016)
10a[c]	0.1156 (0.0132)	–	**12b**[c]	0.0722 (0.0031)	0.0950 (0.0044)
11a[c]	0.1217 (0.0024)	0.1146 (0.0025)	**13**[c]	0.1001 (0.0028)	0.0998 (0.0012)
12a[c]	0.1129 (0.0055)	0.1317 (0.0016)			

[a]*Values in parentheses indicate standard deviations.* [b]*Protein, 1 μM in buffer (20 mM Tris, 160 mM NaCl, 50 μM $ZnSO_4$, pH 7.4).* [c]*DAG, **1**–**13**, 10 μM; protein, 1 μM in buffer (20 mM Tris, 160 mM NaCl, 50 μM $ZnSO_4$, pH 7.4).*

To gain more information about ligand–protein interactions, we performed steady-state fluorescence anisotropy measurements of the proteins in the absence and presence of the ligands and DAGs. The increase in anisotropy values of the proteins in the presence of the

ligands support their ligand binding. The degree of anisotropy of pure PKCδ C1b protein increases from 0.0439 in buffer to 0.0874 and 0.0850 upon interaction with 10-fold excesses of ligands **5b** and **8b**, respectively (*Table 4.1.2*). Similar increases in anisotropy values were observed for the proteins in the presence of DAGs and other compounds. Although the changes in anisotropy values were different for the compounds, this experiment still suggests that the presence of the compounds increases the rigidity of the surrounding environment of the protein in a manner similar to that of DAGs.

Interaction with Ligand-Associated Liposomes─ Peripheral proteins such as PKCs are reported to interact with the membrane surface through their lipid-binding C1 and C2 domains. The C1 domains have both a membrane-binding surface and a lipid-binding groove. The C1 domain responds to increased DAG levels at the plasma membrane. To measure the binding properties of the C1b subdomains of PKC isoforms with the long-chain (hydroxymethyl)phenyl ester analogues, we performed protein-to-membrane FRET-based liposome binding assay and competitive binding assay. In this assay, one Trp residue in the C1b subdomains of PKC serve as the FRET donor and a low density of membrane-embedded, dansyl-PE (dPE) lipids serve as the acceptors.[161,162] A FRET-based liposome binding assay was employed to compare the qualitative ligand selectivity of the C1b subdomains in a liposomal environment. The protein-to-membrane FRET signal was monitored to measure the protein docking to the ligand-associated liposome surface. In a separate experiment, liposomes without the ligands were titrated into a solution of protein, to control the increasing background emission arising from direct dansyl-PE excitation and PS binding of C1b subdomains. Following subtraction of the background signal and correction for dilution, the binding isotherm was generated. The qualitative ligand selectivity pattern shows that C1b subdomains have better binding affinity for **5a**-, **6**-, and **8a**-associated liposomes than for DAG_{16}-associated liposomes, under similar experimental conditions (*Table 4.1.3*). The liposomes of ligands **5a**, **6**, and **8a** show more than 5-fold stronger binding affinity than DAG_{16}. Such titration experiments are useful for measuring relative binding affinities under similar liposomal environments, but not for accurate determination of affinities. The dansyl-PE concentration needed for the FRET assay significantly exceeds the binding constant of the interaction. We used a FRET-based competitive binding assay to compare quantitatively the binding affinities and specificities of C1b subdomains for the liposome-associated targeted ligand.

In this method, competitive inhibitor DAG_8 was titrated into the solution containing C1b-subdomain-bound liposomes. The decrease in the protein-to-membrane FRET signal (*Figure 4.1.4*) was monitored to measure the displacement of protein from liposomes by DAG_8 and to calculate an apparent inhibitory constant [$K_I(DAG_8)_{app}$].

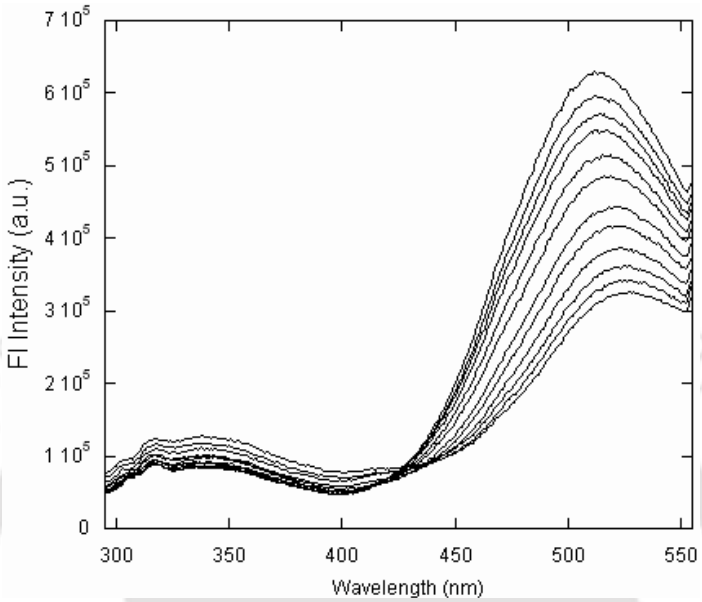

Figure 4.1.4*: Representative plot of competitive binding of DAG_8 to PKCδ C1b protein bound liposome. The curve represents the emission spectrum (λ_{ex} = 284 nm) of a sample in which the protein (1 μM) was added to PC/PE/PS/dPE/***8a*** liposome (55/15/20/5/5). The decrease in FRET efficiency between Trp residues of PKCδ C1b subdomain and dansyl group, caused by the displacement of protein from labeled liposome, is demonstrated by the increase in Trp fluorescence (340 nm) and the concomitant decrease in dansyl emission (522 nm).*

Figure 4.1.5 represents the DAG_8-induced competitive displacement of C1b subdomain from 5% targeted-ligand-associated liposomes. The apparent inhibition constant [$K_I(DAG_8)_{app}$] for DAG_8 depends on ligand concentration in the liposomes and the background lipid composition, as well as the affinities of the C1b subdomains for ligands and DAG_8. This assay confirmed that the synthesized ligands interact with the C1 domains through the DAG/phorbol ester binding site. The results also showed that higher concentrations of DAG_8 were required for the displacement of both proteins from the ligand **5a**-, **6**-, **8a**-, and **13**-associated liposomes (*Table 4.1.3*).

Finally, the equilibrium dissociation constant [$K_D(L_{16})$] for the C1b subdomain binding to the liposome-associated targeted ligand was calculated using the standard equation for competitive inhibition.[162] Comparison of the equilibrium dissociation constant for competitive inhibitor DAG_8 revealed that C1b subdomains have higher binding affinities for the compound **5**-, **6**-, **8**-, and **13**-associated liposomes (*Table 4.1.3*).

Table 4.1.3: *Equilibrium Parameters for PKCδ C1b and PKCθ C1b Protein[a] Binding to the Ligand-Associated Liposomes[b] at Room Temperature*

compound	K_D(LL) (nM)		$K_I(DAG_8)_{app}$ (μM)		$K_D(L_{16})$ (nM)	
	PKCδ C1b	PKCθ C1b	PKCδ C1b	PKCθ C1b	PKCδ C1b	PKCθ C1b
5a	3.36 ± 0.58	2.80 ± 0.19	23.43 ± 1.03	21.54 ± 0.69	129.56 ± 5.51	137.48 ± 3.96
6	3.24 ± 0.64	2.76 ± 0.11	23.85 ± 1.85	23.22 ± 1.22	117.78 ± 3.11	–
7a	6.40 ± 0.45	3.53 ± 0.34	19.79 ± 1.05	13.85 ± 0.54	183.47 ± 5.23	267.76 ± 6.78
8a	2.87 ± 0.27	2.53 ± 0.21	28.02 ± 1.82	24.11 ± 1.77	89.29 ± 3.11	92.49 ± 2.19
11a	9.06 ± 0.61	6.98 ± 0.60	13.13 ± 0.90	12.02 ± 1.54	434.85 ± 9.14	415.89 ± 6.98
12a	6.76 ± 0.30	4.64 ± 0.89	14.14 ± 01.75	12.91 ± 1.79	356.76 ± 4.59	406.87 ± 10.15
13	2.98 ± 0.28	2.19 ± 0.18	30.14 ± 2.22	25.79 ± 1.93	75.33 ± 1.87	59.02 ± 2.59
DAG_{16}	17.13 ± 0.98	14.70 ± 1.34	–		–	

[a]Protein, 1 μM in buffer (20 mM Tris, 150 mM NaCl, 50 μM $ZnSO_4$, pH 7.4). [b]Active liposome composition, PC/PE/PS/dPE/ligand$_{16}$ (55:15:20:5:5).

The molecular docking and binding analysis shows that the synthesized ligands interact differentially with the C1b subdomains of PKCδ and PKCθ, both in monomeric form and in a liposomal environment. Modifications of the ester side chains have a modest effect on the binding. Compounds **5**–**8** and **13** have both of the phorbol ester pharmacophores. However, compound **7**, with a shorter ester group at the ortho position, shows a weaker binding affinity. These results highlight the similarity in the importance of hydrophobicity in the ligands as for other C1-domain ligands. Our studies with compounds **9**–**12** show that lack of an ester group at the ortho position contributes to diminished binding affinity. The only difference in functionality at the ortho position between compounds **8** and **12** causes more than a 2-fold difference in binding affinity for the two proteins under similar experimental conditions. Our studies with compounds **6** and **13**, having unsaturated acyl groups, showed higher binding affinities than compound **5**, having saturated acyl groups. The results are in accordance with the reported binding affinity of unsaturated DAG to C1 domains.[121,168] This could be due to either genuine selectivity of PKC C1 domains for ligands with unsaturated acyl groups or the effect of these ligands on the membrane structure.

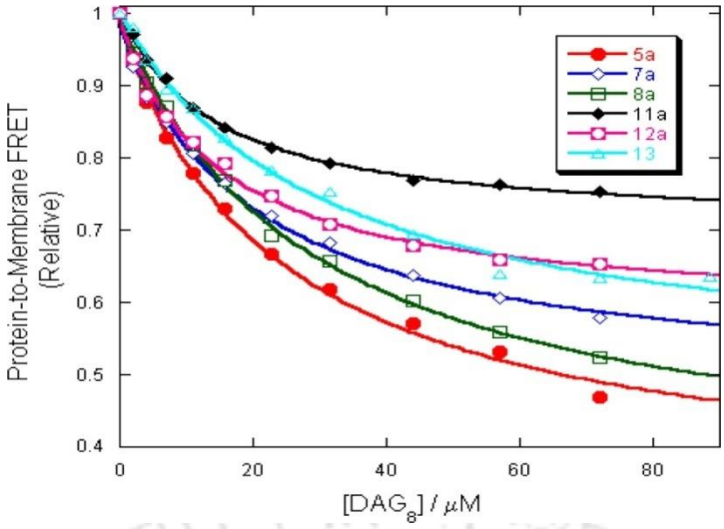

Figure 4.1.5: *Competitive displacement assay for the PKCδ C1b subdomains (1 μM) bound to liposome-containing ligands* ***5a*** *(●),* ***7a*** *(◊),* ***8a*** *(□),* ***11a*** *(♦),* ***12a*** *(□) and* ***13*** *(△). The bound complex was titrated with the competitive inhibitor* DAG_8.

Extent of Membrane Localization─ To evaluate the relationship between the protein binding properties of the ligands and the extent of their localization at the bilayer/water interface, we performed fluorescence quenching experiments using PC/cholesterol/$ligand_{16}$/NBD-PE liposomes. The NBD dye is embedded close to the bilayer interface, providing a useful marker for surface interactions of membrane-active C1-domain ligands.

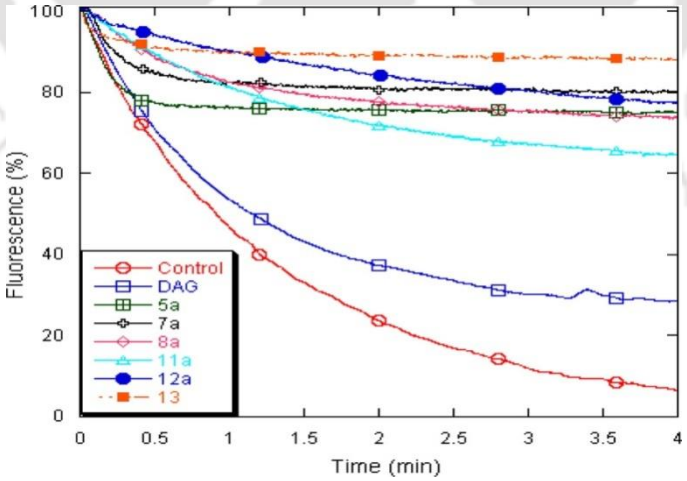

Figure 4.1.6: *Fluorescence quenching of NBD-PE embedded in PC/cholesterol/*$ligand_{16}$*/NBD-PE (44.5:44.5:10:1) liposomes. Sodium dithionite, 0.6 μM; control no ligand*

The NBD fluorescence quenching by sodium dithionite provided a measure of the membrane interactions of the ligands.[125,160] *Figure 4.1.6* demonstrates that ligand-associated fluorescent liposomes yielded significant changes in the rate of dithionite-induced fluorescence quenching of the bilayer-embedded dye. All of the examined ligands yielded lower quenching rates than the control liposomes (without any ligands). The results suggest that the NBD dye became more "shielded" from the soluble dithionite quencher, because of the presence of (hydroxymethyl)phenyl ester analogues in the liposomes. The results also imply that these ligands are more localized at the liposome surface than DAG is. Thus, in a liposome environment, the (hydroxymethyl)phenyl ester analogues (**5a**, **7a**, **8a**, **11a**, and **12a**) are more accessible for protein binding than DAG is. This is in complete correlation with their protein binding properties in the liposome environment.

Docking Analysis─ Our molecular docking analysis showed that the (hydroxymethyl)phenyl ester analogues are anchored to binding site of the C1 domain of PKC in a similar fashion, as phorbol esters, DAG-lactones, and dialkyl 5-(hydroxylmethyl)isophthalate.[119,127,147] The ligand's hydroxyl group is also hydrogen-bonded to the backbone amide proton of Thr-242 and the carbonyls of Thr-242 and Leu-251 (*Figure 4.1.7*). The model structure also showed that one carbonyl group of ligands **5b**, **7b**, and **8b** is also hydrogen-bonded to the backbone amide proton of Gly-253. The other carbonyl group might be involved in interactions with charged lipid head groups, including phosphatidylserine for activation.[126] In contrast, the hydrogen bond with the backbone amide proton of Gly-253 is missing for ligands **9b**–**12b**, because of the presence of the ether group (*Figure 4.1.7).* Overall, these results demonstrate that a hydroxymethyl group and one ester group with hydrophobic side chain at the ortho position are needed for binding activity of the compounds to the C1 domain, but if the compound has one ether group at the ortho position, another ether-/ester-linked hydrophobic side chain are also required. The results also show that long-chain (hydroxymethyl)phenyl esters can differentially influence the in vitro membrane interaction properties of PKCθ and PKCδ. The affinity differences between the proteins are solely because of the differences in the residues and surface areas of the activator binding pockets. The activating effect of (hydroxymethyl)phenyl esters can be lower than that of phorbol esters or other natural ligands under similar experimental conditions.

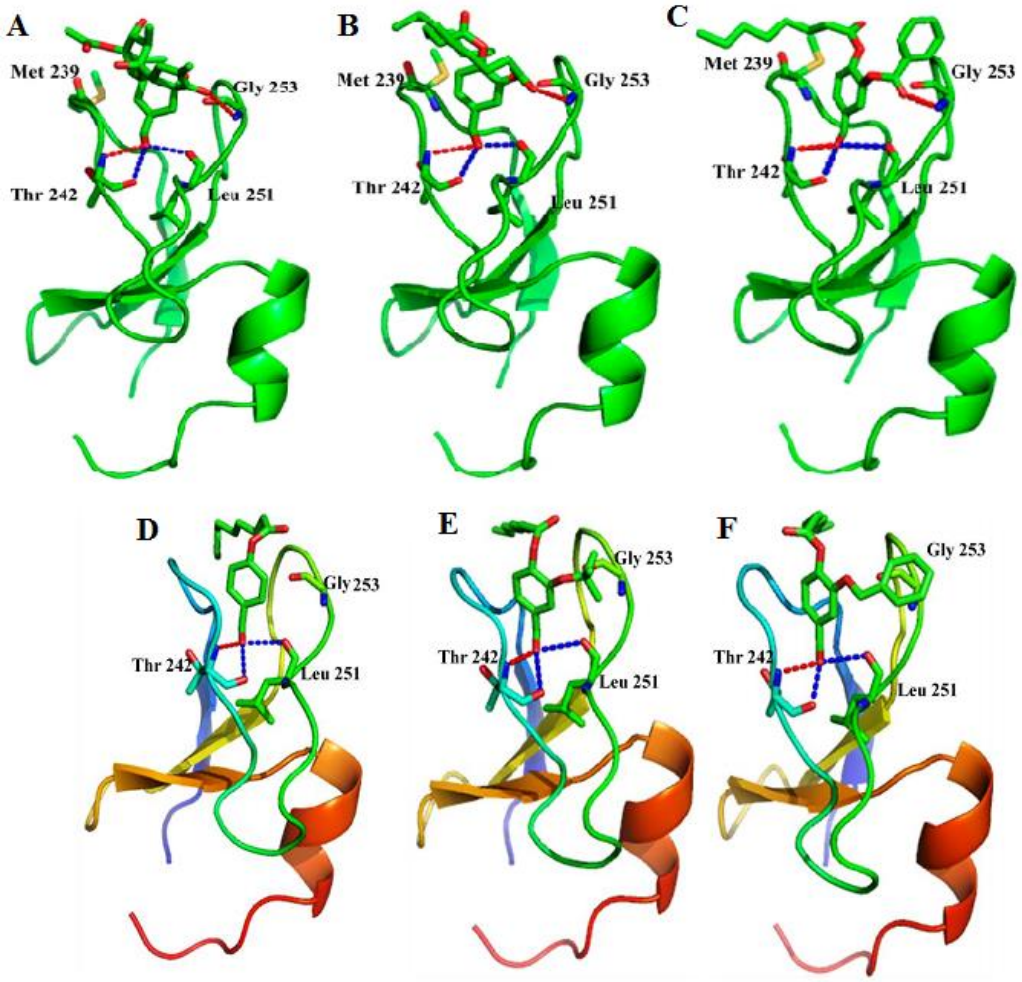

Figure 4.1.7: *Structures of ligand-bound PKCδ C1b subdomain. (A) Crystal structure of phorbol-13-O-acetate-bound PKCδ C1b; (B) modeled structure of* ***5b****; (C) modeled structure of* ***8b****; (D) modeled structure of* ***3b****; (E) modeled structure of* ***11b****;* ***(F)*** *modeled structure of* ***12b.*** *The modeled structures were generated using Molegro Virtual Docker, version 4.3.0. The oxygen and nitrogen atoms are shown in red and blue, respectively. The dotted lines indicate possible hydrogen bonds.*

Table 4.1.4: *Docking score values obtained from the docking of ligands into the PKCδ C1b subdomain using Molegro Virtual Docker, version 4.3.0.*

Compound	MolDock Score	Rerank Score
5b	-114.519	-78.846
7b	-118.402	-94.292
8b	-105.553	-71.561
11b	-124.388	-81.594
12b	-115.101	-95.105

Conclusion

This chapter described the synthesis of (hydroxymethyl)phenyl ester analogues that interact with the C1 domain of PKC isoforms through the DAG/phorbol ester binding site. Synthesis of these compounds from the corresponding aldehydes provided the ability to generate pure samples and the freedom to explore the roles of a hydroxymethyl group, hydrophobic side chains, and an ester group at the ortho position. The measured binding parameters indicate that the active compounds can also compete with DAG for binding to C1 domains of PKC under liposomal environment. This makes these compounds, in particular the derivatives of protocatechualdehyde, potential regulators of PKC isoforms and can be further developed as research tools or lead compounds in drug development.

Encouraged by the C1 domain binding properties of the (hydroxymethyl)phenyl ester analogues, synthesized from protocatechualdehyde; we also studied the C1 domain binding properties of alkyl cinnamates, the other compounds synthesized from the same protocatechualdehyde. The cinnamates are already known to alter the PKC enzyme activities. Therefore, the C1 domain binding properties would further help to understand their ability to alter PKC enzyme activities. In the next chapter we described the synthesis, spectral analysis and C1 domain binding properties of the alkyl cinnamates.

4.2. Experimental Section

4.2.1. Instrumentations and Characterization

As described in chapter 2 section 2.2.1

4.2.2. General Procedure for the Synthesis of Formyl-phenyl Monoester Analogues:

Hexadecanic acid/octonic acid (1.1 equiv), dicyclohexylcarbodiimide (1.1 equiv), and *N*,*N*-dimethylaminopyridine (0.1 equiv) were added to a stirring solution of monohydroxybenzaldehyde (1.0 equiv) in anhydrous dichloromethane (8 mL) under a N_2 atmosphere. Stirring was continued for 12 h at room temperature. After completion of the reaction (monitored by TLC), the reaction mixture was filtered and washed (three times) with dichloromethane. The filtrate was concentrated under reduced pressure, and column chromatography was performed with silica gel and a gradient solvent system of 0–8% ethyl acetate/hexane to provide corresponding esters. The average yields were 77–90%.

4.2.3. General Procedure for the Synthesis of Formylphenyl Diester Analogues[167]: Palmitic acid/octonic acid (2.2 equiv), dicyclohexylcarbodiimide (2.2 equiv), and *N*,*N*-dimethylaminopyridine (0.1 equiv) were added to a stirring solution of dihydroxybenzaldehyde (1.0 equiv) in anhydrous dichloromethane (8 mL) under a N_2 atmosphere. Stirring was continued for 12 h at room temperature. After completion of the reaction, the reaction mixture was filtered and washed (three times) with dichloromethane. The filtrate was concentrated under reduced pressure, and column chromatography was performed with silica gel and a gradient solvent system of 0–8% ethyl acetate/hexane, yielding the corresponding esters. The average yields were 77–90%.

4.2.4. General procedure for the Reduction of Aldehydes: To a stirring solution of formylphenyl ester analogues (1.0 equiv) in THF, $NaBH_4$ (2.0 equiv) was added portion-wise at 0 °C over 5 min, and stirring was continued for another 15 min at room temperature. After completion of the reaction (monitored by TLC), the mixture was cooled to 0 °C; the reaction was carefully quenched with 1 mL of acetic acid, followed by 3 mL of water; and the mixture was extracted with ethylacetate (3 × 10 mL). The organic layer was dried over anhydrous Na_2SO_4 and concentrated under reduced pressure. Column chromatography with silica gel and a gradient solvent system of 10–30% ethyl acetate/hexane yielded the corresponding (hydroxymethyl)phenyl ester analogues as final products. The average yields were 80–96%.

4.2.5. General Procedure for the Synthesis of 2-*tert*-Butoxy and 2-(Benzyloxy)-4-formylphenyl Hexadecanoate/Octanoate: To a solution of 4-formyl-2-hydroxyphenyl hexadecanoate/octanoate (1.0 equiv) in anhydrous dichloromethane (10 mL), were added silver oxide (1.5 equiv) and benzyl bromide/*tert*-butyl iodide (1.2 equiv) under a N_2 atmosphere. Stirring was continued for 8 h at room temperature. After completion of the reaction, the reaction mixture was filtered off through a pad of Celite. The solvent was removed under reduced pressure. Column chromatography with silica gel and a gradient solvent system of 6–10% ethyl acetate to hexane yielded the target compounds. The average yields were 80–92%.

4.2.6. Protein Purification: The PKCδ and PKCθ C1b subdomains were expressed in *E. coli* as a glutathione-S-transferase (GST) tagged protein and purified by glutathione

sepharose column, and the GST tag was removed by the thrombin treatment using methods similar to those described earlier.[138,151,160,164]

4.2.7. Fluorescence Measurements:

As described in chapter 3 in section 3.3.10

4.2.8. Extent of Membrane Localization: The extent of localization of the ligands at the liposome interface was studied by the fluorescence quenching method, using PC/cholesterol/ligand$_{16}$/NBD-PE liposomes (44.5:44.5:10:1) in 50 mM Tris buffer, pH 8.2, containing 150 mM NaCl, according to the reported procedure.[125,160]

4.2.9. Molecular Modeling: Molecular docking modeling was performed using the crystal structure of PKCδ C1b (Protein Data Bank code 1PTR).[127] The generation of energy-minimized three-dimensional structures of ligands and ligand–protein docking was performed using the methods similar to those described earlier.[151,160]

4.3. Characterization of the Synthesized Compounds

4-hydroxylphenyl palmitate (1a): Yield (300 mg, 86%), white solid; mp: 56-58 $^{\circ}$C; ^{1}H NMR (400 MHz, $CDCl_3$): δ_{ppm} 6.82 (d, 2H, J = 8.0 Hz), 6.71 (d, 2H, J = 8.0 Hz), 4.06 (br s, 1H), 2.45 (t, 2H, J = 8.0 Hz), 1.64 (m, 2H), 1.18 (m, 24H), 0.80 (t, 3H, J = 6.0 Hz); ^{13}C NMR (100 MHz, $CDCl_3$): δ_{ppm} 173.3, 153.7, 144.3, 122.6, 116.2, 34.6, 34.3, 33.0, 32.1, 31.2, 30.0, 29.7, 29.6, 29.5, 29.3, 25.0, 23.0, 14.3; HR-MS m/z (%): calcd. for $C_{22}H_{36}O_3Na^+$ [M+ Na]$^+$: 371.2557, found:371.2560.

4-hydroxylphenyl octanoate (1b): Yield (210 mg, 89%), colourless oil; ^{1}H NMR (400 MHz, $CDCl_3$): δ_{ppm} 7.00 (br s, 1H), 6.80 (d, 2H, J = 9.2 Hz), 6.73 (d, 2H, J = 8.8 Hz), 2.31-2.22 (m, 2H), 1.72-1.52 (m, 2H), 1.31-1.20 (br s, 8H), 0.83-0.77 (m, 3H); ^{13}C NMR (100 MHz, $CDCl_3$): δ_{ppm} 171.2, 151.1, 129.2, 118.5, 115.2, 34.0, 31.5, 28.8, 28.7, 24.6, 22.4, 13.8; HR-MS m/z (%): calcd. for $C_{14}H_{20}O_3Na^+$ [M+ Na]$^+$: 259.1305, found: 259.1310.

3-hydroxylphenyl palmitate (2a): Yield (305 mg, 89%), white solid; mp: 67-68 $^{\circ}$C; ^{1}H NMR (400 MHz, $CDCl_3$): δ_{ppm}; 7.20 (t, 1H, J = 8.2 Hz), 6.50 (t, 1H, J = 9.4 Hz), 6.53 (s, 1H),

6.20 (br s, 1H), 2.54 (t, 2H, J = 7.4 Hz), 1.76-1.70 (m, 2H), 1.26 (m, 24H), 0.88 (t, 3H, J = 6.4 Hz); ^{13}C NMR (100 MHz, $CDCl_3$); δ_{ppm}173.3, 157.0, 151.7, 130.2, 113.6, 113.4, 109.4, 34.7, 32.1, 29.9, 29.7, 29.6, 29.5, 29.3, 25.1, 22.9, 14.3; HR-MS m/z (%): calcd. for $C_{22}H_{36}O_3Na^+$ $[M+ Na]^+$: 371.2557, found: 371.2553.

3-hydroxylphenyl octanoate (2b): Yield (200 mg, 85%), colourless oil; ^{1}H NMR (400 MHz, $CDCl_3$): δ_{ppm}; 7.13 (t, 1H, J = 8.0 Hz), 6.92 (br s, 1H), 6.66 (s, 1H), 6.65 (d, 1H, J = 8.0 Hz), 6.55 (d, 1H, J = 8.0 Hz), 2.36-2.29 (m, 2H), 1.76-1.58 (m, 2H), 1.36-1.24 (br s, 8H), 0.87 (t, 3H, J = 5.8); ^{13}C NMR (100 MHz, $CDCl_3$): δ_{ppm} 172.1, 157.3, 151.4, 129.6, 113.1, 112.8, 109.0, 34.2, 31.5, 29.0, 28.9, 28.8, 24.8, 24.7, 22.5, 13.9; HR-MS m/z (%): calcd. for $C_{14}H_{20}O_3Na^+$ $[M+ Na]^+$: 259.1305, found: 259.1308.

4-(hydroxymethyl)phenyl palmitate (3a): Yield (95 mg, 94%), white solid; mp:73-76 $^\circ$C; ^{1}H NMR (400 MHz, $CDCl_3$): δ_{ppm} 7.32 (d, 2H, J = 8.0 Hz), 7.03 (d, 2H, J = 8.4 Hz), 4.60 (s, 2H), 2.54 (t, 2H, J = 7.6 Hz), 2.4 (br s, 1H), 1.78-1.70 (m, 2H), 1.26 (br s, 24H), 0.88 (t, 3H, J = 6.6 Hz); ^{13}C NMR (100 MHz, $CDCl_3$): δ_{ppm} 172.7, 150.2, 138.6, 128.2, 121.8, 64.7, 34.5, 32.1, 29.9, 29.6, 29.5, 29.4, 29.3, 25.1, 22.9, 14.3; HR-MS m/z (%): calcd. for $C_{23}H_{38}O_3Na^+$ $[M+ Na]^+$: 385.2713, found: 385.2716.

4-(hydroxymethyl)phenyl octanoate (3b): Yield (92 mg, 92%), white solid; mp: 36-38 $^\circ$C (lit.[1] mp 35-36 $^\circ$C); ^{1}H NMR (400 MHz, $CDCl_3$): δ_{ppm} 7.25 (d, 2H, J = 8.0 Hz), 6.95 (d, 2H, J = 8.4 Hz), 4.53 (s, 2H), 2.46 (t, 2H, J = 7.6 Hz), 2.37 (br s, 1H), 1.68-1.63 (m, 2H), 1.86 (br s, 8H), 0.80 (t, 3H, J = 6.4 Hz); ^{13}C NMR (100 MHz, $CDCl_3$): δ_{ppm} 172.7, 150.2, 138.6, 128.2, 121.8, 64.7, 34.5, 32.1, 29.9, 29.6, 29.5, 29.4, 29.3, 25.1, 22.9, 14.3; HR-MS m/z (%): calcd. for $C_{15}H_{22}O_3Na^+$ $[M+ Na]^+$: 273.1467, found: 273.1466.

3-(hydroxymethyl)phenyl palmitate (4a): Yield (97mg, 96%), white solid; mp: 59-60 $^\circ$C; ^{1}H NMR (400 MHz, $CDCl_3$): δ_{ppm} 7.34 (t, 1H, J = 7.8 Hz), 7.19 (d, 1H, J = 7.6 Hz), 7.08 (s, 1H), 6.97 (d, 1H, J = 8.0 Hz), 4.66 (s, 2H), 2.54 (t, 2H, J = 7.6 Hz), 2.21 (br s, 1H); 1.76-1.71 (m, 2H), 1.40-1.26 (br s, 24H), 0.88 (t, 3H, J = 6.6 Hz); ^{13}C NMR (100 MHz, $CDCl_3$): δ_{ppm} 172.7, 151.0, 142.9, 129.6, 124.2, 120.7, 120.2, 64.7, 34.6, 32.1, 29.9, 29.7, 29.5, 29.4, 29.3, 25.1, 22.9, 14.3; HR-MS m/z (%): calcd. for $C_{23}H_{38}O_3Na^+$ $[M+ Na]^+$: 385.2713, found: 385.2712.

3-(hydroxymethyl)phenyl octanoate (4b): Yield (90 mg, 90%), colourless oil; ^{1}H NMR (400 MHz, $CDCl_3$): δ_{ppm} 7.30 (t, 1H, J = 8 Hz), 7.20 (d, 1H, J = 7.8 Hz), 6.91 (s, 1H), 6.88 (d, 1H, J = 7.8 Hz), 4.66 (s, 2H), 2.54 (t, 2H, J = 7.6 Hz), 2.21 (br s, 1H), 1.76-1.71 (m, 2H), 1.40-1.26 (br s, 8H), 0.88 (t, 3H, J = 6.6 Hz); ^{13}C NMR (100 MHz, $CDCl_3$): δ_{ppm} 172.7, 151.0, 142.9, 129.6, 124.2, 120.7, 120.2, 64.9, 34.6, 32.1, 29.9, 29.7, 29.5, 29.4, 29.3, 25.1, 22.9, 14.3; HR-MS m/z (%): calcd. for $C_{15}H_{22}O_3Na^+$ $[M+Na]^+$: 273.1467, found: 273.1470.

4-formyl-2-hydroxyphenyl palmitate: Yield (86 mg, 85%), white solid; mp: 73-74 $^{\circ}$C; ^{1}H NMR (400 MHz, $CDCl_3$): δ_{ppm} 9.86 (s, 1H), 7.64 (d, 1H, J = 8.8 Hz), 7.61 (s, 1H), 7.10 (d, 1H, J = 8.8 Hz), 2.61 (t, 2H, J = 7.6 Hz), 1.80-1.73 (m, 2H), 1.41-1.26 (br s, 24H), 0.86 (t, 3H, J = 6.8 Hz);^{13}C NMR (100 MHz, $CDCl_3$): δ_{ppm} 191.3, 172.6, 154.6, 139.0, 130.2, 129.4, 124.5, 117.6, 34.2, 32.1, 29.9, 29.8, 29.7, 29.6, 29.5, 29.4, 29.2, 25.0, 24.9, 22.8, 14.2; HR-MS m/z (%): calcd. for $C_{23}H_{36}O_4Na$ $[M+Na]^+$: 399.2506, found: 399.2510.

4-formyl-2-hydroxyphenyl octanoate: Yield (84 mg, 83%), brown coloured oil; ^{1}H NMR (400 MHz, $CDCl_3$): δ_{ppm} 9.12 (s, 1H), 7.54 (d, 1H, J = 8.8 Hz), 7.53 (s, 1H), 6.96 (d, 1H, J = 8.8 Hz), 2.54 (t, 2 H, J = 7.6 Hz), 1.71-1.64 (m, 2H), 1.33-1.21 (m, 8H), 0.82 (t, 3H, J = 6.8 Hz); ^{13}C NMR (100 MHz, $CDCl_3$): δ_{ppm} 191.4, 172.5, 154.8, 139.0, 130.2, 129.1, 124.5, 117.4, 34.0, 31.6, 29.0, 28.9, 24.8, 22.6, 14.1; HR-MS m/z (%): calcd. for $C_{15}H_{20}O_4Na$ $[M+Na]^+$: 287.1254, found: 287.1250.

4-(hydroxymethyl)-2-(hexadecanoyloxy)phenyl palmitate (5a): Yield (90 mg, 90%), white solid; mp: 67-68°C; ^{1}H NMR (400 MHz, $CDCl_3$): δ_{ppm} 7.21 (d, 1H, J = 8.4 Hz), 7.18 (s, 1H), 7.13 (d, 1H, J = 8.4 Hz), 4.64 (s, 2H), 2.52 (t, 4H, J = 7.6 Hz), 1.76-1.69 (m, 4H), 1.40-1.26 (br s, 48H), 0.88 (t, 6H, J = 6.6 Hz); ^{13}C NMR (100 MHz, $CDCl_3$): δ_{ppm} 171.4, 142.2, 141.4, 140.1, 124.8, 123.5, 121.9, 64.2, 34.3, 32.1, 30.0, 29.7, 29.5, 29.4, 29.3, 25.1, 22.9, 14.3; HR-MS m/z (%): calcd. for $C_{39}H_{68}O_5Na^+$ $[M+Na]^+$: 639.4959, found: 639.4961.

4-(hydroxymethyl)-2-(octanoyloxy)phenyl octanoate (5b): Yield (92 mg, 92%), colourless oil; ^{1}H NMR (400 MHz, $CDCl_3$): δ_{ppm} 7.20-7.04 (m, 3H), 4.54 (s, 2H), 2.45 (t, 4H, J = 7.2 Hz), 1.65-1.64 (m, 4H), 1.23 (br s, 16H), 0.82 (m, 6H); ^{13}C NMR (100 MHz, $CDCl_3$): δ_{ppm};171.4, 142.0, 141.0, 140.2, 124.7, 123.2, 121.7, 63.6, 34.1, 31.7, 29.1, 29.0, 24.9, 22.6, 14.1; HR-MS m/z (%): calcd. for $C_{23}H_{36}O_5Na^+$ $[M+Na]^+$: 415.2455, found: 415.2453.

2-(Z)-(octadec-9-enoyloxy)-4-(hydroxymethyl)phenyl oleate (6): Yield (95 mg, 95%), yellow oil; ^{1}H NMR (400 MHz, $CDCl_3$): δ_{ppm} 7.21 (d, 1H, J = 8.4 Hz), 7.18 (s, 1H), 7.14 (d, 1H, J = 8.0 Hz), 5.39-5.31 (m, 4H), 4.65 (s, 2H), 2.52 (t, 4H, J = 7.4 Hz), 2.04-2.00 (m, 8H), 1.76-1.69 (m, 4H), 1.34-1.24 (br s, 40H), 0.88 (t, 6H, J = 6.6 Hz); ^{13}C NMR (100 MHz, $CDCl_3$): δ_{ppm} 171.3, 142.1, 141.2, 140.1, 130.3, 130.1, 130.0, 129.7, 128.2, 128.0, 124.8, 123.4, 121.8, 64.0, 34.1, 32.7, 32.0, 31.6, 30.0, 29.8, 29.6, 29.4, 29.3, 29.2, 27.3, 27.2, 25.7, 25.0, 22.8, 22.7, 14.2; HR-MS m/z (%): calcd. for $C_{43}H_{72}O_5Na^+$ $[M+Na]^+$: 691.5272, found: 691.5273.

2-acetoxy-4-(hydroxylmethyl)phenyl palmitate (7a): Yield (92 mg, 93%), white solid; mp: 45-47 $^{\circ}$C; ^{1}H NMR (400 MHz, $CDCl_3$): δ_{ppm} 7.20 (s, 1H), 7.15 (d, 1H, J = 8.8 Hz), 7.10 (d, 1H, J = 8.0 Hz), 4.62 (s, 2H), 2.47 (t, 2H, J = 7.6 Hz), 2.21 (s, 3H), 1.76-1.63 (m, 2H), 1.31-1.20 (br s, 24H), 0.81 (t, 3H, J = 6.6 Hz); ^{13}C NMR (100 MHz, $CDCl_3$): δ_{ppm} 171.5, 168.6, 142.2, 141.3, 140.2, 124.8, 123.5, 121.9, 64.2, 34.2, 32.1, 29.79, 29.82, 29.6, 29.5, 29.4, 29.3, 25.1, 22.8, 20.8, 14.3; HR-MS m/z (%): calcd. for $C_{24}H_{40}O_5Na^+$ $[M+Na]^+$: 443.2768, found: 443.2770.

2-acetoxy-4-(hydroxymethyl)phenyl octanoate (7b): Yield (95 mg, 94%), yellow oil; ^{1}H NMR (400 MHz, $CDCl_3$): δ_{ppm} 7.15 (d, 1H, J = 8.0 Hz), 7.13 (s, 1H), 7.10 (d, 1H, J = 8.4 Hz), 4.56 (s, 2H), 2.50 (t, 2H, J = 7.4 Hz), 2.24, (s, 3H), 1.72-1.66 (m, 2H), 1.38-1.28 (br s, 8H), 0.87 (t, 3H, J = 6.6 Hz); ^{13}C NMR (100 MHz, $CDCl_3$): δ_{ppm} 171.2, 168.4, 141.7, 140.8, 140.2, 124.5, 123.0, 121.5, 63.3, 33.8, 31.5, 28.9, 28.8, 24.8, 22.4, 20.3, 13.9; HR-MS m/z (%): calcd. for $C_{17}H_{24}O_5Na^+$ $[M+Na]^+$: 331.1516, found: 331.1515.

5-(hydroxymethyl)-2-(palmitoyloxy)phenyl benzoate (8a): Yield (94 mg, 94%), white solid; mp: 53-55 $^{\circ}$C; ^{1}H NMR (400 MHz, $CDCl_3$): δ_{ppm} 8.10 (d, 2H, J = 7.2 Hz), 7.56 (t, 1H, J = 7.2 Hz), 7.43 (t, 2H, J = 7.4 Hz), 7.25-7.12 (m, 3H), 4.64 (s, 2H), 2.33 (t, 2H, J = 7.6 Hz), 1.50-1.46 (m, 2H), 1.19 (br s, 24H), 0.81-0.79 (m, 3H); ^{13}C NMR (100 MHz, $CDCl_3$): δ_{ppm} 171.6, 164.4, 142.4, 141.6, 140.4, 133.9, 130.3, 128.9, 128.7, 125.0, 124.9, 123.5, 121.9, 64.1, 34.2, 32.0, 29.8, 29.5, 29.4, 29.2, 25.1, 22.8, 14.2; HR-MS m/z (%): calcd. for $C_{30}H_{42}O_5Na^+$ $[M+Na]^+$: 505.2924, found: 505.2925.

5-(hydroxymethyl)-2-(octanoyloxy)phenyl benzoate (8b): Yield (96 mg, 95%), yellow oil; ^{1}H NMR (400 MHz, $CDCl_3$): δ_{ppm} 8.04 (d, 2H, J = 8.4 Hz), 7.51 (t, 1H, J = 6.8 Hz), 7.37 (t, 2H, J = 7.6 Hz), 7.16-7.03 (m, 3H), 4.47 (s, 2H), 2.27 (t, 2H, J = 7.6 Hz), 1.45-1.38 (m, 2H),

1.16-1.00 (br s, 8H), 0.73 (t, 3H, J = 7.2 Hz); ^{13}C NMR (100 MHz, $CDCl_3$): δ_{ppm} 171.5, 164.3, 142.2, 141.4, 140.3, 133.9, 130.2, 128.8, 128.7, 125.0, 124.9, 123.3, 121.8, 63.7, 34.0, 31.5, 28.9, 28.8, 24.9, 22.5, 14.0; HR-MS m/z (%): calcd. for $C_{22}H_{26}O_5Na^+$ $[M+Na]^+$: 393.1672, found: 393.1675.

4-(hydroxy methyl)-2-methoxyphenyl palmitate (9a): Yield (90 mg, 89%), white solid; mp: 43-45 °C; ^{1}H NMR (400 MHz, $CDCl_3$): δ_{ppm} 6.93 (s, 1H), 6.91 (d, 1H, J = 8.0 Hz), 6.84 (d, 1H, J = 8.0 Hz), 4.56 (s, 2H), 3.77 (s, 3H), 2.54 (t, 2H, J = 7.4 Hz), 1.75-1.69 (m, 2H), 1.38-1.21 (br s, 24H), 0.89-0.83 (m, 3H); ^{13}C NMR (100 MHz, $CDCl_3$): δ_{ppm} 172.3, 151.1, 140.2, 138.9, 122.6, 118.9, 111.0, 64.6, 55.8, 34.1, 32.0, 29.8, 29.6, 29.5, 29.39, 29.2, 25.1, 22.8, 14.2; HR-MS m/z (%): calcd. for $C_{24}H_{40}O_4Na^+$ $[M+Na]^+$: 415.2819, found: 415.2820.

4-(hydroxymethyl)-2-methoxyphenyl octanoate (9b): Yield (92 mg, 91%), colourless oil; ^{1}H NMR (400 MHz, $CDCl_3$): δ_{ppm} 7.67 (d, 1H, J = 8.4 Hz), 7.66 (s, 1H), 7.04 (d, 1H, J = 8.4 Hz), 4.50 (s, 2H), 3.81 (s, 3H), 2.52 (t, 2H, J = 7.6 Hz), 1.73-1.35 (m, 2H), 1.33-1.23 (br s, 8H), 0.83 (t, 3H, J = 6.6 Hz); ^{13}C NMR (100 MHz, $CDCl_3$): δ_{ppm} 171.6, 151.3, 144.7, 128.1, 123.6, 123.1, 113.9, 56.2, 34.2, 31.8, 29.9, 29.2, 29.1, 25.1, 22.8, 14.2; HR-MS m/z (%): calcd. for $C_{16}H_{24}O_4Na^+$ $[M+Na]^+$: 303.1567, found: 303.1569.

5-(hydroxymethyl)-2-methoxyphenyl palmitate (10a): Yield (87 mg, 87%), white solid; mp: 51-53 °C; ^{1}H NMR (400 MHz, $CDCl_3$): δ_{ppm} 7.15 (d, 1H, J = 8.0 Hz), 7.02 (s, 1H), 6.91 (d, 1H, J = 8.4 Hz), 4.55 (s, 2H), 3.79 (s, 3H), 2.56 (t, 2H, J = 7.4 Hz), 1.77-1.73 (m, 2H), 1.42-1.26 (br s, 24H), 0.88 (t, 3H, J = 6.8 Hz); ^{13}C NMR (100 MHz, $CDCl_3$): δ_{ppm} 172.2, 150.6, 139.8, 134.0, 125.5, 122.0, 112.4, 64.4, 56.0, 34.2, 32.1, 29.8, 29.7, 29.5, 29.4, 29.2, 25.2, 22.8, 14.3; HR-MS m/z (%): calcd. for $C_{25}H_{40}ONa^+$ $[M+Na]^+$: 415.2819, found: 415.2822.

5-(hydroxymethyl)-2-methoxyphenyl octanoate (10b): Yield (90 mg, 90%), yellow oil; ^{1}H NMR (400 MHz, $CDCl_3$): δ_{ppm} 7.11 (d, 1H, J = 8.4 Hz), 6.98 (s, 1H), 6.88 (d, 1H, J = 8.4 Hz), 4.53 (s, 2H), 3.75 (s, 3H), 2.51 (t, 2H, J = 7.6 Hz), 1.71-1.67 (m, 2H), 1.37-1.24 (br s, 8H), 0.82 (t, 3H, J = 6.8 Hz); ^{13}C NMR (100 MHz, $CDCl_3$): δ_{ppm} 172.2, 150.2, 139.4, 133.8, 125.3, 121.6, 112.1, 63.7, 55.7, 33.9, 31.6, 28.9, 24.9, 22.5, 14.0; HR-MS m/z (%): calcd. for $C_{16}H_{24}O_4Na^+$ $[M+Na]^+$: 303.1567, found: 303.1567.

2-tert-butoxy-4-(hydroxymethyl)phenyl palmitate (11a): Yield (90 mg, 90%), white solid; mp: 35-38 °C; ^{1}H NMR (400 MHz, $CDCl_3$): δ_{ppm} 7.00 (d, 1H, J = 8.0 Hz), 6.90 (s, 1H), 6.77 (d, 1H, J = 8.4 Hz), 4.40 (s, 2H), 2.46 (t, 2H, J = 7.4 Hz), 1.70-1.60 (m, 2H), 1.32-1.18 (br s, 24H), 0.91 (s, 9H), 0.80 (t, 3H, J = 6.4 Hz); ^{13}C NMR (100 MHz, $CDCl_3$): δ_{ppm} 172.1, 150.1, 139.9, 133.7, 125.5, 121.8, 113.2, 75.0, 64.3, 34.1, 32.1, 29.8, 29.6, 29.5, 29.4, 29.3, 28.4, 25.1, 22.8, 19.3, 14.2; HR-MS m/z (%): calcd. for $C_{27}H_{46}O_4Na^+$ $[M+Na]^+$: 457.3288, found: 457.3289.

2-tert-butoxy-4-(hydroxymethyl)phenyl octanoate (11b): Yield (93 mg, 92%), yellow oil; ^{1}H NMR (400 MHz, $CDCl_3$): δ_{ppm} 7.02 (d, 1H, J = 8.4 Hz), 6.93 (s, 1H), 6.80 (d, 1H, J = 8.4 Hz), 4.39 (s, 2H), 2.51 (t, 2H, J = 7.4 Hz), 1.75-1.67 (m, 2H), 1.38-1.23 (br s, 8H), 0.96 (s, 9H), 0.87 (t, 3H, J = 6.0 Hz); ^{13}C NMR (100 MHz, $CDCl_3$): δ_{ppm} 172.0, 149.8, 139.7, 133.6, 125.3, 121.6, 113.0, 74.8, 63.9, 34.0, 31.6, 29.1, 28.9, 28.3, 25.0, 22.6, 19.1, 14.0; HR-MS m/z (%): calcd. for $C_{19}H_{30}O_4Na^+$ $[M+Na]^+$: 345.2036, found: 345.2035.

2-(benzyloxy)-4-(hydroxymethyl)phenyl palmitate (12a): Yield (91 mg, 91%), white solid; mp: 45-46 °C; ^{1}H NMR (400 MHz, $CDCl_3$): δ_{ppm} 7.33-7.25 (m, 5H), 7.00 (d, 1H, J = 8.4 Hz), 6.96 (s, 1H), 6.84 (d, 1H, J = 8.4 Hz), 4.94 (s, 2H), 4.40 (s, 2H), 3.45 (br s, 1H), 2.45 (t, 2H, J = 7.6 Hz), 1.64-1.60 (m, 2H), 1.27-1.24 (br s, 24H), 0.86 (t, 3H, J = 6.4 Hz); ^{13}C NMR (100 MHz, $CDCl_3$): δ_{ppm} 172.2, 149.5, 140.1, 136.7, 134.3, 128.5, 127.9, 127.4, 125.3, 121.8, 113.7, 70.7, 64.0, 34.1, 32.0, 29.8, 29.7, 29.5, 29.4, 29.3, 29.2, 25.1, 22.8, 14.2; HR-MS m/z (%): calcd. for $C_{30}H_{44}O_4Na^+$ $[M+Na]^+$: 491.3132, found: 491.3135.

2-(benzyloxy)-4-(hydroxymethyl)phenyl octanoate (12b): Yield (90 mg, 90%), yellow oil; ^{1}H NMR (400 MHz, $CDCl_3$): δ_{ppm} 7.29-7.19 (m, 5H), 7.00 (d, 1H, J = 8.4 Hz), 6.94 (s, 1H), 6.83 (d, 1H, J = 8.4 Hz), 4.93 (s, 2H), 4.41 (s, 2H), 2.42 (t, 2H, J = 7.4 Hz), 1.60-1.55 (m, 2H), 1.25-1.16 (br s, 8H), 0.79 (t, 3H, J = 7.0 Hz); ^{13}C NMR (100 MHz, $CDCl_3$): δ_{ppm} 172.2, 149.7, 140.2, 136.7, 134.3, 128.6, 128.1, 127.5, 125.4, 121.9, 113.9, 70.8, 64.4, 34.2, 31.7, 29.2, 29.0, 25.1, 22.7, 14.2; HR-MS m/z (%): calcd. for $C_{22}H_{28}O_4Na^+$ $[M+Na]^+$: 379.1880, found: 379.1883.

4-(hydroxymethyl)-2-[(5Z,8Z,11Z,14Z)-icosa-5,8,11,14-tetraenoyloxy]phenyl(5Z,8Z, 11Z,14Z)-icosa-5,8,11,14-tertaenoate (13): Yield (22 mg, 91%); white solid; mp: 50-52 °C; ^{1}H NMR (400 MHz, $CDCl_3$): δ_{ppm} 7.64 (d, 1H, J = 8.0 Hz), 7.62 (s, 1H), 7.07 (d, 1H, J = 8.4

Hz), 5.43-5.30 (m, 16H), 4.61 (s, 2H), 2.83-2.77 (m, 12H), 2.63 (t, 4H), 2.12-2.18 (m, 8H), 2.03-2.00 (m, 4H), 1.86-1.84 (m, 4H), 1.35-1.23 (m, 8H), 0.83 (t, 6H, J = 6.6 Hz); ^{13}C NMR (100 MHz, $CDCl_3$): δ_{ppm} 171.3, 142.1, 141.2, 140.1, 130.3, 130.1, 130.0, 129.7, 128.2, 128.0, 124.8, 123.4, 121.8, 64.0, 34.1, 32.7, 32.0, 31.6, 30.0, 29.8, 29.7, 29.4, 29.3, 29.2, 27.3, 27.2, 25.7, 25.0, 22.8, 22.7, 14.2.

4.4. Selected Spectra of (Hydroxymethyl)phenyl Ester Analogues

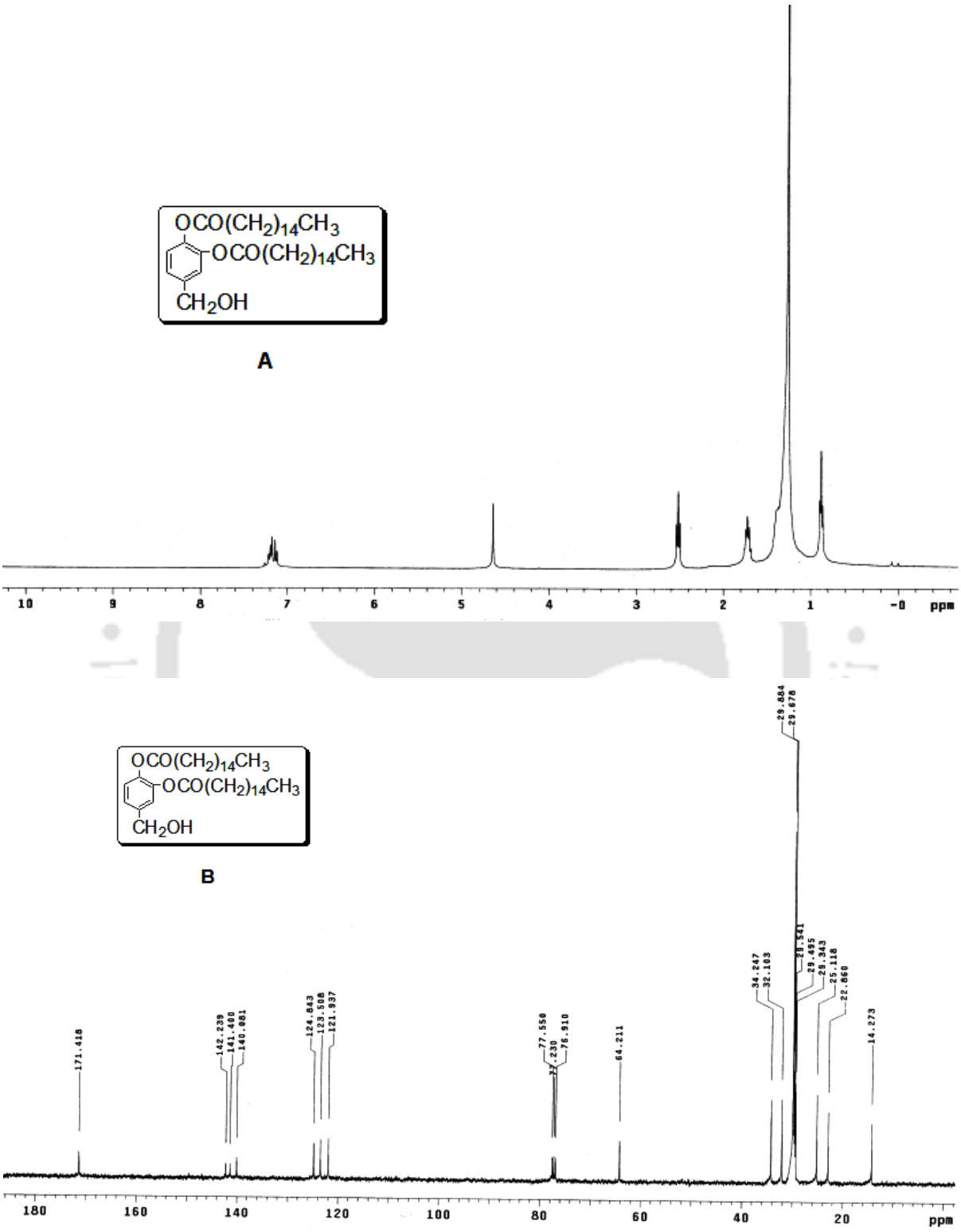

Figure 4.4.1: *^{1}H NMR (**A**) and ^{13}C NMR (**B**) of 4-(hydroxymethyl)-2-(hexadecanoyloxy)phenyl palmitate (**5a**)*

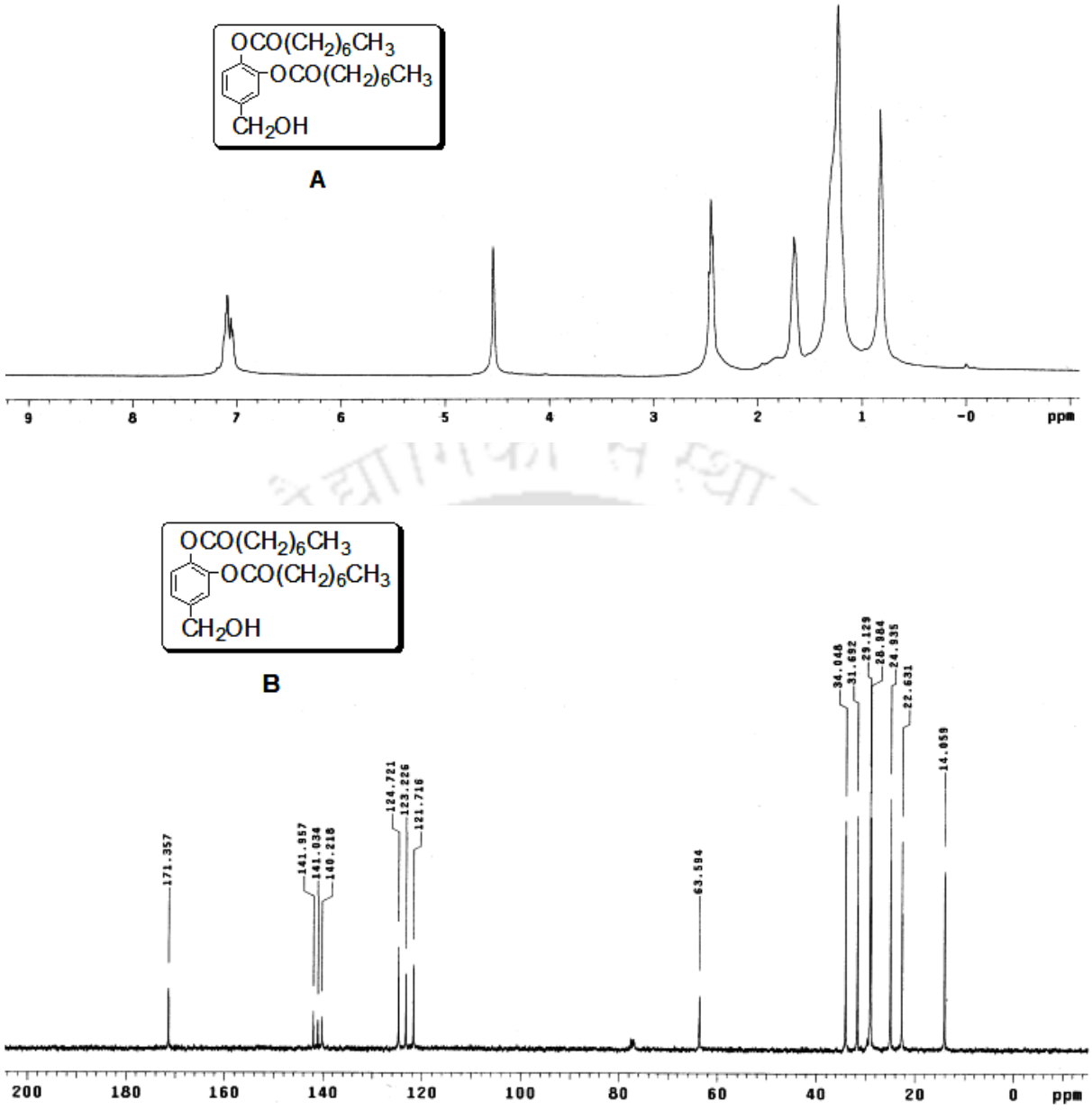

Figure 4.4.2: *^{1}H NMR (**A**) and ^{13}C NMR (**B**) of 4-(hydroxymethyl)-2-(octanoyloxy)phenyl octanoate (**5b**)*

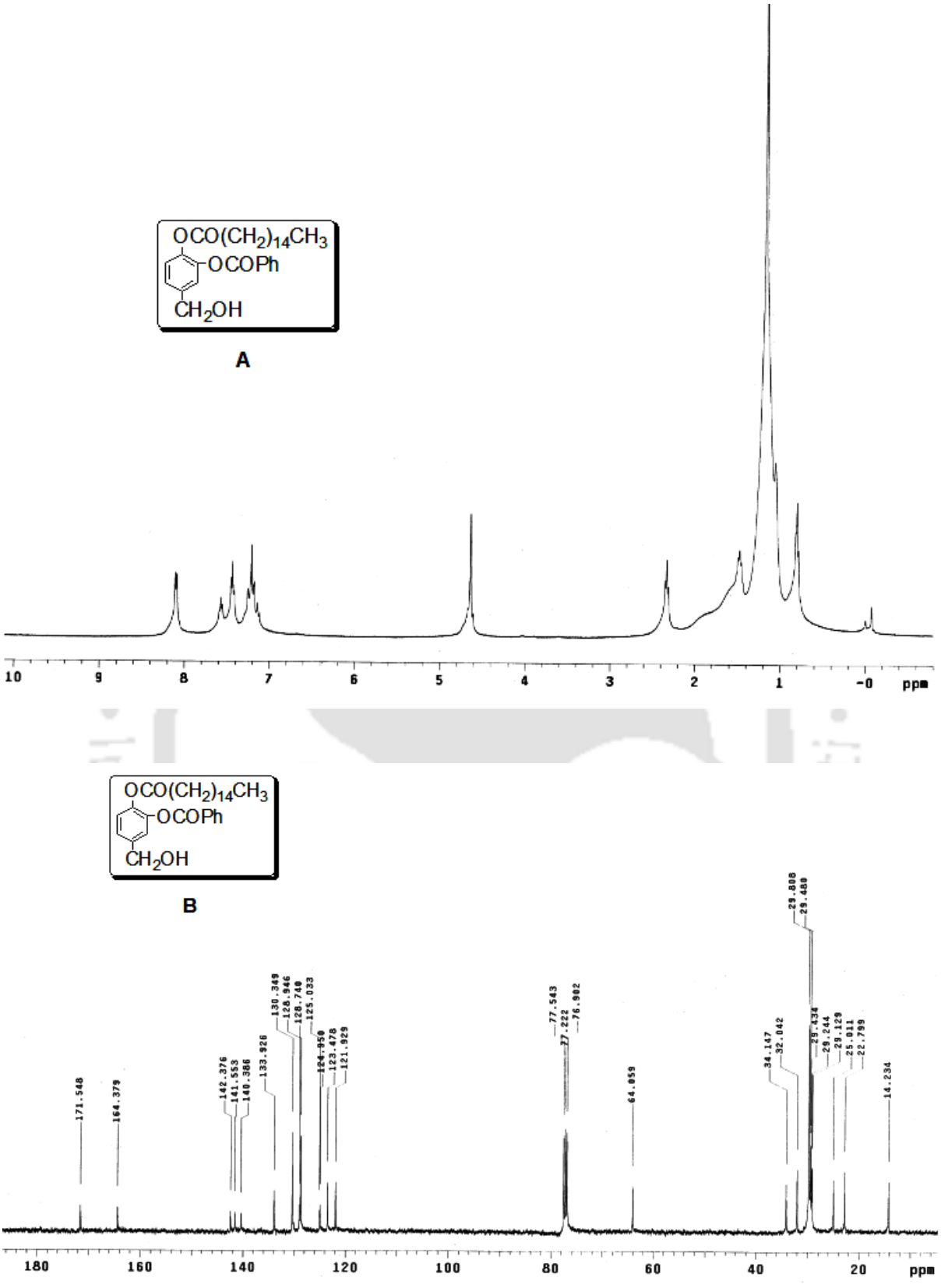

Figure 4.4.3: *^{1}H NMR (**A**) and ^{13}C NMR (**B**) of 5-(hydroxymethyl)-2-(palmitoyloxy)phenyl benzoate (**8a**)*

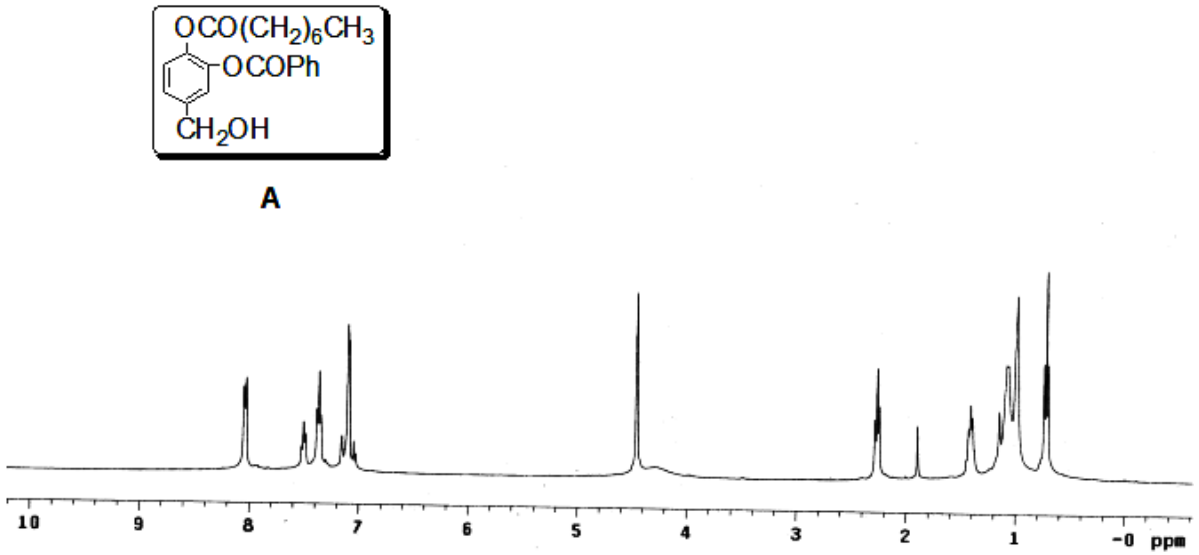

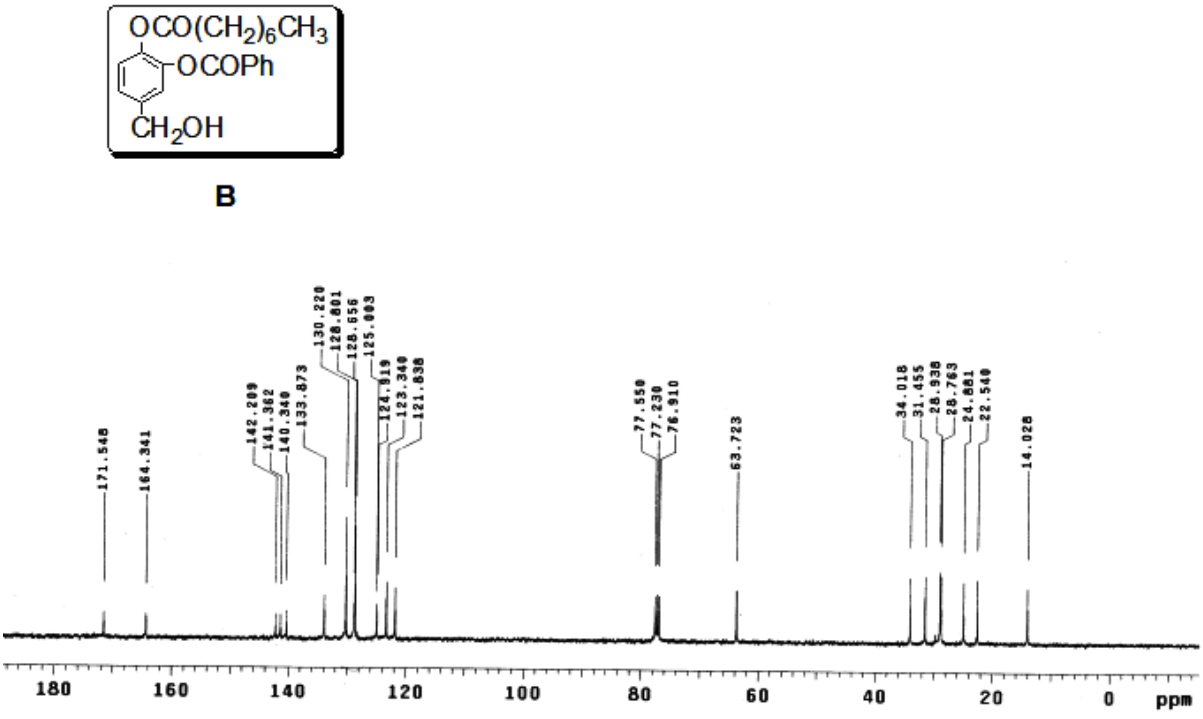

Figure 4.4.4: *^{1}H NMR (**A**) and ^{13}C NMR (**B**) of 5-(hydroxymethyl)-2-(octanoyloxy)phenyl benzoate (**8b**)*

CHAPTER 5

Synthesis of Protein Kinase C (PKC)-C1 Domain Targeted Alkyl Cinnamates

The present chapter describes design and synthesis of alkyl cinnamates using Verley–Doebner modification of Knoevenagel condensation reaction. The structure of the synthesized alkyl cinnamates are closely related to the curcumin structure. It also illustrates the detailed spectral properties and PKC-C1domain binding properties of alkyl cinnamates.

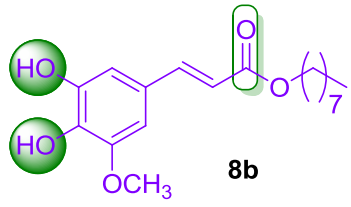

8b

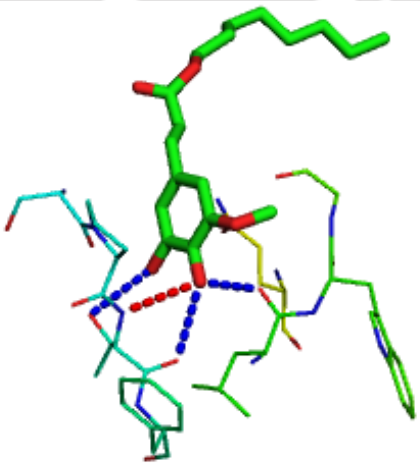

5.1 Background and Focus of the Present Work

The antioxidant cinnamic acids such as ferulic, caffeic, sinapic, chlorogenic, coumaric acids and their conjugates are aromatic secondary plant metabolites exist ubiquitously in nature. They are also very important intermediates in the bio-synthetic pathways of most of the natural products. Most of the cinnamic acids and their derivatives exhibit a broad spectrum of bio-activities such as antibacterial, antiviral, anti-inflammatory, antiatherosclerotic, anti-HIV, antitumor and others mainly due to their antioxidant properties. Numerous studies highlighted the effects of natural and synthetic cinnamates in a variety of human disease models. They are also good scavenger of a number of reactive species, including 2,2-diphenyl-1-picrylhydrazyl (DPPH) radicals, and peroxyl and hydroxyl radical.[169] The caffeic acid phenethyl ester (CAPE) induces apoptosis on transformed cell lines, inhibit lipoxygenases and cyclooxygenase (COX)-2 enzymes from free radical generation and lipid hydroperoxidation. CAPE is also known to play an important role in PKC regulation.[170] Long chain alkyl cinnamates have been reported to be free radical scavengers. The antioxidant activity of radish sprout (*Raphanus sativus* L.) has been attributed to be related mainly with the presence of sinapic acid long chain esters. The esters of long chain alcohols with caffeic acid have been shown to inhibit COX-1 enzymes. Recently, the relation-ship between the redox potentials and the antioxidant activity of hydroxy cinnamic acids and derivatives has been also demon-strated.[171] Esters of sinapic and ferulic acids with alkanols have been also used in commercial applications as sunscreens.[172-174]

Caffeic acid and ferulic acid are reported to be weak inhibitors of 12-O-Tetradecanoylphorbol-13-acetate (TPA)-induced tumor promotion and ornithine decarboxylase activity in mouse skin. The long chain esters of both caffeic and ferulic acid are also inhibitor of tumor cell proliferation, COX enzyme, and lipid peroxidation.[175,176] In this context, the present chapter describes the synthesis and binding properties to the C1b subdomains of PKCδ and PKCθ using fluorescence spectroscopy and molecular modeling studies. The alkyl cinnamates interact with the C1b subdomains of PKC isoforms through the DAG or phorbol ester binding site and forms hydrogen bonds with the residues at the activator binding site. The results also show that the hydroxyl groups and methoxy groups of curcumin plays an important role in recognizing the C1 domain of PKC isoforms.

Design and synthesis─ Curcumin is one of the thoroughly studied natural compounds. It has potential uses against several diseases including, HIV-infections, cancer, cystic fibrosis and others. It is reported to be implicated in altering the activity of membrane ATPases, protein kinases and transcription factors. It has also been reported to inhibit phorbol esters induced tumor promotion and some of the phorbol esters-responsive markers in cancer.[10,38,177] Recent studies showed that both curcumin and phorbol ester modulate PKC activity through the common C1 domains. Curcumin is a symmetric molecule and it is reported that long chain derivatives of curcumin interact with the C1 domain more efficiently than natural curcumin in membrane-free systems.[138,177] The reported binding affinity and molecular docking analysis of curcumin and long chain curcumin derivatives show that the two halves of the symmetric curcumin molecule might act as two separate units under the experimental conditions and specifically direct the hydrophilic pharmacophores of the ligand for their interaction with C1 domains of PKC isoforms. To understand the role of both sides of the symmetric curcumin molecule and to develop cinnamic acid derivatives for improved PKC binding and activity, we prepared alkyl esters of selected cinnamic acids related to the curcumin structure (*Scheme 5.1.1*). Most of the compound also contains two of the phorbol ester pharmacophores, the hydroxyl and the carbonyl functionalities within the same molecule.

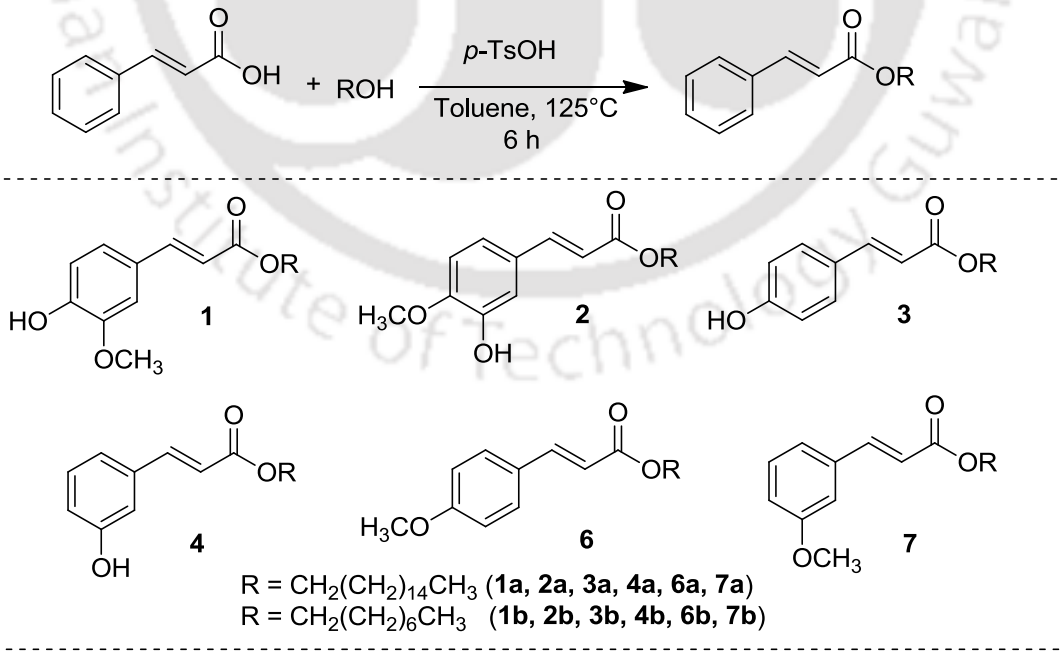

Scheme 5.1.1: *p-TsOH catalyzed esterification of cinnamic acid derivatives (**1-4**, **6** and **7**)*

The compounds also contain hydrophobic alkyl chains for their possible interaction either with the hydrophobic residues of the C1 domain or with the membrane lipids. To investigate the role of hydroxyl and methoxy groups of curcumin for their interaction with PKC C1b subdomains, we prepared alkyl cinnamates according to the reported and modified procedures. The vanillin derivatives closely resemble to the one half of the natural curcumin molecule. To determine the effect of both the functional groups for PKC binding, we prepared isovanillin, where only the positions of the functional groups were switched. Monohydroxy, dihydroxy, monomethoxy and dimethoxy alkyl cinnamates were synthesized to understand the importance of hydroxyl and methoxy groups separately. To extend our findings for better PKC binding cinnamic acid derivatives, we also prepared 3,4-dihydroxy-5-methoxy alkyl cinnamates. The alkyl cinnamates were prepared from the respective benzaldehydes through Knoevenagel condensation and Verley–Doebner modification of Knoevenagel condensation in two steps.[172,178,179] The alkyl cinnamates **1**–**4**, **6** and **7** were prepared from the respective benzaldehydes using malonic acid, pyridine and catalytic amount of piperidine, followed by refluxing with octanol or 1-hexadecanol in presence of p-toluenesulfonic acid (*Scheme 5.1.1*). The other alkyl cinnamates **5** and **8** were prepared from the corresponding half esters of malonic acids and benzaldehydes.

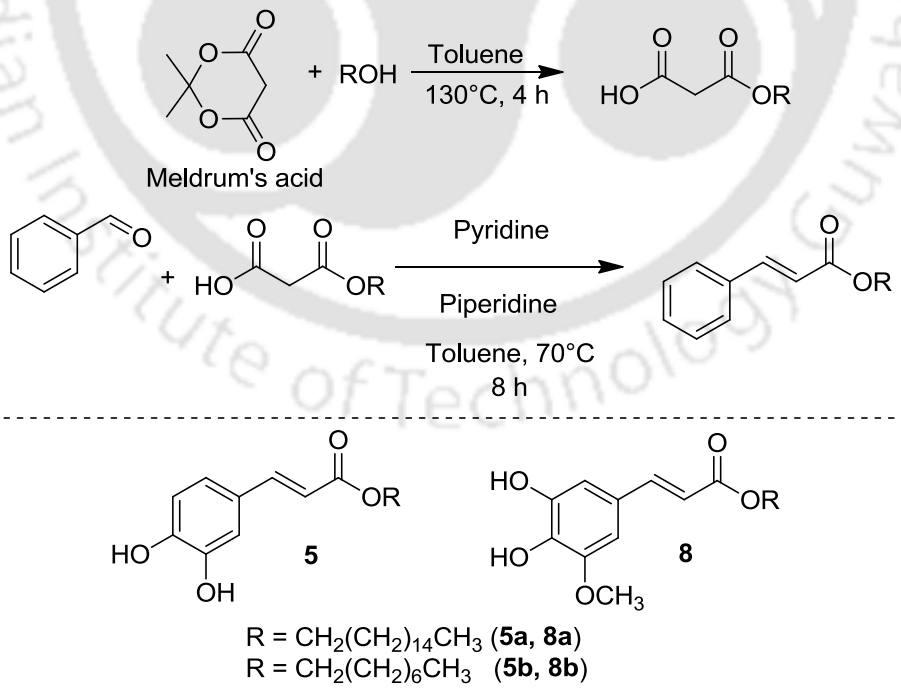

Scheme 5.1.2: *Synthesis of long chain alkyl cinnamates (**5** and **8**) from monomalonates*

The monomalonates were obtained in high yields by refluxing Meldrum's acid (2,2-dimethyl- 1,3-dioxane-4,6-dione) with octanol and 1-hexadecanol in toluene. Condensation of monomalonates with protocatechualdehyde and 5-hydroxyvanillin in presence of pyridine and piperidine produced the respective alkyl cinnamates in moderate to good yields (*Scheme 5.1.2*). All the compounds were fully characterized on the basis of their spectral data (^{1}H and ^{13}C NMR and HRMS). The alkyl cinnamates were prepared both with long (1-hexadecanol) and short chain (octanol) alcohols to study the impact of hydrophobicity on the binding affinity.

Spectral Properties— Cinnamic acid derivatives of our interest show a broad absorbance peaks in the range of 304-330 nm. The absorption maxima show significant solvent dependency both in polar and non-polar environment. The compounds show one major absorption peak in polar, non-polar and liposome environments (*Table 5.1.1 and Table 5.1.2*). The absorption spectra of the compounds in ethanol are shown in Figure 5.1.1. The fluorescence emission maximums of the compounds are in the range of 341- 444 nm (*Table 5.1.1 and Table 5.1.2*). For all the compounds one major broad emission peak were observed in polar, non-polar and liposome environment. The emission maxima were blue shifted in the non-polar solvent such as hexane as compared with ethanol or water. This could be due to the effect of polarity in intermolecular hydrogen bond formation.

***Table 5.1.1**: Absorption and emission properties*[a] *of alkyl cinnamates and curcumin in different solvents at room temperature.*

compound	Hexane	EtOH	Water	Hexane	EtOH	Water
1a	313	325	324	360	410	418
1b	314	323	323	360	410	417
2a	313	324	322	358	410	416
2b	312	323	323	357	409	417
3a	311	313	319	345	400	404
3b	310	315	320	346	400	408
5a	322	330	328	358	412	425
5b	323	329	329	358	413	424
6a	305	309	317	342	400	402
6b	304	310	319	341	400	402
8a	315	324	324	373	426	437
8b	313	325	326	372	425	444
Curcumin	404	427	425	474	560	572

[a] *Compound, 2 µM. Absorbance maximum was used for recording emission spectra.*

In non-polar solvents like hexane the intramolecular hydrogen bond formation and in polar solvents like ethanol the intermolecular hydrogen bond formation may affect the position of fluorescence emission maxima.

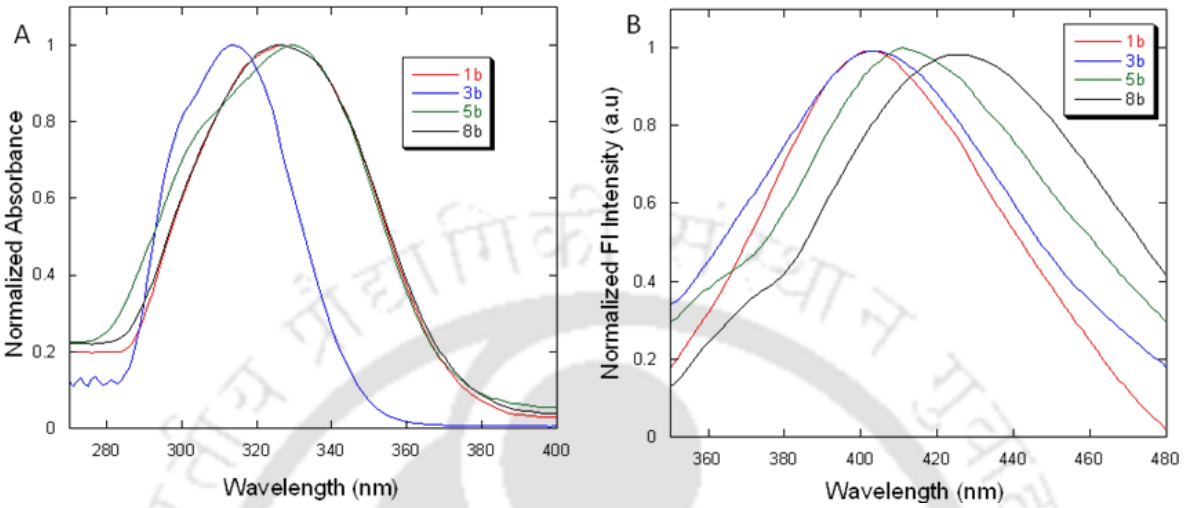

Figure 5.1.1: *(A) Normalized absorption spectra and (B) fluorescence emission spectra of cinnamic acid derivatives* ***1b***, ***3b***, ***5b*** *and* ***8b*** *in ethanol.*

In water, the compounds showed much lower and broader fluorescence intensity compared to the organic solvent indicating lower quantum yields in water. The emission spectra of the compounds in ethanol are shown in Figure 5.1.1. We also measured the spectral properties of liposomes containing long chain alkyl cinnamates in buffer solution (20 mM Tris, 150 mM NaCl, 50 µM ZnSO4, pH 7.4). The results show that the absorption and fluorescence properties of the liposomes containing alkyl cinnamates are very similar to that of compounds in polar medium (*Table 5.1.2*).

Table 5.1.2: *Absorption and emission properties*[a] *of alkyl cinnamates embedded in liposome at room temperature.*

Compound	Absorbance maximum (λ_{max}), (nm)	Emission maximum (λ_{em}), (nm)
1a	331	412
3a	316	405
5a	332	413
6a	312	411
8a	334	441

[a)] *Compound, 2 µM. Absorbance maximum was used for recording emission spectra*

The alkyl chain length did not show any significant effect in the absorption and emission maxima.

Protein Binding Properties

Interaction with ligands in monomeric form— The PKC protein family consists of at least eleven known isoforms, categorized into conventional (calcium, DAG and phospholipid-dependent), novel (calcium-independent, but DAG and phospholipids dependent), and atypical (calcium and DAG-independent) subgroups.[11,18] DAG, phorbol esters and others interacts with the PKC isoforms through the C1 domain. This interaction activates these enzymes and promotes their association with the membrane lipids, by inducing the translocation of cytosolic PKC to the cellular membrane.[11,119,120] The C1 domain is duplicated into a tandem C1 domain consisting of C1a and C1b subdomains in classical and novel PKC isoforms.[121] In the present study we selected PKCθ and PKCδ C1b subdomains to measure the *in vitro* binding affinity of the alkyl cinnamates due to their intrinsic fluorescence properties. The C1b subdomains of PKCδ and PKCθ have better DAG binding activity than C1a subdomains.

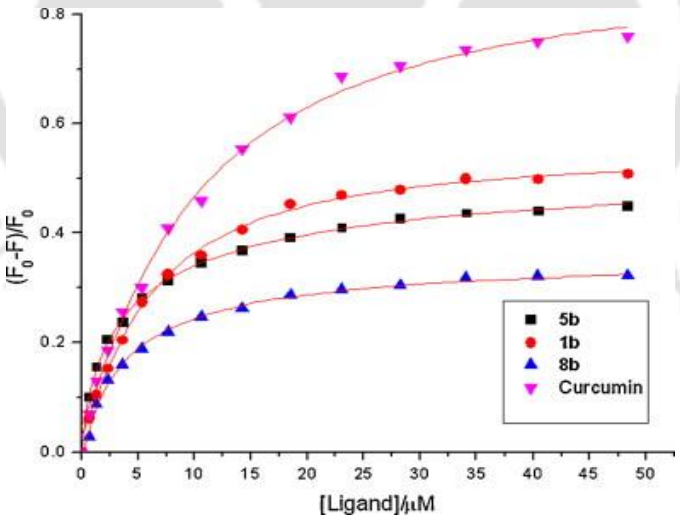

Figure 5.1.2: *Binding of alkyl cinnamates with PKCδ C1b. Representative plot of fluorescence intensity of PKCδ C1b (2 μM) in buffer (20 mM Tris, 150 mM NaCl, 50 μM $ZnSO_4$, pH 7.4) in the presence of varying concentration of* ***5b*** *(▪),* ***1b*** *(●),* ***8b*** *(▲) and curcumin (▼), where F and F_0 are fluorescence intensity in the presence and absence of the alkyl cinnamates, respectively. Solid lines indicate the fit using Hill equation.*

The intrinsic fluorescence of these PKC C1b subdomains is due to the presence of a single Trp (Trp-252 in delta, and Trp-253 in theta) and tyrosine residues (Tyr-236 and Tyr-238 in delta, Tyr-249 and Tyr-251 in theta). The C1b subdomains of PKCδ, PKCθ, PKCη and PKCε contain single Trp residue close to the binding pocket.[10] The binding affinity of alkyl cinnamates, curcumin and DAG to C1b subdomains of PKC isoforms were assessed *in vitro* by fluorescence quenching method under similar experimental condition and the EC_{50} values were calculated using Hill equation. Figure 5.1.2 shows the representative plot of fluorescence quenching data for PKCδ C1b in presence of different concentrations (0.67-48 μM) of **1b**, **5b**, **8b** and curcumin in buffer. The binding affinity values indicate that compound **8b** has good binding affinity for the C1b subdomain of PKCθ (EC_{50} = 3.51 μM, Hill coefficient = 1.02) and other compounds have comparable binding affinity for both the proteins (*Table 5.1.3*). The EC_{50} values of DAG_8, DAG_{16} and curcumin are in accordance with the reported results.[138] The results also demonstrate that the compounds have higher binding affinity for PKCθ C1b as compared to the PKCδ C1b, possibly due to additional hydrogen bonds. To understand the importance of the alkyl chain length of the compounds for their binding to C1b subdomains similar binding analyses were performed (*Table 5.1.3*). Compound **8b** shows 4.1-fold and 1.7-fold stronger binding affinity than $DDAG_8$ for PKCδ-C1b and PKCθ-C1b protein, respectively.

Table 5.1.3: *EC_{50} values for the binding of alkyl cinnamates, curcumin and DAGs with the PKCδ C1b and PKCθ C1b proteins*[a] *at room temperature.*

Compound	**EC_{50} (μM)**		**Hill coefficients (nH)**	
	PKCθ C1b	PKCδ C1b	PKCθ C1b	PKCδ C1b
1a	5.18 ± 0.29	5.95 ± 0.35	1.01 ± 0.22	0.91 ± 0.11
1b	5.31 ± 0.37	6.30 ± 0.65	1.09 ± 0.13	1.21 ± 0.15
2a	6.30 ± 0.31	–	1.24 ± 0.19	–
2b	6.97 ± 0.39	–	1.18 ± 0.17	–
3a	20.60 ± 0.89	–	1.13 ± 0.19	–
3b	21.22 ± 0.87	–	0.93 ± 0.17	–
5a	4.21 ± 0.21	4.16 ± 0.19	1.08 ± 0.21	0.69 ± 0.11
5b	4.78 ± 0.22	4.57 ± 0.25	1.05 ± 0.28	0.72 ± 0.12
6a	11.13 ± 0.51	–	1.07 ± 0.12	–
6b	13.83 ± 0.67	–	1.15 ± 0.16	–
8a	2.98 ± 0.16	3.35 ± 0.21	1.06 ± 0.19	1.06 ± 0.35
8b	3.51 ± 0.33	3.76 ± 0.18	1.02 ± 0.13	0.87 ± 0.28
Curcumin	10.61 ± 0.81	10.19 ± 0.51	1.16 ± 0.12	1.17 ± 0.17
DAG_{16}	7.59 ± 0.56	6.68 ± 0.85	1.12 ± 0.16	0.92 ± 0.20
DAG_8	6.12 ± 0.61	15.39 ± 0.91	0.91 ± 0.11	0.99 ± 0.19

[a] *Protein, 2 μM in buffer (20 mM Tris, 150 mM NaCl, 50 μM $ZnSO_4$, pH 7.4)*

For compound **1a** (XLOGP3 = 9.59) and **1b** (XLOGP3 = 5.25), although there is a distinct difference in hydrophobicity due to alkyl chain length, but the difference in binding affinity among them are very small for both the proteins. This could be due to their binding orientations with the C1b subdomains. The octanol-water partition coefficients (log *P*) for all compounds were calculated according to the program XLOGP3.

Fluorescence anisotropy measurements— To gain more information about ligand‑protein interactions, we performed steady-state fluorescence anisotropy measurements of the alkyl cinnamates and curcumin in presence or absence of the proteins. The increase in anisotropy values of the compounds in presence of proteins support their bindings to the proteins. For **8b** the anisotropy value changed from 0.0677 in buffer to 0.1204 in PKCδ C1b and 0.1171 in PKCθ C1b, respectively, whereas for **1b**, the changes were from 0.0575 in buffer to 0.1144 in PKCδ C1b and 0.1109 in PKCθ C1b (*Table 5.1.4*). Under similar experimental condition the degree of anisotropy of curcumin increases from 0.0694 in buffer to 0.1291 in PKCδ C1b and 0.1623 in PKCθ C1b.

Table 5.1.4: *Anisotropy*[a] *values of alkyl cinnamates and curcumin in the presence and absence of the PKCδ and PKCθ C1b proteins at room temperature.*

Compound[b]	buffer[c]	PKCδ-C1b	PKCθ-C1b
1a	0.0577 (0.0114)	0.1111 (0.0049)	0.1076 (0.0025)
1b	0.0575 (0.0056)	0.1144 (0.0031)	0.1109 (0.0032)
2a	0.0511 (0.0043)	–	0.1043 (0.0111)
2b	0.0606 (0.0008)	–	0.1076 (0.0134)
3a	0.0563 (0.0009)	–	0.0815 (0.0039)
3b	0.0445 (0.0035)	–	0.0930 (0.0061)
5a	0.0603 (0.0061)	0.1122 (0.0021)	0.1001(0.0053)
5b	0.0561 (0.0100)	0.1109 (0.0029)	0.1088 (0.0325)
6a	0.0455 (0.0015)	–	0.0941 (0.0045)
6b	0.0508 (0.0083)	–	0.0792 (0.0007)
8a	0.0657 (0.0104)	0.1181 (0.0029)	0.1190 (0.0058)
8b	0.0677 (0.0110)	0.1204 (0.0025)	0.1171 (0.0066)
Curcumin	0.0694 (0.0093)	0.1291 (0.0046)	0.1623 (0.0050)
DAG_8[d]	–	0.0978 (0.0063)	0.1069 (0.0051)

[a] Values in the parenthesis indicate standard deviations. [b] Compound, 20 μM; protein, 2 μM in buffer (20 mM Tris, 160 mM NaCl, 50 μM $ZnSO_4$, pH 7.4). [c] Anisotropy values of compounds in buffer. [d] Anisotropy values of PKCδ and PKCθ C1b protein in buffer were 0.05793 (0.0056) and 0.05529 (0.0032).

Although the changes in anisotropy values were different for the compounds, still this experiment suggested that presence of proteins increase the rigidity of the surrounding environment of the compounds in a similar manner to that of curcumin.

Interaction with ligand containing liposomes─ Lipid-binding domains and proteins must first interact with the membrane surface for specific lipid recognition, because most of the lipids are located at the membranes. In general the lipid binding domains and proteins have a membrane-binding surface as well as a lipid-binding groove.[180] The C1 domain of PKC isoforms has both membrane binding surface and lipid-binding groove. The C1 domains respond to increased DAG levels at the plasma membrane.[121]

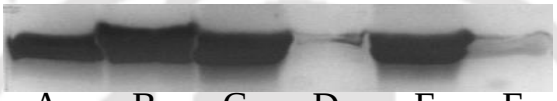

Figure 5.1.3: *Coomassie blue stained SDS-PAGE gel image of liposome binding assay. A, C, E are liposome bound fraction and B, D, F are unbound fraction of PKCδ C1b protein. The lipid compositions were PC/PS (80/20) for A, PC/PS/**8a** (70/20/10) for C and PC/PS/DAG_{16} (70:20:10) for E.*

To investigate the binding properties of the C1b subdomains of PKC isoforms to long chain alkyl cinnamates containing liposomes, we performed liposome binding assay and fluorescence quenching assay. The qualitative binding properties of the alkyl cinnamates containing liposomes were first analyzed by SDS-PAGE gel. The Coomassie blue staining of the SDS-PAGE gel shows the comparable protein binding to the DAG/ligand containing liposomes (*Figure 5.1.3*). We also performed Trp fluorescence quenching assay with the DAG/ligand containing liposomes. Figure 5.1.4 shows the representative plot of fluorescence quenching data for PKCδ C1b in the presence of different concentrations (0.15-2.80 nM) of **1a**, **5a** and **8a** and DAG containing liposomes. The liposome binding assay for compound **8a** also shows 2.2-fold stronger binding affinity than DAG_{16} for PKCδ C1b and other compounds have comparable binding affinity (*Table 5.1.5*) under the similar experimental conditions. The experimental values suggest that the long chain alkyl cinnamates interacts with the C1b subdomain of PKC isoforms in a similar manner to that of DAG and the PKC C1b subdomains could be recruited from cytoplasm and activated by the alkyl cinnamates at the plasma membrane.

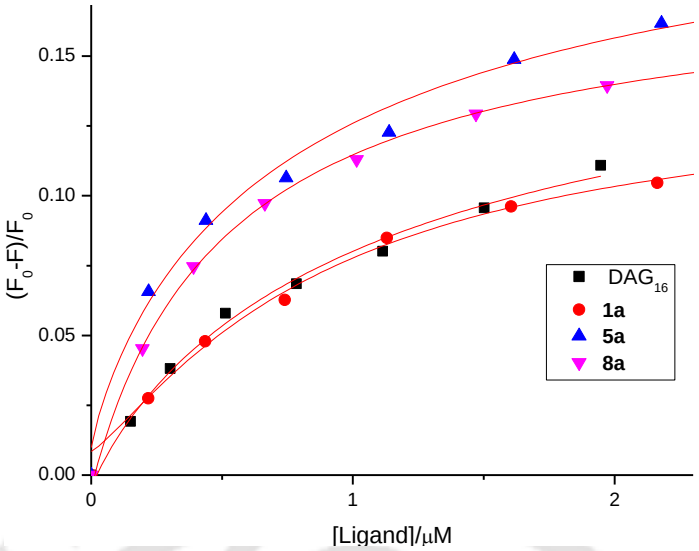

Figure 5.1.4: *Binding of liposome containing ligands with PKCδ C1b. Representative plot of fluorescence intensity of PKCδ C1b (500 nM) in buffer (20 mM Tris, 150 mM NaCl, 50 μM $ZnSO_4$, pH 7.4) in presence of varying concentration of liposome containing DAG_{16} (■), **1a** (●), **5a** (▲) and **8a** (▼), where F and F_0 are fluorescence intensity in the presence and absence of the ligand, respectively. Solid lines indicate the fit using Hill equation.*

The decrease of Trp fluorescence intensity (at ~338 nm) and the increase in the compound fluorescence intensity (at ~415 nm) with the concomitant addition of alkyl cinnamates (*Figure 5.1.5*) or alkyl cinnmates containing liposomes to the protein in buffer solution shows the energy transfer process from the single Trp residue of the C1b subdomain (donor) to the alkyl cinnamates (acceptor). Similar type of energy transfer was observed for human serum albumin-curcumin interactions[181] and PKCα C1a subdomain-resveratrol derivatives.[182]

Table 5.1.5: *EC_{50} values for the binding of alkyl cinnamates (**1a**, **5a** and **8a**) and DAG_{16} containing liposome[b] with the PKCδ C1b protein[a] at room temperature.*

PKCδ C1b	DAG_{16}	**1a**	**5a**	**8a**
EC_{50} (nM)	1.17 ± 0.11	0.91 ± 0.10	0.85 ± 0.07	0.54 ± 0.08
Hill coefficients (nH)	1.08 ± 0.08	1.13 ± 0.12	0.98 ± 0.10	1.01 ± 0.07

[a] Protein, 0.5 μM in buffer (20 mM Tris, 150 mM NaCl, 50 μM $ZnSO_4$, pH 7.4).

[b] Liposome composition, PC/PS/$Ligand_{16}$ (80-x: 20: x, where x = 0-10 mol%).

The Hill coefficient values (*Table 5.1.3*) and energy transfer process (*Figure 5.1.5*) indicates that one alkyl cinnamate bind to one C1b subdomain in such a way that the distance of ligand molecules residing within the C1b subdomain are within the limit of Forster Resonance Energy Transfer (FRET) distance. It is also reported that the ligand binding to the C1b subdomains expose the Trp residue to the buffer, causing decrease in Trp fluorescence intensity.[138,151] Thus, the decrease in Trp fluorescence could be due to both the displacement of Trp residue and FRET process. The only FRET process due to binding will not produce complete Trp fluorescence quenching, because in such event the extent of quenching will depend on the Förster radius, as well as the Trp-cinnamate chromophore distance. A similar FRET process also occurs for protein binding to the alkyl containing liposomes. Additionally, FRET can occur to randomly distributed alkyl cinnamates in the solution and bilayer, without actual binding. In this study all the ligands have similar chromosphore, so relative binding affinity (EC_{50}) measured by modified Hill equation would not vary, but the quantitative binding affinity for all the compounds may vary. Here, EC_{50} is the measure of half maximal effective concentration of the ligands required to induce the Trp fluorescence change halfway between the baseline and maximum.

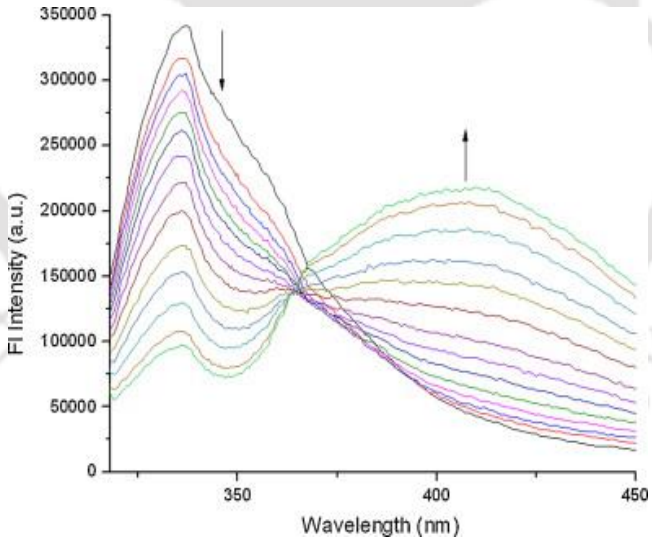

Figure 5.1.5: *Quenching of intrinsic fluorescence of PKCδ C1b by* ***8b****. Addition of increased concentration of* ***8b*** *(0.67-48 µM) to PKCδ C1b (2 µM) quenched the intrinsic fluorescence at 338 nm and increased fluorescence intensity at 415 nm.*

To calculate the quantitative binding affinity, it is also required to consider the inner filter effect and FRET effect. The presence of single Trp residue close to the binding pocket and energy transfer from Trp to alkyl cinnamates/curcumin also shows their interaction through the DAG/phorbol ester binding site.

Extent of membrane localization— To evaluate the relationship between the protein binding properties of the ligands (under membrane environment) and the extent of their localization at the liposome interface, we performed fluorescence quenching experiments using PC/Cholesterol/Ligand$_{16}$/NBD-PE liposomes. The NBD dye is embedded close to the bilayer interface, providing a useful marker for surface interactions of membrane-active compounds. The NBD fluorescence quenching by sodium dithionite provided a measure of membrane interactions of the ligands. Figure 5.1.6 demonstrates that ligand containing fluorescent liposomes yielded significant changes in the rate of dithionite-induced fluorescence quenching of the bilayer-embedded dye. All the ligands examined yielded lower quenching rates compared to the control liposomes (without any ligands). The result suggests that the NBD dye became more 'shielded' from the soluble dithionite quencher, due to the presence of alkyl cinnamates in the liposomes. The results also imply that these ligands are more localized at the liposome surface compared to DAG.

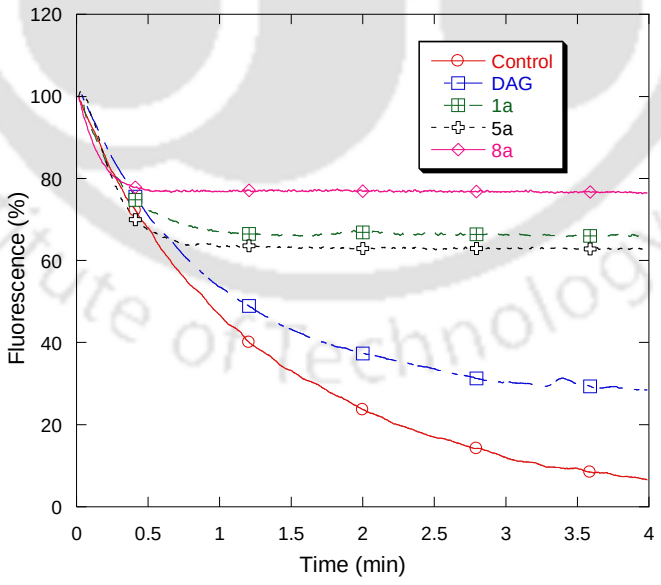

Figure 5.1.6: *Fluorescence quenching of NBD-PE embedded in PC/Cholesterol/Ligand$_{16}$/NBD-PE (44.5:44.5:10:1) liposomes. Sodium dithionite = 0.6 µM. Control: no ligand.*

Thus, the alkyl cinnamates (**1a**, **5a** and **8a**) are more accessible for the protein binding than DAG, under liposome environment. This is in complete correlation with their protein binding properties, under the liposome environment.

Molecular docking analysis─ To gain more details of the possible binding mode of the compounds and the interacting residues of the C1b subdomains, we performed molecular docking analysis. The molecules were docked into the activator binding site using the crystal structure of PKCδ C1b and NMR structure of PKCθ C1b [Protein Data Bank code: 1PTR, 2ENZ].[183,184] The models revealed the possible binding orientation when ligands were docked into the empty C1b subdomains and also showed that ligands were anchored to the binding pocket *via* similar fashion, as phorbol esters and curcumin (*Figure 5.1.7*). The hydroxyl and methoxy groups of ligands were hydrogen bonded to the backbone amide proton and the carbonyls of C1b subdomain. They could also be involved in additional hydrogen bonding with the side chain of polar amino acid of PKCδ C1b protein.

All the compounds showed negative MolDock score and rerank score values and most of them formed hydrogen bonds (up to ~3.2 Å) with the protein residues. Curcumin, compounds **1b** and **8b** interacted with the PKCδ C1b by forming two, three and four hydrogen bonds, respectively (*Figure 5.1.7*). The C-11 hydroxyl and C-5 methoxy groups of curcumin were hydrogen bonded to the backbone carbonyl group of Leu-251 and the amide proton of Thr-242, respectively. In case of **1b** the C-35 methoxy and C-36 hydroxyl groups were hydrogen bonded to the backbone amide proton of Thr-242 and carbonyl groups of Thr-242 and Leu-251, respectively. The C-16 hydroxyl groups of compound **8b** were hydrogen bonded to the backbone amide protons of Thr-242 and carbonyl groups of Thr-242 and Leu-251, respectively. The C-15 hydroxyl group of **8b** was hydrogen bonded to the side-chain hydroxyl groups of Thr-242. Therefore, in general, both hydroxyl and methoxy groups of these molecules are important for their interaction with PKCs. The molecular docking analysis of the ligands with the PKCθ C1b subdomain indicates the similar binding pattern with additional hydrogen bonds. The experimental binding results and docking score values obtained from the models do not always corroborate (*Table 5.1.6*). This difference indicates that both proteins and compounds can undergo conformational changes under experimental conditions. The molecular docking analysis also indicates that the overall high binding affinities of compounds **1**, **5** and **8** are probably associated with the position and number of hydroxyl and methoxy groups, helping them anchoring to the bottom of the binding site, which may not be possible for compounds **3**, **4**, **6** and **7.**

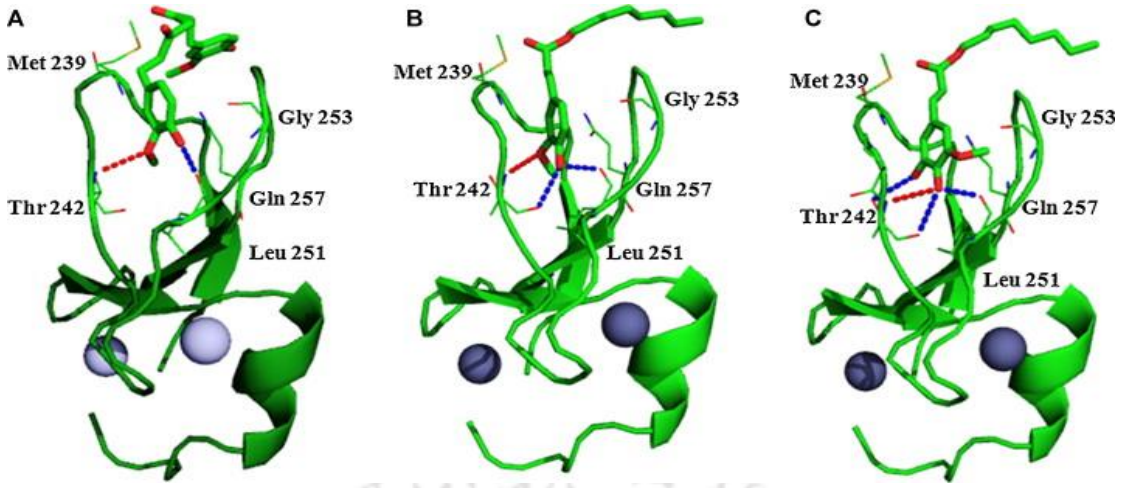

Figure 5.1.7: *Structures of ligand bound PKCδ C1b subdomain (Protein Data Bank code: 1PTR). Modeled structure of curcumin and short chain alkyl cinnamates (**1b**, **8b**) docked into PKCδ C1b (A–C). The modeled structures were generated using the Molegro Virtual Docker, version 4.3.0. The oxygen atoms and nitrogen atoms are shown in red and blue, respectively. The dotted line indicates possible hydrogen bonds. (For interpretation of the references to color in this figure legend, the reader is referred to the web version of the article.)*

Therefore, binding affinities of the compounds highlight the importance of ligand hydrophobicity and binding orientation, in similar manner to those reported for C1 domain ligands. It is also proposed that the hydrophobic amino acids such as Met-239, Phe-243, Leu-250, and Leu-254 for PKCδ C1b, surrounding the ligand binding site of the C1 domain interact with the hydrophobic moiety of the C1 domain ligands. The long alkyl chain containing compounds may interact with the membrane lipid bilayer, because the PKC isoforms interacts with the membrane through the C1 domain for activation and regulation of other cellular pathways. Thus, the fluorescence binding assay using water soluble ligands and ligand containing liposomes confirms that the alkyl cinnamates interact with C1b subdomains. The results also indicate that the long chain alkyl cinnamates can differentially influence the activation and membrane translocation properties of PKCθ and PKCδ. The affinity differences between the proteins are solely because of the differences in the residues and surface area of the activator binding pockets. The results also indicate that their activating effect could be lower than the phorbol esters or other natural compounds under similar experimental conditions.

Table 5.1.6: *Docking score values obtained from the docking of cinnamic acid derivatives (with short chain length) and curcumin into the PKCθ and PKCδ C1b subdomains using Molegro Virtual Docker, version 4.3.0.*

Compound	MolDock score		Rerank score	
	PKCδ C1b	PKCθ C1b	PKCδ C1b	PKCθ C1b
1b	-110.233	-100.4	-80.9186	-76.4443
2b	-107.465	-	-75.2924	-
3b	-104.961	-	-74.5324	-
5b	-103.906	-114.96	-81.116	-93.8836
6b	-103.868	-	-78.2321	-
8b	-116.893	-102.31	-96.1726	-76.1319
Curcumin	-119.661	-	-98.8156	-

The binding measurements also suggest that, the C1b subdomains interact differentially with the alkyl cinnamates and their interactions can specifically modulate the PKC isoforms.

Conclusion

We described here the synthesis, spectral properties and binding of alkyl cinnamates related to the curcumin structure, to the C1b subdomains of PKCθ and PKCδ isoenzymes. Synthesis of these alkyl cinnamates from the corresponding aldehydes provided the ability to generate pure samples and freedom to explore the role of hydroxyl and methoxy groups at different positions. The experimental results showed that alkyl cinnamates interact with the C1b subdomain of PKC isoforms through the DAG or phorbol ester binding site and forms hydrogen bonds with the residues at the activator binding site. The monomeric and liposome binding assays shows that the long chain alkyl cinnamate derivatives can differentially influence the activation and membrane translocation properties of PKCθ and PKCδ. The membrane localization study shows that the alkyl cinnamtes are more localized at the liposome surface, thus more accessible for the protein binding than DAG. The long chain alkyl derivatives of each halves of symmetric curcumin have comparable binding affinity under the experimental conditions. In contrast to phorbol esters, which are tumorogenic, cinnamic acids and its ester derivatives are non-toxic and have anticancer, anti-inflammatory, antioxidant and several other properties. This makes these ligands, in particular the derivatives of 5-hydroxyvanillin, vanillin and protocatechualdehyde as potential regulator of PKC isoforms and can be further developed as research tools or lead compound in drug

development. Undoubtedly, further studies are needed to fully understand the importance of the alkyl cinnamates in activation and regulation of PKC isoenzymes.

In chapters 2-5, we have described the synthesis of ester based C1 domain ligands. There are several methods to prepare ester analogues; however most of the reported methods are not always strong and/or selective enough for the synthesis of complex substrates, including hydroxyl group bearing carboxylic acids. In the next chapter, we described a mild and selective esterification method for a series of hydroxyl group bearing acids, including the cinnamic acids via formation of a more reactive species, zinc co-ordinated acyloxyphosphonium ion intermediate.

5.2. Experimental Section

5.2.1 Instrumentations and Characterization

As described in chapter 2 section 2.2.1

5.2.2. General experimental procedure for the preparation of half esters of malonic acid (I): Meldrum's acid (1 equiv.) and cetyl alcohol or 1-octanol (1 equiv.) were refluxed in toluene (30 ml) for 4 h. After completion of the reaction (monitored by TLC), the reaction mixture was cooled to room temperature followed by 0 °C. The reaction was quenched by saturated $NaHCO_3$ solution and neutralized by concentrated HCl. The resulted solution was extracted with ethyl acetate (3 × 30 ml) and washed with brine (30 ml). The combined organic layer was dried over anhydrous Na_2SO_4 and the solvent was removed under reduced pressure to yield 2-((hexadecyloxy)carbonyl)acetic acid and 2-((octyloxy)carbonyl)acetic acid as white solid and colourless oil respectively.

5.2.3. General experimental procedure for the preparation of esters of trans-cinnamic acids (II):- Method A: A solution of trans-cinnamic acid (1.0 equiv.), cetyl alcohol or 1-octanol (1.0 equiv.), p-toluenesulfonic acid (0.1 equiv.) in toluene was refluxed for 6 h and the azeotrope was collected in a Dean‑Stark trap. After completion of the reaction (monitored by TLC), the reaction mixture was cooled to room temperature and 20% (W/W) solid sodium bicarbonate was added. After stirring for another 30 min at room temperature, the reaction mixture was filtered off and filtrate was

concentrated under reduced pressure. The resulted crude product was purified by silica gel column chromatography with a gradient solvent system of 0‑10% ethyl acetate to hexanes yielded trans-cinnamic acid ester analogue.

Method B: To a stirring solution of 2-((hexadecyloxy)carbonyl)acetic acid or 2-((octyloxy)carbonyl)acetic acid, corresponding benzaldehyde derivative in toluene (15 ml) were added pyridine (1.5 equiv.), piperidine (0.1 equiv.) and the resulting mixture was stirred for 8 h at 70 °C. After completion of reaction (monitored by TLC), the reaction mixture was cooled to room temperature and quenched by adding 3(N) HCl. The resulted solution was extracted with ethyl acetate (3 × 20 ml) and washed with brine (30 ml). The combined organic layer was dried over anhydrous Na_2SO_4 and the solvent was removed under reduced pressure. The crude reaction mixture was purified by column chromatography with silica gel and a gradient solvent system of 0‑10% of ethyl acetate to hexane to provide trans-cinnamic acid ester analogue.

5.2.4. Protein purification:

As described in chapter 2 in section 2.2.8

5.2.5. Fluorescence studies:

As described in chapter 2 in section 2.2.9

5.2.6. Liposome binding assay

As described in chapter 2 in section 2.2.10

5.2.7. Extent of membrane localization

As described in chapter 3 in section 2.2.11

5.2.8. Molecular docking

As described in chapter 2 section 2.2.11

5.3. Characterization of the Synthesized Compounds

(E)-hexadecyl 3-(4-hydroxy-3-methoxyphenyl)acrylate (1a)[172]**:** White solid; m.p. 65-67 °C (lit. m.p. 69 °C); ^{1}H NMR (400 MHz, $CDCl_3$): δ_{ppm} 7.59 (d, 1H,*J* = 16.0 Hz), 7.14 (s, 1H), 7.02 (d, 1H, *J* = 8.4 Hz), 6.84 (d, 1H, *J* = 8.4 Hz), 6.29 (d, 1H, *J* = 16.0 Hz), 5.71 (s, 1H), 4.10 (t, 2H, *J* = 6.0 Hz), 3.84 (s, 3H), 1.61(m, 2H), 1.22 (m, 26H), 0.79 (t, 3H, *J* = 6.0 Hz); ^{13}C NMR (100 MHz, $CDCl_3$): δ_{ppm} 167.6, 148.7, 146.1, 144.6, 128.3, 122.0, 116.5, 113.3, 110.7, 64.8, 56.1, 32.1, 30.0, 29.8, 29.7, 29.6, 29.5, 28.9, 26.2, 22.9, 14.3; HRMS (ESI) Calcd for $C_{26}H_{42}O_4$ $[M+1]^+$ 419.3156. Found 419.2211.

(E)-octyl 3-(4-hydroxy-3-methoxyphenyl) acrylate (1b): Colorless oil; ^{1}H NMR (400 MHz, $CDCl_3$): δ_{ppm} 8.8 (br s, 2H), 7.51 (d, 1H, *J* = 16.0 Hz), 7.07 (s, 1H), 6.95 (d, 1H,*J* = 8.4 Hz), 6.76 (d, 1H, *J* = 8.4 Hz), 6.22 (d, 1H, *J* = 16.0 Hz), 5.69 (s, 1H), 4.11 (t, 2H, *J* = 6.6 Hz), 3.84 (s, 3H), 1.62 (m, 2H), 1.21 (m, 10H), 0.81 (t, 3H, *J* = 6.6 Hz); ^{13}C NMR (100 MHz, $CDCl_3$): δ_{ppm} 167.7, 148.8, 146.0, 144.6, 128.2, 121.9, 116.3, 113.3, 110.7, 64.8, 56.0, 31.9, 29.8, 29.4, 29.3, 28.9, 26.1, 22.8, 14.2; HRMS (ESI) Calcd for $C_{18}H_{26}O_4$ $[M+1]^+$ 307.1904. Found 307.1271.

(E)-hexadecyl 3-(3-hydroxy-4-methoxyphenyl)acrylate (2a): White solid; m.p. 69-70 °C; ^{1}H NMR (400 MHz, $CDCl_3$): δ_{ppm} 7.53 (d, 1H, *J* = 16.0 Hz), 6.98 (d, 1H, *J* = 8.0 Hz), 6.94 (s, 1H), 6.83 (d, 1H, *J* = 8.0 Hz), 6.21 (d, 1H, *J* = 16.0 Hz), 5.8 (br s, 1H), 4.11 (t, 2H, *J* = 6.8 Hz), 3.82 (s, 3H), 1.63 (m, 2H), 1.23 (m, 26H), 0.79 (t, 3H, *J* = 6.8 Hz); ^{13}C NMR (100 MHz, $CDCl_3$): δ_{ppm} 167.6, 148.2, 147.02, 144.9, 127.2, 123.2, 115.8, 115.0, 109.5, 64.8, 56.1, 33.0, 32.1, 30.0, 29.6, 29.6, 29.0, 26.2, 26.0, 22.9, 14.3; HRMS (ESI) Calcd for $C_{26}H_{42}O_4$ $[M+1]^+$ 419.3156. Found 419.2211.

(E)-octyl 3-(3-hydroxy-4-methoxyphenyl) acrylate (2b): Colorless oil; ^{1}H NMR (400 MHz, $CDCl_3$): δ_{ppm} 7.54 (d, 1H, *J* = 16.0 Hz), 7.0 (d, 1H, *J* = 8.4 Hz), 6.96 (s, 1H), 6.84 (d, 1H, *J* = 8.4 Hz), 6.22 (d, 1H, *J* = 16.0 Hz), 5.88 (s, 1H), 4.11 (t, 2H, *J* = 6.8 Hz), 3.85 (s, 3H), 1.62 (m, 2H), 1.23 (m, 10H), 0.81 (t, 3H, *J* = 5.6 Hz); ^{13}C NMR (100 MHz, $CDCl_3$): δ_{ppm} 167.6, 148.2, 147.0, 144.9, 127.2, 123.2, 115.8, 115.0, 109.5, 64.8, 56.2, 31.9, 29.8, 29.4, 29.3, 28.9, 26.1, 22.8, 14.2; HRMS (ESI) Calcd for $C_{18}H_{26}O_4$ $[M+1]^+$ 307.1904. Found 307.1271.

(E)-hexadecyl 3-(4-hydroxyphenyl)acrylate (3a)[173]**:** White solid; m.p.84-85 °C (lit. m.p. 84-86 °C); ^{1}H NMR (400 MHz, $CDCl_3$): δ_{ppm} 7.63 (d, 1H, *J* = 16.0 Hz), 7.42 (d, 2H, *J* = 8.4 Hz), 6.86 (d, 2H, *J* = 8.4 Hz), 6.30 (d, 1H, *J* = 16.0 Hz), 6.25 (br s, 1H), 4.20 (t, 2H, *J* = 6.6 Hz), 1.68 (m, 2H), 1.29 (m, 26H), 0.88 (t, 3H, *J* = 6.6 Hz); ^{13}C NMR (100 MHz, $CDCl_3$): δ_{ppm} 168.2, 158.3, 145.0, 130.2, 127.1, 116.1,115.5, 65.0, 32.1, 30.0, 29.8, 29.7, 29.6, 29.5, 29.0, 26.2, 23.0, 14.3; HRMS (ESI) Calcd for $C_{25}H_{40}O_3$ $[M+1]^+$ 389.3050. Found 389.3053.

(E)-octyl 3-(4-hydroxyphenyl)acrylate (3b): Yellow oil; ^{1}H NMR (400 MHz, $CDCl_3$): δ_{ppm} 7.64 (d, 1H, *J* = 16.0 Hz), 7.41 (d, 2H, *J* = 8.4 Hz), 7.20 (br s 1H), 6.88 (d, 2H, *J* = 8.4 Hz), 6.30 (d, 1H, *J* = 16.0 Hz), 4.20(t, 2H, *J* = 6.8 Hz), 1.70 (m, 2H), 1.27 (m, 10H), 0.87 (t, 3H, *J* = 6.6 Hz); ^{13}C NMR (100 MHz, $CDCl_3$): δ_{ppm} 168.7, 158.7, 145.4, 130.2, 126.8, 116.2, 115.0, 65.2, 31.9, 29.9, 29.4, 29.3, 28.8, 26.1, 22.8, 14.2; HRMS (ESI) Calcd for $C_{17}H_{24}O_3$ $[M+1]^+$ 277.1798. Found 277.0797.

(E)-hexadecyl 3-(3-hydroxyphenyl)acrylate (4a)[173]**:** White solid; m.p. 83-85 °C (lit. m.p. 75-76.5 ° C); ^{1}H NMR (400 MHz, $CDCl_3$): δ_{ppm} 7.55 (d, 1H, *J* = 16.0 Hz), 7.16 (t, 1H, *J* = 8.0 Hz), 6.99 (d, 1H, *J* = 8.0 Hz), 6.59 (s, 1H), 6.81 (d, 1H, *J* = 8.0 Hz), 6.59 (br s, 1H), 6.33 (d, 1H, *J* = 16.0 Hz), 4.13 (t, 2H, *J* = 5.4 Hz), 1.62 (m, 2H), 1.18 (m, 26H), 0.80 (t, 3H,*J* = 6.6 Hz); ^{13}C NMR (100 MHz, $CDCl_3$): δ_{ppm} 167.8, 156.6, 145.0, 136.0, 130.3, 120.8, 118.5, 117.8, 114.8, 65.3, 32.1, 29.9, 29.8, 29.7, 29.6, 29.5, 28.9, 26.2, 22.9, 14.3; HRMS (ESI) Calcd for $C_{25}H_{40}O_3$ $[M+1]^+$389.3050. Found 389.3052.

(E)-octyl 3-(3-hydroxyphenyl)acrylate (4b): Yellow oil; ^{1}H NMR (400 MHz, $CDCl_3$): δ_{ppm} 7.55 (d, 1H, *J* = 16.0 Hz), 7.14 (t, 1H, *J* = 8.0 Hz), 7.04 (s, 1H), 6.97 (d, 2H, *J* = 8.0 Hz), 6.83 (d, 1H, *J* = 8 Hz), 6.32 (d, 1H, *J* = 16 Hz), 4.12 (t, 2H, *J* = 6.8 Hz), 1.61 (m, 2H), 1.19 (m, 10H), 0.80 (t, 3H, *J* = 6.8 Hz); ^{13}C NMR (100 MHz, $CDCl_3$): δ_{ppm} 168.2, 156.7, 145.4, 135.8, 130.2, 120.7, 118.0, 114.9, 65.4, 32.0, 29.9, 29.4, 28.8, 26.1, 22.8, 14.3; HRMS (ESI) Calcd for $C_{17}H_{24}O_3$ $[M+1]^+$277.1759. Found 277.1759.

(E)-hexadecyl 3-(3,4-dihydroxyphenyl)acrylate (5a) [172]**:** White solid; m.p. 105-107 °C (lit. m.p. 102 °C); ^{1}H NMR (400 MHz, $CDCl_3$ + DMSO-d_6): δ_{ppm} 7.43 (d, 1H, *J* = 16 Hz), 6.98 (s, 1H), 6.82 (d, 1H, *J* = 8.4 Hz), 6.75 (d, 1H, *J* = 6.6 Hz), 6.13 (d, 1H,*J* = 16 Hz), 4.05 (m, 2H),

1.60 (m, 2H), 1.18 (m, 28H), 0.80 (m, 3H); ^{13}C NMR (100 MHz, $CDCl_3$ + DMSO-d_6): δ_{ppm} 166.9, 147.7, 145.1, 144.6, 125.8, 121.1, 115.4, 114.1, 63.9, 31.4, 29.2, 28.8, 28.3, 28.0, 25.5, 25.3, 22.2, 13.7; HRMS (ESI) Calcd for $C_{25}H_{40}O_4$ $[M+1]^+$ 405.2999. Found 405.2996.

(E)-octyl 3-(3,4-dihydroxyphenyl)acrylate (5b): White solid; m.p. (64-66 °C); ^{1}H NMR (400 MHz, $CDCl_3$ + DMSO-d_6): δ_{ppm} 7.45 (d, 1H, *J* = 16 Hz), 6.97 (s, 1H), 6.83 (d, 1H, *J* = 8.0 Hz), 6.73 (d, 1H, *J* = 6.4 Hz), 6.11 (d, 1H, *J* = 16 Hz), 4.06 (t, 2H, *J* = 6.6 Hz), 1.57 (m, 2H), 1.17 (br, 12H), 0.79 (t, 3H, *J* = 6.4 Hz); ^{13}C NMR (100 MHz, $CDCl_3$ + DMSO-d_6): δ_{ppm} 168.4, 147.4, 145.5, 144.8, 126.8, 122.0, 115.3, 114.6, 114.1, 64.8, 31.7, 29.2, 29.1, 28.6, 26.0, 22.6, 14.0; HRMS (ESI) Calcd for $C_{17}H_{24}O_4$ $[M+1]^+$ 293.1747. Found 293.1745.

(E)-hexadecyl 3-(4-methoxyphenyl)acrylate (6a): White solid; m.p. (76-77 °C); ^{1}H NMR (400 MHz, $CDCl_3$): δ_{ppm} 7.54 (d, 1H, *J* = 16.0 Hz), 7.36 (d, 2H, *J* = 8.4 Hz), 6.79 (d, 2H, *J* = 8.4 Hz), 6.21 (d, 1H, *J* = 16.0 Hz), 4.08 (t, 2H, *J* = 6.6 Hz), 3.71 (s, 3H), 1.59 (m, 2H), 1.16 (m, 26H), 0.78 (t, 3H, *J* = 6.4 Hz), ^{13}C NMR (100 MHz, $CDCl_3$): δ_{ppm} 167.5, 161.4, 144.3, 130.0, 128.0, 116.0, 114.4, 64.7, 55.5, 32.1, 29.9, 29.8, 29.7, 29.5, 29.4, 29.1, 29.0, 26.2, 25.5, 22.9, 14.3; HRMS (ESI) Calcd for $C_{26}H_{42}O_3$ $[M+1]^+$ 403.3207. Found 403.3210.

(E)-octyl 3-(4-methoxyphenyl)acrylate (6b): Yellow oil; ^{1}H NMR (400 MHz, $CDCl_3$): δ_{ppm} 7.53 (d, 1H, *J* = 16.0 Hz), 7.35 (d, 2H, *J* = 8.8 Hz), 6.78 (d, 2H,*J* = 8.8 Hz), 6.20 (d, 1H, *J* = 16.0 Hz), 4.08 (t, 2H, *J* = 6.8 Hz), 3.69 (s, 3H), 1.58 (m, 2H), 1.18 (m, 10H), 0.78 (t, 3H, *J* = 6.0 Hz); ^{13}C NMR (100 MHz, $CDCl_3$): δ_{ppm} 167.4, 161.4, 144.2, 129.8, 129.7, 128.0, 127.2, 115.6, 114.3, 64.5, 55.3, 31.9, 29.9, 29.4, 29.3, 29.0, 28.8, 26.1, 22.7, 14.1; HRMS (ESI) Calcd for $C_{18}H_{26}O_3[M+Na]^+$ 313.1774. Found 313.1776.

(E)-hexadecyl 3-(3-methoxyphenyl)acrylate (7a): White solid; m.p. (75-76 °C); ^{1}H NMR (400 MHz, $CDCl_3$): δ_{ppm} 7.54 (d, 1H, *J* = 16 Hz), 7.16 (t, 1H, *J* = 7.8 Hz), 7.00 (d, 1H, *J* = 8.0 Hz), 6.93 (s, 1H), 6.81 (d, 1H, *J* = 8.0 Hz), 6.32 (d, 1H, *J* = 16 Hz), 4.09 (t, 2H, *J* = 6.6 Hz), 3.69 (s, 3H), 1.58 (m, 2H), 1.61 (m, 26H), 0.78 (t, 3H, *J* = 6.8 Hz); ^{13}C NMR (100 MHz, $CDCl_3$): δ_{ppm} 166.8, 160.0, 144.4, 135.9, 129.8, 120.7, 118.6, 116.0, 113.0, 64.6, 55.1, 32.0, 29.8, 29.7, 29.6, 29.5, 29.4, 28.8, 26.1, 22.8, 14.1; HRMS (ESI) Calcd for $C_{26}H_{42}O_3$ $[M+1]^+$ 403.3207. Found 403.2229.

(E)-octyl 3-(3-methoxyphenyl)acrylate (7b): Yellow oil; ^{1}H NMR (400 MHz, $CDCl_3$): δ_{ppm} 7.52 (d, 1H, *J* = 16 Hz), 7.14 (t, 1H, *J* = 7.4 Hz), 6.87 (d, 1H,*J* = 8.2 Hz), 6.95 (s, 1H), 6.83 (d, 1H, *J* = 8.2 Hz), 6.30 (d, 1H, *J* = 16 Hz), 4.07 (t, 2H, *J* = 6.8 Hz), 3.66 (s, 3H), 1.55 (m, 2H), 1.17 (m, 26H), 0.77 (t, 3H, *J* = 6.8 Hz); ^{13}C NMR (100 MHz, $CDCl_3$): δ_{ppm} 166.8, 159.9, 144.3, 135.8, 129.7, 120.6, 118.5, 116.0, 112.9, 64.6, 55.0, 31.8, 29.2, 29.1, 28.7, 26.0, 22.6, 14.0; HRMS (ESI) Calcd for $C_{18}H_{26}O_3$ $[M+1]^+$ 291.1955. Found 291.1955.

(E)-hexadecyl 3-(3,4-dihydroxy-5-methoxyphenyl)acrylate (8a): White solid; m.p. (105-106 °C); ^{1}H NMR (400 MHz, $CDCl_3$): δ_{ppm} 7.51 (d, 1H, *J* = 16 Hz), 6.80 (s, 1H), 6.66 (s, 1H), 6.25 (d, 1H, *J* = 15.6 Hz), 4.17 (t, 2H, *J* = 6.6 Hz), 3.83 (s, 3H), 1.67 (m, 2H), 1.24 (m, 26H), 0.86 (t, 3H,*J* = 6.6 Hz); 13 C NMR (100 MHz, $CDCl_3$): δ_{ppm} 168.0, 147.4, 145.3, 144.4, 135.4, 126.5, 116.0, 109.5, 103.5, 65.0, 56.3, 32.1, 29.8, 29.5, 28.9, 26.1, 22.8, 14.2; HRMS (ESI) Calcd for $C_{26}H_{42}O_5$ $[M+1]^+$ 435.3066. Found 435.3064.

(E)-octyl 3-(3,4-dihydroxy-5-methoxyphenyl)acrylate (8b): Yellow oil, ^{1}H NMR (400 MHz, $CDCl_3$): δ_{ppm} 7.41 (d, 1H, *J* = 15.6 Hz), 6.69 (s, 1H), 6.49 (s, 1H), 6.14 (d, 1H,*J* = 15.6 Hz), 5.92 (br, 2H), 4.08 (t, 2H, *J* = 6.6 Hz), 3.71 (s, 3H), 1.59 (m, 2H), 1.17 (m, 10H), 0.79 (t, 3H,*J* = 6 Hz); ^{13}C NMR (100 MHz, $CDCl_3$): δ_{ppm} 168.0, 147.5, 145.4, 144.4, 135.5, 126.2, 115.7, 109.5, 103.5, 65.0, 56.2, 31.8, 29.7, 29.3, 29.2, 28.7, 26.0, 25.9, 22.7, 14.1; HRMS (ESI) Calcd for $C_{18}H_{26}O_5$ $[M+1]^+$ 323.1814. Found 323.1817.

5.4. Selected Spectra of Alkyl Cinnamates

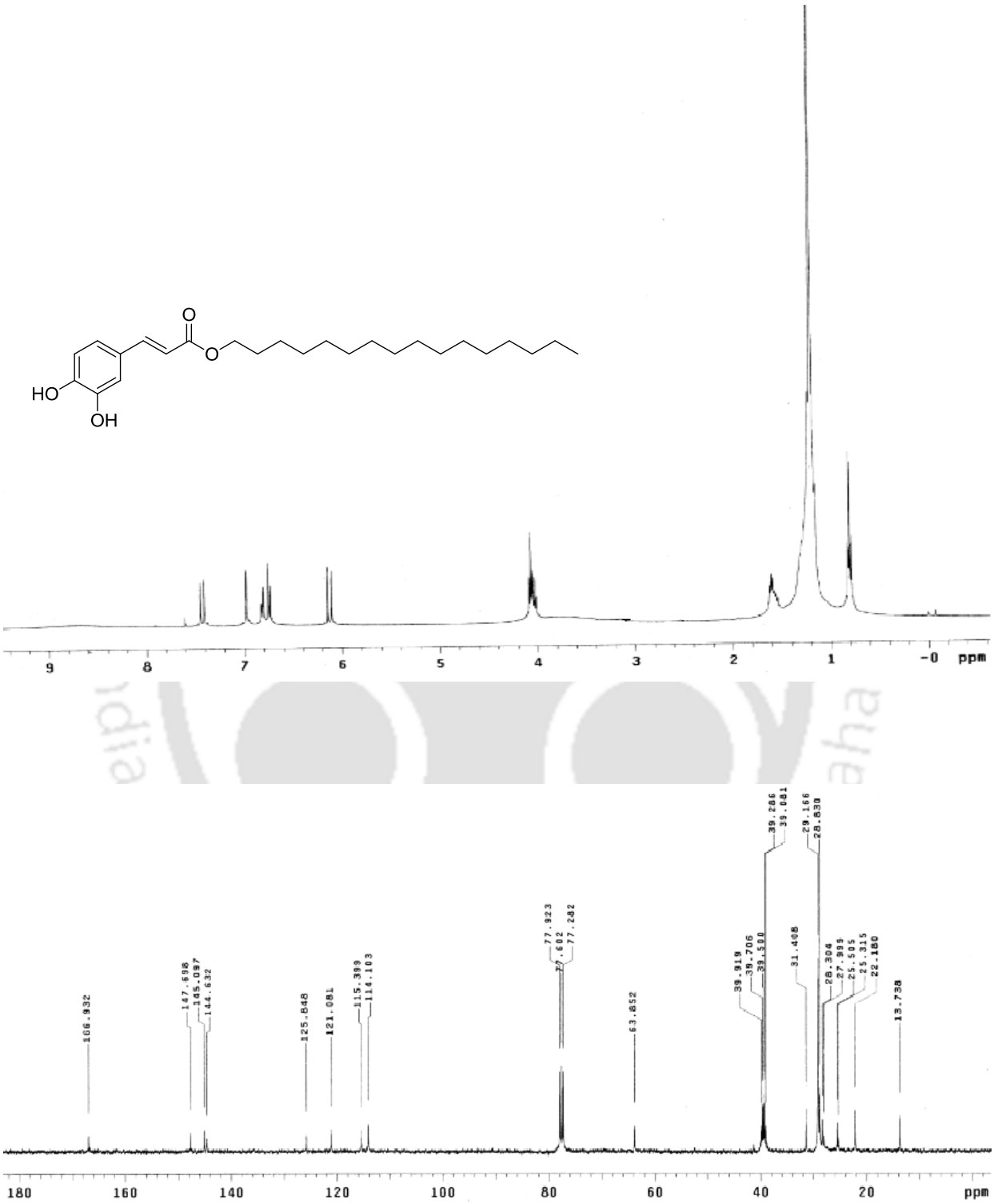

Figure 5.4.1: *^{1}H NMR and ^{13}C NMR of (E)-hexadecyl 3-(3,4-dihydroxyphenyl)acrylate* ***(5a)***

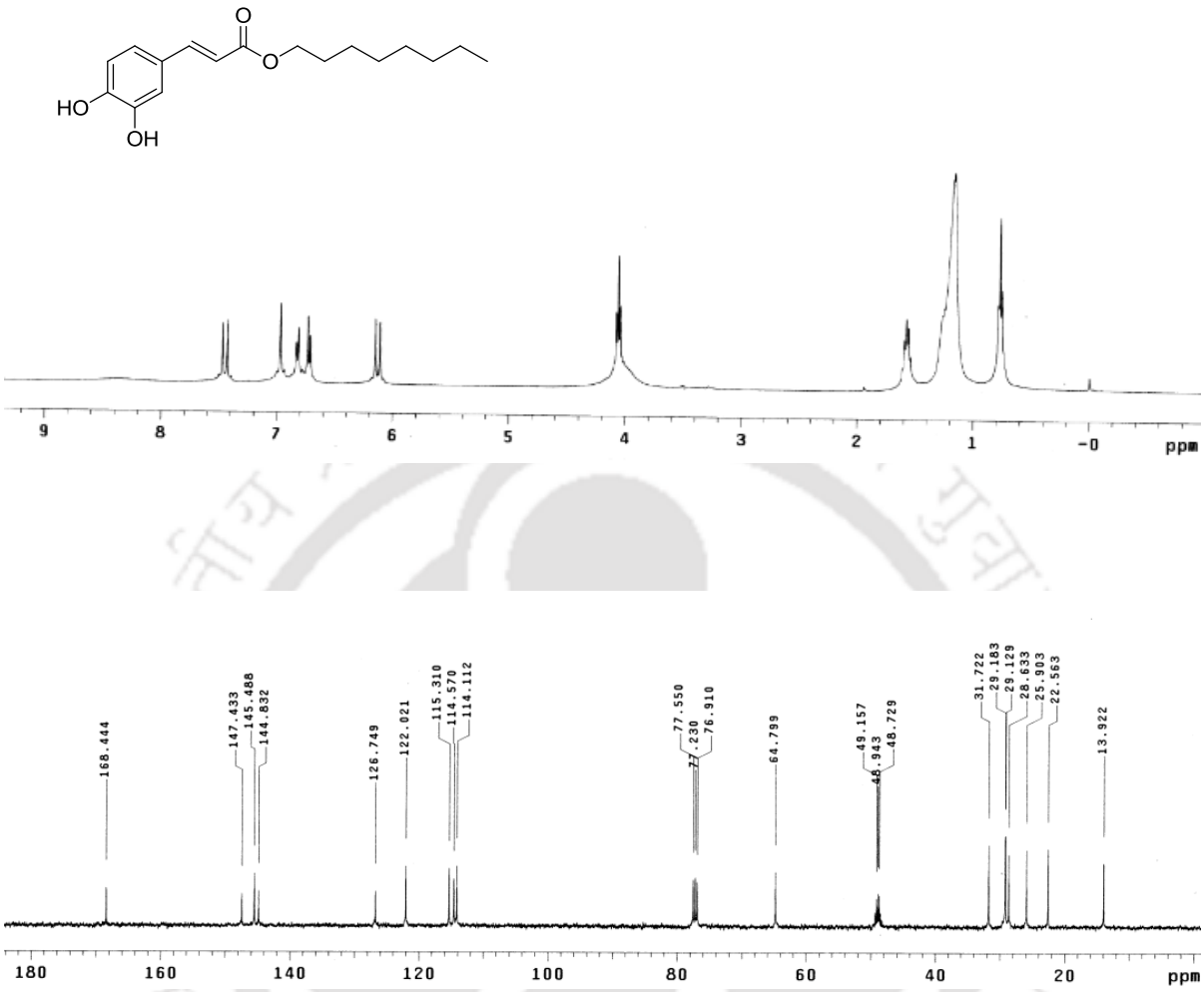

Figure 5.4.2: *^{1}H NMR and ^{13}C NMR of (E)-octyl 3-(3,4-dihydroxyphenyl)acrylate* ***(5b)***

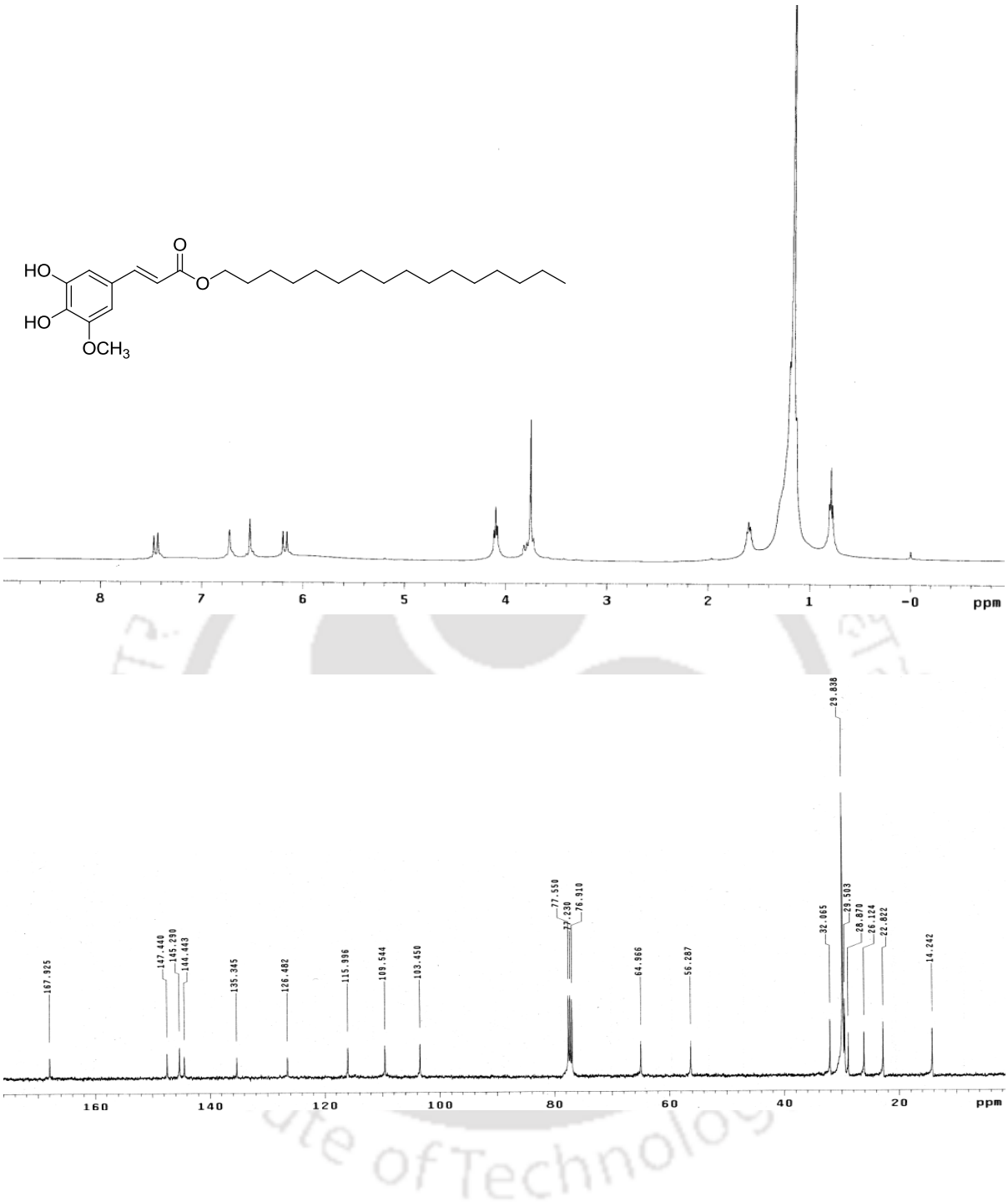

Figure 5.4.3: *^{1}H NMR and ^{13}C NMR of (E)-hexadecyl 3-(3,4-dihydroxy-5methoxyphenyl)acrylate* ***(8a)***

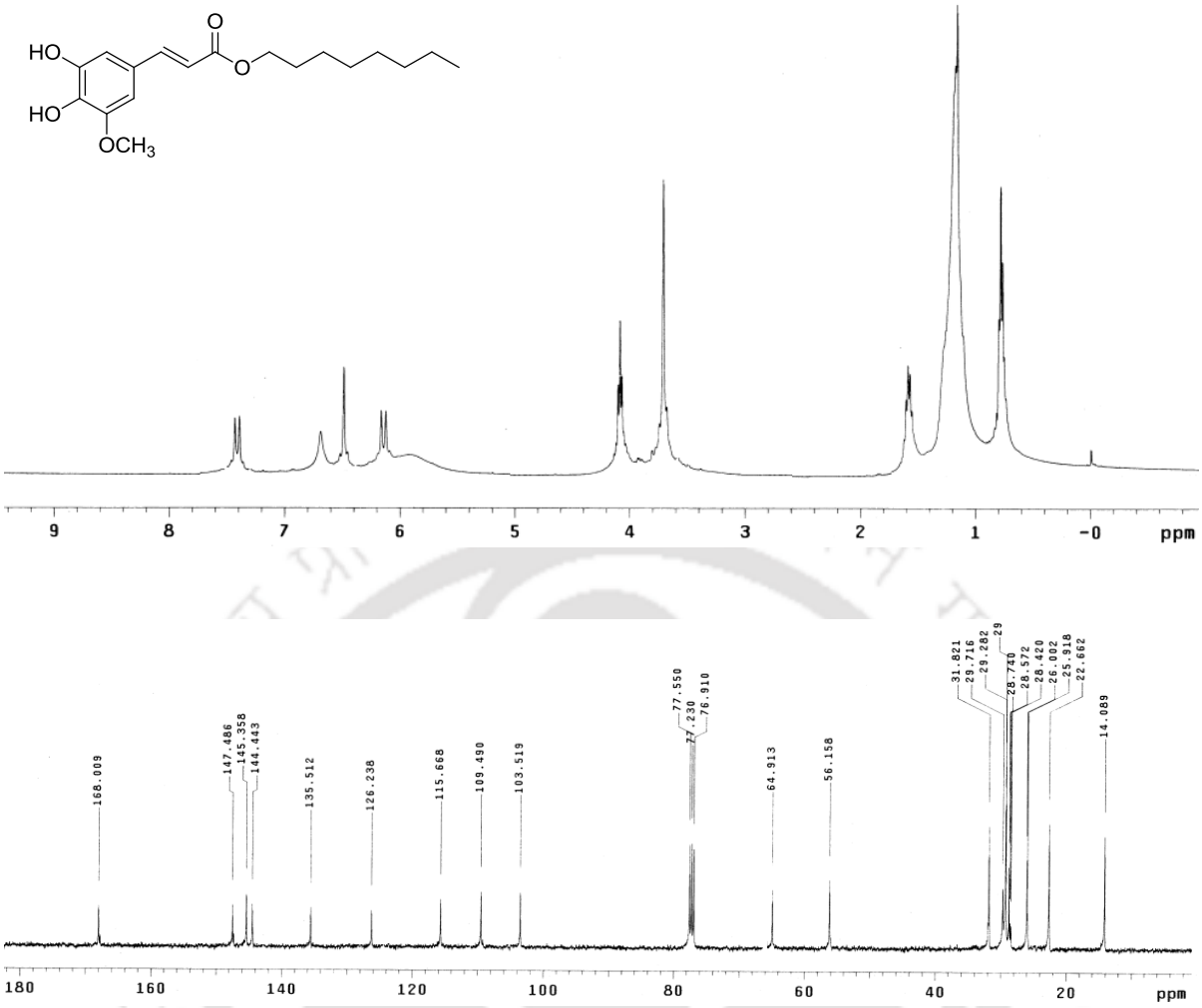

Figure 5.4.4: *^{1}H NMR and ^{13}C NMR of (E)-octyl 3-(3,4-dihydroxy-5-methoxyphenyl)acrylate* ***(8b)***

CHAPTER 6

$Zn(OTf)_2$ Catalyzed Chemoselective Esterification of Carboxylic Acids Usable for the PKC Activation and other Biological Applications

The present chapter demonstrates the utility of triphenylphosphine, iodine and a catalytic amount of $Zn(OTf)_2$ for chemoselective esterification/amidation of hydroxyl groups bearing, phenolic carboxylic acids with a library of alcohols and amines, respectively in higher yields. The activation of in-situ generated acyloxyphosphonium ion intermediate was the key step for esterification/amidation reactions. It also reveals that the acid sensitive protecting groups, internal and terminal alkynes and alkenes bearing both carboxylic acids and alcohols are highly stable under the optimised reaction conditions.

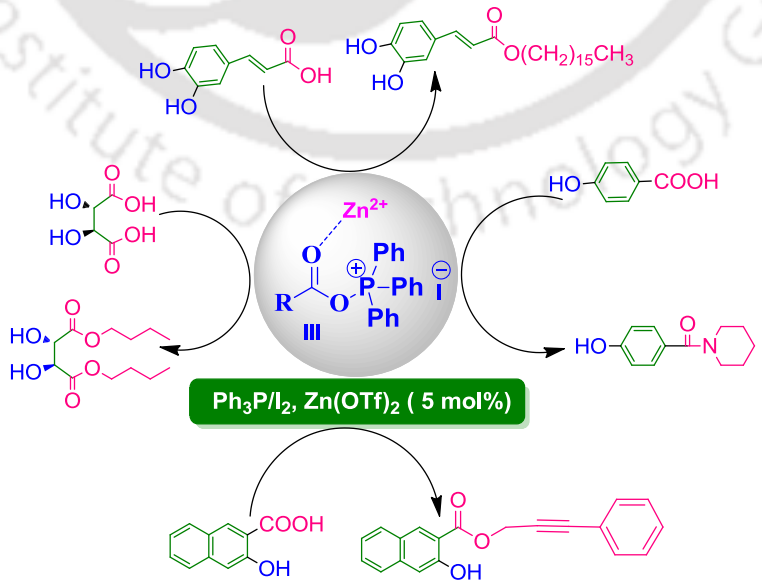

6.1. Background and Focus of the Present Work

Hydroxyl group bearing aliphatic and aromatic esters are immensely valuable compounds in the field of medicinal and pharmaceutical chemistry.[185a,b] Epicatechin gallate, epigallocatechin gallate, caffeic acid, and phenethyl esters are good examples of the hydroxyl group bearing biologically active esters (*Figure 6.1.1*).[186a-g] In addition, structurally complex esters including, phorbol esters, bryostatins, DAG-lactones and others also received importance in the cancer field as PKC modulators (*Figure 6.1.1).*[96,122,123] Chemoselective synthesis of these compounds in fewer steps using the regular esterification reaction conditions are exceedingly difficult because of the requirement of other functional group protection or the use of harsh reaction condition and/or a large excess of reactants.[186a-g] However, there are only few limited methods available in the literatures to achieve the synthesis of these complex esters in a mild and chemoselective/regioselective manner.

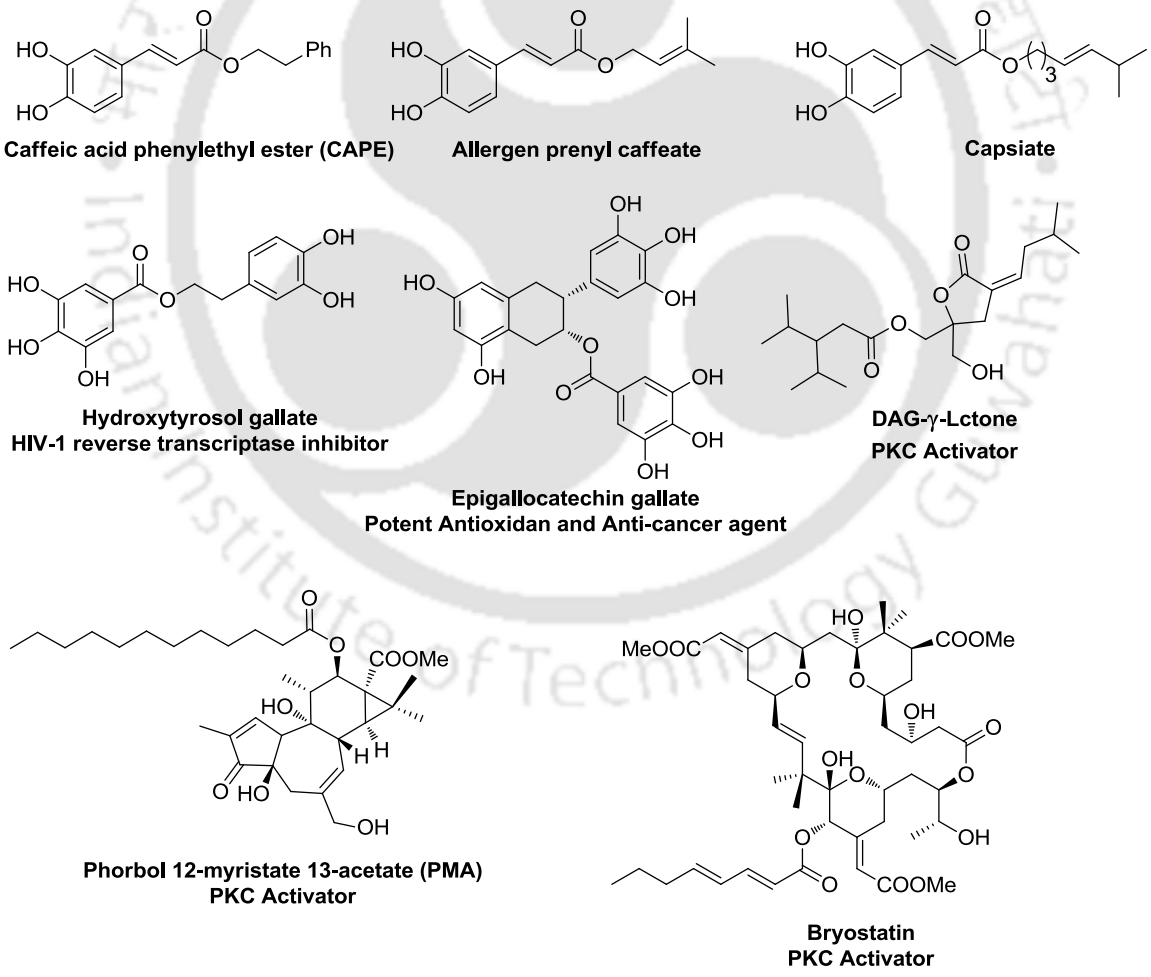

Figure 6.1.1: *Ester subunit contained some of the biologically active molecules*

In order to develop a mild and chemoselective esterification method, Robles and co-workers demonstrated a selective esterification method based on the Garegg−Samuelsson reaction conditions.[187] Zhang and co-workers reported the direct esterification/amidation of carboxylic acids with iodosodilactone coupling reagent in the presence of triphenylphosphine/4-dimethylaminopyridine (Ph_3P/DMAP) via in situ generated acyloxyphosphonium ion mechanism.[188] Earlier, Mukaiyama and co-workers also reported the esterification/amidation of carboxylic acids based on oxidative activation of Ph_3P by di(2-pyridyl)disulfide followed by in situ generated acyloxyphosphonium ion intermediate.[189] All these methods demonstrated in-situ activation of acids for the direct esterification/amidation. However, the activation is not always well enough for the complex substrates. Therefore, the key feature for further development of mild and selective esterification methods is that the acid should be activated to more reactive species.

In chapter 2-5, we described the synthesis of ester based DATs,[151] DAT-anionic phospholipids,[167] (hydroxymethyl)phenyl esters[159] and alkyl cinnamates[160] respectively, as C1 domain ligands. During the synthesis of these PKC modulators, we used DCC/DMAP reaction conditions for the esterification reaction. Unfortunately, we faced problems like chemo/regioselectivity, racemization, requirement of a large number of protecting groups, harsh reaction conditions, lower yield of products and longer reaction time. It is well documented that inversion of the stereochemistry has been observed in case of the Mitsunobu esterification.[190] Therefore, this method is also not suitable for the synthesis of some of these C1 domain modulators. Hence, there is a clear and unmet need to develop chem/regioselective esterification of hydroxyl groups bearing carboxylic acids to overcome these drawbacks in the synthesis of C1 domain modulators, as well as complex natural products. In an attempt to work out these problems, in this chapter we described a mild, highly efficient, and chemoselective esterification of the hydroxyl group bearing of carboxylic acids in the presence of Ph_3P, I_2 and a catalytic amount of $Zn(OTf)_2$ as an activator. We presumed that the reaction proceeds via in situ production of the zinc-coordinated acyloxyphosphonium ion intermediate, which might enhance the electrophilicity well enough to assist the intermolecular attack of alcohol or amine at a faster rate (within 3−5 h) to generate the corresponding ester/amide with good to excellent yield.

Synthesis of Esters— It is well known that the Lewis acid catalyzed esterification is extremely proficient due to the enhancement of electrophilicity of carboxylic acids and anhydrides.[106,107,191] Accordingly, substantial attention has been aimed at the investigation of a wide variety of Lewis acids such as $CoCl_2$, $InCl_3$, $TiCl_4$, $AgClO_4$, $ZnCl_2$, $CeCl_3$, $Yb(OTf)_3$, $HfCl_4{\cdot}(THF)_2$, and others for their role in esterification.[108-111] Recently, a catalytic amount of $Zn(OTf)_2$ was used for amide cleavage and esterification of β-hydroxyethylamides.[192] The $Zn(OTf)_2$ was also used for the microwave-irradiated esterification of simple acids and alcohols.[193] However, there is no previous report of zinc-catalyzed chemoselective esterification/amidation using Ph_3P/I_2. The chemoselective esterification of phenolic acids and alcohols has been successfully achieved by a few methods. However, the reaction conditions are either harsh, or their purifications are troublesome. [106,107,191] Whereas, the reported Lewis acid catalyzed esterifications for most of these phenolic acids/alcohols are very slow, and yields are poor to moderate only.[194,195]

We assumed that the combination of in situ generated carboxylic acid activation, followed by the Lewis acid activation would give us an otherwise unattainable enhanced reactivity. We selected caffeic acid (**1a**) and cetyl alcohol (**2a**) as a substrate for the model reaction, using Ph_3P (2.0 equiv), I_2 (2.0 equiv), a catalytic amount of (5 mol %) $Zn(OTf)_2$ in CH_3CN solvent at 60 °C (*scheme 6.1.1*). This led to the formation of the target ester **3aa** in 86% yield within 4 h. Encouraged by this positive results, the esterification reaction conditions were optimized by studying several Lewis acids, solvents, and at different temperature (*Table 6.1.1*).

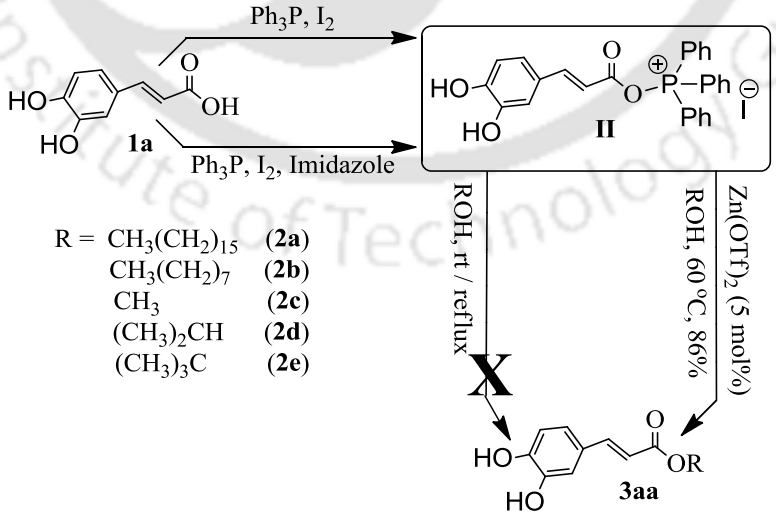

Scheme 6.1.1: *Model Reaction of Zn(OTf)$_2$-Catalyzed Esterification of Carboxylic Acids*

The best results were obtained in the presence of 5 mol % of Zn(OTf)$_2$ catalyst and CH_3CN as solvent. However, in the presence of lower amount of catalyst yields were poor *(Table 6.1.1, entries 1 and 2),* whereas there was no significant improvement in the yield at higher and lower temperature the reaction was sluggish (*Table 6.1.1, entry 4 and 5).* Exclusion of either Ph_3P/I_2 or Zn(OTf)$_2$ did not produce the desired ester (entries 6 and 7) with high yield.

Table 6.1.1: *Screening of Lewis Acids and Solvent System for the Esterification Reaction*[a]

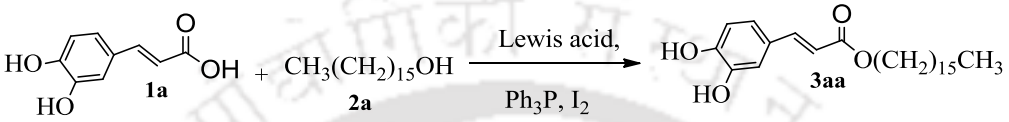

Entry	Lewis acid (mol%)	Phosphine/I_2	Solvent	Temp ($^\circ$C)	Time (h)	Yield (%)[c]
1	Zn(OTf)$_2$; (1)	Ph_3P/I_2	CH_3CN	100[b]	24	23
2	Zn(OTf)$_2$; (2)	Ph_3P/I_2	CH_3CN	80	12	41
3	**Zn(OTf)$_2$; (5)**	**Ph_3P/I_2**	**CH_3CN**	**60**	**4**	**86**
4	Zn(OTf)$_2$; (5)	Ph_3P/I_2	CH_3CN	80	4	87
5	Zn(OTf)$_2$; (5)	Ph_3P/I_2	CH_3CN	rt	24	ND
6	Zn(OTf)$_2$; (5)	-	CH_3CN	60	24	ND
7	-	Ph_3P/I_2	CH_3CN	60	24	ND
8	Zn(OTf)$_2$; (5)	Ph_3P/I_2	CH_2Cl_2	60[b]	48	26
9	Zn(OTf)$_2$; (5)	Ph_3P/I_2	THF	60	30	20
10	Zn(OTf)$_2$; (5)	Ph_3P/I_2	DMF	60	24	13
11	Zn(OTf)$_2$; (5)	Ph_3P/I_2	Toluene	60	24	10
12	$Zn(OAc)_2$; (5)	Ph_3P/I_2	CH_3CN	80	28	10
13	$ZnCl_2$; (5)	Ph_3P/I_2	CH_3CN	80	24	8
14	$Zn(ClO_4)_2 \cdot 6H_2O$; (5)	Ph_3P/I_2	CH_3CN	100[b]	24	7
15	$Cu(OTf)_2$; (5)	Ph_3P/I_2	CH_3CN	100[b]	20	6
16	$FeCl_3$; (5)	Ph_3P/I_2	CH_3CN	80	24	5

[a]*Performed with carboxylic acid (1.0 equiv), Ph_3P (2.0 equiv), I_2 (2.0 equiv), Lewis acid (1- 5 mol%) and alcohol (1.1 equiv) in dry acetonitrile.* [b]*Reactions were performed under the sealed tube conditions.* [c]*Isolated yield. ND: Not detectable.*

Thus, both Ph_3P/I_2 and Zn(OTf)$_2$ are indispensable for chemoselctive esterification of less reactive 3,4-dihydroxybenzoic acid. In addition, a set of solvents and Lewis acids was also studied and the obtained results were outlined in the Table 6.1.1. Therefore, Ph_3P/I_2 (2.0 equiv) and Zn(OTf)$_2$ (5 mol %) in CH_3CN solvent are the best reaction conditions at 60 $^\circ$C. We also observed that, in the presence of the lower amount of Ph_3P/I_2 (less than 2.0 equiv), the activated intermediate can suffer the attack of a second molecule of the acid to generate

significant amounts of anhydride and Ph_3PO.[114] Therefore, Ph_3P/I_2 (2.0 equiv) and $Zn(OTf)_2$ (5 mol %) in CH_3CN solvent are the best reaction conditions at 60 °C.

Table 6.1.2: *Esterification of Cinnamic Acids under Optimized Reaction Conditions*[a]

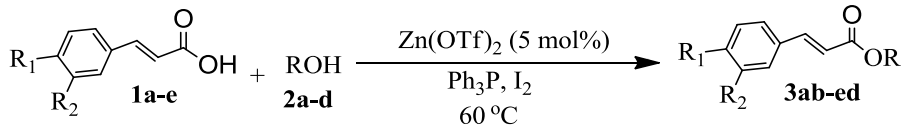

Entry	Acid	Alcohol	Time (h)	Product	Yield (%)[b]
1	**1a:** R_1 = OH, R_2= OH	**2b**	4	**3ab**	86
2	**1a:** R_1 = OH, R_2= OH	**2d**	5	**3ad**	70
3	**1a:** R_1 = OH, R_2= OH	**2e**	12	**3ae**	ND
4	**1b:** R_1 = OH, R_2= OMe	**2a**	4	**3ba**	86
5	**1b:** R_1 = OH, R_2= OMe	**2b**	4	**3bb**	86
6	**1b:** R_1 = OH, R_2= OMe	**2d**	5	**3bd**	73
7	**1c:** R_1 = OMe, R_2= OH	**2a**	4	**3ca**	86
8	**1c:** R_1 = OMe, R_2= OH	**2b**	4	**3cb**	86
9	**1c:** R_1 = OMe, R_2= OH	**2c**	3.5	**3cc**	90
10	**1c:** R_1 = OMe, R_2= OH	**2d**	5	**3cd**	73
11	**1d:** R_1 = OH, R_2= H	**2a**	3.5	**3da**	90
12	**1d:** R_1 = OH, R_2= H	**2b**	3.5	**3db**	90
13	**1d:** R_1 = OH, R_2= H	**2d**	5	**3dd**	73
14	**1e:** R_1 = H, R_2= OH	**2a**	3.5	**3ea**	90
15	**1e:** R_1 = H, R_2= OH	**2b**	3.5	**3eb**	90
16	**1e:** R_1 = H, R_2= OH	**2c**	3.5	**3ec**	90
17	**1e:** R_1 = H, R_2= OH	**2d**	5	**3ed**	75

[a]*Performed with carboxylic acid (1.0 equiv.), Ph_3P (2.0 equiv.), I_2 (2.0 equiv.), $Zn(OTf)_2$ (5 mol %), and alcohol (1.1 equiv.) in dry acetonitrile.* [b]*Isolated yield. ND: Not detectable.*

The scope of the esterification/amidation reaction was tested by analysing the reactivity of various carboxylic acids, alcohols, and amines under these optimized reaction conditions. We first performed the esterification of cinnamic acids (**1a**–**e**) with primary (**2a**–**c**), secondary (**2d**), and tertiary alcohol (**2e**). The esterification of caffeic acids with primary alcohols produced the desired ester with good to excellent yields (86–90%). The reaction with the secondary alcohol (**2c**) resulted moderate to good yields (70–75%) only, whereas failed with the hindered tertiary alcohol (*Table 6.1.2*). The chemoselectivity was investigated by using various hydroxyl group bearing aromatic and aliphatic carboxylic acids and different types of alcohols (*Table 6.1.3, entries 1–18*). Except for secondary alcohol and gallic acid, the overall yields were generally good. Similar results were also obtained for the esterification aliphatic acids with secondary benzylic alcohols (*Table 6.1.3, entries 17 and 18*). The α-hydroxycarboxylic acid (L-tartaric acid) also produced an excellent yield of

98%.[105] Exclusively regioselective esterification at the primary alcohol over secondary alcohol was observed for an unsymmetrical diol (*Table 6.1.3, entry 11*).

Similarly, selective esterification of aliphatic acid in the presence of aromatic acid was also observed (*Table 6.1.3, entry 12*). It is well documented that acid sensitive protecting groups contained carboxylic acids/alcohols do not result the desire esters under Lewis acid conditions with good yield.[196] Consequently, to investigate the stability of deferent protecting groups under these optimized reaction conditions, we performed esterification with Ts-, Boc-, Tr-, TBDPS-, TBDMS-, and acetonide- protecting groups of acids/alcohols.

Table 6.1.3: *Chemoselective Esterification of Carboxylic Acids and Alcohols under Optimized Reaction Conditions*[a]

Entry	Acid	Alcohol	Time (h)	Product	Yield (%)[b]
1	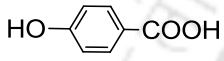	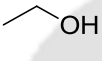	4	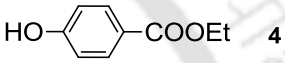 **4**	91
2	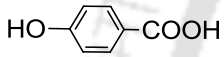	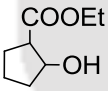	5	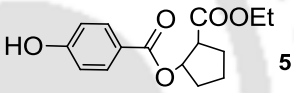 **5**	69
3	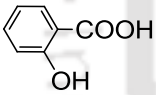	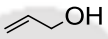	4	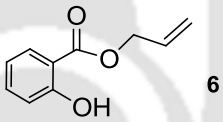 **6**	87
4	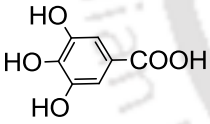	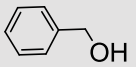	4	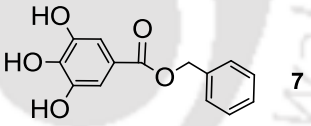 **7**	65
5	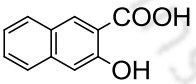	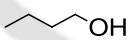	4	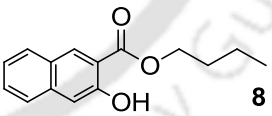 **8**	90
6	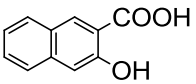	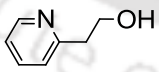	4	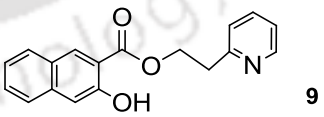 **9**	88
7	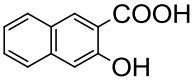	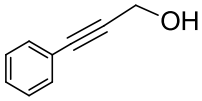	4	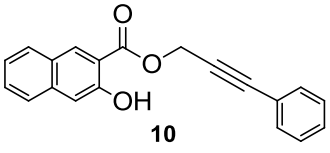 **10**	81
8	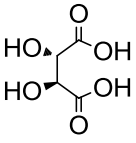	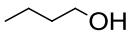	4	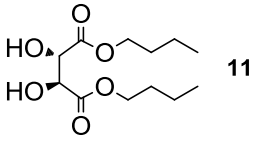 **11**	98[c]

Continued...

9	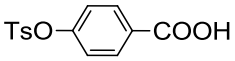	**2c**	4	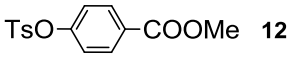 **12**	89
10	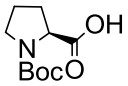	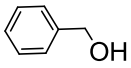	4	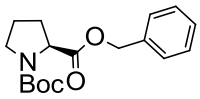 **13**	89
11	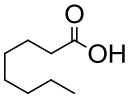	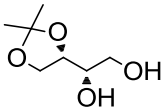	3.5	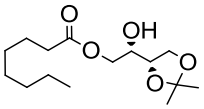 **14**	97
12	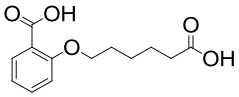	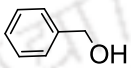	4	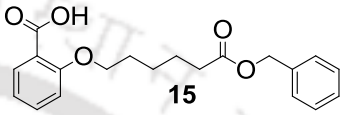 **15**	96
13	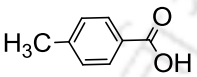	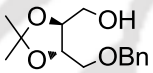	4	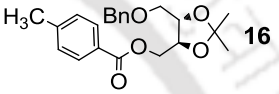 **16**	95
14	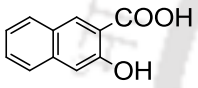	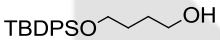	4	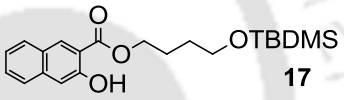 **17**	97
15	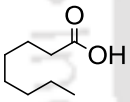	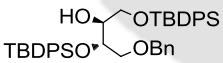	5	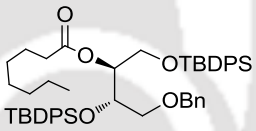 **18**	75
16	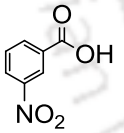	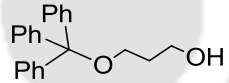	4	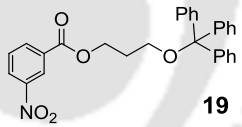 **19**	98
17	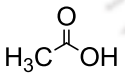	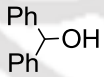	6	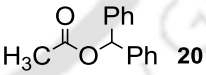 **20**	61
18	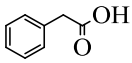		6	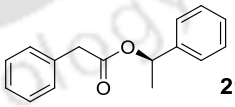 **21**	70

[a]Performed with carboxylic acid (1.0 equiv.), Ph_3P (2.0 equiv), I_2 (2.0 equiv.), $Zn(OTf)_2$ (5 mol %), and alcohol (1.1 equiv.) in dry acetonitrile. [b]Isolated yield. [c]Ph_3P (4.0 equiv.), I_2 (4.0 equiv.), $Zn(OTf)_2$ (10 mol %), and alcohol (2.2 equiv.) in dry acetonitrile

We found excellent yields (89–97%) of the corresponding esters without any deprotection/decomposion of protecting groups (*Table 6.1.3, entries 9–11 and 13–16).* In the presence of $Zn(OTf)_2$, both electron-donating and electron-withdrawing functional groups bearing acids produced the desired esters in excellent yields (*Table 6.1.4, entries 1–5*). As

expected, the reactions with secondary alcohols were sluggish. However, both terminal and internal alkenes and alkynes bearing alcohols also selectively produced esters without the addition of I_2 over these multiple bonds (*Table 6.1.3, entries 3 and 7; Table 6.1.4, entries 1, 2 and 4).*

Table 6.1.4: *Substrate Scope of Esterification under Optimized Reaction Conditions*[a]

Entry	Acid	Alcohol	Time (h)	Product	Yield (%)[b]
1	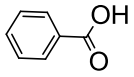	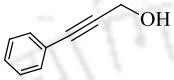	3.5	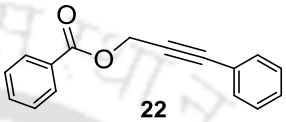 **22**	96
2	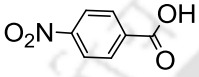		3.5	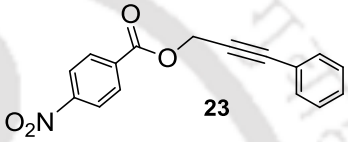 **23**	98
3	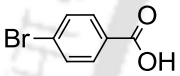	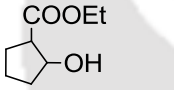	5	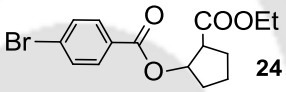 **24**	76
4	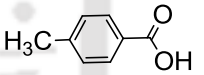	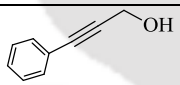	4	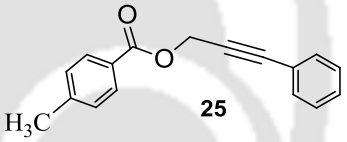 **25**	95
5	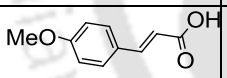 **2b**		4	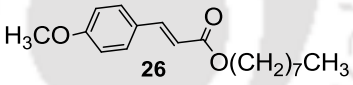 **26**	93

[a] *Performed with carboxylic acid (1.0 equiv.), Ph_3P (2.0 equiv.), I_2 (2.0 equiv.), Zn(OTf)$_2$ (5 mol %), and alcohol (1.1 equiv.) in dry acetonitrile.* [b] *Isolated yield.*

In addition, carbonyl, nitro, bromo, and methoxy groups of carboxylic acids and alcohols were also highly stable under optimized reaction condition. The results clearly showed that the presence of Zn(OTf)$_2$ in the reaction medium surmounts the direct effect of these functional groups on esterification. After that, we decided to extend the applicability of this method towards the synthesis of biologically active molecules/intermediates.

The esterification of saturated fatty acids (palmitic acid and octanoic acid), unsaturated fatty acid (oleic acid), (+)-menthol, cholesterol, indole-3-propionic acid, quinoline-2-carboxylic (*Table 6.1.5, entries 1–9*), and gallic acid (*Table 6.1.3, entry 4*) resulted in a corresponding ester with moderate to excellent yield, which is very important in

the synthesis of complex molecules. This could be due to the mild reaction conditions, avoiding possible decomposition or simultaneous reactions with other functional groups within the same molecule.

Table 6.1.5: *Synthesis of Biologically Active Esters*[a]

Entry	Acid	Alcohol	Time (h)	Product	Yield (%)[b]
1	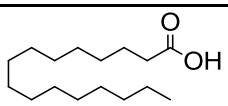	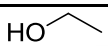	3.5	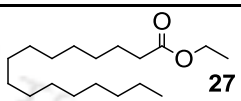 **27**	98
2	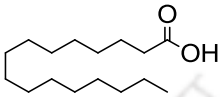	2d	5	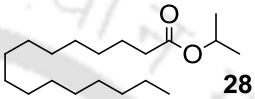 **28**	77
3	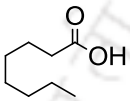	2e	6	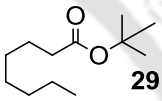 **29**	20
4	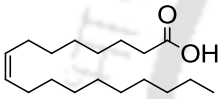	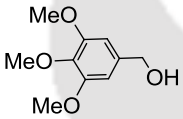	3.5	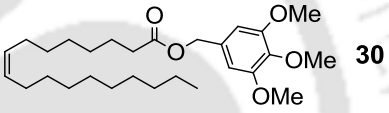 **30**	98
5	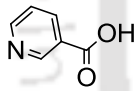	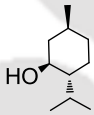	5	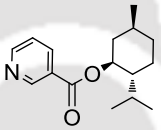 **31**	73
6	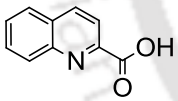	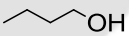	3.5	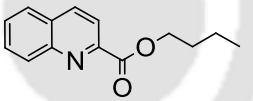 **32**	96
7	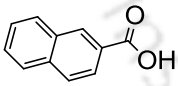	Cholesterol	5	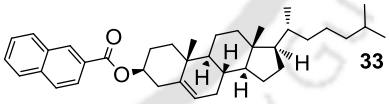 **33**	72
8	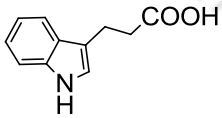	**2a**	4	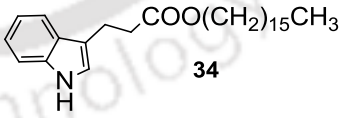 **34**	97
9	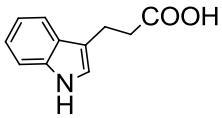	**2d**	5	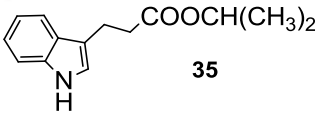 **35**	80

[a]*Performed with carboxylic acid (1.0 equiv.), Ph_3P (2.0 equiv.), I_2 (2.0 equiv.), $Zn(OTf)_2$ (5 mol %), and alcohol (1.1 equiv.) in dry acetonitrile.* [b]*Isolated yield.*

The esterification yields were higher for primary alcohols compared to secondary and tertiary alcohols as expected. Significantly, when chiral carboxylic acids and alcohols were

used, retention of the stereochemistry was also observed. The chiral ester **13** and **21** showed >99% ee as measured by HPLC.

To extend the use of this methodology beyond esterification, we tested amidation reaction. The amidation of various carboxylic acids with *n*-butylamine, benzylamine, (pyridin-2-yl)methanamine, *N′*,*N′*-dimethylethane-1,2-diamine and piperidine under the optimized reaction condition resulted the desired amide in 75–98% yields (*Table 6.1.6, entries 1–8*).

Table 6.1.6: *Amidation of Carboxylic Acids under Optimized Reaction Conditions*[a]

Entry	Acid	Amine	Time (h)	Product	Yield (%)[b]
1	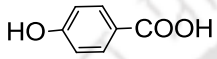	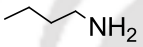	4	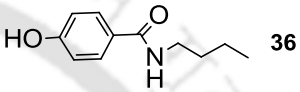 **36**	85
2	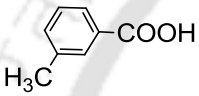	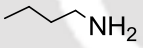	4	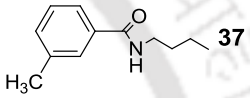 **37**	94
3	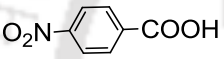	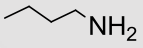	4	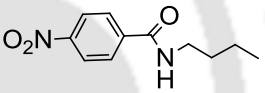 **38**	98
4	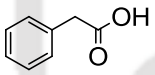	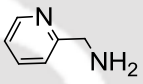	4	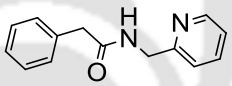 **39**	95
5	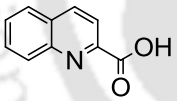	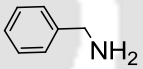	4	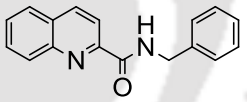 **40**	95
6	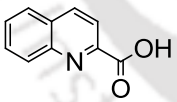	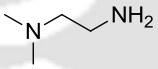	4	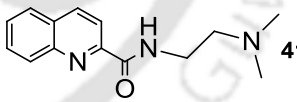 **41**	98
7	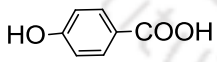		6	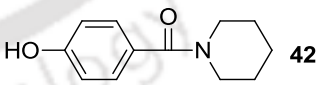 **42**	75
8	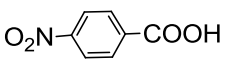		6	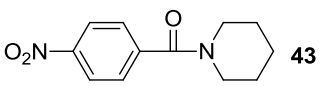 **43**	78

[a]*Performed with carboxylic acid (1.0 equiv.), Ph_3P (2.0 equiv.), I_2 (2.0 equiv.), $Zn(OTf)_2$ (5 mol %), and amine (1.1 equiv.) in dry acetonitrile.* [b]*Isolated yield.*

Therefore, this reaction condition is a good alternative to the methods known for amidation. It is worth noting that adopted reaction condition worked well for several

heterocyclic substrates *(Table 6.1.3, entries 6 and 10; Table 6.1.5, entries 5, 6, 8, and 9; Table 6.1.6, entries 4–8).*

The results obtained in our study suggest that the reaction between Ph_3P and I_2 yielded the triphenylphosphonium iodide intermediate (**I**), and subsequent attack of carboxylic acid generates the acyloxyphosphonium ion intermediate (**II**), in accordance with the Garegg−Samuelsson reaction mechanism,[187,197a,b] whereas addition of $Zn(OTf)_2$ to intermediate (**II**) proposed the formation of zinc-coordinated active intermediate (**III**) as reported earlier.[192] This could enhance the electrophilicity toward a carbonyl center of acyloxyphosponium ion intermediate (**III**) and facilitate the nucleophilic attack of the alcohol.

Figure 6.1.2: *Possible Reaction Mechanism for the Zn(OTf)$_2$-Mediated Esterification*

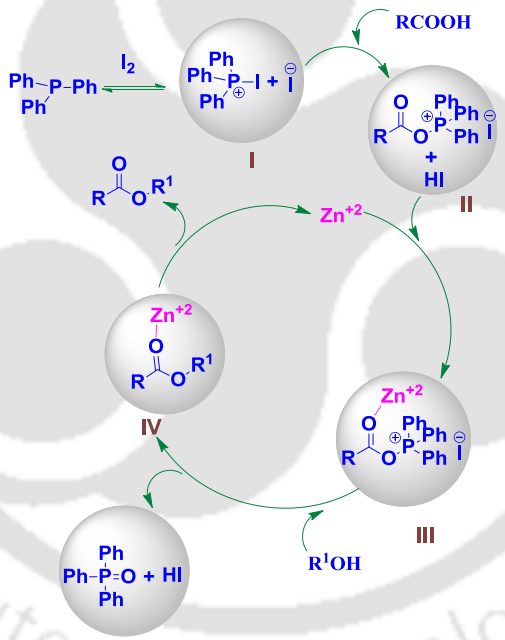

The downfield shift of the ^{31}P NMR signal ($\Delta\delta$ = 3.0 ppm) and the ^{13}C NMR signal for the C=O group ($\Delta\delta$ = 0.5 ppm), after addition of $Zn(OTf)_2$ to the intermediate **II**, indicate the formation of intermediate **III**. These spectral changes also propose the coordination of zinc ion to the C=O group of intermediate III. This highly hindered intermediate **III** is mainly responsible for the selectivity of esterification using this method.

Table 6.1.7: *^{31}P and ^{13}C Chemical Shifts for esterification reaction intermediates/species*

		^{31}P Chemical Shifts		^{13}C Chemical Shifts	
Entry	Species	δ^a (ppm)	Reported δ^a (ppm)	Species	δ^a (ppm)
1	Ph_3P	-4.29	-4.25	**II**	175.401
2	$Ph_3P{\bullet}I_2$	-15.76	-15.77	**III**	175.916
3	**II**	48.22	–	**3aa**	166.707
4	**III**	51.19	–	–	–
5	$Ph_3P{=}O$	30.68	30.60	–	–

[a]Chemical shifts

When this intermediate suffers attack by more hindered secondary and tertiary alcohols, a bigger steric repulsion between the ligands of phosphine and substituent of the alcohols minimizes the probability of nucleophilic addition.[198-200] Under this optimized reaction condition, the phenolic hydroxyl group present on either substrate acts as inert spectators even though Ph_3P and I_2 have been largely employed for the synthesis of iodoalkanes. Therefore, the reaction mechanism rules out phenolic carbons as substrate for S_N2-type reactions, while the generation of the nucleophilic species due to deprotection, a relatively weak base, secures that carboxylate rather than phenolates are formed, in the presence of stoichiometric amounts of reagents. This could be the main reason behind the selectivity of esterification.

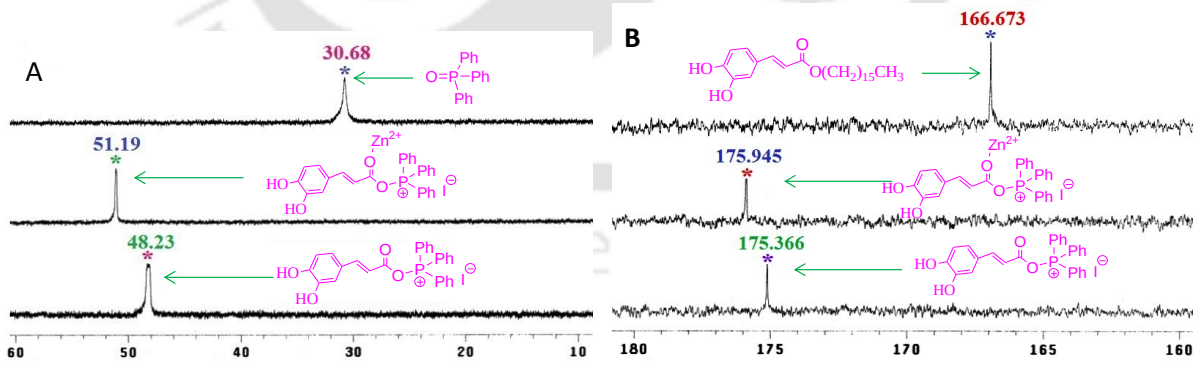

Figure 6.1.3: *Monitoring the progress of reaction by ^{31}P NMR (A) and ^{13}C NMR spectra (B) in $CDCl_3$.*

Conclusion

In conclusion, we have developed $Zn(OTf)_2$ catalysed a facile and highly chemoselective esterification/amidation method for aromatic and aliphatic carboxylic acids in the presence of triphenylphosphine, and I_2. In particular, the utility of zinc ion assisted activation of acyloxyphosphonium ion intermediate has been demonstrated. In addition, we showed regioselective esterification of unsymmetrical alcohols as well as regioselective esterification of aliphatic carboxylic acids over aromatic carboxylic acids, which could be very important in the synthesis of polyfunctionalized substrates. We have also successfully synthesized most of the ester based PKC-C1 domain regulators in chapters 2-5 with high yields. This facile and efficient method will serve as a useful alternative to the existing esterification methods and will decrease the burden of protecting groups in the synthesis of several complex molecules, which represents an important objective in modern organic chemistry.

6.2. Experimental Section

6.2.1. Instrumentations and Characterization

As shown in chapter 2 section 2.2.1

6.2.2. General Procedure for the $Zn(OTf)_2$ Catalysed Esterification/Amidation of Carboxylic Acids: To a stirring solution of I_2 (2.0 equiv) and triphenylphosphine (2.0 equiv) in dry acetonitrile (10 mL) was added carboxylic acid (1.0 equiv) under a N_2 atmosphere, and the reaction mixture was stirred for 10 min, then (5 mol%) of $Zn(OTf)_2$ was added. Stirring was continued for 30 min at 60 $^{\circ}$C, and then alcohol/amine (1.1 equiv) in dry acetonitrile was added. After completion of the reaction (monitored by TLC), the mixture was cooled to room temperature and the solvent was removed under reduced pressure. The residue was dissolved in ethylacetate and washed with saturated $NaHCO_3$ followed by brine solution. The organic layer was dried over anhydrous Na_2SO_4 and concentrated under reduced pressure. Column chromatography with silica gel and a gradient solvent system of ethylacetate to hexane yielded the target compound. Title compound were properly characterized by NMR, HRMS (ESI) and Melting points.

6.3. Spectral Characterization of the New Compounds

2-(Pyridin-2-yl)ethyl 3-hydroxynaphthanele-2-carboxylate (9): Yellow solid (69 mg, 88%); m.p. 95-97 °C; ^{1}H NMR (400 MHz, $CDCl_3$): δ_{ppm} 10.42 (br, s, 1H), 8.57 (d, 1H, J = .8 Hz), 8.35 (s, 1H), 7.73 (d, 1H, J = 8.4 Hz), 7.65-7.61 (m, 2H), 7.45 (t, 1H, J = 7.4 Hz), 7.30-7.23 (m, 3H), 7.17 (t, 1H, J = 6.3 Hz), 4.79 (t, 2H. J = 6.6 Hz), 3.31 (t, 2H, J = 6.8 Hz); ^{13}C NMR (100 MHz, $CDCl_3$): δ_{ppm} 169.7, 157.6, 156.3, 149.6, 137.9, 136.8, 132.5, 129.3, 129.2, 127.1, 126.3, 124.0, 123.7, 122.0, 114.4, 111.7, 64.8, 37.2; HRMS (ESI) Calcd for $C_{18}H_{16}NO_3$ $[M+H]^+$: 294.1130, Found: 294.1131.

3-Phenylprop-2-ynyl 3-hydroxynaphthanele-2-carboxylate (10): Gray color solid (65 mg, 81%); m.p.72-73 °C; ^{1}H NMR (400 MHz, $CDCl_3$): δ_{ppm} 10.27 (br, s, 1H), 8.58 (s, 1H), 7.82 (d, 1H, J = 8.4 Hz), 7.68 (d, 1H, J = 8.4 Hz), 7.52-7.48 (m, 3H), 7.36-7.31 (m, 5H), 5.25 (s, 2H); ^{13}C NMR (100 MHz, $CDCl_3$): δ_{ppm} 169.4, 156.4, 138.2, 133.0, 132.2, 129.5, 129.2, 128.5, 127.2, 126.5, 124.2, 122.1, 113.9, 111.9, 87.6, 82.4, 54.1; HRMS (ESI) Calcd for $C_{20}H_{15}O_3$ $[M+H]^+$: 303.1021, Found: 303.1023.

(S)-2-Hydroxy-2-((S)-2,2-dimethyl-1,3-dioxolane-4-yl)ethyl octanoate (14): Yellow oil (97 mg, 97%); $[\alpha]^{20}_D$ = +5.2° (0.2 c, CH_2Cl_2) ; ^{1}H NMR (400 MHz, $CDCl_3$): δ_{ppm} 5.14-5.10 (m, 1H), 4.27-4.18 (m, 2H), 4.12-4.07 (m, 1H), 3.99-3.95 (m, 1H), 3.74-3.70 (m, 1H), 2.30 (t, 2H, J = 7.4 Hz), 1.60-1.53 (m, 2H), 1.37 (s, 3H), 1.29 (s, 3H), 1.25-1.20 (br s, 8H), 0.82 (t, 3H, J = 6.6 Hz); ^{13}C NMR (100 MHz, $CDCl_3$): δ_{ppm} 173.5, 110.0, 74.6, 70.8, 65.7, 62.9, 34.3, 31.8, 29.2, 29.1, 26.3, 25.5, 25.1, 22.8, 14.2; HRMS (ESI) Calcd for $C_{15}H_{28}O_5K^+$ $[M+K]^+$: 327.1574, Found: 327.1577.

2-(5-((benzyloxy)carbonyl)pentyloxy)benzoic acid (15): Yellow solid (71mg, 96%); m.p. 82-83 °C; ^{1}H NMR (400 MHz, $CDCl_3$): δ_{ppm} 10.83 (s, 1H), 7.82 (d, 1H, J = 8.0 Hz), 7.45 (t, 1H, J = 7.0 Hz), 7.38-7.32 (m, 5H), 6.98 (d, 1H, J = 8.4 Hz), 6.87 (d, 1H, J = 7.0 Hz), 5.12 (s, 2H), 4.33 (t, 2H, J = 6.4 Hz), 2.40 (t, 2H, J = 7.4 Hz), 1.83-1.78 (m, 2H), 1.76-1.72 (m, 2H), 1.52-1.4 (m, 2H); ^{13}NMR (100 MHz, $CDCl_3$): δ_{ppm} 173.3, 170.2, 156.6, 135.9, 135.7, 129.8, 128.6, 128.3, 128.2, 119.1, 117.6, 112.5, 66.2, 65.1, 34.1, 29.7, 28.3, 25.5, 24.5; IR (neat) cm^{-1}; 3083, 2985, 1731, 1698, 1614, 1524, 1416;HRMS (ESI): Calcd for $C_{20}H_{23}O_5$ $[M+H]^+$: 343.1545, Found: 343.1543.

((4S,5S)-5-((benzyloxy)methyl)-2,2-dimethyl-1,3-dioxolan-4-yl)methyl 4-methylbenzoate (16): Colorless oil (129 mg, 95%); $[\alpha]^{20}_D$ = +9.2 ° (0.3 c, CH_2Cl_2); ^{1}H NMR (400 MHz, $CDCl_3$): δ_{ppm} 7.91 (d, 2H, J = 8.0 Hz), 7.40-7.35 (m, 2H), 7.32-7.18 (m, 5H), 4.58 (s, 2H), 4.52 (dd, 1H, J = 3.6 Hz), 4.36 (dd, 1H, J = 5.2 Hz), 4.22-4.18 (m, 1H), 4.16-4.12 (m, 1H), 3.69-3.61 (m, 2H), 2.60 (s, 3H), 1.44 (s, 6H); ^{13}C NMR (100 MHz, $CDCl_3$): δ_{ppm} 167.3, 140.6, 137.9, 132.3, 131.8, 130.8, 129.3, 128.6, 127.9, 127.8, 125.9, 110.1, 76.9, 76.8, 73.8, 70.5, 64.4, 27.2, 21.9; HRMS (ESI) Calcd for $C_{22}H_{26}O_5Na^+$ $[M+Na]^+$:393.1678, Found: 393.1678.

4-[Tert-butyldimethylsilyl)oxy]butyl 3-hydroxynapthalene-2-carboxylate (17): Light yellow solid (96 mg, 97%); m.p.118-120 °C; ^{1}H NMR (400 MHz, $CDCl_3$): δ_{ppm} 8.57 (s, 1H), 7.93 (d, 1H, J = 8.4 Hz), 7.78 (d, 1H, J = 8.4 Hz), 7.55 (t, 2H, J = 7.6 Hz), 7.43 (s, 2H), 4.96-4.90 (m, 2H), 2.67-2.57 (m, 2H), 1.86-1.78 (m, 2H), 1.47-1.39 (m, 2H), 0.89 (s, 9H), 0.05 (s, 6H); ^{13}C NMR (100 MHz, $CDCl_3$): δ_{ppm} 170.4, 160.5, 149.4, 138.8, 136.8, 129.8, 129.2, 127.2, 125.6, 115.7, 110.4, 63.3, 56.1, 29.5, 28.7, 26.7, 26.3, 26.2, 18.6, 15.1; HRMS (ESI): Calcd for $C_{21}H_{31}O_4Si$ $[M+H]^+$: 375.1992, Found: 375.1991.

2,2,10,10-Tetramethyl-5-(phenoxymethyl)-3,3,9,9-tetraphenyl-4,8-dioxa-3,9-disilaundecan-6-yl octanoate (18): Clear viscous oil (208 mg, 75%); $[\alpha]^{20}_D$ = +19.5 ° (0.2 c, CH_2Cl_2); ^{1}H NMR (400 MHz, $CDCl_3$): δ_{ppm} 7.65-7.62 (m, 10H), 7.42-7.30 (m, 10H), 7.28-7.23 (m, 5H), 5.34-5.30 (m, 1H), 4.58 (dd, 2H, J = 11.6, 11.6 Hz), 3.88-3.81 (m, 2H), 3.78-3.74 (m, 1H), 2.21 (t, 2H, J = 7.4 Hz), 1.60-1.53 (m, 2H), 1.25 (br s, 10H), 1.02 (s, 18H), 0.86 (t, 3H, J = 6.4 Hz); ^{13}C NMR (100 MHz, $CDCl_3$): δ_{ppm} 173.3, 138.7, 135.8, 135.7, 133.6, 129.9, 128.4, 127.7, 78.4, 73.4, 63.2, 62.3, 34.5, 31.8, 29.9, 29.3, 29.1, 27.0, 25.1, 22.8, 19.4, 14.3; HRMS (ESI): Calcd for $C_{51}H_{66}O_5Si_2Na^+$ $[M+Na]^+$: 837.4346, Found: 837.4347.

3-(Trityloxy)propyl 3-nitrobenzoate (19): White solid (137 mg, 98%); m.p. 85-87 °C; ^{1}H NMR (400 MHz, $CDCl_3$): δ_{ppm} 8.64 (s, 1H), 8.23 (d, 1H, J = 8.0 Hz), 8.16 (d, 1H, J = 7.6 Hz), 7.42-7.34 (m, 6H), 7.21-7.09 (m, 10H), 4.45 (t, 2H, J = 6.2 Hz), 3.22 (t, 2H, J = 5.8 Hz), 2.00 (m, 2H); ^{13}C NMR (100 MHz, $CDCl_3$): δ_{ppm} 164.4, 148.2, 147.0, 144.5, 144.1, 135.3, 132.1, 129.6, 128.8, 128.7, 128.0, 127.9, 127.8, 127.3, 127.2, 127.0, 126.9, 124.5, 86.7, 63.3, 59.7, 29.3; HRMS (ESI): Calcd for $C_{29}H_{25}NO_5Na^+$ $[M+Na]^+$: 490.1630, Found: 490.1633.

2-(Ethoxycarbonyl)cyclopentyl 4-bromobenzoate (24): Clear oil (65 mg, 76%); ^{1}H NMR (400 MHz, $CDCl_3$): δ_{ppm} 7.86-7.79 (m, 2H), 7.56-7.46 (m, 2H), 5.58-5.53 (m, 1H), 4.15 (q, 2H, J = 7.2 Hz), 2.97-2.92 (m, 1H), 2.18-2.09 (m, 2H), 1.58-1.78 (m, 4H), 1.23 (t, 3H, J = 7.2 Hz); ^{13}C NMR (100 MHz, $CDCl_3$): δ_{ppm} 174.1, 165.4, 131.8, 131.2, 129.4, 128.2, 79.4, 60.9, 50.7, 32.8, 29.0, 23.7, 14.3; HRMS (ESI): Calcd for $C_{15}H_{17}BrO_4Na^+$ $[M+Na]^+$: 363.0208, Found: 363.0208.

3-Phenylprop-2-ynyl 4-methylbenzoate (25): White solid (87 mg, 95%); m.p. 80-82 $^\circ$C; ^{1}H NMR (400 MHz, $CDCl_3$): δ_{ppm} 7.90 (d, 2H, J = 8.0 Hz), 7.39-7.36 (m, 2H), 7.31 (t, 2H, J = 7.4 Hz), 7.22-7.20 (m, 1H), 7.17-7.13 (m, 2H), 5.03 (s, 2H), 2.54 (s, 3H); ^{13}C NMR (100 MHz, $CDCl_3$): δ_{ppm} 166.9, 140.7, 132.5, 132.1, 131.9, 131.0, 129.1, 128.9, 128.5, 125.9, 122.4, 86.6, 83.4, 53.2, 21.9; HRMS (ESI) Calcd for $C_{17}H_{14}O_2Na^+$ $[M+Na]^+$: 273.0891, Found: 273.0891.

(Z)-3,4,5-Trimethoxybenzyl octadec-8-enoate (30): Yellow oil (80 mg, 98%); ^{1}H NMR (400 MHz, $CDCl_3$): δ_{ppm} 6.51 (s, 2H), 5.26-5.25 (m, 2H), 4.96 (s, 2H), 3.78 (s, 6H), 3.75 (s, 3H), 2.30-2.26 (m, 2H), 1.93-1.92 (m, 4H), 1.57-1.55 (m, 2H), 1.22-1.18 (br s, 20H), 0.80 (t, 3H, J = 6.4 Hz); ^{13}C NMR (100 MHz, $CDCl_3$): δ_{ppm} 173.7, 153.4, 131.8, 130.1, 129.8, 105.5, 66.4, 60.9, 56.2, 34.4, 32.0, 31.0, 29.8, 29.6, 29.4, 29.3, 27.3, 25.1, 22.8, 14.2; HRMS (ESI): Calcd for $C_{28}H_{46}O_5Na^+$ $[M+Na]^+$: 485.3243, Found: 485.3245.

Hexadecyl 3-(1H-indol-3-yl)propanoate (34): Crystalline white solid (106 mg, 97%); m.p.80-82 $^\circ$C; ^{1}H NMR (400 MHz, $CDCl_3$): δ_{ppm} 8.02 (br s, 1H), 7.61 (d, 1H, J = 8.0 Hz), 7.35 (d, 1H, J = 8.0 Hz), 7.19 (t, 1H, J = 7.4 Hz), 7.12 (t, 1H, J = 7.4 Hz), 7.01 (s, 1H), 4.06 (t, 2H, J = 6.8 Hz), 3.10 (t, 2H, J = 7.4 Hz), 2.72 (t, 2H, J = 7.8), 1.60-1.53 (m, 4H), 1.29-1.22 (br s, 24H), 0.88 (t, 3H, J = 6.6 Hz); ^{13}C NMR (100 MHz, $CDCl_3$): δ_{ppm} 173.8, 136.5, 127.3, 122.0, 121.6, 119.3, 118.8, 114.9, 111.3, 63.0, 35.2, 32.9, 32.1, 29.9, 29.7, 29.6, 29.5, 29.4, 28.8, 26.1, 25.9, 22.9, 20.9, 14.3; HRMS (ESI): Calcd for $C_{27}H_{43}NO_2Na^+$ $[M+Na]^+$: 436.3191, Found: 436.3190.

Isopropyl 3-(1H-indol-3-yl)propanoate (35): Colorless oil (49 mg, 80%); ^{1}H NMR (400 MHz, $CDCl_3$): δ_{ppm} 8.03 (br s, 1H), 7.60 (d, 1H, J = 8.0 Hz), 7.30 (d, 1H, J = 8.0 Hz), 7.15 (t, 1H, J = 7.4 Hz), 7.10 (t, 1H, J = 7.4 Hz), 6.94 (s, 1H), 5.04-4.98 (m, 1H), 3.08 (t, 2H, J = 7.8 Hz), 2.67 (t, 2H, J = 7.8 Hz), 1.20 (d, 6H, J = 6.4 Hz); ^{13}C NMR (100 MHz, $CDCl_3$): δ_{ppm}

173.3, 136.4, 127.3, 122.0, 121.6, 119.3, 118.8, 114.9, 111.3, 67.8, 35.5, 21.9, 20.8; HRMS (ESI): Calcd for $C_{14}H_{18}NO_2$ $[M+H]^+$: 232.1338, Found: 232.1339.

6.4. ^{31}P and ^{13}C-NMR Titration-Spectra for the Zn(OTf)$_2$ Catalyzed Esterification Reaction.

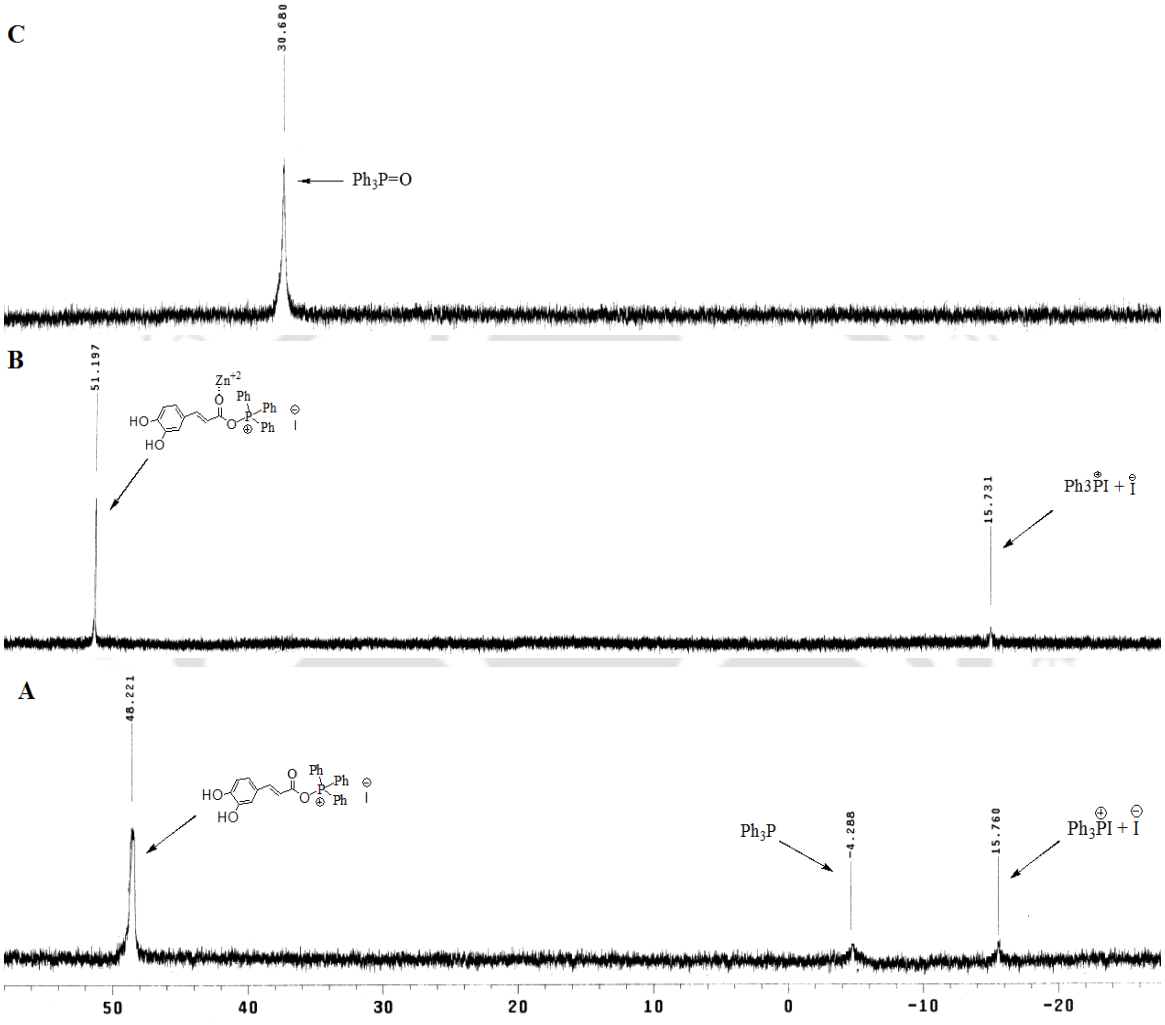

Figure 6.4.1: *Monitoring the progress of the esterification reaction between the carboxylic acid (**1a**) and alcohol (**2a**) in the presence of PPh$_3$, I$_2$ and a catalytic amount of Zn(OTf)$_2$by ^{31}P-NMR in CDCl$_3$; (A) 10 min after addition of **1a** to the stoichiometric mixture of Ph$_3$P and I$_2$; (B) 30 min after addition of Zn(OTf)$_2$ to the mixture of **1a**, Ph$_3$P and I$_2$; (C) 4 h after addition of **2a** to the mixture of Zn(OTf)$_2$, **1a**, Ph$_3$P and I$_2$.*

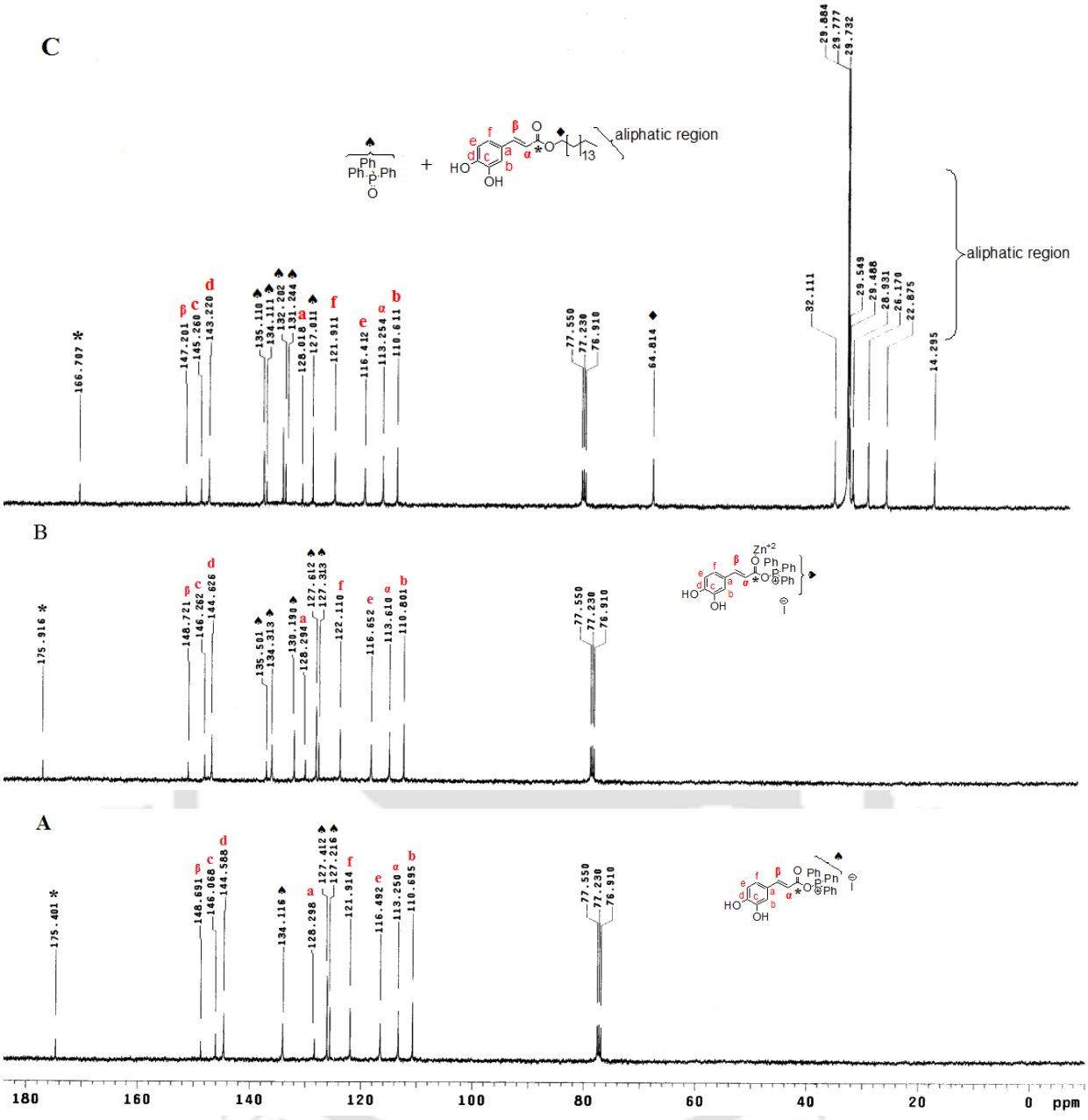

Figure 6.4.2: *Monitoring the progress of the esterification reaction between the carboxylic acid (**1a**) and alcohol (**2a**) in the presence of PPh_3, I_2 and a catalytic amount of $Zn(OTf)_2$ by ^{13}C-NMR in $CDCl_3$; (A) 10 min after addition of **1a** to the stoichiometric mixture of Ph_3P and I_2; (B) 30 min after addition of $Zn(OTf)_2$ to the mixture of **1a**, Ph_3P and I_2; (C) 4 h after addition of **2a** to the mixture of $Zn(OTf)_2$, (**1a**), Ph_3P and I_2.*→Represents the C=O of phosphate ester intermediate and compound **3aa**; ♠→Represents the phenyl protons of triphenylphosphine (Ph_3P)and triphenylphosphine oxide (Ph_3P=O); ♦→Represents the OCH_2 protons of cetyl alcohol aliphatic chain.*

6.5. NMR Spectra of Some of the Selected Esters

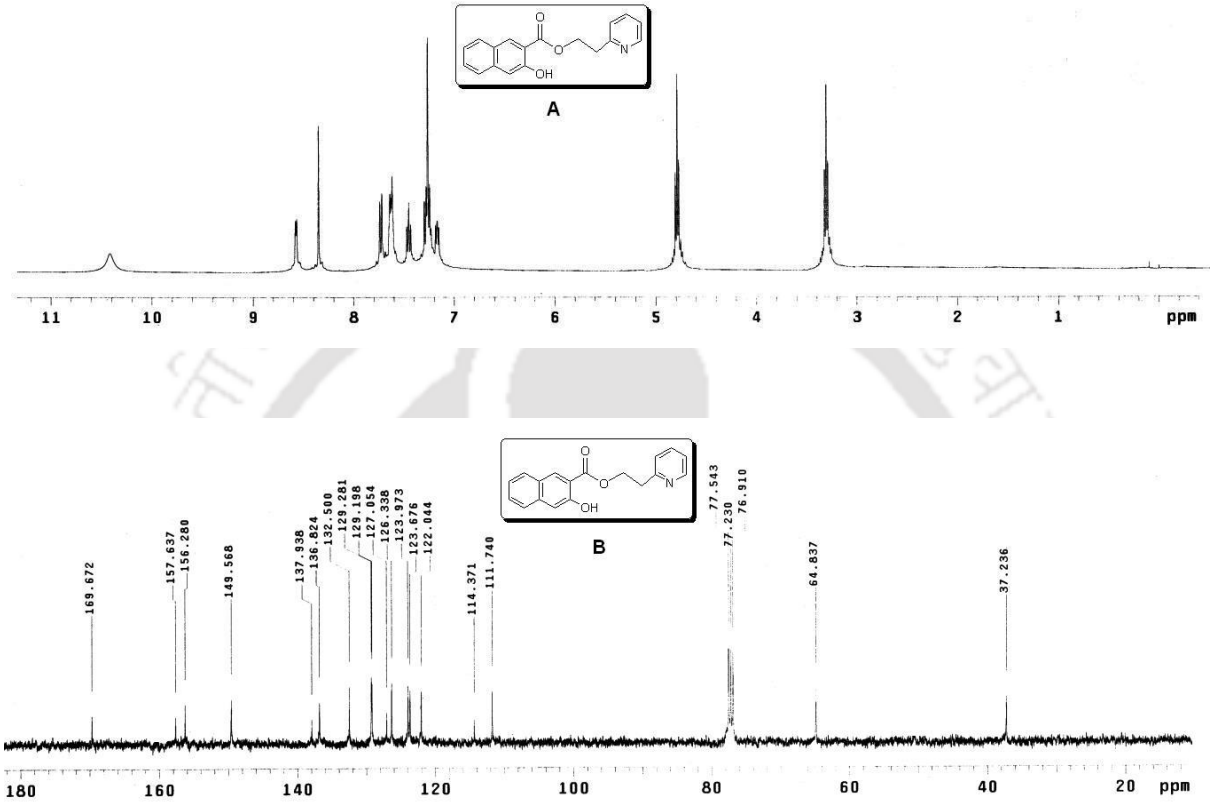

Figure 6.5.1: *^{1}H NMR (**A**) and ^{13}C NMR (**B**) of 2-(Pyridin-2-yl)ethyl 3-hydroxynaphthanele-2-carboxylate (**9**)*

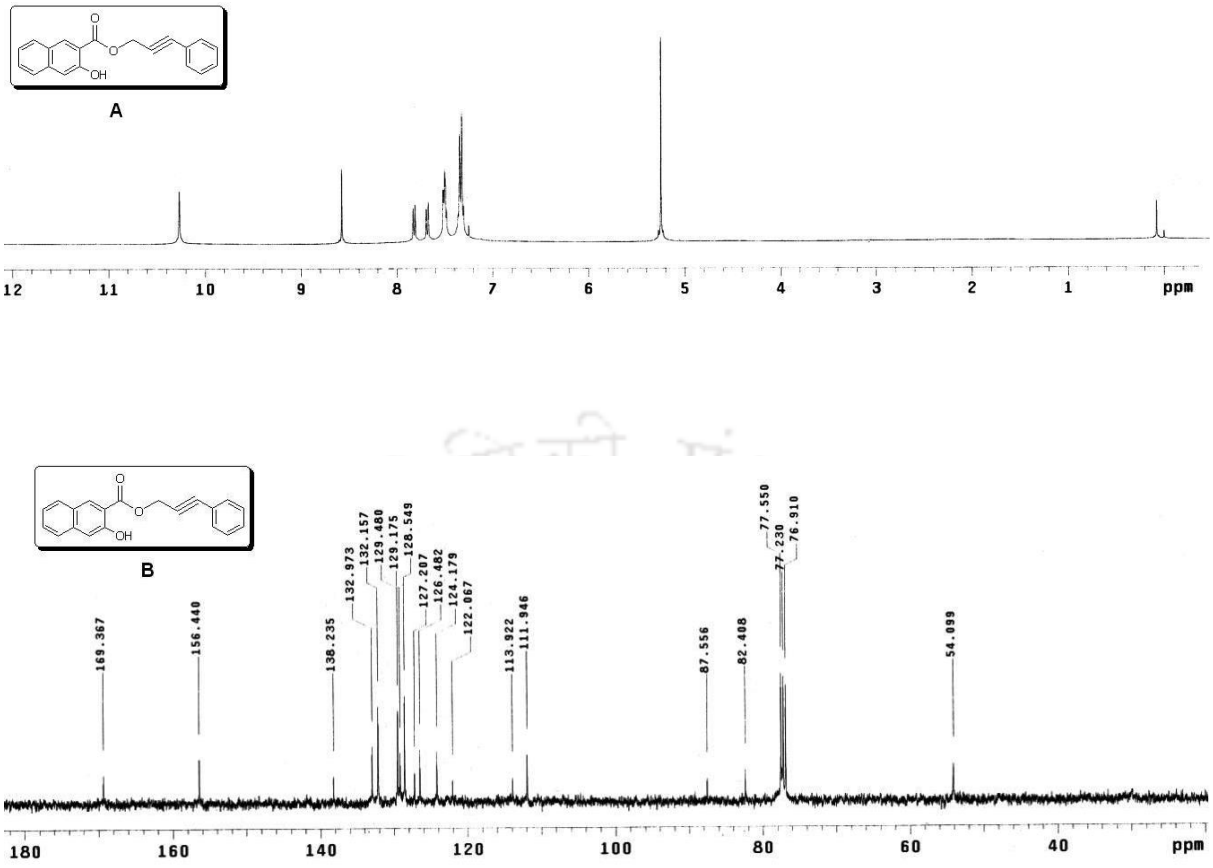

Figure 6.5.2: *^{1}H NMR (**A**) and ^{13}C NMR (**B**) of 3-Phenylprop-2-ynyl 3-hydroxynaphthanele-2-carboxylate (**10**)*

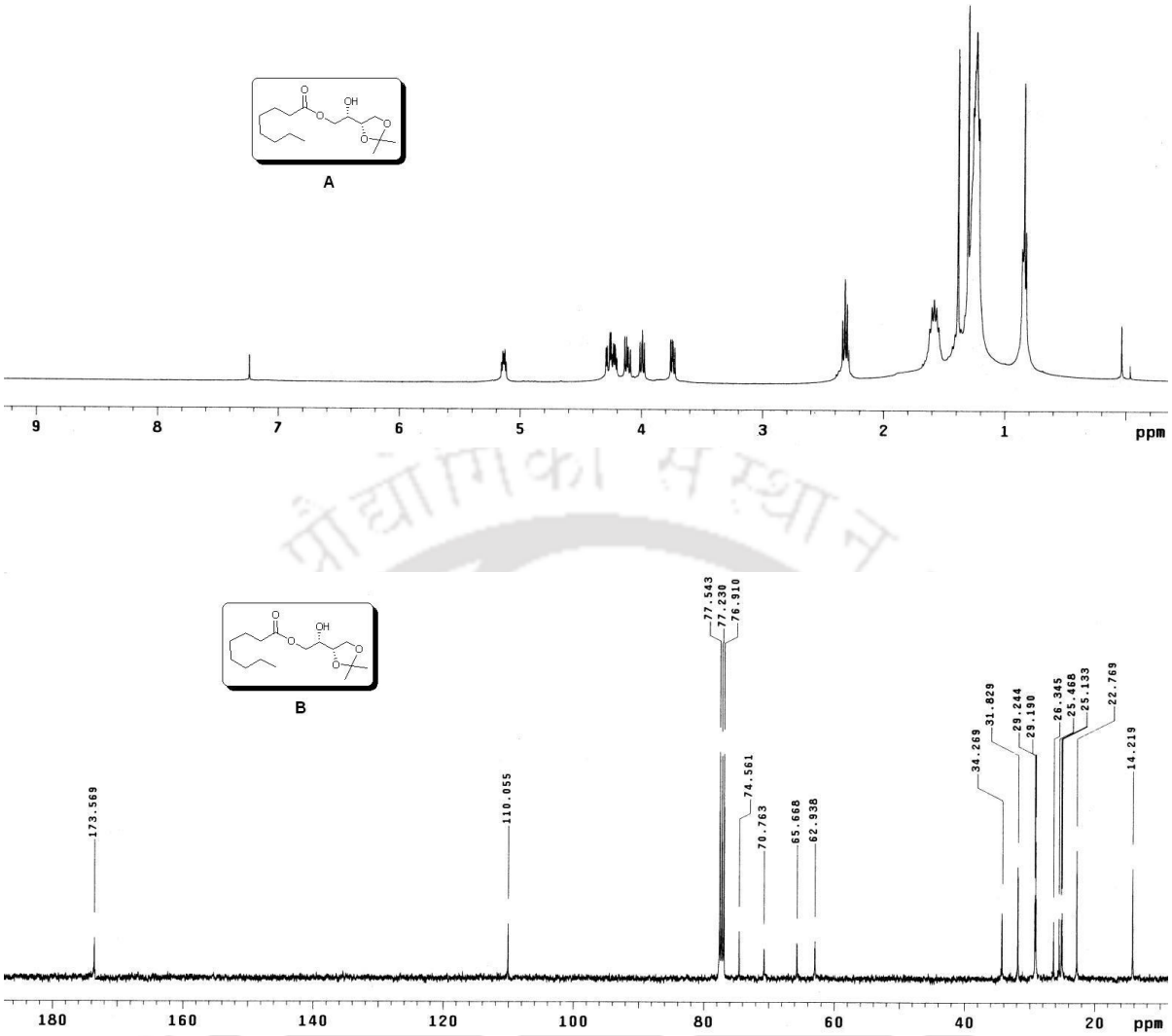

Figure 6.5.3: *^{1}H NMR (**A**) and ^{13}C NMR (**B**) of (S)-2-Hydroxy-2-((S)-2,2-dimethyl-1,3-dioxolane-4-yl)ethyl octanoate (**14**)*

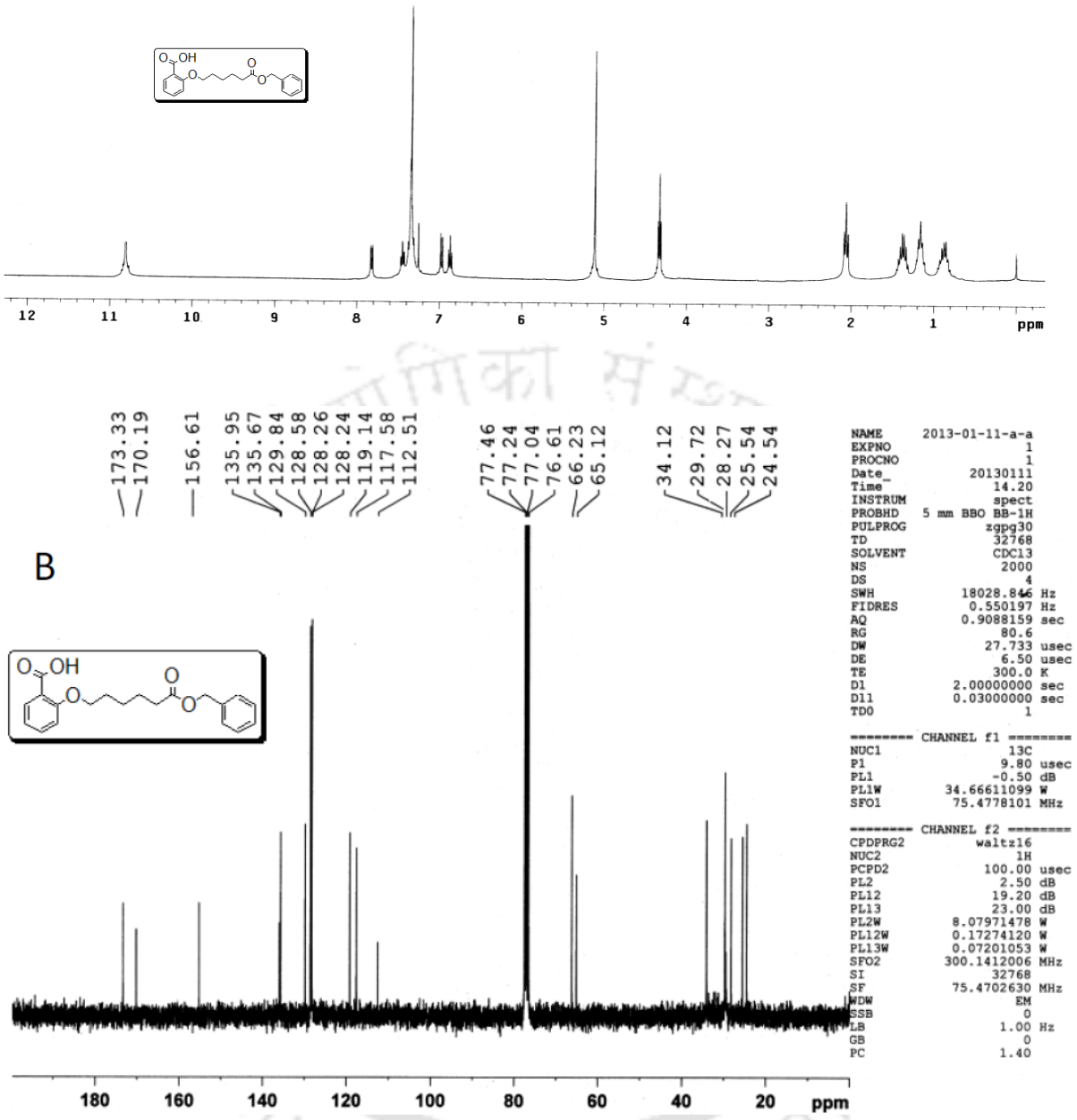

Figure 6.5.4: *^{1}H NMR (**A**) and ^{13}C NMR (**B**) of2-(5-((benzyloxy)carbonyl)pentyloxy)benzoic acid (**15**)*

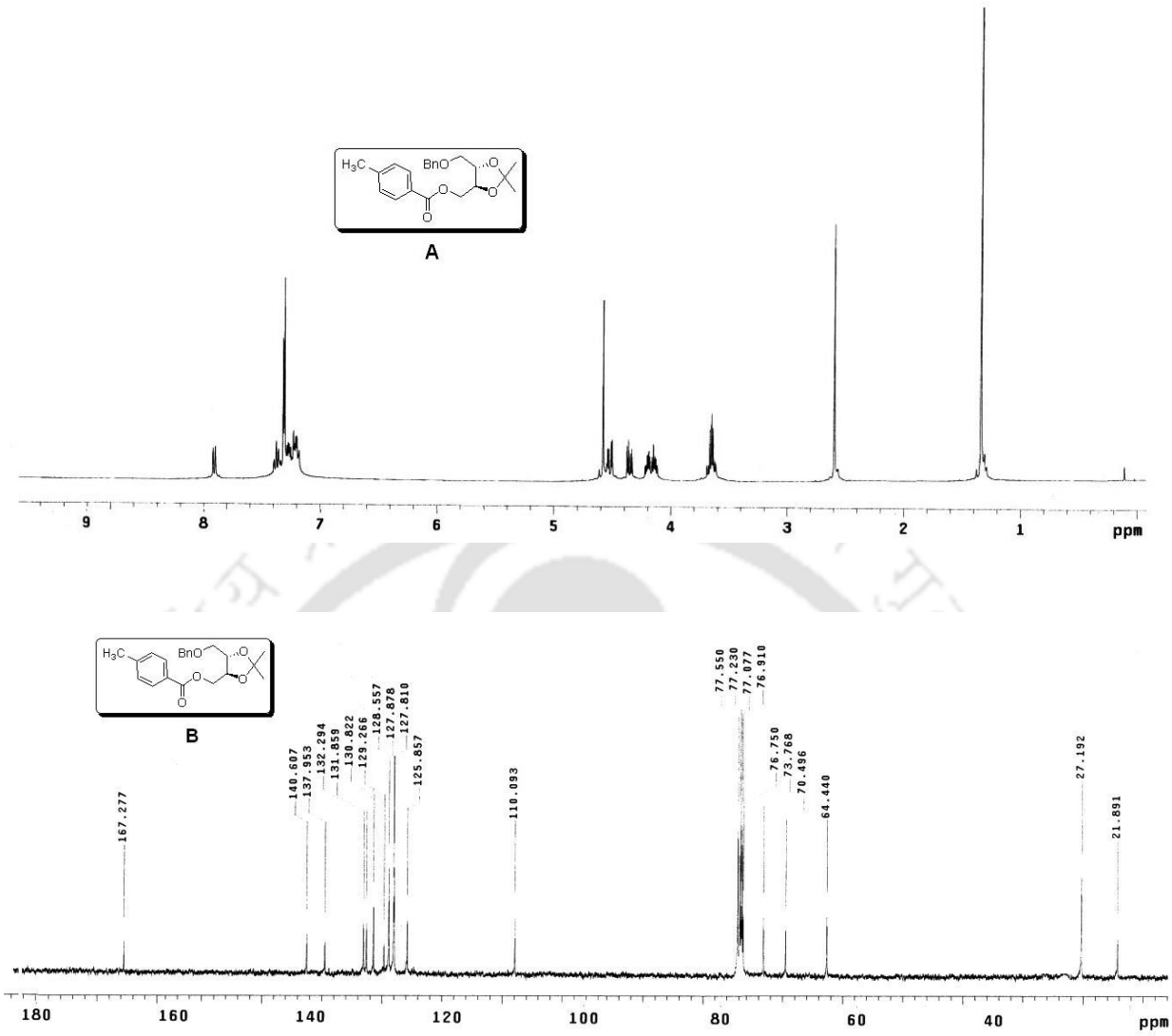

Figure 6.5.5: *^{1}H NMR (**A**) and ^{13}C NMR (**B**) of (4S,5S)-5-((benzyloxy)methyl)-2,2-dimethyl-1,3-dioxolan-4-yl)methyl 4-methylbenzoate (**16**)*

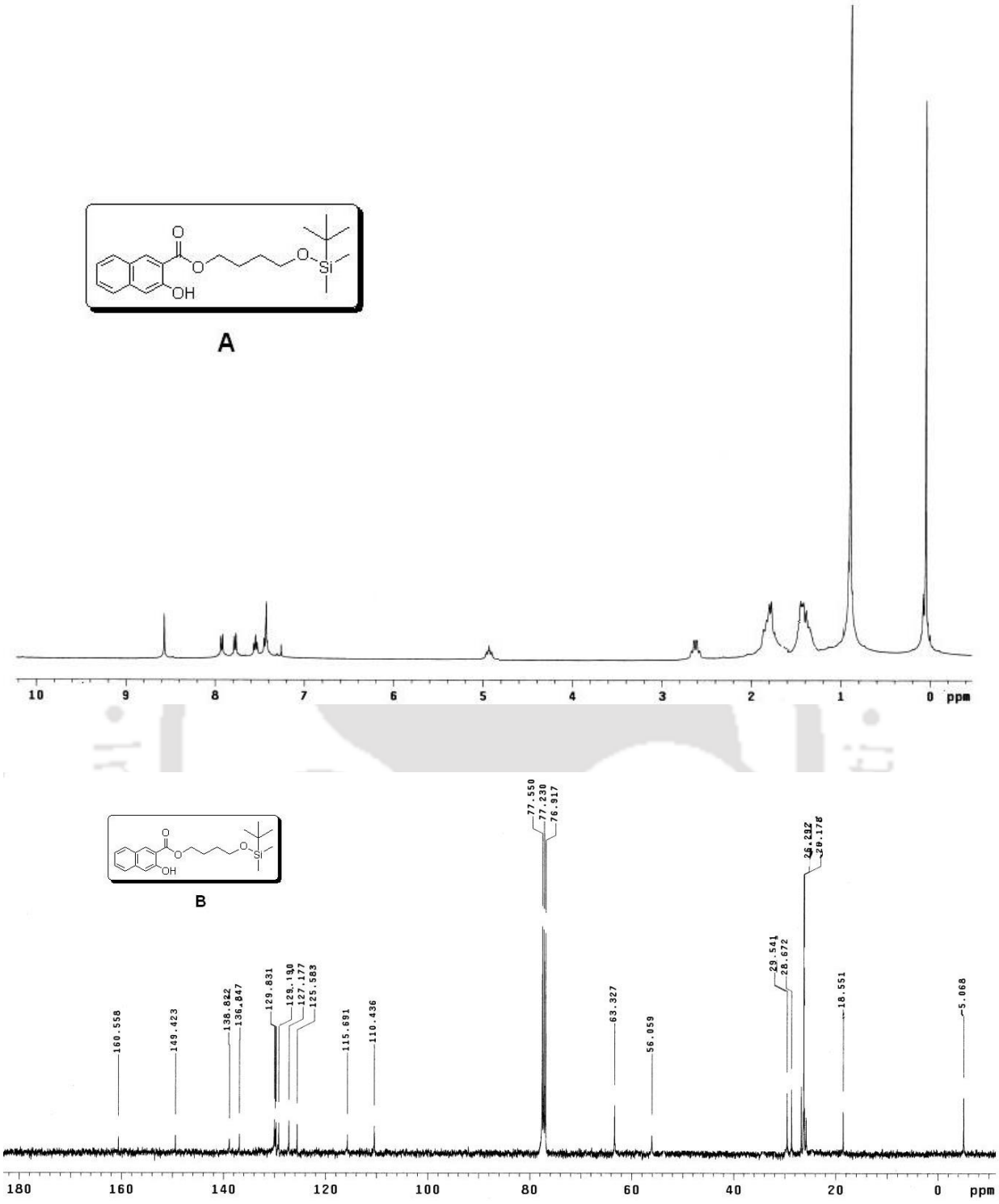

Figure 6.5.6: *^{1}H NMR (**A**) and ^{13}C NMR (**B**) of 4-[Tert-butyldimethylsilyl)oxy]butyl 3-hydroxynapthalene-2-carboxylate (**17**)*

Conclusion and Future Perspective

The significant findings and future perspective of the present investigation described in this dissertation/thesis have been summarized below. In this thesis, rational design and synthesis of lipid probes/ester derivatives have been described using multi-step organic synthesis as well as development of new methodologies to construct Protein Kinase C (PKC)-C1 domain targeted ester molecules. The interactions of these synthesized esters with the C1 domain of PKC isoforms have been investigated extensively based on *in-vitro* binding studies using Trp-fluorescence quenching assay both in monomeric form and under the liposomal environment, FRET-based competitive binding assay and molecular docking analysis.

We successfully described the designed and synthesized DAT lipids in the **chapter 2**. The DAT-lipid probes were synthesized within four to seven steps as a single isomer from (+)-diethyl L-tartrate as starting material in a good yield. Compound DAT-**4** showed 4-fold stronger binding affinity than DAG for C1b subdomain of PKCδ, whereas 2.4-fold stronger binding affinity than DAG for PKCθ it indicates that there is a modest selectivity in the binding affinities for PKCδ. In addition, molecular docking study revealed that DAT-**4** with hydroxymethyl and hydroxyl group at 1,2 positions respectively is more appropriate within C1 domain binding site. In **chapter 3**, we the synthesized diacyltetrol based-anionic hybrid lipids (DAT-PA/PS/PG) within seven to nine reaction steps in a good yield. We developed one-pot synthetic methodology for the phosphorylation reaction and time depended catalytic hydrogenation reaction conditions for selective deprotection of benzyl group in the presence of olefin double bond, which are quite demanding in the synthetic organic chemistry. In addition, based on the apparent inhibition constant (K_I) values, we concluded that PKCδ selectively interact with DAT-PS, whereas PKCθ selectively interact with DAT-PA lipid probes respectively. Particularly, DAT-PS showed 5-fold stronger binding affinity than DAG for C1b subdomain of PKCδ, whereas DAT-PA and DAT-PG showed 2.5 and 1.7-fold stronger than DAG for PKCθ respectively. Molecular docking analyses showed that these anionic lipids interact with the C1 domain through both DAG/phorbol ester binding site as well

as anionic lipid binding site, but with minimal preferable towards anionic lipid binding site.

In **chapter 4**, we designed and synthesized rigid phenyl backbone bearing (hydroxymethyl)phenyl ester analogs as PKC regulators within two reaction steps. The best compounds (**13**, **5**, and **8**, from chapter 4) showed 5-fold stronger binding affinity than natural DAG for C1 domain. Based on K_I values comparison, isoform selectivity was observed between PKCδ and PKCθ. In particularly, (hydroxymethyl)phenyl ester analogs were more specific for PKCδ than PKCθ. In addition, molecular docking studies showed that these ester analogs were binding with C1 domain of PKC isoforms at DAG/phorbol ester binding site. In **chapter 5**, we synthesized curcumin structure related alkyl cinnamates within two steps. Compound **8** showed 3.6-fold stronger binding affinity than DAG for C1 domain. A modest selectivity was observed among the PKC (δ and θ). Docking analyses revealed that alkyl cinnamates interact with the PKC-C1 domains through its DAG/phorbol ester binding site. **Chapter 6** described, a mild and efficient $Zn(OTf)_2$ promoted chemoselective esterification/amidation of the hydroxyl group bearing carboxylic acids in the presence of Ph_3P and I_2 *via* acyloxyphosponium ion intermediate. Acid sensitive protecting groups contained acids and alcohols were successfully esterified under $Zn(OTf)_2$ catalyzed conditions without loss of such protecting groups. In addition, this methodology was used for the synthesis of PKC regulators in high yield. Therefore, we believe that this method can be alternative to the existing esterification methods; it may decrease the burden of protecting groups in the parallel organic synthesis of natural products.

Thus, this thesis demonstrated some of the core and erratic concepts of organic and bio-organic chemistry. New synthetic methods (one-pot phosphorylation, time depended hydrogenation and $Zn(OTf)_2$ catalyzed esterification) developed in this study will be useful tools in further development of PKC regulators as well as other biological active compounds. All these small organic molecules can be further used as research tools or lead compounds in PKC based drug development as well as in design of other biomolecules, agonists, and antagonists and therapeutic agents.

Especially, DATs and DAT-anionic hybrid lipids may immense useful in the drug delivery, transmembrane anion transport. In addition, these compounds can be useful not

only for PKC activation but also other drug design like diabetes, stroke, heart failure and Alzheimer's disease. Hydroxymethyl-phenyl esters and alkyl cinnamates may be useful in a wide range of bio-activities such as Anticancer, anti-angiogenesis, antibacterial, antiviral, anti-inflammatory, antiatherosclerotic, anti-HIV, antitumor and antioxidants properties. Therefore, these studies performed in the thesis, reveals that the in-sight of small organic molecules and protein interactions. This also finds several parameters to control the interaction phenomena between proteins and small organic molecules in both monomeric and liposome environment. These aforementioned facts demonstrate the significance of nature and structure of esters or small organic molecules i.e. the headgroup and chain length of esters controls their activity on interaction with protein. Further studies are going on in our laboratory to develop more effective PKC regulators based on these findings and detailed interatomic structural analysis.

References

1) Lander, E. S. *Nature* **2001**, *409*, 860-921.
2) Rubin, G. M. *Science* **2000**, *287*, 2204-2215.
3) Manning, G. Plowman, T. Hunter, S. Sudarsanam, *Trends Biochem. Sci.* **2002**, 27, 514-520.
4) Venter, J. C. *Science* **2001**, *291*, 1304-1351.
5) Hunter, T.; Plowman, G. D. *Trends Biochem Sci.* **1997**, *22*, 18-22.
6) Manning, G.; Whyte, D. B.; Martinez, R.; Hunter, T.; Sudarsanam, S. *Science* **2002**, *298*, 1912-1934.
7) Hofmann, J. *Curr. Cancer Drug Targets* **2004**, *4*, 125-146.
8) Castagna, M.; Takai, Y, Kaibuchi, K.; Sano, K, Kikkawa, U.; Nishizuka Y. *J. Biol. Chem.* **1982**, *257*, 7847-7851.
9) Evcimen, N. D.; King, G. L. *Pharm. Res*. **2007**, *55*, 498-510.
10) Koivunen, J.; Aaltonen, V.; Peltonen, J. *Cancer Lett.* **2006**, *235*, 1-10.
11) Newton, A. C. *Chem. Rev*. **2001**, *101*, 2353-2364.
12) (a) Otera, J. *Angew. Chem., Int. Ed.* **2001**, *40*, 2044-2045. (b) Nahmany, M.; Melman, A. *Org. Biomol. Chem.* **2004**, *2*, 1563-1572.
13) Mitsunobu, O. *Synthesis* **1981**, 1–28.
14) Matthews, D. A.; Gerritsen, M. E. *John Wiley & Sons, Inc.: New Jersey, USA.* **2010**; 87-91.
15) Ubersax, J. A.; Ferrell, J. E. *Nat. Rev. Mol. Cell Biol.* **2007**, *8*, 530-541.
16) Blume-Jensen, P.; Hunter, T. *Nature* **2001**, *411*, 355-365.
17) Cohen, P. *Nat. Rev. Drug Discov.* **2002**, *1*, 309–315.
18) Steinberg, S. F. *Physiol. Rev.* **2008**, *88*, 1341-1378.
19) Nishizuka, Y. *Science* **1992**, *258*, 607-614.
20) Oude Weernink, P. A.; Han, L.; Jakobs, K. H.; Schmidt, M. *Biochim. Biophys. Acta* **2007**, *1768*, 888-900.
21) Nishizuka, Y. *Nature* **1984**, *308*, 693-698.
22) Nishizuka, Y. *FASEB J.* **1995**, *9*, 484-496.
23) Griner, E. M.; Kazanietz, M. G. *Nat. Rev. Cancer* **2007**, *7*, 281-294.

24) Battaini, F. *Pharmacol. Res*. **2001**, *44*, 353-361.

25) Pascale, A.; Amadio, M.; Govoni, S.; Battaini, F. *Pharmacol. Res.* **2007**, *55*, 560-569.

26) Olariu, A.; Yamada, K.; Nabeshima, T. *J. Pharmacol. Sci.* **2005**, *97*, 1-5.

27) Alkon, D. L.; Sun, M. K.; Nelson, T. J. *Trends Pharmacol. Sci.* **2007**, *28*, 51-60.

28) Newton, A. C.; Keranen, L. M. *Biochemistry* **1994**, *33*, 6651-6658.

29) Colon-Gonzalez, F.; Kazanietz, M. G. *Biochim. Biophys. Acta* **2006**, *1761*, 827-837.

30) Yang, C.; Kazanietz, M. G. *Trends Pharmacol. Sci.* **2003**, *24*, 602-608.

31) Wakelam, M. J. *Biochim. Biophys. Acta* **1998**, *1436*, 117-126.

32) Rhee, S. G. *Annu. Rev. Biochem.* **2001**, *70*, 281-312.

33) Meyer-Bertenrath, J. G. *Experientia*. **1969**, *25*, 1-5.

34) Kraft, A. S.; Anderson, W. B.; Cooper, H. L.; Sando, J. J. *J. Biol. Chem.* **1982**, *257*, 13193-13196.

35) Ashendel, C. L. *Biochim. Biophys. Acta* **1985**, *822*, 219-242.

36) Blumberg, P. M.; Kedei, N.; Lewin, N. E.; Yang, D.; Czifra, G.; Pu, Y.; Peach, M. L.; Marquez, V. E. *Curr. Drug Targets* **2008**, *9*, 641-652.

37) Newton, A. C. *J. Biol. Chem.* **1995**, *270*, 28495-28498.

38) Battaini, F.; Mochly-Rosen, D. *Pharmacol. Res*. **2007**, *55*, 461-466.

39) Orr, J. W.; Keranen, L. M.; Newton, A. C. *J. Biol. Chem.* **1992**. *267*, 15263-15266.

40) Keranen, L. M.; Dutil, E. M.; Newton, A. C. *Curr. Biol.* **1995**, *5*, 1394-1403.

41) Cenni, V.; Doppler, H.; Sonnenburg, E. D.; Maraldi, N.; Newton, A. C.; Toker, A. *Biochem. J.* **2002**, *363*, 537-545.

42) Parekh, D.; Ziegler, W.; Yonezawa, K.; Hara, K.; Parker, P. J. *J. Biol. Chem.* **1999**, *74*, 34758-34764.

43) Inoue, M.; Kishimoto, A.; Takai, Y.; Nishizuka, Y. *J. Biol. Chem.* **1977**, *252*, 7610-616.

44) Dutil, E. M.; Keranen, L. M.; DePaoli-Roach, A. A.; Newton, A. C. *J. Biol. Chem.* **1994**, *269*, 29359-29362.

45) Hansra, G.; Garcia-Paramio, P.; Prevostel, C.; Whelan, R. D.; Bornancin, F.; Parker, P. J. *Biochem. J.* **1999**, *342*, 337-344.

46) Prevostel, C.; Alice, V.; Joubert, D.; Parker, P. J. *J. Cell. Sci.* **2000**, *113*, 2575-2584.

47) Lee, H. W.; Smith, L.; Pettit, G. R.; Smith, J. B. *Mol. Pharmacol.* **1997**, *51*, 439-447.

48) Lu, Z.; Liu, D.; Hornia, A.; Devonish, W.; Pagano, M.; Foster, D. A. *Mol. Cell. Biol.* **1998**, *18*, 839-845.

49) Gao, T.; Newton, A. C. *J. Biol. Chem.* **2002**, *277*, 31585-31592.

50) Hurley, J. H.; Newton, A. C.; Parker, P. J.; Blumberg, P. M.; Nishizuka, Y. *Protein Sci*. **1997**, *6*, 477-480.

51) Kazaneitz, M. G. Mol. *Carcinog*. **2000**, *28*, 5-11.

52) Mott, H. R.; Carpenter, J. W.; Zhong, S.; Ghosh, S.; Bell, R. M.; Campbell, S. L. *Proc. Natl. Acad. Sci. USA.* **1996**, *93*, 8312-8317.

53) Leonard, T. A.; Rozycki, B.; Saidi, L. F.; Hummer, G.; Hurley, J. H. *Cell* **2011**, *144*, 55-66.

54) Xu, R. X.; Pawelczyk, T.; Xia, T. H.; Brown, S. C. *Biochemistry* **1997**, *36*, 10709-10717.

55) Hommel, U.; Zurini, M.; Luyten, M. *Nat. Struct. Biol.* **1994**, *1*, 383-387.

56) Lomize, A. L.; Pogozheva, I. D.; Lomize, M. A.; Mosberg, H. I. *BMC Struct. Biol.* **2007**, *7*, 44-74.

57) Parker, P. J.; Coussens, L.; Totty, N.; Rhee, L.; Young, S.; Chen, E.; Stabel, S.; Waterfield,M. D.; Ullrich, A. *Science* **1986**, *233*, 853-859.

58) Boije af Gennas, G.; Talman, V.; Tuominen, R.; Yli-Kauhaluoma, J.; Ekokoski, E. *Curr.Top. Med. Chem.* **2011**, *11*, 1370-1392.

59) Szallasi, Z.; Krausz, K. W.; Blumberg, P. M. *Carcinogenesis* **1992**, *13*, 2161-2167.

60) Gustafson, K. R.; Cardellina, J. H., 2nd; McMahon, J. B.; Gulakowski, R. J.; Ishitoya, J.; Szallasi, Z.; Lewin, N. E.; Blumberg, P. M.; Weislow, O. S.; Beutler, J. A. *J. Med. Chem.* **1992**, *35*, 1978-1986.

61) Wender, P. A.; Kee, J. M.; Warrington, J. M. *Science* **2008**, *320*, 649-652.

62) Wender, P. A.; Heumann, L. V.; Kramer, R.; Gauntlett, C.; Mieuli, E.; Fournogerakis, D.; Boudreault, P.; Schrier, A.; Dechristopher, B. *U.S. Pat. Appl.* **2011**/0014699A1.

63) Jassbi, A. R. *Phytochemistry* **2006**, *67*, 1977-1984.

64) Ogbourne, S. M.; Hampson, P.; Lord, J. M.; Parsons, P.; De Witte, P. A.; Suhrbier, A. *Anti-cancer Drugs* **2007**, *18*,357-362.

65) Winkler, J. D.; Hong, B.; Bahador, A.; Kazanietz, M. G.; Blumberg, P. M. *Bioorg. Med. Chem. Lett.* **1993**, *3*, 577-580.

66) Hecker, E. *Cancer Res.* **1968**, *28*, 2338–2349.

67) Kedei, N.; Lundberg, D. J.; Toth, A.; Welburn, P.; Garfield, S. H.; Blumberg, P. M. *Cancer Res.* **2004**, *64*, 3243-3255.

68) Hecker, E. *Toxicol. Pathol.* **1987**, *15*, 245-258.

69) Mason, S. A.; Cozzi, S. J.; Pierce, C. J.; Pavey, S. J.; Parsons, P. G.; Boyle, G. M. *Invest New Drugs* **2010**, *28*, 575-586.

70) Pettit, G. R.; Herald, C. L.; Doubek, D. L.; Herald, D. L. *J. Am. Chem. Soc*. **1982**, *104*, 6846-6848.

71) Sudek, S.; Lopanik, N. B.; Waggoner, L. E.; Hildebrand, M.; Anderson, C.; Liu, H.; Patel, A.; Sherman, D. H.; Haygood, M. G. *J. Nat. Prod.* **2007**, *70*, 67-74.

72) Reyland, M. E.; Insel, P. A.; Messing, R. O.; Dempsey, E. C.; Newton, A. C.; Mochly-Rosen, D.; Fields, A. P. *Am. J. Physiol. Lung Cell. Mol. Physiol.* **2000**, *279*, 429-438.

73) Wender, P. A.; Brabander, J. D.; Harran, P. G.; Jimenez, J.M.; Koehler, M. F. T.; Lippa, B.; Park, C.M.; Siedenbiedel, C.; Pettit, G. R. *Proc. Natl. Acad. Sci. U.S.A.* **1998**, *95*,6624–6629.

74) Hale, K. J.; Hummersome, M. G.; Manaviazar, S.; Frigerio, M. *Nat. Prod. Rep.* **2002**, *19*, 413-453

75) Wang, Q. J.; Bhattacharyya, D.; Garfield, S.; Nacro, K.; Marquez, V. E.; Blumberg, P. M. *J. Biol. Chem.* **1999**, *274*, 37233-37239.

76) Wender, P. A.; Baryza, J. L.; Bennett, C. E.; Bi, F. C.; Brenner, S. E.; Clarke, M. O.; Horan, J. C.; Kan, C.; Lacote, E.; Lippa, B.; Nell, P. G.; Turner, T. M. *J. Am. Chem. Soc.* **2002**, *124*, 13648-13649.

77) Wender, P. A.; Verma, V. A. *Org. Lett.* **2008**, *10*, 3331-3334.

78) Wender, P. A.; Baryza, J. L.; Brenner, S. E.; Clarke, M. O.; Craske, M. L.; Horan, J.C. Meyer, T. *Curr. Drug Discovery Technol.* **2004**, *1*, 1-11.

79) Wender, P. A.; Dechristopher, B. A.; Schrier, A. J. *J. Am. Chem. Soc.* **2008**, *130*, 6658-6659.

80) Endo, Y.; Takehana, S.; Ohno, M.; Driedger, P. E.; Stabel, S.; Mizutani, M. Y.; Tomioka, N.; Itai, A.; Shudo, K. *J. Med. Chem.* **1998**, *41*, 1476-1496.

81) Fujiki, H.; Suganuma, M.; Nakayasu, M.; Tahira, T.; Endo, Y.; Shudo, K.; Sugimura, T. *Jpn. J. Cancer Res.* **1984**, *75*, 866-870.

82) Nakagawa, Y.; Irie, K.; Yanagita, R. C.; Ohigashi, H.; Tsuda, K. *J. Am. Chem. Soc.* **2005**, *127*, 5746-5747.

83) Endo, Y.; Ohno, M.; Hirano, M.; Itai, A.; Shudo, K. *J. Am. Chem. Soc.* **1996**, *118*, 1841-1855.

84) Boije af Gennäs, G.; Talman, V.; Tuominen, R.; Yli-Kauhaluoma, J.; Ekokoski, E. *Curr. Top. Med. Chem.* **2011**, *11*, 1370-1392.

85) Yanagita, R. C.; Nakagawa, Y.; Yamanaka, N.; Kashiwagi, K.; Saito, N.; Irie, K. J. *Med. Chem.* **2008**, *51*, 46-56.

86) Irie, K.; Nakagawa, Y.; Ohigashi, H. *Chem. Rec.* **2005**, *5*, 185-195.

87) Kozikowski, A. P.; Wang, S.; Ma, D.; Yao, J.; Ahmad, S.; Glazer, R. I.; Bögi, K.; Acs, P.; Modarres, S.; Lewin, N. E.; Blumberg, P. M. *J. Med. Chem.* **1997**, *40*, 1316-1326.

88) Ma, D.; Tang, G.; Kozikowski, A. P. *Org. Lett.* **2002**, *4*, 2377-2380.

89) Nakagawa, Y.; Irie, K.; Masuda, A.; Ohigashi, H. *Tetrahedron* **2002**, *58*, 2101-2115.

90) Nakagawa, Y.; Irie, K.; Yanagita, R. C.; Ohigashi, H.; Tsuda, K.; Kashiwagi, K.; Saito, N. *J. Med. Chem.* **2006**, *49*, 2681-2666.

91) Marner, F.; Krick, W.; Gellrich, B.; Jaenicke, L. *J. Org. Chem.* **1982**, *47*, 2531-2536.

92) Takahashi, K.; Suzuki, S.; Hano, Y.; Nomura, T. *Biol. Pharm. Bull.* **2002**, *25*, 432-436.

93) Shao, L.; Lewin, N. E.; Lorenzo, P. S.; Hu, Z.; Enyedy, I. J.; Garfield, S. H.; Stone, J. C.; Marner, F. J.; Blumberg, P. M.; Wang, S. *J. Med. Chem.* **2001**, *44*, 3872-3880.

94) Bonfils, J. P.; Pinguet, F.; Culine, S.; Sauvaire, Y. *Planta Med.* **2001**, *67*, 79-81.

95) Corbu, A.; Aquino, M.; Pratap, T. V.; Retailleau, P.; Arseniyadis, S. *Org. Lett.* **2008**, *10*, 1787-1790.

96) Marquez, V. E.; Blumberg, P. M. *Acc. Chem. Res.* **2003**, *36*, 434-443.

97) Nacro, K.; Bienfait, B.; Lee, J.; Han, K. C.; Kang, J. H.; Benzaria, S.; Lewin, N. E.; Bhattacharyya, D. K.; Blumberg, P. M.; Marquez, V. E. *J. Med. Chem.* **2000**, *43*, 921-944.

98) Kang, J. H.; Siddiqui, M. A.; Sigano, D. M.; Krajewski, K.; Lewin, N. E.; Pu, Y.; Blumberg, P. M.; Lee, J.; Marquez, V. E. *Org. Lett*. **2004**, *6*, 2413-2416.

99) Kang, J. H.; Peach, M. L.; Pu, Y.; Lewin, N. E.; Nicklaus, M. C.; Blumberg, P. M.; Marquez, V. E. *J. Med. Chem.* **2005**, *48*, 5738-5748.

100) Comin, M. J.; Czifra, G.; Kedei, N.; Telek, A.; Lewin, N. E.; Kolusheva, S.; Velasquez, J. F.; Kobylarz, R.; Jelinek, R.; Blumberg, P. M.; Marquez, V. E. *J. Med. Chem.* **2009**, *52*, 3274-3283.

101) Pu, Y.; Perry, N. A.; Yang, D.; Lewin, N. E.; Kedei, N.; Braun, D. C.; Choi, S. H.; Blumberg, P. M.; Garfield, S. H.; Stone, J. C.; Duan, D.; Marquez, V. E. *J. Biol. Chem.* **2005**, *280*, 27329-27338.

102) Garcia-Bermejo, M. L.; Leskow, F. C.; Fujii, T.; Wang, Q.; Blumberg, P. M.; Ohba, M.; Kuroki, T.; Han, K. C.; Lee, J.; Marquez, V. E.; Kazanietz, M. G. *J. Biol. Chem.* **2002**, *277*, 645-655.

103) Truman, J. P.; Rotenberg, S. A.; Kang, J. H.; Lerman, G.; Fuks, Z.; Kolesnick, R.; Marquez, V. E.; Haimovitz-Friedman, A. *Cancer. Biol. Ther.* **2009**, *8*, 54-63.

104) Hamer, D. H.; Bocklandt, S.; McHugh, L.; Chun, T. W.; Blumberg, P. M.; Sigano, D. M.; Marquez, V. E. *J. Virol.* **2003**, *77*, 10227-10236.

105) Houston, T. A.; Wilkinson, B. L.; Blanchfield, J. T. *Org. Lett.* **2004**, *5*, 679-681.

106) Burke, T. R.; Fesen, M. R.; Mazumder, A.; Wang, J.; Carothers, A. M.; Grunberger, D.; Driscoll, J.; Kohn, K.; Pommier, Y. *J. Med. Chem.* **1995**, *38*, 4171−4178.

107) Appendino, G.; Minassi, A.; Daddario, N.; Bianchi, F.; Tron, G. C. *Org. Lett.* **2002**, *4*, 3839−3841.

108) Iqbal, J.; Srivastava, R. R. *J. Org. Chem.* **1992**, *57*, 2001−2007.

109) Miyashita, M.; Shiina, I.; Miyoshi, S.; Mukaiyama, T. *Bull. Chem. Soc. Jpn.* **1993**, *66*, 1516−1527.

110) Kumareswaran, R.; Gupta, A.; Vankar, Y. D. *Synth. Commun.* **1997**, *27*, 277−282.

111) Ishihara, K.; Ohara, S.; Yamamoto, H. *Science* **2000**, *290*, 1140−1142.

112) Heller, S. T.; Sarpong, R. *Org. Lett.* **2010**, *12*, 4572-4575.

113) Boden, P. E.; Keck, G. E. *J. Org. Chem.* **1985**, *50*, 2394–2395.

114) Morcillo, S. P.; de Cienfuegos, L. A.; Mota, A. J.; Justicia, J.; Robles, R. *J. Org. Chem.* **2011**, *76*, 2277–2281.

115) Tian, J.; Gao, W. C.; Zhou, G. M.; Zhang, C. *Org. Lett.* **2012**, *14*, 3020-3023.

116) (a) Selva, M.; Tundo, P. *J. Org. Chem.* **2005**, *71*, 1464-1470. (b) Gopinath, P.; Nilaya, S.; Muraleedharan, K. M. *Org. Lett*. **2011**, *13*, 1932-1935. (c) Torregiani, E.; Seu, G.; Minassi, M.; Appendino, G. *Tetrahedron Lett*. **2005**, *46*, 2193-2196. (d) Maki, T.; Ishihara, K.; Yamamoto. H. *Org. Lett*. **2005**, *7*, 5047-5050. (e) Ohshima, T.; Iwasaki, T.; Maegawa, Y.; Yoshiyama, A.; Mashima, K. J. *Am. Chem. Soc*. **2008**, *130*, 2944-2945. (f) Hayashi, Y.; Santoro, S.; Azuma, Y.; Himo, F.; Ohshima, T.; Mashima, K. *J. Am. Chem. Soc*. **2013**, *135*, 6192−6199.

117) Das, N.; Evcimen; King, G. L. *Pharm. Res.* **2007**, *55*, 498–510.

118) Koivunen, V. J.; Aaltonen, J. Peltonen. *Cancer Lett.* **2006**, *235*, 1-10.

119) Boije af Gennas, G.; Talman, V.; Aitio, O.; Ekokoski, E.; Finel, M.; Tuominen, R. K.; Yli-Kauhaluoma, J. *J. Med. Chem.* **2009**, *52*, 3969–3981.

120) Kazanietz, M. G. *Mol. Pharmacol.* **2002**, *61*, 759–767.

121) Stahelin, R. V. *J. Lipid Res.* **2009**, *50*, 299–304.

122) Ono, Y.; Fujii, T.; Igarashi, K.; Kuno, T.; Tanaka, C.; Kikkawa, U.; Nishizuka, Y. *Proc. Natl. Acad. Sci. U. S. A.* **1989**, *86*, 4868–4871.

123) Smith, J. B.; Smith, L.; Pettit, G. R.; *Biochem. Biophys. Res. Commun.* **1985**, *132*, 939–945.

124) Kong, F. H.; Kishi, Y.; Perezsala, D.; Rando, R. R. *Proc. Natl. Acad. Sci. U. S. A.* **1991**, *88*, 1973–1976.

125) Raifman, O.; Kolusheva, S.; Comin, M. J.; Kedei, N.; Lewin, N. E.; Blumberg, P. M.; Marquez, V. E.; Jelinek, R. *FEBS J*. **2010**, *277*, 233–243.

126) Duan, D.; Sigano, D. M.; Kelley, J. A.; Lai, C. C.; Lewin, N. E.; Kedei, N.; Peach, M. L.; Lee, J.; Abeyweera, T. P.; Rotenberg, S. A.; Kim, H.; Kim, Y. H.; El Kazzouli, S.; Chung, J. U.; Young, H. A.; Young, M. R.; Baker, A.; Colburn, N. H.; Haimovitz-Friedman, A.; Truman, J. P.; Parrish, D. A.; Deschamps, J. R.; Perry, N. A.; Surawski, R. J.; Blumberg, P. M.; Marquez, V. E. J. *Med. Chem.* **2008**, *51*, 5198–5220.

127) El Kazzouli, S.; Lewin, N. E.; Blumberg, P. M.; Marquez, V. E. *J. Med. Chem.* **2008**, *51*, 5371–5386.

128) Keck, G. E.; Poudel, Y. B.; Rudra, A.; Stephens, J. C.; Kedei, N.; Lewin, N. E.; Peach, M. L.; Blumberg, P. M. *Angew. Chem., Int. Ed.* **2010**, *49*, 4580–4584.

129) Zhang, G. G.; Kazanietz, M. G.; Blumberg, P. M.; Hurley, J. H. *Cell* **1995**, *81*, 917–924.

130) Linclau, B.; Boydell, A. J.; Clarke, P. J.; Horan, R.; Jacquet, C. *J. Org. Chem.* **2003**, *68*, 1821–1826.

131) Smith, M. D.; Sudhahar, C. G.; Gong, D.; Stahelin, R. V.; Best, M. D. *Mol. Biosyst.* **2009**, *5*, 962–972.

132) Smith, M. D.; Gong, D.; Sudhahar, C. G.; Reno, J. C.; Stahelin, R. V.; Best, M. D. *Bioconjugate Chem.* **2008**, *19*, 1855–1863.

133) McDonald, F. E.; Boone, M. A.; Lichter, J.; Lutz, S.; Cao, R.; Hardcastle, K. I.; *Org. Lett.* **2009**, *11*, 851–854.

134) Boden, E. P.; Keck, G. E. *J. Org. Chem.* **1985**, *50*, 2394–2395.

135) Hsieh, H. P.; Shiao, H. Y.; Liao, C. C. *Org. Lett.* **2008**, *10*, 449–452.

136) Bouzide, A.; LeBerre. N.; Sauve, G.; *Tetrahedron Lett.* **2001**, *42*, 8781–8783.

137) Sureshan, K. M.; Shashidhar, M. S.; Praveen, T.; Das, T. *Chem. Rev.* **2003**, *103*, 4477–4503.

138) Majhi, A.; Rahman, G. M.; Panchal, S.; Das, J. *Bioorg. Med. Chem.* **2010**, *18*, 1591–1598.

139) Nacro, K.; Sigano, D. M.; Yan, S.; Nicklaus, M. C.; Pearce, L. L.; Lewin, N. E.; Garfield, S. H.; Blumberg, P. M.; Marquez, V. E.; *J. Med. Chem.* **2001**, *44*, 1892–1904.

140) Wang, S.; Zaharevitz, D. W.; Sharma, R.; Marquez, V. E.; Lewin, N. E.; Du, L.; Blumberg, P. M.; Milne, G. W. *J. Med. Chem.* **1994**, *37*, 4479–4489.

141) Das, J.; Pany, S.; Rahman, G. M.; Slater, S. J. *Biochem. J.* **2009**,*421*, 405–413.

142) Manna, D.; Albanese, A.; Park, W. S.; Cho, W. *J. Biol. Chem.* **2007**, *282*, 32093–32105.

143) Thomsen, R.; Christensen, M. H. *J. Med. Chem.* **2006**, *49*, 3315–3321.

144) Battaini, F.; Mochly-Rosen, D. *Pharmacol. Res.* **2007**, *55*, 461-466.

145) Hodgkin, M. N.; Pettitt, T. R.; Martin, A.; Michell, R. H.; Pemberton, A. J.; Wakelam, M. J. *Trends Biochem. Sci.* **1998**, *23*, 200-204.

146) Alkon, D. L.; Sun, M. K.; Nelson, T. J. *Trends Pharmacol. Sci.* **2007**, *28*, 51-60.

147) Benzaria, S.; Bienfait, B.; Nacro, K.; Wang, S. M.; Lewin, N. E.; Beheshti, M.; Blumberg, P. M.; Marquez, V. E. *Bioorg. Med. Chem. Lett.* **1998**, *8*, 3403-3408.

148) Sanchez-Bautista, S.; Corbalan-Garcia, S.; Perez-Lara, A.; Gomez-Fernandez, J. C. *Biophys J.* **2009**, *96*, 3638-3647.

149) Medkova, M.; Cho, W. *Biochemistry* **1998**, *37*, 4892-4900.

150) Newton, A. C.; Keranen, L. M. *Biochemistry* **1994**, *33*, 6651-6658.

151) Mamidi, N.; Gorai, S.; Mukherjee, R.; Manna, D. *Mol. Biosyst.* **2012**, *8*, 1275-1285.

152) Wakelam, M. J. Biochim. *Biophys. Acta* **1998**, *1436*, 117−126.

153) Brose, N.; Rosenmund, C. J. *Cell Sci.* **2002**, *115*, 4399−4411.

154) Chen, J.; Feng, L.; Prestwich, G. D. *J. Org. Chem.* **2006**, *63*, 6511-6522.

155) Xu, Y.; Sculimbrene, B. R.; Miller, S. J. *J. Org. Chem.* **2006**, *71*, 4919-4928.

156) BouzBouz, S.; Cossy, J. *Org. Lett.* **2004**, *6*, 3569-3572.

157) Khaled, A.; Gravier-Pelletier, C.; Merrer, Y. L. *Tetrahedron: Asymmetry* **2007**, *18*, 2121-2124.

158) Vaiquea, E.; Guy, A.; Couedelo, L.; Gosse, I.; Durand, T.; Cansell, M.; Sandra Pinet, S. *Tetrahedron* **2010**, *66*, 8872-8879.

159) Mamidi, N.; Borah, R.; Sinha, N.; Jana, C.; Manna, D. *J. Phys. Chem. B* **2012**, *116*, 10684-10692.

160) Mamidi, N.; Gorai, S.; Sahoo, J.; Manna, D. *Chem. Phys. Lipids* **2012**, *165*, 320-330.

161) Landgraf, K. E.; Pilling, C.; Falke, J. J. *Biochemistry* **2008**, *47*, 12260−12269.

162) Corbin, J. A.; Dirkx, R. A.; Falke, J. J. *Biochemistry* **2004**, *43*, 16161−16173.

163) Ahn, T.; Peter Guengerich, F.; Yun, C. –H. Biochemistry **1998**, *37*, 12860-12866.

164) Das, A.; Base, C.; Manna, D.; Cho, W.; Dubreuil, R. R. *J. Biol. Chem.* **2008**, *283*, 12643−12653.

165) Blumberg, P. M.; Kedei, N.; Lewin, N. E.; Yang, D.; Czifra, G.; Pu, Y.; Peach, M. L.; Marquez, V. E. *Curr. Drug Targets* **2008**, *9*, 641–652.

166) Kim, K. J.; Kim, M. A.; Jung, J. H. *Arch. Pharm. Res.* **2008**, *31*, 1572−1577.

167) Mamidi, N.; Panda, S.; Borah, R.; Manna, D. *Mol. Biosyst.* **2014**, *10*, 3002-30013.

168) Mackay, H. J.; Twelves, C. J. *Nat. Rev. Cancer* **2007**, *7*, 554−562.

169) Figueroa-Espinoza, M. C.; Villeneuve, P. *J. Agric. Food Chem.* **2005**, *53*, 2779–2787.

170) Hsiao, G.; Lee, J. J.; Lin, K. H.; Shen, C. H.; Fong, T. H.; Chou, D. S.; Sheu, J. R. *Cardiovasc. Res.* **2007**, *75*, 782–792.

171) Gaspar, A.; Garrido, E. M. Esteves, M.; Quezada, E.; Milhazes, N.; Garrido, J.; Borges, F. *Eur. J. Med. Chem.* **2009**, *44*, 2092–2099.

172) Menezes, J.C.; Kamat, S.P.; Cavaleiro, J.A.; Gaspar, A.; Garrido, J.; Borges, F. *Eur. J. Med. Chem.* **2011**, *46*, 773–777.

173) Maurice, E.S. D.; Snook, E.; Kays, S. J. *J. Agric. Food Chem.* **1994**, *42*, 2589–2595.

174) Nishimura, K.; Takenaka, Y.; Kishi, M.; Tanahashi, T.; Yoshida, H.; Okuda, C.; Mizushina, Y. *Chem. Pharm. Bull. (Tokyo).* **2009**, *57*, 476–480.

175) Jayaprakasam, B.; Vanisree, M.; Zhang, Y.; Dewitt, D. L.; Nair, M. G. *J. Agric. Food Chem.* **2006**, *54*, 5375–5381.

176) Murakami, A.; Kadota, M.; Takahashi, D.; Taniguchi, H.; Nomura, E.; Hosoda, A.; Tsuno, T.; Maruta, Y.; Ohigashi, H.; Koshimizu, K. *Cancer Lett.* **2000**, *157*, 77–85.

177) Perez-Lara, A.; Corbalan-Garcia, S.; Gomez-Fernandez, J.C. *Biochem. Biophys.* **2011**, *513*, 36–41.

178) Xia, C. N.; Li, H. B.; Liu, F.; Hu, W. X. *Bioorg. Med. Chem. Lett.* **2008**, *18*, 6553–6557.

179) Kolb, K. E.; Field, K. W.; Schatz, P. F. *J. Chem. Educ.* **1990**, *67*, 304-306.

180) Cho, W.; Stahelin, R. V. *Annu. Rev. Biophys. Biomol. Struct.* **2005**, *34*, 119–151.

181) Barik, A.; Mishra, B.; Kunwar, A.; Priyadarsini, K. I. *Chem. Phys. Lett.* **2007**, *436*, 239–243.

182) Das, J.; Pany, S.; Majhi, A. *Bioorg. Med. Chem.* **2011**, *19*, 5321–5333.

183) Zhang, G. G.; Kazanietz, M. G.; Blumberg, P. M.; Hurley, J.H. *Cell* **1995**, *81*, 917–924.

184) Nagashima, T.; Hayashi, F.; Yokoyama, S.; *PDB code: 2ENZ, in press.*

185) (a) Carey, J. S.; Laffan, D.; Thomson, C.; Williams, M. T. *Org. Biomol. Chem.* **2006**, *4*, 2337–2347. (b) Dugger, R. W.; Ragan, J. A.; Ripin, D. H. B. *Org. Process Res. Dev.* **2005**, *9*, 253–258.

186) (a) Sancho, R.; Lucena, C.; Macho, A.; Calzado, M. A.; Blanco-Molina, M.; Minassi, A.; Appendino, G.; Munoz, E. *Eur. J. Immunol.* **2002**, *32*, 1753–1763. (b) Nakane, H.; Ono, K. *Biochemistry* **1990**, *29*, 2841–2845. (c) Tillekeratne, L. M. V.; Sherette, A.; Grossman, P.; Hupe, L.; Hupe, D.; Hudson, R. A. *Bioorg. Med. Chem. Lett.* **2001**, *11*, 2763–2767. (d) Natarajan, K.; Singh, S.; Burke, T. R.; Grunberger, D.; Aggarwal, B. B. *Proc. Natl. Acad. Sci. U.S.A.* **1996**, *93*, 9090–9095. (e) Stuwe, H. T.; Bruhn, G.; Konig, W. A.; Hausen, B. M. *Naturwissenschaften* **1989**, *76*, 426–427. (f) Orita, A.; Tanahashi, C.; Kakuda, A.; Otera, J. *J. Org. Chem.* **2001**, *66*, 8926–8934. (g)

Ishihara, K.; Kubota, M.; Kurihara, H.; Yamamoto, H. *J. Org. Chem.* **1996**, *61*, 4560–4567.

187) Garegg, P. J.; Samuelsson, B. *J. Chem. Soc., Chem. Commun.* **1979**, 978–980.

188) Tian, J.; Gao, W. C.; Zhou, D. M.; Zhang, C. *Org. Lett.* **2012**, *14*, 3020–3023.

189) Mukaiyama, T. *Angew. Chem., Int. Ed.* **1976**, *15*, 94–103.

190) Lipshutz, B. H.; Chung, D. W.; Rich, B.; Corral, R. *Org. Lett.* **2006**, *8*, 5069-5072.

191) Kim, D. S. H. L.; Kim, J. Y. *Bioorg. Med. Chem. Lett.* **2001**, *11*, 2541–2543.

192) Kita, Y.; Nishii, Y.; Higuchi, T.; Mashima, K. *Angew. Chem., Int. Ed.* **2012**, *51*, 5723–5726.

193) Shekarriz, M.; Taghipoor, S.; Khalili, A. A.; Jamarani, M. S. *J. Chem. Res. Synop.* **2003**, 172–173.

194) Chandra, K. L.; Saravanan, P.; Singh, R. K.; Singh, V. K. *Tetrahedron* **2002**, *58*, 1369–1374.

195) Damen, E. W. P.; Braamer, L.; Scheeren, H. W. *Tetrahedron Lett.* **1998**, *39*, 6081–6082.

196) Bartoli, G.; Boeglin, J.; Bosco, M.; Locatelli, M.; Massaccesi, M.; Melchiorre, P.; Sambria, L. *Adv. Synth. Catal.* **2005**, *347*, 33–38.

197) (a) The NMR spectra in $CDCl_3$ were recorded 10 min after addition of **1a** to the stoichiometric mixture of Ph_3P and I_2; 30 min after addition of $Zn(OTf)_2$ to the mixture of 1a, Ph_3P and I_2; and 4 h after addition of **2a** to the mixture of $Zn(OTf)_2$, **1a**, Ph_3P, and I_2. (b) Bae, S.; Lakshman, K. M. *J. Org. Chem.* **2008**, *73*, 1311–1319.

198) Tolman, C. A. *Chem. Rev.* **1977**, *77*, 313–348.

199) Smith, A. B.; Safonov, I. G.; Corbett, R. M. *J. Am. Chem. Soc.* **2002**, *124*, 11102–11113.

200) Shull, B. K.; Sakai, T.; Nichols, J. B.; Koreeda, M. *J. Org. Chem.* **1997**, *62*, 8294–8303.

List of Publications

1. **Mamidi**, **N**.; Manna, D. "Design, Synthesis and Biophysical Study of γ-Butyrolactone Derivatives and Targeted to the C1 Domain of Protein Kinase C (PKC)" (*Manuscript under Preparation*).
2. **Mamidi**, **N**.; Manna, D. "An Efficient CuCN.2LiCl Promoted Diasteoselective Synthesis of γ-Butyrolactones *via* Aldol C-C Bond Formation Reactions" (*Manuscript under Preparation*).
3. **Mamidi**, **N**.; Panda, S.; Borah, R.; Manna, D. "Synthesis and Protein Kinase C (PKC)-C1 Domain Binding Properties of Diacyltetrol Based Anionic Lipids" *Mol. Biosyst*. **2014**, *10*, 3002-3013.
4. **Mamidi**, **N**.; Gorai, S.; Ravi, B.; Manna, D. "Hybrid Lipid: Mimic of Diacylglycerol and Conventional Phospholipids" *RSC Adv.* **2014**, *4*, 21971-21978.
5. **Mamidi**, **N**.; Manna, D. "$Zn(OTf)_2$ Promoted Chemoselective Esterification of Hydroxyl Group Bearing Carboxylic Acids" *J. Org. Chem.* **2013**, *78*, 2386-2396.
6. **Mamidi**, **N**.; Borah, R.; Sinha, N.; Jana, C.; Manna, D. "Effects of Ortho Substituent Groups of Protocatechualdehyde Derivatives on Binding to the C1 Domain of Novel Protein Kinase C" *J. Phys. Chem. B* **2012**, *116*, 10684-10692.
7. **Mamidi**, **N**.; Gorai, S.; Sahoo, J.; Manna, D. "Alkyl Cinnamates as Regulator for the C1 Domain of Protein Kinase C isoforms" *Chem. Phys. Lipids* **2012**, *165*, 320-330.
8. **Mamidi**, **N**.; Gorai, S.; Mukherjee, R.; Manna, D. "Development of Diacyltetrol Lipids as Activators for the C1 Domain of Protein Kinase C" *Mol. Biosyst.* **2012**, *8*, 1275-1285.